DEVELOPMENT OF HYBRID HAEMAGGLUTININ PSEUDOTYPED LENTIVIRUSES TO ASSESS HETEROSUBTYPIC IMMUNITY TO INFLUENZA

By George Carnell

A thesis submitted for

THE DEGREE OF DOCTOR OF PHILOSOPHY

IN THE SUBJECT OF PHARMACY

Viral Pseudotype Unit

Medway School of Pharmacy

Universities of Kent and Greenwich at Medway

Central Avenue, Chatham Maritime, Chatham, Kent, ME4 4TB

Submitted in October 2017

DECLARATION OF ORIGINALITY

I hereby declare that this thesis and the work reported herein was composed by and originated entirely from me. Information derived from the published and unpublished work of others has been acknowledged in the text and references are given in the list of sources.

Place and date: .....

Signature: .....

Abstract

The influenza virus still causes hundreds of thousands of deaths globally, on top of morbidity and associated economic burden. We are currently at the height of efforts surrounding the development and employment of 'universal' vaccines against this virus, with clinical trials commencing on the most promising candidates. Despite this, the influenza virus poses more of a threat to human life than it ever has previously, with multiple subtypes of pandemic potential circulating around the globe. The key to current efforts lies in the priming of the immune system towards generating long lasting defences against conserved epitopes and conferring heterosubtypic immunity against the surface glycoprotein haemagglutinin. While vaccine strategies have expanded rapidly over recent years with the advent of 'headless' constructs as well as those derived from consensus, mosaic or chimeric sequences, the serological techniques to test how effective these vaccines are, have advanced less rapidly. Classical serological assays have been shown to be ineffective at detecting the antibodies which modern 'universal' vaccines strife to elicit, replaced by ELISA based approaches combined with mouse models measuring *in vivo* protection. In this thesis, an alternative method for the detection of heterosubtypic antibodies is used in depth across multiple platforms. Influenza pseudotypes have been employed using chimeric haemagglutinin constructs in a comprehensive project aimed at dissecting head and stalk directed antibodies present in human serum. Characterised broadly neutralising monoclonal antibodies have been tested on panels of influenza pseudotypes including divergent bat influenza viruses which hitherto have not been encountered in humans. A further aspect of influenza immunity has been covered in the detection of anti neuraminidase antibodies which have an important role to play in influenza heterosubtypic immunity. Finally, influenza pseudotypes bearing the glycoproteins from the less studied influenza B virus have been assayed in a large scale project aimed at correlating pseudotype assays with classical approaches.

TABLE OF CONTENTS

LIST OF FIGURES

LIST OF TABLES

ACKNOWLEDGEMENTS

First I would like to thank my supervisors Dr. Nigel Temperton and Dr. Simon Scott for their excellent mentorship and support. They have always put my interests first and encouraged me to present and publish my work at any and every opportunity, to which I am eternally grateful. I look forward to future conferences and networking sessions!

I'm grateful to the members of VPU for all the troubleshooting sessions and making the VPU such a dynamic place to work: Keith, Rebecca, Stuart, Martin and Yasser. A special thanks to Francesca for your instrumental role in the VPU and for the training and advice. To Fabrizio, thank you for making the hardest part of this PhD enjoyable, it would not have been possible without your unfailing enthusiasm and drive to get results! I would also like to thank the staff at the Medway School of Pharmacy as well as the Universities of Greenwich and Kent.

To Prof. Sarah Gilbert and Dr. Teresa Lambe, thank you very much for having me at the Jenner Institute, and for making collaborations look easy! Many thanks to Craig Thompson for the multitude of talks on interesting influenza and pseudotype subjects, your enthusiasm is infectious!

To my family, thank you for your endless and unwavering support, without it I would not have gotten very far at all.

ABBREVIATIONS

ADCC	Antibody dependent cellular cytotoxicity
APHA	Animal and Plant Health Agency
ATP	Adenosine triphosphate
BEAST	Bayesian evolutionary analysis by sampling trees
BHK-21	Baby hamster kidney cells
bnAb	Broadly neutralising antibody
bnmAb	Broadly neutralising monoclonal antibody
Bris CHM	H11 head, H1 A/Brisbane/59/2007 stalk cHA
BSA	Bovine serum albumin
BSL	Bio safety level
Cat:	Catalogue number
CA/09	A/California/7/2009 (H1N1)
CD4+	Cluster of differentiation 4 positive T lymphocyte
CD8+	Cluster of differentiation 8 positive T lymphocyte
cDNA	Complementary deoxyribonucleic acid
CF	Complement fixation test
cHA	Chimeric haemagglutinin
CONSISE	Consortium for the standardization of influenza seroepidemiology
CPE	Cytopathic effect
cRNA	Complementary ribonucleic acid
CS CHM	H11 head, H1 2009pdm stalk cHA
DC	Dendritic Cell
DMEM	Dulbecco's Modified Eagle's Medium
DMSO	Dimethyl sulfoxide
DNA	Deoxyribonucleic acid
dNTPs	Deoxyribonucleotides
ECD	Extracellular domain

EDTA	Ethylenediaminetetracetic acid
ED	Effector domain
EIF2α	Eukaryotic initiation factor 2α
ELLA	Enzyme-linked lectin assay
ELISA	Enzyme-linked immunnosorbent assay
ER	Endoplasmic reticulum
exNA	Exogenous neuraminidase
FBS	Foetal bovine serum
FcR	Fragment crystallisable region
FDA	U.S Food and Drug Administration agency
Flu B CHM	H10 head, influenza B stalk cHA
Fwd	Forward primer
GISRS	Global Influenza Surveillance and Response System (WHO)
GFP	Green fluorescence protein
GMT	Geometric mean titre
HA	Haemagglutinin
HAT	Human airway trypsin-like protease
hCMV	Human cytomegalovirus
HE	Haemagglutinin esterase
HEF	Haemagglutinin esterase fusion protein
HI	Haemagglutinin inhibition
HIV-1	Human immunodeficiency virus type-1
HPAI	Highly pathogenic avian influenza
H1N1pdm09	2009 pandemic H1N1
IAV	Influenza A virus
IC_{50}	50% inhibitory concentration
IC_{90}	90% inhibitory concentration
IE	Immediate early
IFN	Interferon

IFITM3	Interferon induced transmembrane protein 3
Ig	Immunoglobulin
IL	Interleukin
IRF	Interferon regulatory factor
ISG	Interferon stimulated gene
IU	International Units
LAIV	Live attenuated influenza vaccine
LB	Luria Bertani
LPAI	Low pathogenic avian influenza
LTR	Long terminal repeat
M1	Matrix protein 1
mAb	Monoclonal antibody
MAVS	Mitochondrial antiviral signalling protein
MCS	Multiple cloning site
MDCK	Madin Darby Canine Kidney
MEGA	Molecular evolutionary genetics analysis
MHC	Major histocompatability complex
MLV	Murine leukemia virus
MN	Microneutralisation assay
mRNA	Messenger ribonucleic acid
MVA	Modified vaccinia virus Ankara
M2e	M2 protein ectodomain
NA	Neuraminidase
Nanobody	Camelid/Llama derived antibody
NCBI	National Center for biotechnology information
NEP	Nuclear export protein
NF- $\varkappa$B	Nuclear factor $\varkappa$B
NIBSC	National institute for biological standards and controls
NIH	National institutes of health

NK	Natural killer cell
NP	Nucleoprotein
NPC	Nuclear pore complex
NS1	Non-structural protein 1
NS2	Non-structural protein 2 (NEP)
OD	Optical density
OIE	Office international des epizooties
Opt	Optimised
Ori	Origin of replication
PA	Polymerase acidic protein
PB1	Polymerase basic protein 1
PB2	Polymerase basic protein 2
PBS	Phosphate buffered saline
PCR	Polymerase chain reaction
Pdm	Pandemic
PEI	Polyethylenimine
pELLA	pseudotype based ELLA
pH1N1	Pandemic H1N1
pMN	Pseudotype based microneutralisation assay
PNA-HRPO	Peanut agglutinin conjugated to horseradish peroxidise
Polybrene	Hexamethrine bromide
PSI Ψ	Packaging signal element
PV	Pseudotype virus
P3	Polymerase 3 (Influenza C)
QIV	Quadrivalent influenza vaccine
RBC	Red blood cell
RBD	Receptor binding domain
RBS	Receptor binding site
Rev	Reverse primer

RIG-I	Retinoic acid inducible gene 1
RLA	Relative luciferase activity
RLU	Relative luminescence units
RNA	Ribonucleic acid
Rpm	Revolutions per minute
RRE	Rev responsive element
RT	Room temperature (20°C)
RT-qPCR	Reverse transcriptase quantative PCR
sH1N1	Seasonal H1N1
SIN	Self inactivating vector
SFFV	Spleen focus forming virus
SOC	Super optimal broth with catabolite repression
Sol CHM	H11 head, H1 A/Solomon islands/3/2006 stalk cHA
SRID	Single radial immuno-diffusion
SRH	Single radial haemolysis
SV40	Simian vacuolating virus 40
TAE	Tris-acetate-ethylendiaminetetraacetic acid buffer
$TCID_{50}$	50% tissue culture infectious dose
TCR	T cell receptor
TIV	Trivalent influenza vaccine
TLR	Toll like receptor
TMPRSS2	Type II Transmembrane protease, serine 2
TMPRSS3	Type II Transmembrane protease, serine 3
TMPRSS4	Type II Transmembrane protease, serine 4
TMPRSS6	Type II Transmembrane protease, serine 6
TPCK-Trypsin	L-tosylamido-2-phenyl ethyl chloromethyl ketone treated trypsin
TRIM	Tripartite motif
VLP	Virus like particle

vRNA	Viral ribonucleic acid
vRNP	Viral ribonucleoprotein
VSV	Vesicular stomatitis virus
VSV-G	VSV glycoprotein
WHO	World Health Organisation
WPRE	Woodchuck hepatitis virus post transcriptional regulatory element
WT	Wild type
-ssRNA	Negative sense single stranded ribonucleic acid

Chapter 1 : Introduction

1.1 Influenza virus basics and disease

Influenza is a respiratory syndrome caused by three of six genera in the orthomyxoviridae family, influenza A, B and C. A putative fourth genus (Influenza D) has recently been characterised and proposed (Hause et al. 2014). Influenza A virus (IAV) is the most widespread, its various subtypes are classified according to their antigenically variable surface glycoproteins: haemagglutinin (HA, H1-H18) and neuraminidase (NA, N1-N11). The virion consists of a segmented negative sense genome encapsidated within ribonucleoprotein complexes (vRNP), which are surrounded by a matrix shell and lipid envelope containing the two surface glycoproteins and the M2 ion channel. Influenza A is the primary source of the seasonal form of the disease, responsible for up to 500,000 deaths per annum as well as deaths caused by pandemics such as those occurring in 1918, 1957, 1968, and 2009 (WHO factsheet N°211, 2014). Influenza B is also of importance, with two antigenically distinct lineages co-circulating worldwide causing 20-30% of global morbidity (Ambrose and Levin 2012; Glezen et al. 2013; Mccullers et al. 2004). Vaccines against influenza need to be regularly updated to match predicted circulating strains that are constantly escaping from vaccine protection through a mechanism known as antigenic drift. Influenza A is primarily associated with wild fowl/birds in the case of the majority of subtypes and can reassort with human strains through antigenic shift to yield human compatible viruses with previously un-encountered surface epitopes. Pigs are usually considered to be the mixing vessel for reassortment as they express a mixture of α-2,3 and α-2,6 sialic acid linkages which are the preferred receptor for avian and human influenza viruses respectively (Skehel and Wiley 2000). Research on influenza viruses is often hindered by the requirement for expensive bio safety level (BSL) precautions, especially in the case of the Highly Pathogenic Avian influenza (HPAI, e.g. H5N1, H7N1) or pandemic strains. Symptoms caused by influenza virus infection range from a non-febrile upper respiratory tract illness to severe or fatal pneumonia. The majority of infections have been reported to be self-limiting fevers with respiratory symptoms and many cases have been indistinguishable from the common cold. (Komiya et al. 2009; Liang et al. 2009; Ong et al.

2009; S. I. Park et al. 2010; Plessa et al. 2010). However as many as one third of the infected are thought to be asymptomatic (Carrat et al. 2008; C. J. Williams et al. 2010). Nevertheless, the WHO estimates suggest that influenza A and B seasonal epidemics cause between 3-5 million severe cases of influenza disease and 250 to 500,000 deaths per annum (WHO 2003).

1.2 Influenza virus molecular biology

The influenza A virus is contains a segmented genome consisting of 8 genes, coding for up to 14 proteins which are described briefly here, and in further detail in the following sections. Segments 1, 2 and 3 form the components of the viral RNA polymerase which associates with the vRNP, and the influenza negative sense RNA (-ssRNA) in complex with nucleoprotein (NP). Segment 4 is the HA glycoprotein which is the main focus of this thesis. Segment 5 codes for the NP and segment 6 the NA glycoprotein which is involved in destruction of the HA-receptor sialic acids on infected cells, allowing release of nascent virions. Segment 7 codes for the M1 matrix protein, also involved in nuclear export of newly synthesised vRNPs, and the M2 ion channel. Segment 8 codes for non-structural proteins NS1 and the Nuclear Export Protein (NEP). These various genes are shown in schematic format in Figure 1.1.

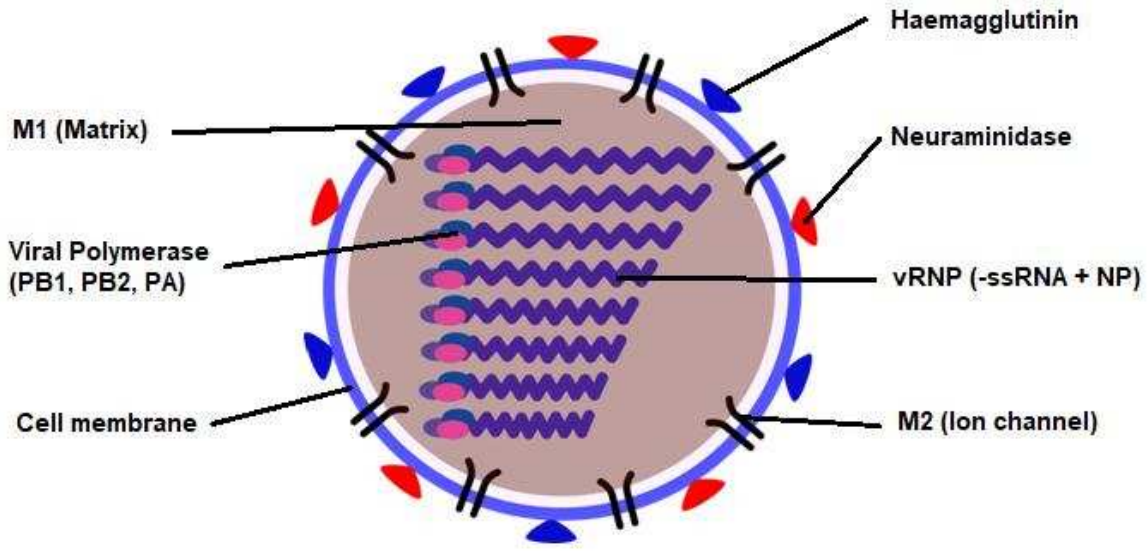

Figure 1.1. Schematic representation of the influenza virus. Surface glycoproteins HA, NA and M2 are embedded in the cell membrane, the latter taken from the host cell. The Matrix protein forms the core or the virus which encapsidates the viral ribonucleoproteins complexed with viral RNA polymerases, on each segment of the multi-partite genome.

The influenza virus infects target ciliated epithelial cells in the respiratory tract through the binding and fusion protein HA, which will bind to terminal sialic acids of glycoproteins or glycolipids on the surface of its target cells (DuBois et al. 2011). Binding initiates endocytosis of the influenza virus and acidification of the resulting endosome, allowing pH mediated conformational changes in the HA trimer and facilitating fusion of the viral and host endosomal membranes, releasing the viral core into the cytoplasm. Endocytosis has been shown to occur both by clathrin-mediated and clathrin/caveolin independent pathways (Lakadamyali et al. 2004; Matlin et al. 1981). The viral core then dissociates after M2 mediated acidification of the viral core, allowing the release of vRNPs coding for the genes which make up the influenza virus (Holsinger et al. 1994; Yoshimura and Ohnishi 1984). vRNPs are transported to the nucleus via interaction with importin-α and importin-β1 and resulting translocation through nuclear pores (Eisfeld et al. 2014). The negative sense genome segments are then transcribed into mRNAs by the transcription complex associated with every vRNP. Cap snatching then occurs, consisting of transfer of the 5' end from cellular mRNAs, including the cap, to the influenza mRNA. This allows viral mRNA stability and transcription after export from the nucleus (Dias et al. 2009; Fechter and Brownlee 2005). Polyadenylation of these mRNAs occurs as a result of transcription from the vRNA. Viral mRNAs subsequently form a template for the production of negative sense viral gene segments as well as being exported to the cytoplasm for translation via the nuclear export protein (NEP) and matrix protein (M1) (Bui et al. 2000; Eisfeld et al. 2014; Martin and Helenius 1991). Viral proteins are translated and trafficked through the endoplasmic reticulum (ER) and golgi apparatus, mediating correct folding and exposure to proteases for post-translational cleaving where necessary (HA protein)(Braakman et al. 1991; Doms et al. 1993; Skehel and Waterfield 1975). Viral glycoproteins are then targeted to the surface of the cell, gathering on lipid rafts and promoting the formation of mature viral particles exiting the cell (D. P. Nayak et al. 2009; Rossman et al. 2010). Exit is facilitated by the action of NA, destroying HA receptors on the surface of the cell and allowing release of viral particles. A life cycle diagram is shown in Figure 1.2.

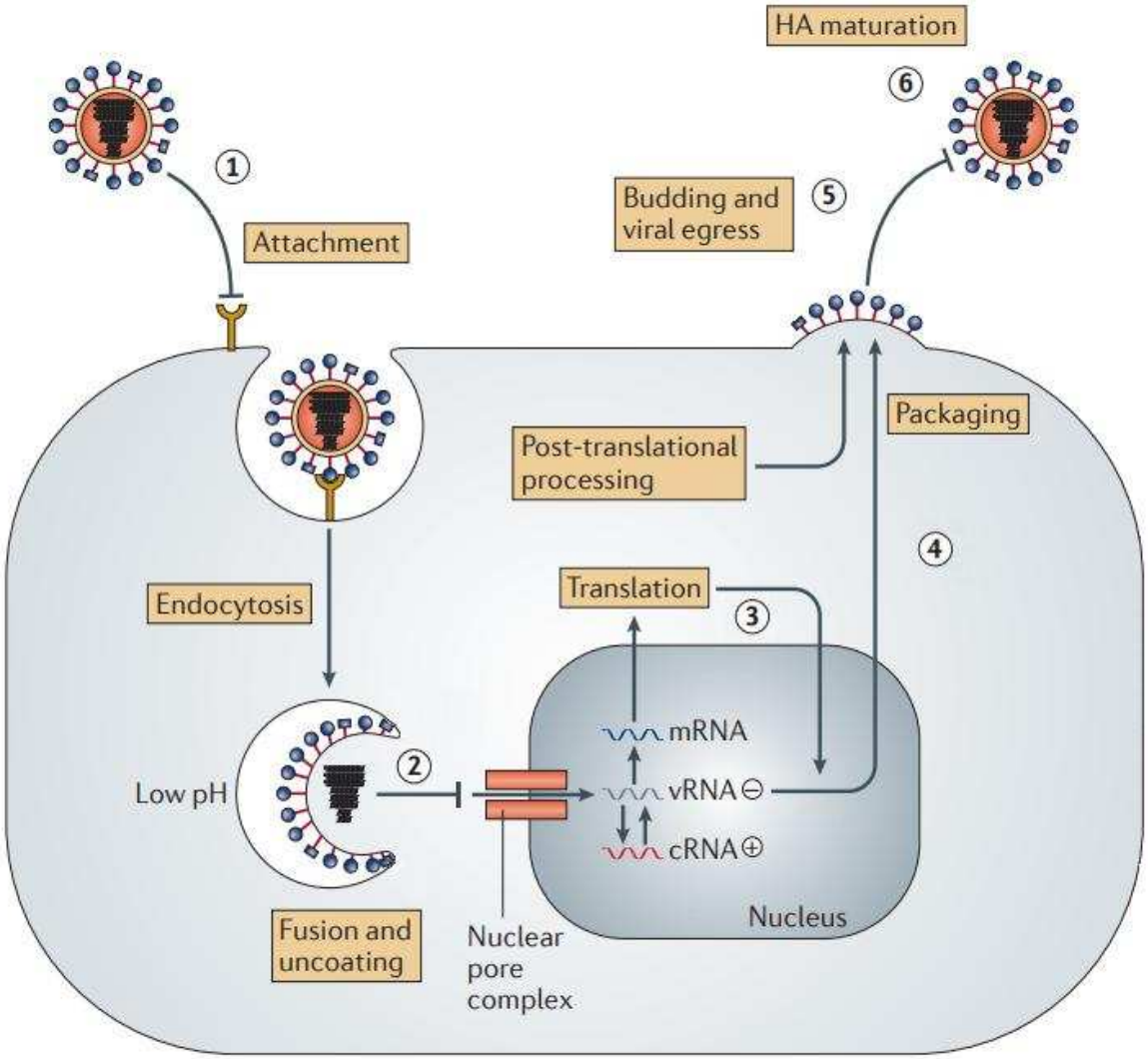

Figure 1.2. Life cycle diagram for the influenza virus. 1) Attachment to target cells is mediated by the HA glycoprotein interaction with terminal sialic acid molecules on the cell surface. 2) Virus internalisation, pH dependent fusion mediated by the HA glycoprotein and influenza virus core acidification mediated by M2 enable release of vRNPs into the cell cytoplasm. 3) Influenza genome replication and protein production is initiated after vRNP nuclear import. 4) Post-translational processing of proteins and packaging occurs, producing progeny viruses. 5) Budding of progeny is facilitated by influenza proteins, allowing viral egress which is further enabled by NA mediated cleavage of surface sialic acid molecules. 6) Cleavage of HA glycoproteins, within the cell or at the cell surface allows maturation of new virions. Figure adapted from (Krammer and Palese 2015)

1.3 HA

The trimeric attachment and fusion protein HA is the principal constituent of the influenza virus envelope, alongside NA and M2. Attachment to sialic acid residues on target cell membranes triggers endocytosis and pH dependent exposure and engagement of the fusion peptide, mediating entry of the virus (Wiley and Skehel 1987). This process is the basis on

which influenza neutralisation assays are founded – the exploitation of attachment and entry for the study of HA-directed antibodies and their neutralising ability. Sequence analysis has permitted classification of influenza A subtypes into two distinct groups: group 1 containing HA subtypes 1, 2, 5, 6, 8, 9, 11, 12, 13, 16, 17 and 18 and group 2 containing 3, 4, 7, 10, 14, and 15. (Fouchier et al. 2005; Tong et al. 2012, 2013). Subtypes within each group are often subdivided into clades with further sequence dissimilarity. A phylogeny of current influenza HA types and subtypes are shown in Figure 1.3.

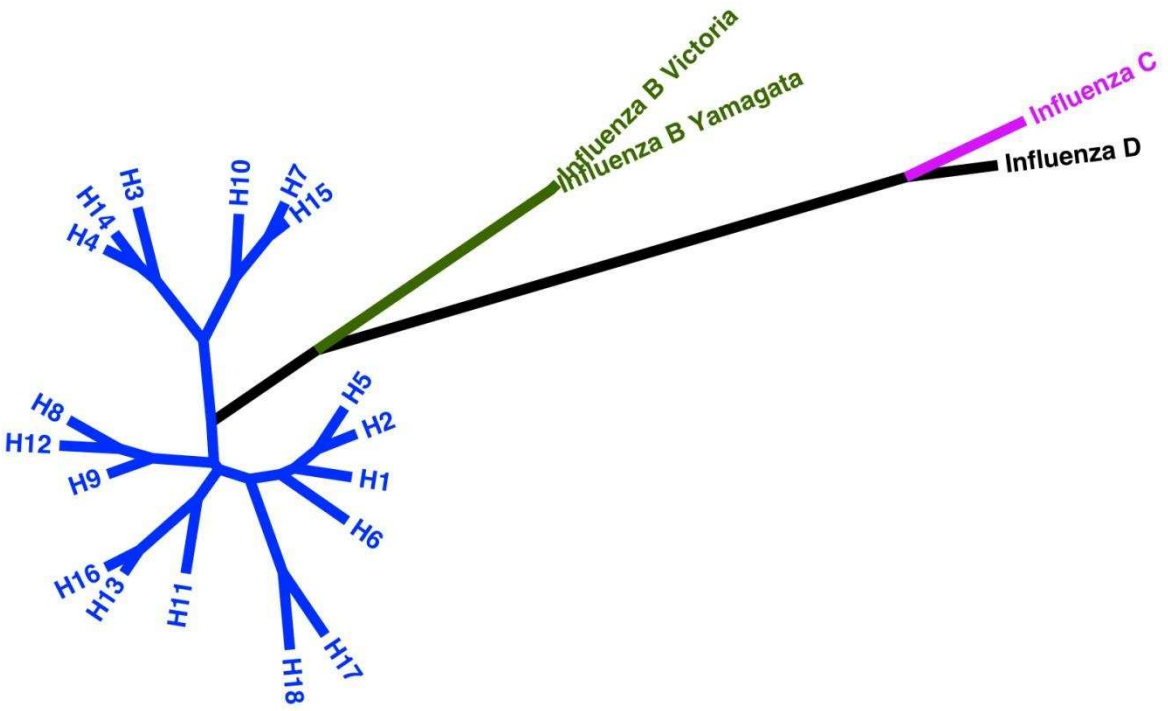

Figure 1.3. Phylogeny of current influenza HA subtypes. Influenza A subtypes form two distinct groups, group 1 consists of subtypes 1, 2, 5, 6, 8, 9, 11, 12, 13, 16, 17 and 18 while group 2 contains subtypes 3, 4, 7, 10, 14, and 15. Influenza B lineages Yamagata and Victoria, Influenza C and influenza D show divergence from influenza A based on this phylogenetic analysis. Figure from (Carnell et al. 2015)

1.3.1 Structural and antigenic properties of HA

There are four primary antigenic sites proximal to the binding site of the HA trimer, to which neutralising antibodies are generally directed. For H1N1, sites Sa, Sb and Cb are found on a single protomer of the HA trimer, and Ca (Ca1 and Ca2) are found in a cleft between two receptor binding domains (RBD) (Brownlee and Fodor 2001; Caton et al. 1982; DuBois et al. 2011; Wiley et al. 1981). These are extensively reviewed and in great detail by Skehel and Wiley (Skehel and Wiley 2000). It has been reported in these cited articles that single amino

acid mutations in these antigenic sites will give rise to drift mutants. For H3N2, the antigenic site A consists of a loop of amino acids from residues 140-146, B consists of the outside residues of an α-helix between residues 187-196, site C is reported from a bulge between cysteine residues 52 and 277 which are linked by a disulphide bridge and the subject of techniques to produce chimeric (or hybrid) HAs (chapter 3). Site D is reported between residues 207 and 220 (Wiley et al. 1981). Aside from these, there are other epitopes on the HA trimer, most notably in the stalk region such as the F domain (Fusion peptide) and membrane proximal stem (Corti et al. 2011; Ekiert et al. 2012; T. T. Wang et al. 2010). Other sites include Pa and Pb on the HA trimer stalk (A. Wu et al. 2010). It would seem that while head proximal antibodies would be involved in obstruction of the RBC, making them haemagglutination inhibition (HI) competent antibodies, stalk antibodies work by preventing unfolding of the HA trimer and neutralising the action of HA in this fashion. These antibodies would not be detected by the HI assay. Despite the notion that high densities of glycoproteins can obscure this stalk region, research has suggested, at least in the case of pandemic H1N1 (pH1N1) that HA are not packed so tightly as to evade stalk reactive antibodies completely. This is partly due to the fluid nature of the influenza envelope in which HA, NA and M2 are embedded. ~75% of HAs were shown to be bound by bnmAb C179 at the membrane proximal stem (A. K. Harris et al. 2013). See Figure 1.4 for a schematic representation of the HA trimer alongside neutral pH and fusion pH conformations, discussed in (Y. Zhou et al. 2014).

1.3.2 Proteases used for cleavage of HA proteins

As HA is produced and trafficked through the secretory pathway it requires proteolytic cleavage in order to become fusion competent. Proteolytic cleavage is mediated by certain host cell proteases and subsequently restricts certain subtypes to epithelial cells where these required proteases are expressed. Newly folded HA0 precursors are cleaved by trypsin or serine proteases (E.g. Human Airway Trypsin) into HA1 and HA2 subunits (S Bertram et al. 2010; Böttcher et al. 2006; Chaipan et al. 2009). Cleavage is necessary for fusion competence of the HA and its resulting role in and viral infectivity (Klenk et al. 1975; Klenk and Rott 1988; Lazarowitz et al. 1973; Lazarowitz and Choppin 1975).

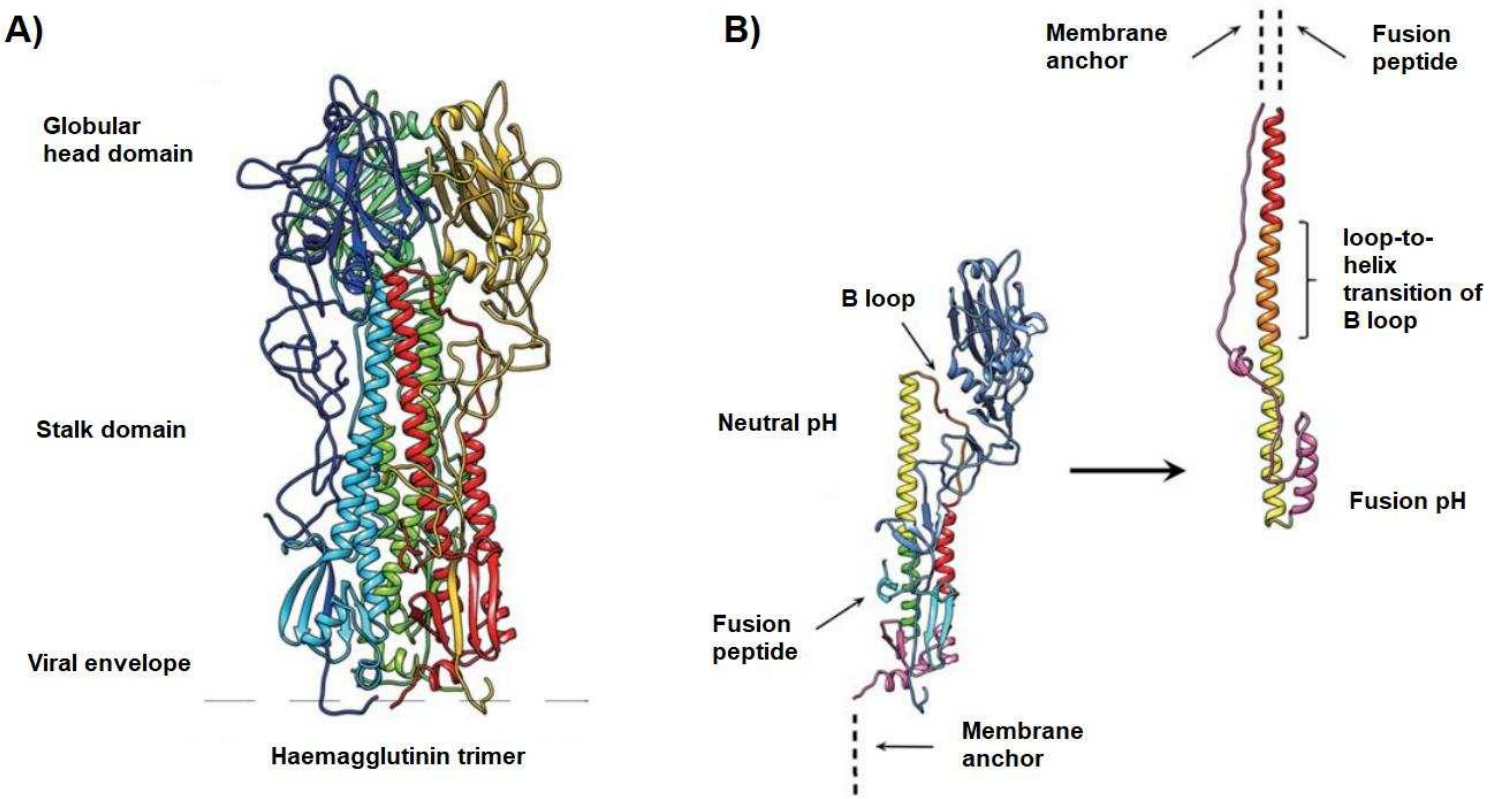

Figure 1.4. Schematic representation of an HA trimer. A) Globular head domain, Stalk domain and region proximal to the viral envelope are shown. B) The conformational changes each HA monomer undergoes are shown, from Neutral pH to Fusion pH whereupon membrane fusion is mediated by HA. Figure adapted from Y. Zhou et al. 2014.

1.4 NA

The NA protein is an enzyme composed of four identical monomers, each 470 amino acid residues in length. They form a homotetramer of which the N-terminal regions form a transmembrane region anchoring the glycoprotein in the membrane and associating with the viral core (matrix, section 1.5). Each influenza virus typically contains 50 NA tetramers on its surface, often arranged in clusters (A. Harris et al. 2006). There are 11 known influenza NA subtypes, arranged into two distinct phylogroups based on nucleotide sequence analysis. N10 and N11, derived from newly described bat species of influenza are divergent with a currently uncharacterised substrate and are discussed in further depth in chapter 7. The N-terminal region forms a cytoplasmic tail which is highly conserved among all NA subtypes of influenza A, but divergent in influenza B (Shtyrya et al. 2009). NA has a globular, mushroom shaped head domain containing the enzymatic active site nestled within a pocket in the space within each NA monomer, shown in Figures 1.5 and 1.6. A thin stalk region extends this head outwards from the virus envelope. NA is an exosialidase, cleaving sialic acid from the surface molecules of infected cells by breaking the α-ketosidic linkage between sialic acid and its adjacent sugar molecule (Varghese and Colman 1991). This allows release of new virions from the cell surface (Lentz and Air 1986; Palese et al. 1974). Sialidase function also aids the virus in evading the heavily sialylated glycoproteins present in the mucus of the respiratory tract, allowing the virus to reach its target cells (Cohen et al. 2013; Matrosovich et al. 2004). In a similar fashion, sialic acid residues on infected cells are cleaved, preventing superinfection (I. C. Huang et al. 2008). The active site of NA is pictured in Figure 1.6, located at the N-terminal end of central parallel strands located within the β-sheet 'propeller' folds of the NA protein (Colman 1994). The active site is conserved among all influenza A and B NAs, with only small differences observed between divergent sequences (Russell et al. 2006).The length of the NA stalk has been associated with pathogenicity in certain highly pathogenic avian influenza (HPAI) strains. These viruses with NAs containing truncated stalk regions showed enhanced replication and shedding in avian species but not other animals tested (Blumenkrantz et al. 2013; T. W. Hoffmann et al. 2012; Y. Li et al. 2014). Further studies have confirmed the relationship of NA stalk deletions with pathogenicity outside of the avian model, showing an increase in lethality to mice resulting from infection by pH1N1 with a truncated NA (S. Park et al. 2017).

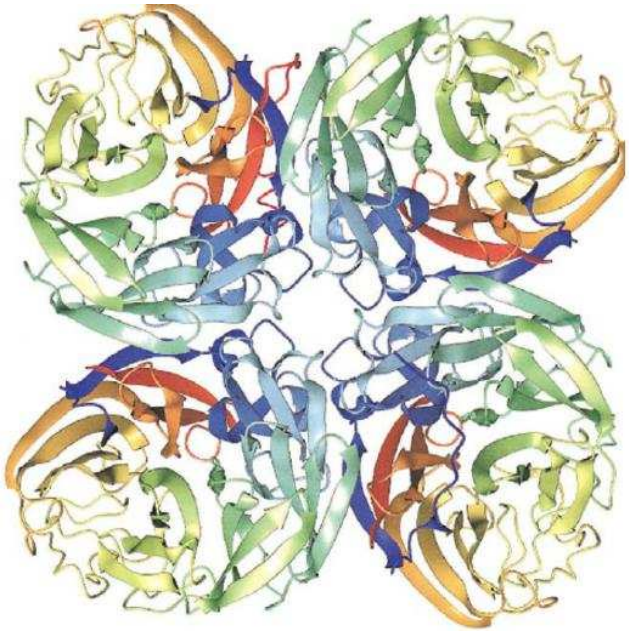

Figure 1.5. Schematic representation of influenza A (N2) tetramer. Each monomer is arranged symmetrically around a central axis. Amino acid ribbon structures coloured from blue to red from N- to C- terminal positions. Figure from (Laver and Garman 2002)

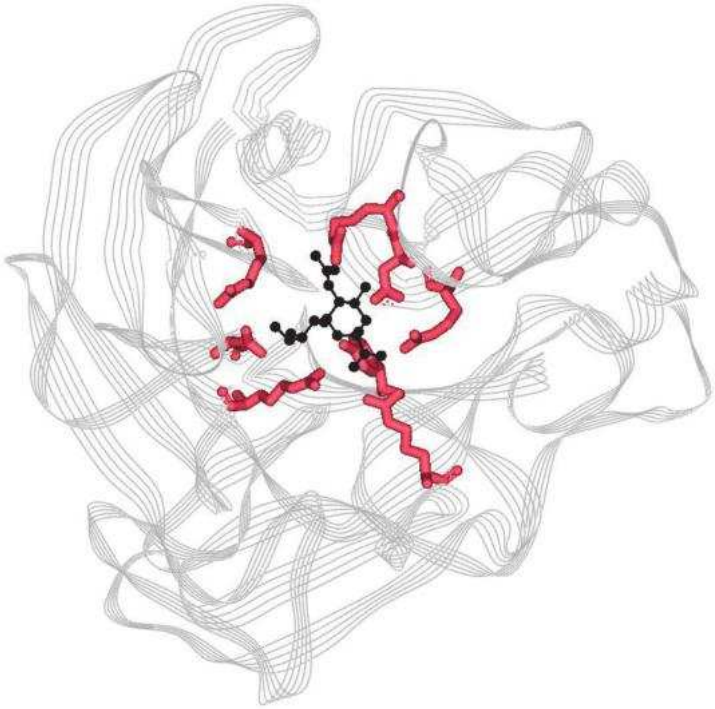

Figure 1.6. Schematic representation of influenza A (N2) NA in complex with 2,3 linked sialic acid (black), with the functional amino acid residues of NA shown in red. Figure from (Shtyrya et al. 2009)

In recent years a binding property of NA has been characterised after discovery that treatment of influenza virus with NA inhibitors reduced its infection efficiency by 1/4 and 1/8 in Madin Darby Canine Kidney (MDCK) and A549 cells respectively (Ohuchi et al. 2006). Mutations (such as D151G and G147R) within the NA of H3N2 viruses have been reported, that increase the receptor-binding activity of NA, also compensating for weaker affinity of the HA glycoprotein for its receptor. Despite this, these NAs still carry out their function in releasing HA from sialic acids in order to mediate release of new particles (Hooper and Bloom 2013; Y. P. Lin et al. 2010). It has been shown that in the presence of non-functional NA, mutations can arise in the HA to reduce its binding affinity, allowing release of viral particles. This shows that HA and NA affinities are carefully balanced to enable the continuation of the influenza life cycle (Mitnaul et al. 2000).

NA is the target for various antiviral drugs which are widely used. Zanamivir, oseltamivir and laninamivir are antivirals which block the action of NA by mimicking its substrate. The latter two are prodrugs, taken in by ingestion or inhalation respectively; these drugs are converted into the active form of the drugs in the liver (oseltamivir) or respiratory tract (laninamivir). Until January 2008 the consensus was that misuse of NA inhibitors would not lead to the rise of resistance mutations, until the first instance occurred with the H274Y mutation conferring resistance to oseltamivir but not zanamivir (Yen et al. 2007). The 2009 pH1N1 strain entering circulation and replacing currently circulating seasonal strains was found to be susceptible to oseltamivir (Shtyrya et al. 2009). However, a recent mutation (H275Y) has arisen, conferring oseltamivir resistance to pH1N1 strains, despite it still being susceptible to zaninamivir and laninamivir (Kamali and Holodniy 2013; Pinilla et al. 2012).

1.5 M1

The matrix protein (M1) of the influenza virus forms the core which acts as a shell interacting closely with the plasma membrane, acting as a bridge between internal proteins, vRNPs and the transmembrane proteins HA, NA and M2, the latter of which interacts with M1 via cytoplasmic tail domains (Gómez-Puertas et al. 2000; K. Zhang et al. 2012). M1 pH dependent dissociation of the influenza virus core, releases vRNPs into the cell cytoplasm upon M2 mediated acidification. M1 is also involved in nuclear import and accumulation of viral structural proteins, and the nuclear export of vRNPs (Akarsu et al. 2003; Whittaker et al. 1996). M1 is a 242 amino acid long protein with a flexible C-terminal domain which may

be responsible for the proteins multiple roles in virion shape/stability and interactions within the viral life cycle (Gómez-Puertas et al. 2000; Shtykova et al. 2013). To date, attempts to determine its full structure have been unsuccessful – no high resolution model has been determined for the entire protein.

1.6 M2

The M2 ion channel is responsible for acidification of the influenza virus core after internalisation by endocytosis, mediating the dissociation of influenza proteins and release of vRNPs into the cell cytoplasm after HA based fusion (Lamb et al. 1985), reviewed in detail by Pinto & Lamb 2006. It is also responsible for regulation of the pH within the Golgi apparatus or endosome, stabilising the pH sensitive HA protein while it is trafficked to the cell surface (Ciampor et al. 1992). M2 is composed of four monomers, each of which is 96 amino acids in length. This resulting homotetramer is a transmembrane protein with an extracellular N-terminal domain 23 amino acids in length, a 19 amino acid transmembrane domain and a cytoplasmic tail 54 amino acids long (Lamb et al. 1985; Pinto et al. 1992). This protein is not only essential for release of vRNPs through its action as a proton channel, but it is also involved in the mediation of virus budding through the action of an amphipathic helix located within its cytoplasmic tail. This 17 amino acid long helix has been shown to be essential for membrane scission, promoting membrane curvature in a cholesterol-dependent manner (Rossman et al. 2010). It is also associated with the M1 protein in its involvement in viral packaging and budding. Mutations in the cytoplasmic region of M2 have been shown to lead to incomplete incorporation of genomc RNA into new viruses, as well as defective budding of new particles (B. J. Chen et al. 2008; Imai et al. 2004, 2008; McCown and Pekosz 2006; Rossman and Lamb 2011). The pore located in the space within the M2 homotetramer contains two essential pore-lining residues which are important for proton selectivity, allowing unidirectional conductance of the M2 ion channel (Y. Tang et al. 2002; C. Wang et al. 1995). M2 is a target for influenza antiviral drugs, discussed in section 1.15.

1.7 vRNP and polymerase

The genetic material of the influenza virus is packaged into eight viral ribonucleoprotein complexes (vRNP) which consist of viral RNA packaged in multiple nucleoprotein (NP) segments and a single trimeric polymerase complex. vRNPs are transported into the host

cell nucleus via nuclear pore complexes (NPC), allowing transcription and genome replication to occur. The NP protein is 498 amino acid residues in length with a positive charge at neutral pH (Ng et al. 2009). It binds to the negative sense single stranded RNA (-ssRNA) gene segment as well as interacting with other NP proteins, and the polymerase basic 1 and 2 (PB1 and PB2) parts of the viral polymerase (Biswas et al. 1998; Eisfeld et al. 2014; Poole et al. 2004).

The viral polymerase complex is composed of PB1 and PB2 alongside the Polymerase acidic protein (PA) in influenza A and B, or Polymerase 3 (P3) in influenza C (Fodor 2013; Resa-Infante et al. 2011; te Velthuis and Fodor 2016). It is complexed to each individual genome segment within the influenza virus, allowing transcription and replication of each vRNA after translocation to the nucleus (Area et al. 2004; Fodor 2013; Hutchinson and Fodor 2013). Transcription occurs in a primer-dependent manner, producing mRNAs with 5' cap and a poly(A) tail (Plotch et al. 1981). The cap is 'snatched' from host mRNAs by action of the PB2 cap-binding domain, that allows the cap to be cleaved 8-14 nucleotides downstream by PA or P3 (Dias et al. 2009; Guilligay et al. 2008; Yuan et al. 2009). The resulting cap and nucleotides are used to prime synthesis of mRNA transcripts for influenza gene segments. Replication of influenza gene segments is primer independent, new vRNAs being produced via a replicative complimentary RNA (cRNA) intermediate. The polymerase complex is intimately linked to host specificity, Nucleoproteins have been shown to co-evolve with the other proteins making up the vRNP complex, possibly as a result of functional restrictions between proteins (Naffakh et al. 2008). Incompatibility between vRNP proteins is a likely hurdle impeding the ability of reassortant influenza viruses from crossing species barriers, limiting interspecies transmission (Cauldwell et al. 2014; Long et al. 2013; Obenauer et al. 2006).

1.8 NEP

The Nuclear Export Protein (NEP), previously known as Non Structural Protein 2 (NS2) is another key protein involved in the cellular functions of the life cycle of the influenza virus. Aside from facilitating the export of vRNPs from the host cell nucleus, NEP also has roles in regulating vRNA, viral mRNA and cRNA accumulation (Inglis et al. 1979; Lamb and Choppin 1979; Lamb and Lai 1980). This role is important as mutations in NEP have been shown to compensate for lack of viral polymerase efficiency when infecting cultured human cells with

avian HPAI viruses (H5N1) (Mänz et al. 2012; Robb et al. 2009). NEP has also been shown to have a role in the budding of progeny viruses through recruitment of a cellular ATPase to the cell membrane for this purpose (Gorai et al. 2012).

1.9 NS1

NS1 is the key influenza protein involved in host cell interactions where it acts to antagonize antiviral responses mediated by interferon (IFN) (Hale et al. 2008). It is expressed at high levels in the nucleus of infected cells where it carries out its primary function in the blocking of cellular innate immunity (Krug and Etkind 1973). In Influenza A viruses, NS1 is typically 230 amino acid residues in length, with distinct genetically divergent clades named A and B, and a third clade for the bat influenza subtypes H17N10 and H18N11 (Tong et al. 2013). Clade B NS1 is mainly found in avian strains whereas Clade A NS1 are the most frequently encountered. Influenza B and C viruses have their own respective NS1 (281 and 246 amino acid residues respectively) variants (Alamgir et al. 2000; Yin et al. 2007). NS1 is a homodimer composed of two distinct structural domains, connected by a flexible linker region (Qian et al. 1994). An RNA-binding domain makes up the first 73 amino acids and an effector domain (ED) completes the protein from residues 80-230. The RNA-binding domain contains six α helices which are involved in the binding of double stranded RNAs (dsRNA) (Cheng et al. 2009). NS1 acts as an IFN antagonist by preventing Retinoic acid inducible gene 1 (RIG-I) activation, preventing the triggering of antiviral responses by recognised viral dsRNAs (Mibayashi et al. 2007; Rehwinkel et al. 2010; Schmidt et al. 2009). It also acts to block the RIG-I signal transduction pathway through its interaction with TRIM25 and Riplet as well as preventing RIG-I ubiquitination (Gack et al. 2009; Rajsbaum et al. 2012). NS1 has been shown to abrogate activation of the protein kinase PKR, preventing this further activation of cellular defensive pathways (S. Li et al. 2006; Lu et al. 1995; Min et al. 2007; Min and Krug 2006). Further capabilities of this dynamic protein include reducing the expression of type I IFN system proteins (such as MxA), delaying or reducing its antiviral effects (García-Sastre et al. 1998; Haye et al. 2009).

1.10 Alternative splicing of Influenza mRNAs

Various novel proteins have been discovered in recent years, produced from alternative splicing of influenza virus mRNAs. PB2-S1 is spliced from Segment 1 mRNA, producing a

protein localized to the mitochondria which acts to inhibit the RIG-I dependent interferon signalling pathway (Yamayoshi et al. 2015). Segment two contains two further non-structural genes, PB1-F2 and N40, the latter which is currently poorly characterised. PB1-F2 is involved in induction of cell death in immune cells and together with N40 these proteins are beneficial to viral replication, but not essential for the viability of influenza virus, as determined by mutational studies (W. Chen et al. 2001; H. M. Wise et al. 2009).

Segment 3 codes for three further non-structural genes, PA-N182, PA-N15S and PA-X. All three proteins are important for viral replication but not essential, as their absence only reduced the efficiency of viral replication and lowered pathogenicity. PA-X plays a role in the regulation of host mRNA degradation. Loss of PA-X was shown to increase inflammatory, apoptotic and T-lymphocyte signalling pathway kinetics (Jagger et al. 2012; Muramoto et al. 2013).

Segment 7 codes for a further ion channel M42 which has an antigenically distinct ectodomain to M2. This protein replaced M2 in an M2 null-mutant virus, through a compensatory mutation inducing an upregulation in M42 synthesis (H. M. Wise et al. 2012).

A schematic diagram of all the genes listed in the previous sections is shown in Figure 1.7.

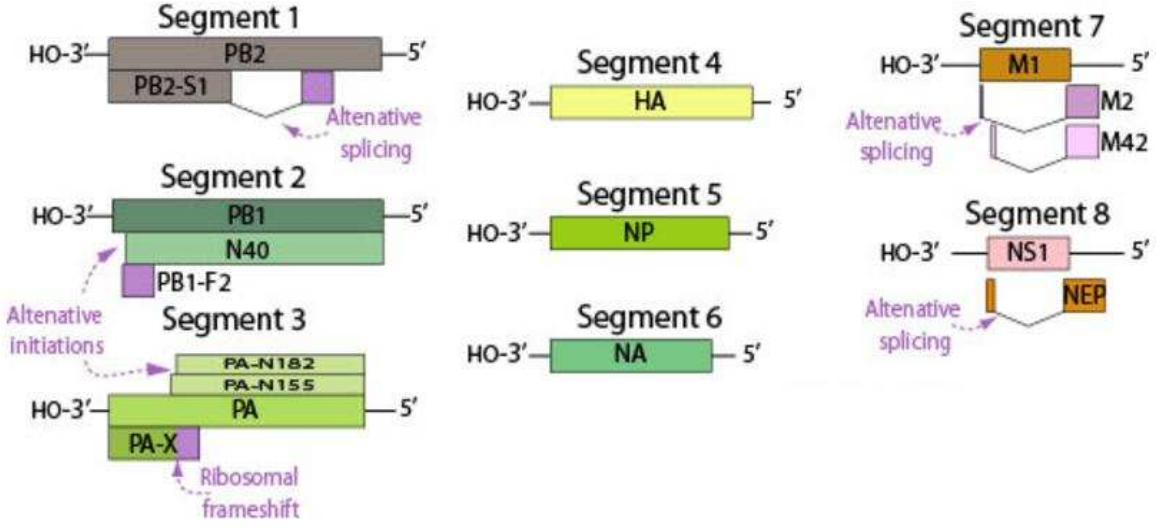

Figure 1.7. Schematic diagram showing the eight gene segments of the influenza virus. Segment 1, 2 and 3 code for PB1, PB2 and PA, the components of the viral polymerase. Segment 4 and 6 code for the glycoproteins HA and NA while segment 5 codes for the nucleoprotein. M1 and M2 are coded for by segment 7 and NS1 and NEP coded for by segment 8. Schematic adapted from Viral Zone, Swiss Institute of Bioinformatics.

1.11 Epidemiology of Influenza virus

1.11.1 Seasonal influenza

Seasonal influenza is the term given to the constant spread of influenza virus around the globe, peaking in seasons each year between September and March in temperate countries. Seasonal influenza viruses are currently composed of human strains of the virus in the H1 and H3 subtypes. Vaccination remains the most effective way to reduce mortality and morbidity against seasonal influenza viruses. The WHO Global Influenza Surveillance and Response System (GISRS), a network of laboratories worldwide, works towards bi-yearly update of vaccine strains to predict and match circulating strains as they evolve (WHO 2003). Due to the dynamics surrounding the circulating strains of influenza, the multiple circulating subtypes and lineages and the time required to produce stocks of vaccine, there are often mismatches in circulating strains and current vaccines (de Jong et al. 2000; Dos Santos et al. 2016; Hoa et al. 2016). This problem is compounded by the elicitation of HA head reactive antibodies (Also HI compatible antibodies) by the traditional inactivated influenza vaccines used globally. The predisposition of the viral polymerase to inducing mutations in progeny influenza virions, alongside the selective pressure on IAVs caused by natural infection, drives antigenic drift in this hyper variable head region, leading to the need for constant updates of the vaccine strain (L. Du, Zhou, et al. 2010; Mossad 2007, 2008; Tosh et al. 2010). Despite this, studies have shown that repeated vaccination or exposure to seasonal influenza can lead to an increase in cross protective antibodies (Pichyangkul et al. 2014).

1.11.2 Pandemic influenza

Upon global spread of a novel strain of influenza to which the human population is naive or lacking immunity to, a pandemic strain is designated. There have been several influenza pandemics in recent human history, the first of note being the H1N1 pandemic (pH1N1) ‘spanish flu’, which caused an estimated 40 million deaths worldwide (WHO 2003). Subsequent pandemics arose from H2N2, the ‘Asian influenza’ of 1957, H3N2, ‘Hong Kong influenza’ of 1968 and the 2009 pandemic ‘swine flu’. Pandemic influenza is generally brought about through antigenic shift, a process by which a virus with novel characteristics but the ability to infect humans results from co-infection of two or more strains/subtypes

within the same cell. It has been reported that infection with pH1N1, whether the 1918 or 2009 strains, leads to increased titres of stalk-directed antibodies which have a role in the pH1N1 strain replacing currently circulating seasonal strains (Pica et al. 2012; Thomson et al. 2012). Also, cross-protection against the 2009 strain was provided by previous infection with the 1918 strain (Medina et al. 2010). This phenomenon has been attributed in part to protection provided by the Fc region (FcR) of stalk antibodies and subsequent protection through antibody dependent cell-mediated cytotoxicity (ADCC) (Tete et al. 2016). The heterosubtypic nature of antibodies elicited by pH1N1 viruses lead to an increased protection against seasonal strains among the elderly, it has been shown that dominant heterosubtypic antibody responses against the HA stalk correlate with absence of memory B cells providing immunity against the HA head. Therefore exposure to a pH1N1 strain early on in a patient's immune history seems to provide them with long lasting heterosubtypic immunity (Thomson et al. 2012).

The 2009 pandemic virus is a triple reassortant influenza virus with internal gene segments from Eurasian and North American Swine, Classic Swine and H3N2 triple reassortant viruses which were circulating in North America (Garten et al. 2009; G. J. D. Smith et al. 2009). The virus itself emerged in Mexico and the United States, spreading rapidly worldwide and becoming pandemic. The virus itself has since evolved, the current WHO recommended vaccine strain originating from the 2009 pandemic being A/Michigan/45/2015 (H1N1) pdm09-like virus. However, this current strain has only 13 amino acid differences in the HA gene with the 2009 strain A/Texas/06/2009, shown in the multiple sequence alignment generated using Clustal Omega (Sievers et al. 2011). See Figure 1.8.

```
CLUSTAL O(1.2.4) multiple sequence alignment

A/Michigan/45/2015(H1N1)      MKAILVVLLYTFTTANADTLCIGYHANNSTDTVDTVLEKNVTVTHSVNLLEDKHNGKLCK
A/Texas/06/2009(H1N1)         MKAILVVLLYTFATANADTLCIGYHANNSTDTVDTVLEKNVTVTHSVNLLEDKHNGKLCK
                              ************:*************************************************

A/Michigan/45/2015(H1N1)      LRGVAPLHLGKCNIAGWILGNPECESLSTASSWSYIVETSNSDNGTCYPGDFINYEELRE
A/Texas/06/2009(H1N1)         LRGVAPLHLGKCNIAGWILGNPECESLSTASSWSYIVETSSSDNGTCYPGDFIDYEELRE
                              ************************************.***********:******

A/Michigan/45/2015(H1N1)      QLSSVSSFERFEIFPKTSSWPNHDSNKGVTAACPHAGAKSFYKNLIWLVKKGNSYPKLNQ
A/Texas/06/2009(H1N1)         QLSSVSSFERFEIFPKTSSWPNHDSNKGVTAACPHAGAKSFYKNLIWLVKKGNSYPKLSK
                              ************************************************************.:

A/Michigan/45/2015(H1N1)      SYINDKGKEVLVLWGIHHPSTTADQQSLYQNADAYVFVGTSRYSKKFKPEIATRPKVRDQ
A/Texas/06/2009(H1N1)         SYINDKGKEVLVLWGIHHPSTSADQQSLYQNADAYVFVGSSRYSKKFKPEIAIRPKVRDQ
                              ********************:****************:*********** *******

A/Michigan/45/2015(H1N1)      EGRMNYYWTLVEPGDKITFEATGNLVVPRYAFTMERNAGSGIIISDTPVHDCNTTCQTPE
A/Texas/06/2009(H1N1)         EGRMNYYWTLVEPGDKITFEATGNLVVPRYAFAMERNAGSGIIISDTPVHDCNTTCQTPK
                              ******************************:************************:

A/Michigan/45/2015(H1N1)      GAINTSLPFQNIHPITIGKCPKYVKSTKLRLATGLRNVPSIQSRGLFGAIAGFIEGGWTG
A/Texas/06/2009(H1N1)         GAINTSLPFQNIHPITIGKCPKYVKSTKLRLATGLRNVPSIQSRGLFGAIAGFIEGGWTG
                              ************************************************************

A/Michigan/45/2015(H1N1)      MVDGWYGYHHQNEQGSGYAADLKSTQNAIDKITNKVNSVIEKMNTQFTAVGKEFNHLEKR
A/Texas/06/2009(H1N1)         MVDGWYGYHHQNEQGSGYAADLKSTQNAIDEITNKVNSVIEKMNTQFTAVGKEFNHLEKR
                              ****************************:***************************

A/Michigan/45/2015(H1N1)      IENLNKKVDDGFLDIWTYNAELLVLLENERTLDYHDSNVKNLYEKVRNQLKNNAKEIGNG
A/Texas/06/2009(H1N1)         IENLNKKVDDGFLDIWTYNAELLVLLENERTLDYHDSNVKNLYEKVRSQLKNNAKEIGNG
                              ********************************************.************

A/Michigan/45/2015(H1N1)      CFEFYHKCDNTCMESVKNGTYDYPKYSEEAKLNREKIDGVKLESTRIYQILAIYSTVASS
A/Texas/06/2009(H1N1)         CFEFYHKCDNTCMESVKNGTYDYPKYSEEAKLNREEIDGVKLESTRIYQILAIYSTVASS
                              ********************************:***********************

A/Michigan/45/2015(H1N1)      LVLVVSLGAISFWMCSNGSLQCRICI
A/Texas/06/2009(H1N1)         LVLVVSLGAISFWMCSNGSLQCRICI
                              *************************
```

Figure 1.8. Multiple HA amino acid sequence alignment between pH1N1 strains A/Texas/06/2009 and A/Michigan/45/2015 13. Amino acid differences are displayed. Amino acid alignment carried out using Clustal Omega (Sievers et al. 2011).

1.12 Innate immunity to Influenza virus

After the influenza virus reaches the respiratory mucosa, it must overcome the protective layer of mucus which lines the respiratory tract. The first defence of the innate immune system, influenza viruses will be caught up in the mucociliary escalator and evacuated into the stomach for disposal. Some viruses will manage to penetrate this layer, avoiding the heavily sialylated mucins present in the mucus through the action of the NA (Cohen et al. 2013; Matrosovich et al. 2004). Once the virus has finally encountered its target cell and initiated an infection, the other aspects of the host cell innate immune system are the next line of defence. Upon initiation of replication, single stranded RNA (ssRNA) and double stranded RNA (dsRNA) will be produced as the virus carries out its life cycle. These will be recognised as pathogen associated molecular patterns (PAMPs), alongside other influenza

life cycle products, by pathogen recognition receptors (PRRs) (Akira et al. 2006; Medzhitov and Janeway 2000; Thompson et al. 2011).

1.12.1 IFN

There are four IFN families of which type I is the most important in regards to the influenza virus, activating key pathways of the innate and adaptive immune system after activation of PRRs (Takeda and Akira 2004). Type I IFN is a multi-gene cytokine family composed of multiple IFN-α subtypes, one IFN-β subtype and several other gene products (Pestka et al. 2004). Type II IFN consists of IFN-λ which is produced by T cells and Natural Killer (NK) cells, acting on cells which contain the IFN-λ receptor (Schoenborn and Wilson 2007). Type III IFN consists of IFN-λ1 IFN-λ2 and IFN-λ3 and IFNλ4 (O'Brien et al. 2014; Prokunina-Olsson et al. 2013). These act in a similar manner to Type I IFN cytokines, but are restricted in activity due to their receptor only being found on epithelial cells surfaces (Witte et al. 2010). Type I IFN are able to induce an antiviral state in infected and bystander cells, interfering with viral replication (Yan and Chen 2012). Almost all cell types are able to produce IFN-α or IFN-β as a result of stimulation of PRRs by PAMPs. A variety of sensors are present in cells for the detection of different PAMPs, recognising ligands or DNA/RNA in different conformations (McNab et al. 2015). Toll like receptor (TLRs) activation also leads to IFN-α/IFN-β production of which the relevant TLRs are described in this section (Leber et al. 2008; Pandey et al. 2009). As well as inducing an antiviral state, IFN also has a direct antiviral action, by increasing the expression of IFITM3, MxA and PKR genes described in subsequent sections, among others such as the Ribonuclease L and ISG15 ubiquitin-like pathways (Julkunen et al. 2000; Anthony J. Sadler and Williams 2008). Type I IFNs are extensively reviewed by McNab et al. 2015, the remainder of this innate immunity subsection will be devoted to the receptors relevant for innate immunity and influenza virus.

1.12.2 TLR7 and TLR8

TLR7 recognises ssRNA influenza genomes within endosomes, resulting in nuclear factor ϰB (NF-ϰB) or interferon regulatory factor 7 (IRF7) activation (Diebold et al. 2004; Lund et al. 2004). These transcription factors stimulate further expression of pro-inflammatory cytokines and type I IFN respectively, blocking viral replication (Honda et al. 2005; Lande et al. 2007; Sasai et al. 2010). TLR8 also recognises ssRNA within endosomes and is involved in

the innate immune response to viruses such as HIV (Heil et al. 2004). It is expressed in human monocytes and macrophages, producing IL-12 upon stimulation by ssRNA (Iwasaki and Pillai 2014).

1.12.3 RIG-I

RIG-I is a protein that is crucial for viral detection as well as the production of type I IFN in infected cells (Kato et al. 2005). It recognises 5' triphosphate viral ssRNA generated after the start of viral replication (Baum et al. 2010; Hornung et al. 2006; Pichlmair et al. 2006; Rehwinkel et al. 2010). RIG-I comes into contact with vRNAs in antiviral stress granules, where it co-localises with viral RNA and interferon stimulated gene (ISG) products such as PKR. Its encounter with vRNA leads to activation of the mitochondrial antiviral signalling protein (MAVS). This results in the production of pro-inflammatory cytokines downstream of NF-$\varkappa$B, and also the production of type I IFNs and ISGs through its activation of IRF3 (West et al. 2011).

1.12.4 ISG

Genes stimulated by IFN which control influenza virus infection include MxA, PKR, IFITM3 (and other IFITM proteins) as well as TRIM22, Viperin and several other genes, reviewed by Iwasaki & Pillai 2014. The Mx proteins were among the first ISGs with anti-influenza roles discovered (Ichinohe et al. 2009). MxA is present in the cytosol, acting against influenza A and other viruses (Hefti et al. 1999; Pavlovic et al. 1995; Turan et al. 2004). It prevents post-transcriptional events in the cytoplasm as well as interacting with NP and the influenza polymerase (Haller et al. 2009; Pavlovic et al. 1992).

IFITM3 acts to block virus-host cell membrane fusion following endocytosis in the first stage of infection. It is expressed constitutively in epithelial and endothelial cells as well as in macrophages (Brass et al. 2009; Desai et al. 2014).

The protein kinase PKR blocks translation of influenza genes through its action in phosphorylating the α subunit of eukaryotic initiation factor 2 α (EIF2α). It also activates the NF-$\varkappa$B pathway and stabilises IFN-α and IFN-β mRNAs (Balachandran et al. 2000; Kumar et al. 1994; A J Sadler and Williams 2007).

The tripartite motif 22 (TRIM22) is located in the nucleus and its mRNA and protein levels are highly unregulated upon influenza virus infection in epithelial cells. It interacts with

influenza NP and this results in NP polyubiquitination and degradation through the proteasome pathway (Di Pietro et al. 2013).

1.13 Cell based immunity

Innate cell based immunity comes in the form of alveolar macrophages, monocytes, neutrophils, and NK cells. Alveolar macrophages secrete chemokines and cytokines in order to recruit further innate cells, as well as initiating an adaptive immune response (Tripathi et al. 2015). These, together with monocytes and neutrophils are recruited to the site of influenza infection and, with macrophages, aid in the clearance of virus-infected cells by recruited phagocytes (Y. Hashimoto et al. 2007). Neutrophils have been shown to produce reactive oxygen species which are responsible for part of the pathology associated with influenza virus infection, through tissue damage (Tripathi et al. 2015). Efforts have been made to reduce this damage, such as investigation of the compound apocynin, which acts to inhibit the NADPH oxidase system involved in neutrophil mediated tissue damage (Vlahos et al. 2011). NK cells act to destroy infected cells alongside the activation of cytotoxic T lymophocytes. They also regulate the production of IFN-λ and interleukin-2 (IL-2). The presence of pre-existing influenza virus specific T cells has been shown to increase NK-mediated innate immunity (He et al. 2004).

1.14 Adaptive immunity

Adaptive immunity is instigated by antigen presenting cells (APC), in particular dendritic cells (DC) which stimulate T cells. DCs encounter viral antigens either through phagocytosis of infected cells, or by being infected. Subsequently, DCs will present viral antigens/peptides on the major histocompatability complexes I or II (MHC I and II) and migrate to the lymph nodes, allowing interaction with CD4+, CD8+ T lymphocytes as well as B lymphocytes (Mildner and Jung 2014). The peptide-MHC complexes will be presented to T cells via the T cell receptor (TCR), mediating their activation.

CD4+ T cells induce the proliferation of CD8+ T cells and B cells, the effectors of the adaptive immune system (Sant et al. 2007). Once activated in the lymphatic system by APC antigen presentation, CD4+ T cells contribute to viral clearance through induction of IFN pathways, described in section 1.12. CD4+ cells can differentiate into two different functional classes of

helper T cells (T_H1, T_H2). T_H1 cells secrete IFN- λ while T_H2 secrete interleukin 4 (IL-4) which is critical for the initiation of humoural immunity (Smiley and Grusby 1998).

CD8+ T cells are activated upon presentation of viral antigens in complex with MHC I, allowing their migration to the site of infection (Cerwenka et al. 1999). Memory CD8+ T cells present in the lymphatic system from a previous exposure to influenza virus will be re-activated, allowing a more rapid protective response to a previously encountered, antigenically similar virus (Tamura and Kurata 2004). These antigen-experienced CD8+ T cells have been shown to immediately degranulate upon recognition of an influenza infected cell, killing them, whereas naive cells have a cytotoxic effect without immediate degranulation (Wolint et al. 2004).

Upon activation, B lymphocytes differentiate into plasma cells and begin to produce antigen specific immunoglobulin (Ig, antibodies). Depending on the epitope or specific protein to which an antibody has been produced, these will either neutralise the action of said protein or act as a primer for the induction of cell-directed immunity, for example through Fc mediated activation leading to ADCC (Zhong et al. 2016). Alternatively, complement mediated cytotoxicity can be induced (Quinnan et al. 1980).

The humoral immune response at the level of the mucosa involves IgA, which is produced locally and transported to the upper respiratory tract via the mucosal epithelium (Palladino et al. 1995; Renegar et al. 2004).The lower respiratory tract is where IgG is primarily found, this class of Ig has been found to diffuse into the blood where it can be collected and analysed as serum. As mentioned previously, the outcome of the production of antibodies is dependent on the epitope and protein presented to B cells.

Antibodies directed against the HA glycoprotein either act to neutralise the virus through masking its RBS, or by preventing its ability to unfold and mediate membrane fusion (Brandenburg et al. 2013). Anti HA antibodies are further detailed in section 1.18 with multiple examples.

Antibodies against the NA have been shown to block viral replication through the inhibition of viral release at the cell surface. Anti NA antibodies therefore have a similar mechanism of action to NA antivirals which do not prevent infection but limit symptoms and further transmission of the virus (Marcelin et al. 2011, 2012; Wohlbold and Krammer 2014).

Antibodies against the M2 channel have been associated with poor protection against infection, but represent a promising target due to the conserved nature of this protein in comparison to other humoral immune targets (B. Nayak et al. 2010; Schotsaert et al. 2009; Treanor et al. 1990).

Anti NP antibodies have been shown to aid cellular immunity against influenza (Carragher et al. 2008). This conserved protein has been targeted alongside other influenza proteins that are conserved between strains, with safety and T cell mediated immunogenicity reported in an NP + M1 MVA vaccine produced and tested in phase I clinical trials by Berthoud et al. 2011.

Due to the virus' ability to drift and shift, evading humoral immune responses, efforts have been made to study the effect of immunological memory against the influenza virus. The Memory B cell populations plays an essential role in prevention of re-infection against similar strains (Ellebedy and Ahmed 2012; K.-Y. Y. A. Huang et al. 2014; Quan et al. 2007).However this immunological memory puts the viral proteins under pressure, driving mutational selection on a global scale and rendering efforts to produce effective vaccines fruitless. A further aspect to consider is the phenomenon of original antigenic sin, in which exposure to an antigen leads to the generation of a sub optimal immune response to a related antigen, such as a from a previously encountered influenza strain (de St.Groth and Webster 1966a, 1966b; Francis 1960; Pan 2011). Due to the worldwide circulation of multiple subtypes and strains of influenza, characterisation of the effects of original antigenic sin on immunity, whether natural or induced by vaccination, is crucial to the future of influenza virus research.

1.15 Influenza virus vaccines and antivirals

Influenza vaccines are available in many forms. Inactivated influenza virus vaccines have been produced in trivalent (TIV) or quadrivalent forms (QIV). In general the TIV will contain one strain from seasonal H1N1 and H3N2 viruses as well as the predicted dominant influenza B lineage strain, whether Yamagata or Victoria. The QIV will generally contain a representative from both influenza B lineages. Alternative vaccines include live attenuated influenza vaccines (LAIV), available commercially as FluMist or Fluenz, consisting of a live and functional influenza virus, attenuated for virulence, often through cold-adaptation (Glezen 2004). Protein based vaccines are produced by recombinant technology – production of HA immunogens or truncated versions of HA, often in bacteria. Finally, reverse genetics based systems utilise cells to grow viruses with desired characteristics (Neumann et al. 2012).

There are various antivirals available against the influenza virus, intercepting the virus in its life cycle at various points. NA inhibitors such as oseltamivir and zanamivir prevent the action of the NA enzyme, reducing the ability of nascent viruses to escape infected cells and thereby slowing down infection and associated symptoms. These are extensively reviewed by De Clercq, 2004 and Moscona, 2005. However, there are NA-inhibitor resistant strains of Influenza circulating, with amino acid changes such as E119V or R292K in the NA gene resulting in decreased sensitivity to the inhibitor. However, some ferret model studies show the drug is still working as intended by reducing spread between ferrets (Herlocher et al. 2002, 2004; Yen et al. 2005). M2 inhibitors are also available, such as amantadine, rimantadine and adamantanamine, which share common features. These block the M2 protein, preventing its action in acidification of the viral core, preventing dissociation and release of vRNPs (Shuck et al. 2000). Various other antivirals are in the process of being characterised and are reviewed by De Clercq, 2006. While this field is currently neglected, research continues to produce novel M2 inhibitor candidates as well as working efforts to overcome resistance mutations in circulating strains of influenza viruses (F. Li et al. 2016; Sulli et al. 2013).

1.16 Universal vaccines and Heterosubtypic immunity: HA

Universal vaccines aim to induce long lasting immunity, generally by eliciting antibodies against conserved regions of the influenza virus. These regions include the HA stalk region in

order to create pan-subtype or pan-group/multi-lineage vaccines, or conserved epitopes between seasonal strains to produce multi-seasonal vaccines (Graham, WHO report). Due to the constraints involved with the active machinery of the HA glycoprotein and its requirement to change conformation to allow membrane fusion, this target is less amenable to antigenic drift and therefore likely less able to evolve around a targeted stalk immune response. However, it is possible that the immunodominance of the head region drives its evolution, and that conservation seen in the stalk is a result of the it's reduced immunogenicity.

Various methods have been employed in order to design and test universal vaccines. One of the most exciting developments in the universal vaccine section of influenza virus research is the progress being made on utilisation of chimeric HA (cHA) based vaccines, reviewed by Kramer and Palese over recent years (Krammer 2016; Krammer and Palese 2013, 2014, 2015). These vaccines employ cHA, originally developed and published by Hai and colleagues (Hai et al. 2012; Krammer et al. 2013) and developed by this group since 2012 in various articles showing this approach's ability to induce broadly neutralising antibodies in mouse models. Cryo EM tomography on these cHAs has shown them to be structurally different to native HAs, with a 60° rotation between stalk and head regions. This leads to a more 'open' arrangement allowing access to the stalk region. Despite these differences, the cHA is still functional and viruses bearing it has been shown to be infectious in the reverse genetics system (Tran et al. 2016). Early work aimed to characterise and build cHAs and utilise them as a serological platform through the production of PV (Hai et al. 2012). This was followed by a study utilising H6/H1 and H9/H1 cHAs to test for bnAbs in serum from H5N1 vaccine clinical trials (Nachbagauer et al. 2014). The H5N1 vaccine elicited bnAbs which were effective in a mouse passive transfer model. A similar approach to the cHA system was evaluated by Eggink et al., 2014, utilising hyperglycosylation as a tool to shield epitopes in the HA head, dampening the immune response elicited against the immunodominant head and redirecting immunity to the stalk region. Mice vaccinated with hyperglycosylated HA vaccines were better protected against mortality and morbidity than those vaccinated with the wild type (WT) HA. This data lends credence to the 'universal vaccine' idea, building up evidence that stalk directed immune responses are to be aimed for. cHAs were further evaluated to be used as vaccines in a system employing head regions from multiple subtypes and stalks from the same H1 subtype, aimed at 'redirecting' the

immune system to the stalk. A panel of influenza viruses were produced bearing cHAs with intra or intergroup head/stalk combinations and examined for growth kinetics and the preservation of epitopes. cHAs were shown to behave in a similar fashion to WT HAs, maintaining stalk epitopes (C.-J. Chen et al. 2016). A vaccine regimen was designed by Nachbagauer et al. whereupon a three stage vaccine regimen using H1N1 followed by cHAs with H5 and then H8 head domains and the same H1N1 stalk. The vaccine regimen induced higher stalk neutralising antibody titres than the seasonal vaccine, with long lasting cross-reactivity observed alongside protection *in vivo* (Nachbagauer, Kinzler, et al. 2016). Similarly, a more recent study achieved the same results, this time using cHAs with influenza A head domains (H5/H7/H8) and an influenza B stalk, mice were protected from lethal challenge post vaccination to a diverse set of influenza B strains (Ermler et al. 2017). The cHA system has also been employed as a vaccine through the use of VSV vectors, administered via intramuscular and intranasal routes – inducing protective heterosubtypic immunity in mice (Ryder et al. 2016).

A different approach has focused on the development of 'headless' HA constructs as protein vaccines allowing the host to produce an immune response against the conserved stalk region in the absence of the immunodominant globular head. This approach has been followed by several research groups with varying levels of success (Mallajosyula et al. 2014; Steel et al. 2010; Valkenburg et al. 2016). Headless HAs, otherwise known as stem constructs or mini HAs were born from early work describing the ability to remove the HA1 region of the influenza HA through acid treatment (Graves et al. 1983). The ability to remove the head of the HA trimer allowed access to the stalk and when used as an immunogen, generating cross-reactive antibodies. Steel et al. produced a headless HA construct and used it to immunize mice, eliciting immunity with broader reactivity than the full length HA tested. They also showed full protection from mortality, and partial protection from morbidity in a lethal challenge experiment (Steel et al. 2010). H1 stem headless HAs designed by the Crucell Vaccine Institute showed structural and bnAb binding properties similar to the full length HA tested (Impagliazzo et al. 2015). This construct was used to vaccinate mice, inducing complete protection in a lethal challenge experiment using heterologous and heterosubtypic strains. This immunogen was also shown to reduce morbidity after sublethal challenge in a primate model. A further headless HA immunogen designed at the National Institutes of Health (NIH) conferred heterosubtypic protection in

mice and ferrets. This design employed a stabilised H1 stem with conserved epitopes, also conferring protection through serum transfer in mice (Yassine et al. 2015). Similarly to previously cited examples, broadly neutralising, yet group 1 specific antibodies were generated by an H5 headless HA generated by Valkenburg et al. Once again, passive transfer of serum protected mice tested from influenza challenge (Valkenburg et al. 2016)

1.17 Other universal vaccines

Influenza vaccine research groups or projects have had success in the elicitation or detection of heterosubtypic immunity to influenza. While seasonal vaccination has been shown to primarily induce head directed antibody responses, some level of heterosubtypic immunity has also been shown (Ding et al. 2011). It is important to note differences between age groups infected with influenza viruses and the immune complement depending on previous exposure history. The elderly are known to have higher stalk directed antibodies due to sequential exposure to strains over the years, as opposed to the young who may have a more head-dominated response. This data was further validated by a recent study (Nachbagauer, Choi, et al. 2016). Sequential sH1N1 vaccination has also been shown to induce heterosubtypic immunity, in a similar fashion to the cHA system utilising divergent HA heads. Kirchenbaum et al showed that sequential vaccination of ferrets with sH1N1 lead to protection from pH1N1 challenge and resulted in poor transmission between ferrets (Kirchenbaum et al. 2015). In 2010, heterosubtypic immunity was elicited through a bivalent H1/H3 vaccine, allowing recipients to produce a bnAb which was able to neutralise an H5 strain (Corti et al. 2010). This group isolated 20 heterosubtypic mAbs which were able to bind group 1 influenza viruses, including the recent pH1N1 strain. bnAbs were found to bind the acid sensitive epitopes in the stalk. Attempts at using exotic H5N1 strains as vaccine candidates has also given rise to heterosubtypic antibodies, for example in the use of a H5N1 DNA vaccine candidate followed by an inactivated vaccine (Joyce et al. 2016). A different approach utilising an MVA delivered recombinant vaccine using a mosaic H5N1 was also successful in generating protection to the matched H5N1 subtype as well as H1N1 (Kamlangdee et al. 2016).

Several recent articles have recently shown that natural infection by G2 subtypes H3 or H7 lead to increases in heterosubtypic antibodies in patients. H3N2 infection was reported to elicit more cross-reactive antibodies than through inactivated virus or HA DNA vaccination

(Margine et al. 2013; Moody et al. 2011). Similarly, natural infection to H7N9 influenza virus has been reported to induce both G1 and G2 specific bnAbs (L. Liu et al. 2017).

Attempts to induce antibodies against the conserved M2 protein ectodomain (M2e) are ongoing, with vaccines in clinical development (Ramos et al. 2015). While the M2 protein is poorly immunogenic, being shielded by HA and NA glycoproteins on the surface of the influenza virion, this protein is present in higher numbers on infected cells and may induce immune responses in the form of ADCC (Nachbagauer and Krammer 2017; Schotsaert et al. 2009). Vaccines against the M1 and NP proteins are also aimed at eliciting heterosubtypic immunity due to their conserved nature between strains. While these proteins are usually shielded from antibodies, they can provide protective immunity in the form of T-cell epitopes (M. Zheng et al. 2014). Vaccination with NA or NA + M2e VLPs from 2009pdm influenza protected mice from subsequent challenge by H3N2 influenza through CD8+ reactive T cell responses, while this was not observed in HA vaccinated mice (Schotsaert et al. 2016). Part of the effectiveness of whole virus vaccines can be attributed to NA targeting antibodies, which have been shown to also contribute to heterosubtypic immunity (Eichelberger and Wan 2014; W.-C. Liu et al. 2015). Various universal vaccines are discussed by Nachbagauer & Krammer 2017 with clinical trial information reported. Figure 1.9 shows a variety of universal vaccine approaches.

1.18 Stalk antibodies

Much of the work in identification of influenza HA epitopes has been carried out using mAbs and associated crystal structures of mAbs bound to their epitopes, via x-ray crystallography. This section will describe some of the main stalk-directed mAbs discovered over recent years. CR9114 was produced by the Crucell Vaccine Institute (now Janssen Pharmaceutical Companies of Johnson and Johnson), binding at the HA stem and was shown to protect mice from lethal challenge with Influenza A and B strains (Dreyfus et al. 2013). This mAb competed with CR6261 which binds to the membrane proximal stem of HA – both of these antibodies therefore act on HA by preventing conformational changes required for the fusion process (Ekiert et al. 2009). The F16 mAb was characterised in 2011 by Corti et al., 2011, binding to the F sub domain of the fusion peptide of influenza HA, neutralising all 16 subtypes of influenza A tested. Another important mAb of note is C179, generated after mice were immunized with A/Okuda/1957 (H2N2) by a group in Japan. This mAb recognises

group 1 influenza viruses, binding two monomers of the HA trimer in the stalk region (Okuno et al. 1993). Finally, yet another stalk binding mAb was characterised, F10. This mAb binds to hydrophobic 'pockets' within the HA stalk, near the fusion peptide. This mAb was shown to neutralise a broad range of group 1 influenza viruses (Jianhua Sui et al. 2009). Interestingly, part of the immunity provided by stalk directed mAbs has been associated with protection through promotion of ADCC through the Fc portion of the bnAb. One study managed to enhance Fc engagement, leading to increased cytotoxicity (DiLillo et al. 2014). Alternative approaches have employed nanobodies – derived from camelids (reviewed by Muyldermans, 2013) – in a similar fashion to mAbs. Nanobodies which bind to HA stalk regions in overlapping epitopes with CR6261 and F10 (fusion peptide) have been characterised and employed successfully in binding and neutralisation assays (Gaiotto and Hufton 2016).

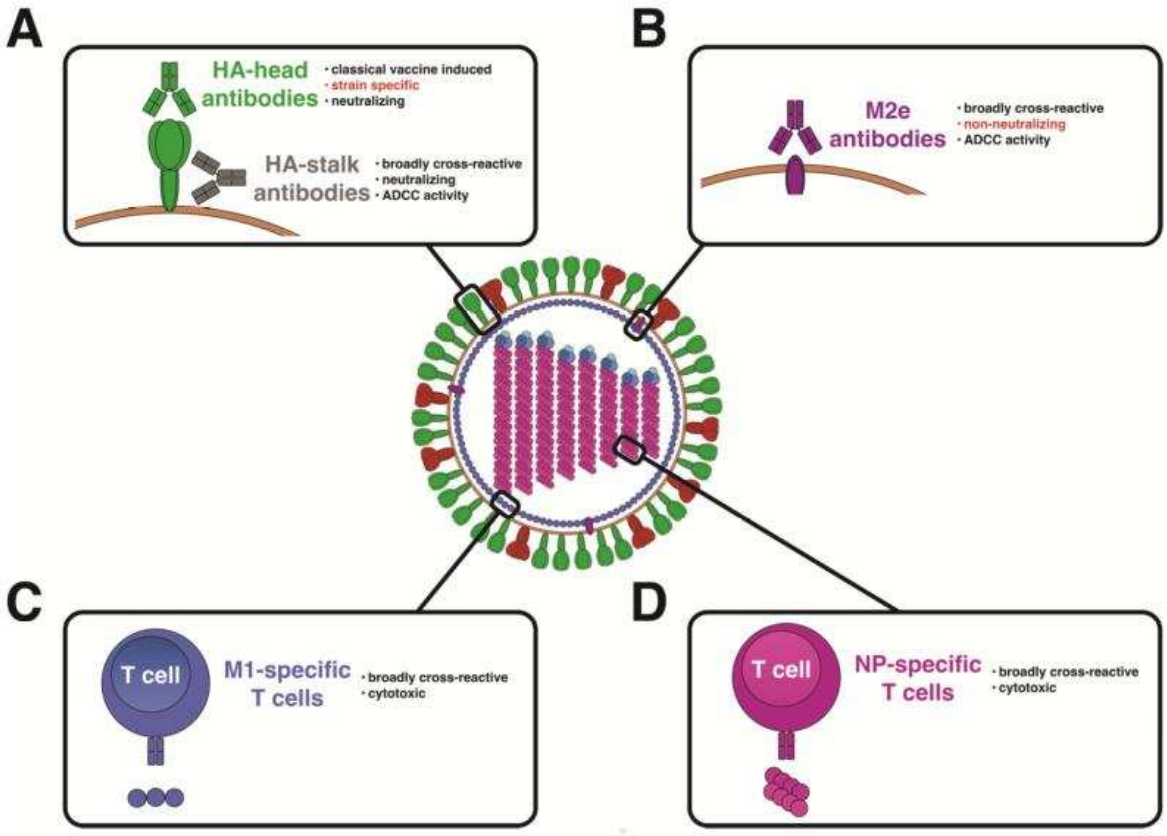

Figure 1.9. Various universal vaccine approaches to the influenza virus. A) Vaccines targeting the HA head are strain specific and neutralising while those targeting the stalk are cross-reactive as well as inducing ADCC based immunity. B) M2 ion channel vaccines targeting the M2 ectodomain are non-neutralising but may induce ADCC. B-D) M2e, M1 and NP vaccine approaches confer broadly cross-reactive immunity due to the conserved nature of these proteins. Figure from (Nachbagauer and Krammer 2017).

1.19 Serology

1.19.1 Basic introduction

Serology takes the form of many different assays when dealing with influenza virus immunity. The primary protein to which antibodies are generated (HA) is used in the majority of assays aimed at detecting immune responses to the virus. Serological experiments for influenza have been reviewed in depth by Trombetta et al., 2014. The HI assay was designed based on the ability of influenza viruses to agglutinate erythrocytes (red blood cells, RBC) through action of its RBS, forming a lattice of RBCs in lieu of a pellet when added to a V-bottom micro titre well. Addition of a known number of HI 'units' to a 96-well micro titre plate with serial dilutions of serum allowed measurement of neutralising antibody titres to different strains of influenza virus. This assay is still widely used to measure immunogenicity of vaccines and immunity after natural infection; however several caveats have arisen since its inception. An HI titre above 40 has been shown to be a good correlate of protection in adults, but not children, the latter of which have a reduced capacity to mount an immune response leading to elicitation of HI competent antibodies (de Jong et al. 2003; Hobson et al. 1972). Currently there is an issue with the type of red blood cell used; with viruses derived from different hosts giving dissimilar results based on the strain in particular's avidity for the various sialic acid moieties on RBCs. As well as this, certain human seasonal strains within the H3N2 subtype have changed their avidity to RBC receptors over the years. For example, H3N2 strains have lost the ability to bind to chicken RBCs used in the 1990s, but since 2003 have regained the ability to bind them (Gulati et al. 2013; Kumari et al. 2007; Yi Pu Lin et al. 2012; Medeiros et al. 2001; Nobusawa et al. 2000). Research suggests amino acid changes in residues 190 and 226 in the HA trimer RBS was involved in the reduction of HI ability of these viruses (Medeiros et al. 2001; Nobusawa et al. 2000). Various groups have also shown that alongside a reduction in binding affinity of the H3 HA over recent years, the NA has compensated and become involved in the infection process by reduced ability to cleave sialic acids and subsequent change in the balance between receptor destroying and receptor binding properties of NA or HA (Y. P. Lin et al. 2010). The balance between HA and NA binding and affinities has further reaching implications, anti NA antivirals are now required to test for HA antigenicity using the HI

assay, in order to prevent false positives arising from NA mediated haemagglutination (Y. P. Lin et al. 2010).

Viral neutralisation or microneutralisation (MN) enables a direct observed response against the cytopathic effect (CPE) of the influenza virus tested (44). Neutralisation is observed by all antibodies which block viral entry and therefore will include stalk as well as head directed antibodies. For this reason this assay is an excellent tool for the detection of antibodies. However, due to the requirement for live virus, this experiment must be carried out under higher BSL conditions when using highly pathogenic or hazardous strains of influenza, reducing the ease at which data can be generated. Furthermore, viruses must be grown for this experiment and therefore must be amenable to growth in eggs or cell based systems. A recent study was carried out in order to compare MN protocols and resulted in a large scale study (Laurie et al. 2015). Single Radial Haemolysis was developed in 1975, utilising antibody diffusion within an agar gel and complement mediated haemolysis induced by antibody-antigen complexes (Schild et al. 1975). This forms zones of haemolysis that can be measured and thus compared between sera (Morley et al. 1995; Schild et al. 1975; Vaerman, J 1981). The Enzyme-linked lectin assay (ELLA) is an ELISA based assay aimed at detecting NA activity through NA-mediated digestion of Foetal bovine serum (FBS) derived Fetuin, which is pre-coated on compatible microtitre plates. This assay is the focus of Chapter 5 where it is described in further detail. ELISA based approaches are used regularly in influenza virus research. Microneutralisation ELISA combines the elements of viral neutralisation and ELISA detection, by detecting NP produced after viral infection, which can be knocked down using serum (de Boer et al. 1990; Rowe et al. 1999; WHO 2011). Other uses of ELISA include using HA or inactivated virus to coat wells as capture antigens for antibodies, with subsequent ELISA colorimetric readout. The ADCC assay measures the effect of the antibody region FcR role in cellular cytotoxicity through its relationship with NK cells. In this way, antibodies which do not neutralise influenza in the traditional assays can be assayed for an *in vivo* role in protection through ADCC (Greenberg et al. 1978; G. Hashimoto et al. 1983a, 1983b; Jegaskanda et al. 2014; Vella et al. 1980; Zhong et al. 2016). See Figure 1.10 for a life cycle diagram of the influenza virus alongside each point in which antibodies can neutralise the virus.

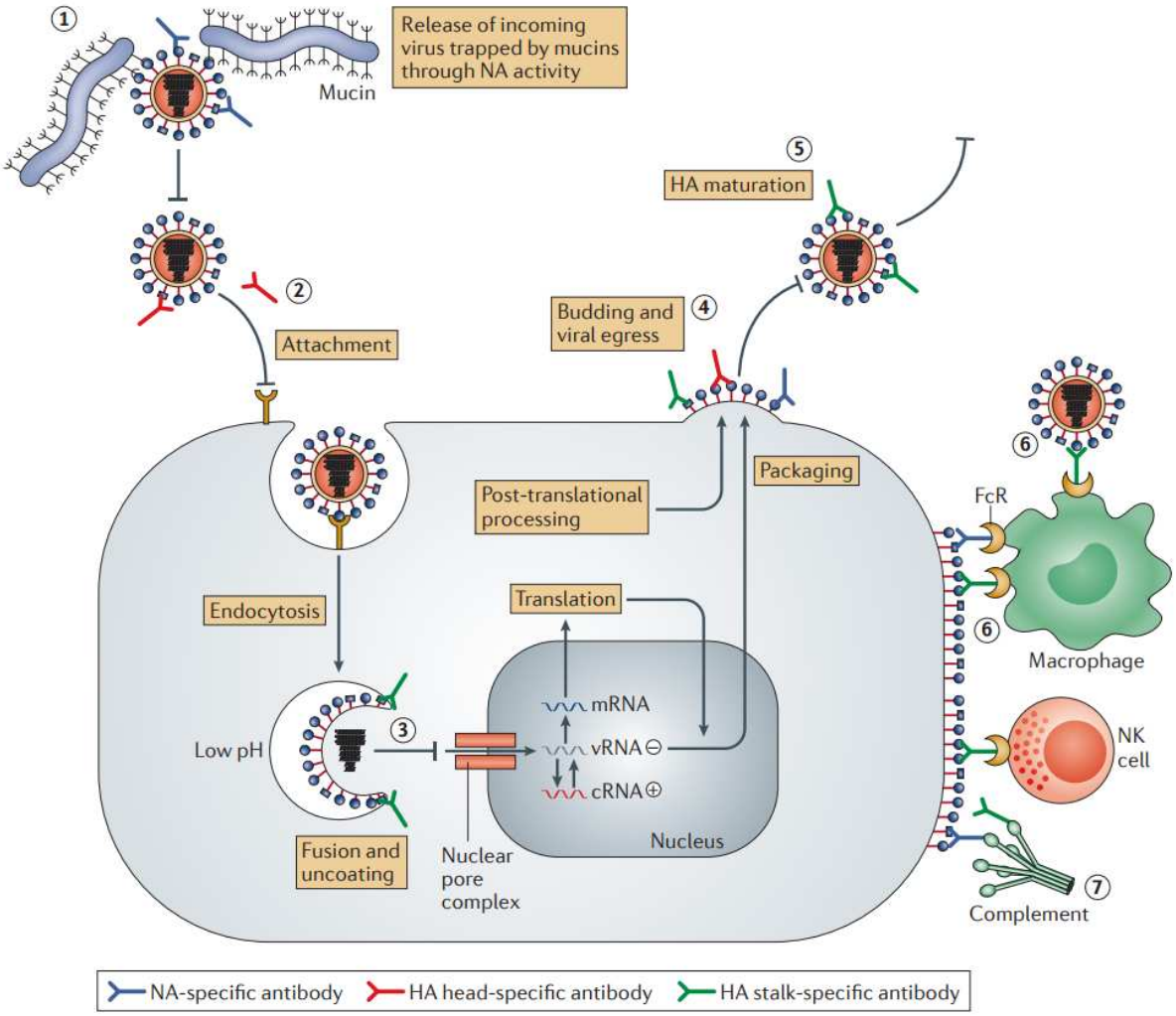

Figure 1.10. Simplified life-cycle diagram for the influenza virus with methods of neutralisation highlighted by bound antibodies. 1) NA targeting antibodies can prevent release of incoming or outgoing influenza viruses from mucins. 2) HA mediated binding of influenza viruses to target cells can be prevented by HA targeting antibodies. 3) HA fusion with endosomal membranes can be prevented by HA stalk targeting antibodies. 4) Nascent influenza viruses can be neutralised during egress from the cell. 5) Maturation of HA through proteolytic cleavage can be prevented by HA stalk bound antibodies. 6-7) Influenza directed antibodies can prime ADCC through FcR interactions as well as NK cells and complement cascade. Figure from (Krammer and Palese 2015)

1.20 CONSISE

The consortium for the standardization of influenza seroepidemiology (CONSISE) is a group of laboratories with the goal of standardising serological techniques in order to inform public health and improve the consistency of intra and inter laboratory data. The CONSISE group will be mentioned in chapter 5 where ELLA was attempted with PV in accordance to CONSISE approved protocols.

1.21 Introduction to influenza virus and pseudotypes

In this section, the methods used for the production and use of PV will be described in the context of the current published literature utilising them, detailed in (Carnell et al. 2015).

1.21.1 Influenza pseudotypes

PV are chimeric 'viruses' consisting of a surrogate virus core surrounded by a lipid envelope with the surface glycoproteins of another virus, such as HA. By removing the genetic element of the virus being studied and replacing it with a suitable reporter, these viruses can be studied in this safer, single cycle system. The comparative safety of PV circumvents the need for restrictive, expensive and widely unavailable BSL facilities, increasing access to research groups interested in highly pathogenic or hazardous viruses.

PV are defined as a replication deficient viruses containing a viral core from one species and bearing glycoproteins from another that are not represented in the genome, in respect to this thesis.

1.21.2 Cores and reporters

The core and its associated genome containing a reporter are the backbone of the PV system which can be used to study the properties of selected entry glycoproteins. The use of cores from lentiviral Human Immunodeficiency Virus 1 (HIV-1) and gammaretroviruses such as Murine Leukemia virus (MLV) predominate in the influenza pseudotype literature. Recent use of systems involving rhabdoviruses, in particular the vesicular stomatitis virus (VSV) has also been used to produce pseudotype cores with promising results (Cheresiz et al. 2014).

1.21.3 Retroviral cores and vectors

Retroviral (including lentiviral) vectors are complex systems which will be explained in simple terms specific to the production and use of pseudotypes. Core and vector systems have been reviewed in great detail (Blesch 2004; Sakuma et al. 2012). The primary genes provided by retroviral or lentiviral systems are *gag* and *pol*. In the case of HIV, *gag* provides the structural proteins p18, p24 and p15, whereas *pol* provides the integrase and reverse transcriptase enzymes in conjunction with the p10 protease required for maturation of each distinct protein from their respective polypeptide chain (Engelman and Cherepanov 2012; Jacks et al. 1988). Reporter constructs are associated with their respective cores based on the packaging signal element (Psi, Ψ) incorporated in the vector design process, making them specific to the surrogate species used. HIV-1 cores are derived from several different origins between laboratory groups. First generation pNL4-3 vectors are well represented in the literature, the pNL4-3-Luc.E-R- variant is the most commonly used (Stephanie Bertram et al. 2012; M. W. Chen et al. 2008, 2011; Labrosse et al. 2010; Pappas et al. 2014; Zmora et al. 2014). This replication deficient proviral HIV-1 clone is derived from the pNL precursor but has inhibitory frame shifts in the *env* and *vpr* genes as well as a luciferase reporter gene cloned into the *nef* gene, the entire construct is incorporated into progeny pseudotypes. Its life cycle mimics that of HIV-1, using the Ψ element to allow encapsidation of the 'genome' into nascent PV and Long Terminal Repeat (LTR) regions (consisting of 3' and 5' untranslated regions U3/U5 and transcription regulatory region R) bearing the U3 promoter, which with the aid of *tat,* permit the expression of the viral proteins after integration into the host genome. The rev responsive element (RRE) allows nuclear export of viral mRNA, including the reporter gene transcript which is the measure of output for this system. Due to the incorporation of the HIV core genes into the same integrated construct as the reporter, transduced cells may possibly produce luciferase containing cores alongside its transcribed enzyme which could potentially interfere with luciferase activity output. Another commonly used HIV-1 core vector is pCMV ΔR8.2, a relation of pCMV ΔR8.9 which still contains intact *vif, vpr, vpu* and *nef* genes (Ding et al. 2011; Hashem et al. 2010; Wei Wang et al. 2008; S. Zhang et al. 2008; F. Zhou et al. 2012; Zufferey et al. 1997).

A further approach uses the second generation HIV vector p8.91 that originates from pCMV ΔR8.9 and ΔR9 (Naldini et al. 1996; Zufferey et al. 1997) which is the vector used in the

projects reported in this thesis. The p8.91 vector is a modified HIV-1 clone, lacking the Ψ sequence as well as the *env, vif, nef, vpu* and *vpr* genes and is widely used in the published literature (Ahmed et al. 2015; Smith et al. 2013; Molesti et al. 2014; Benfield et al. 2015). The human cytomegalovirus (hCMV) promoter is used in lieu of LTR based promotion, meaning that p8.91 provides the necessary genes for the production of the core but the proviral and packaging elements (LTRs, RRE, Ψ) are transferred to a separate plasmid bearing the reporter gene. Thus the reporter construct will be incorporated into nascent PV and integrated into the transduced cell's genome, whereupon the LTRs and RRE will act to enhance expression. In the case of the commonly used firefly luciferase or green fluorescent protein (GFP) containing plasmids pCSFLW or pCSGW, a safety component is incorporated through a deletion in the 3' LTR (U3 promoter region), creating so called self-inactivating (SIN) vectors (E. Wright et al. 2010; Zufferey et al. 1998). Third generation vectors have also been used, in this instance HIV-1 structural and accessory genes are separated from *rev,* which is provided *in cis* on an additional plasmid. The third generation Invitrogen ViraPower Lentiviral Expression System has been used in published research articles, using the plasmids pLP1 and pLP2 (Sawoo et al., 2014; McKay et al., 2006; Finer et al., 1994; Farrell et al., 2002).

MLV cores are less widely used but provide similar *gag* and *pol* elements to HIV-1 vectors (Hatziioannou et al. 1999; Haynes et al. 2009; I. C. Huang et al. 2011; Oh et al. 2009; Tao et al. 2013; Wallerstrom et al. 2014; S.-Y. Wang et al. 2009). One available MLV core used consists of *gag* and *pol* under the effect of a CMV promoter (Bock et al. 2000; Soneoka et al. 1995; Towers et al. 2000). In this instance the vector originates from MLV expression vectors pCI G3 N, B or NB which are differentially restricted in certain murine cells based on the mouse resistant gene alleles $Fv1^N$ and $Fv1^B$ (Hartley et al. 1970). The reporters used in this system are derived from CLONTECH vectors LNCX and pIRES2-EGFP (Bock et al. 2000; Towers et al. 2000). Another described MLV plasmid, pkatgagpolATG originates from ecotropic Moloney MLV and strain 4070A (Wei Wang et al. 2008). Minor differences have been observed when pseudotyping HIV or MLV cores with influenza glycoproteins (Temperton et al. 2007). Therefore the question of which core to use to produce pseudotypes is often down to choice, preference and availability (Garcia and Lai 2011). See Figures 1.11-1.14 for schematic diagrams of the types of PV cores, as well as HIV-1 and MLV packaging constructs and reporters compared to retroviral proviruses.

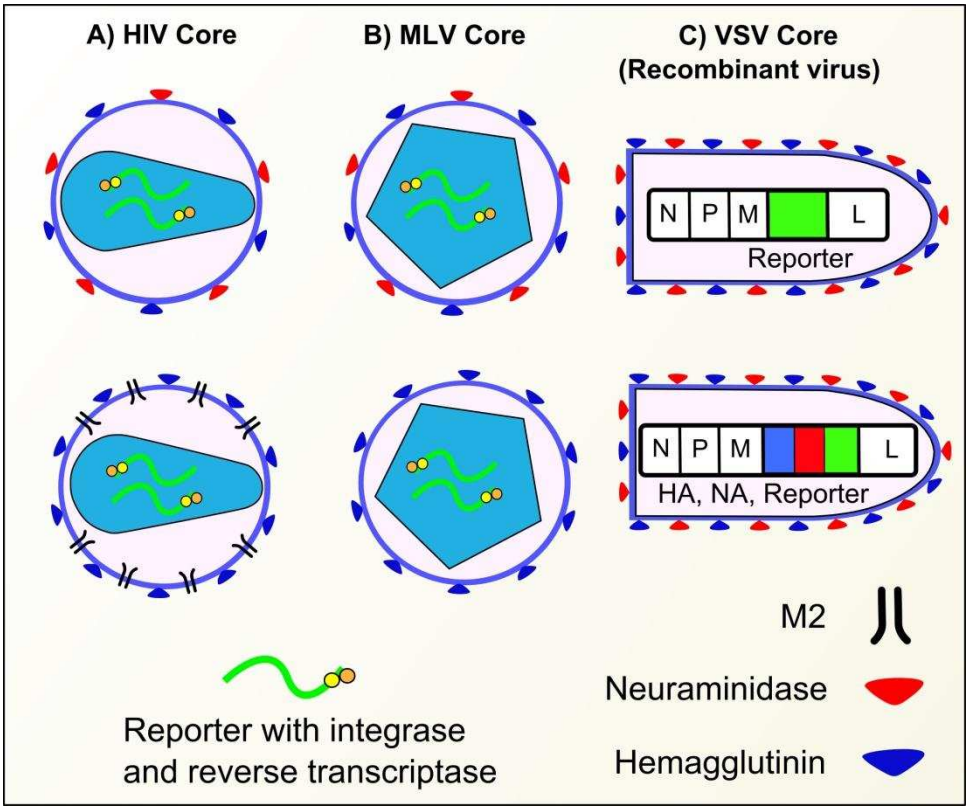

Figure 1.11. Schematic representation of different PV cores.. Components of influenza pseudotypes can be varied according to need. Pseudotypes have been produced with HA, NA, and M2 influenza envelope proteins, with a range of core packaging constructs (HIV, MLV, VSV shown) as well as different reporters. Figure from (Carnell et al. 2015).

1.21.4 VSV PV

Recombinant VSV viruses are produced expressing GFP in lieu of the resident VSV envelope glycoprotein (VSV-G). In certain cases, HA and NA or simply HA are also added to the VSV genome. These additions produce a replication-competent virus which will promote GFP production in infected cells (Zimmer et al. 2014). As these recombinant viruses are not limited to a single cycle of replication, they lack the safety element found within other pseudotypes. A safer VSV based alternative involves transfection of surface protein encoding plasmids (HA/NA) into cells and subsequent infection with a recombinant VSV. In this way one can produce VSV pseudotyped with influenza surface proteins which lack entry-glycoproteins in its resident genome, rendering the second generation of virus infection incompetent (Cheresiz et al. 2014).

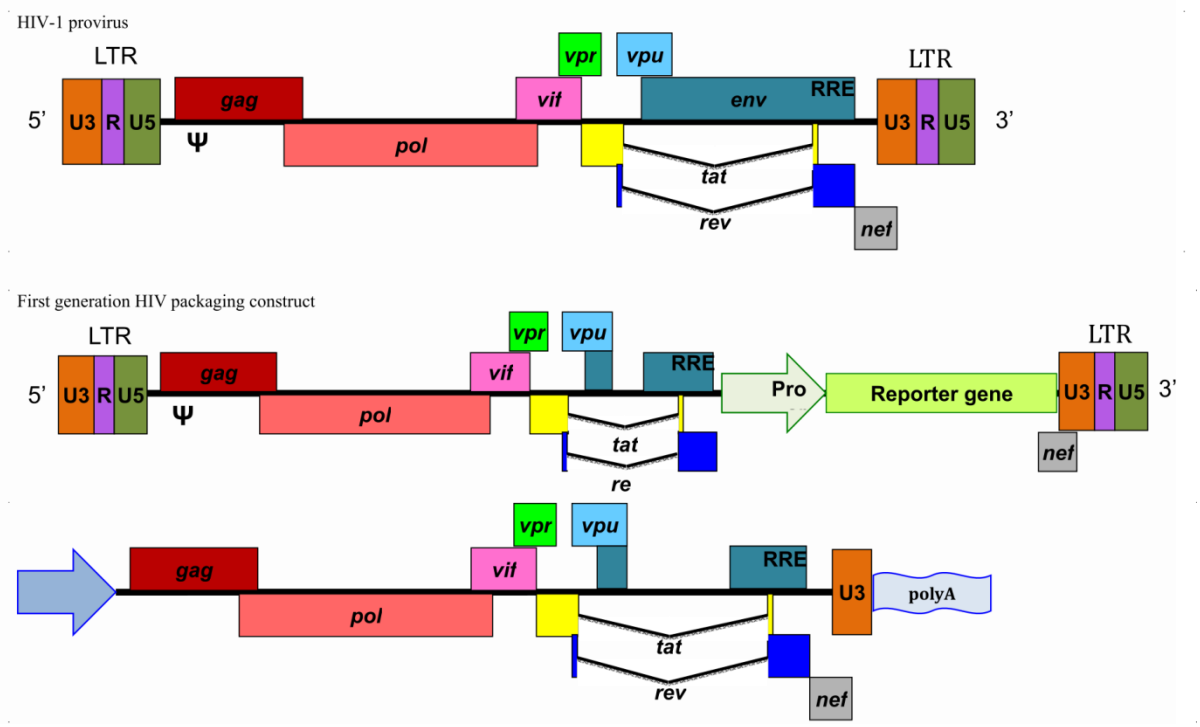

Figure 1.12. Schematic diagram comparing the HIV-1 provirus with first generation HIV-1 packaging constructs. First generation packaging constructs are composed of the HIV-1 provirus with a disrupted glycoprotein gene and often an inserted reporter gene. In this system, the HIV-1 genome depicted is incorporated into PV and transduced into target cells.

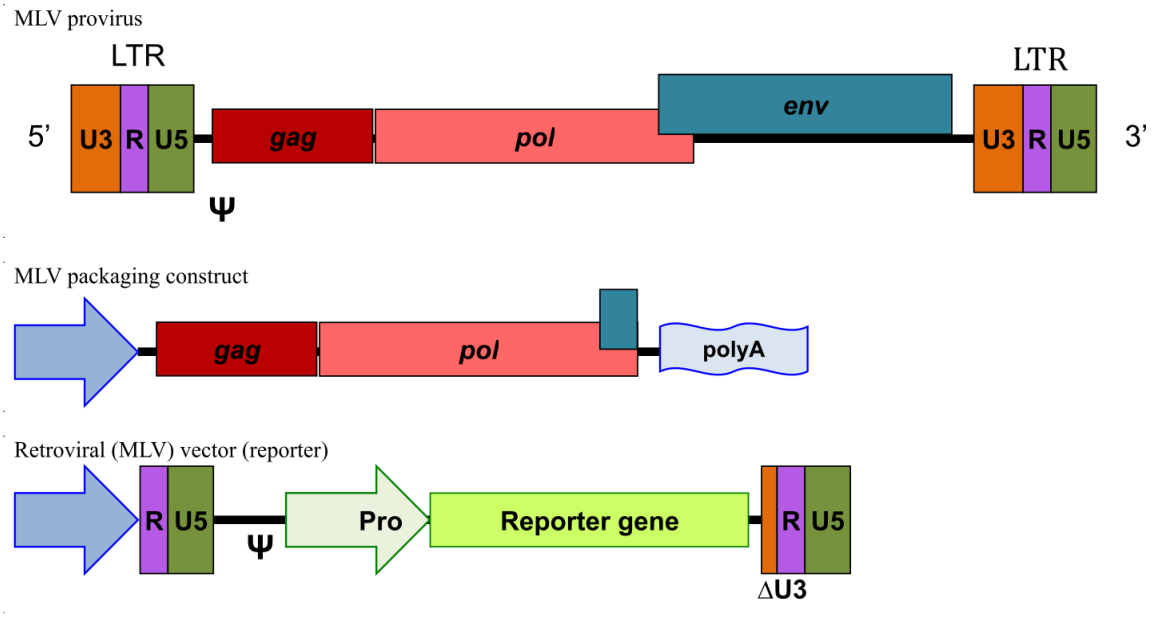

Figure 1.13. Schematic diagram of an MLV provirus and example MLV packaging system. Genes are separated into two plasmids to allow packaging genes *gag* and *pol* to be expressed and a separate retroviral vector containing a reporter gene incorporated into PV.

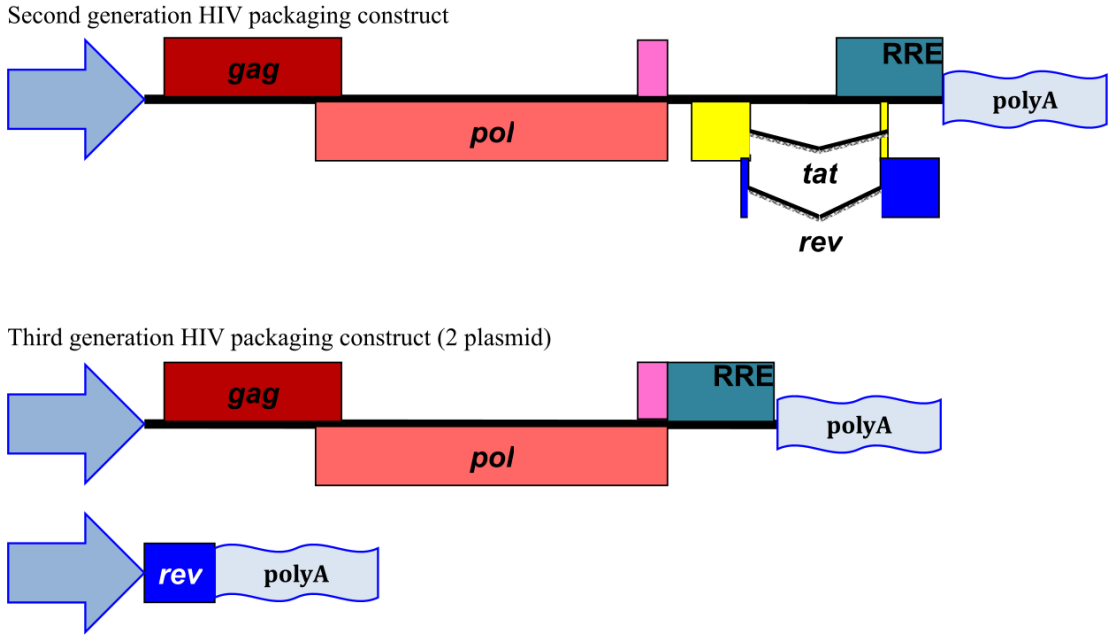

Figure 1.14. Schematic diagram of second and third generation HIV packaging constructs. These differ from first generation packaging constructs as HIV-1 genes have been separated into two plasmids, allowing the expression of *gag* and *pol* structural genes *in cis* while the genome incorporated into PV (shown in figure 1.6) lacks complete HIV-1 genes. The third generation separates *rev* into a third plasmid, preventing the incorporation of *rev* into PV.

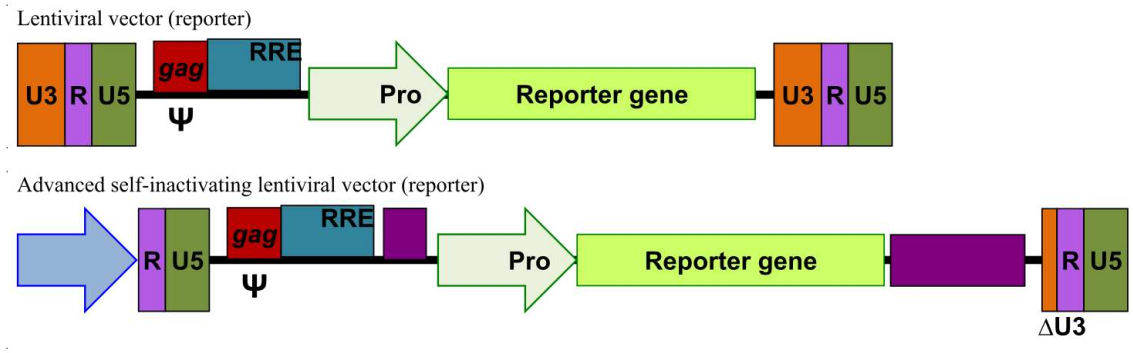

Figure 1.15. Schematic diagram of lentiviral vectors used with second or third generation HIV-1 packaging constructs. Vectors enable the expression of the reporter gene in transduced cells, while limiting the involvement of HIV-1 genes in the use of PVs. Top vector includes HIV-1 LTR regions involved in replication and integration. Lower vector prevents replication through deletion of the U3 region of the LTR, producing self-inactivating

1.21.5 Reporter systems

The output of the PV system is based on the incorporated reporter which mimics the genome of the surrogate virus. In the case of HIV-1 or MLV surrogates, the reporter will often be incorporated into the pseudotype in RNA form, which upon transduction will be reverse transcribed, translocated to the nucleus and integrated into the host cell genome. The reporter will then be transcribed and translated by the host cell and its action used to measure transduction efficiency. The primary reporter used in influenza pseudotypes is firefly luciferase (Mullarkey et al. 2013; Lingwood et al. 2012; Su et al. 2008; Rao et al. 2010; Loureiro et al. 2011; Wei et al. 2012; Ledgerwood et al. 2013; Wei et al. 2008; Wang et al. 2014). Relative luminescence units (RLU) or relative luciferase activity (RLA) are used as output, measured by lysing transduced cells and adding substrate for the luciferase enzyme, the signal from which is then read using a luminometer. GFP is also commonly used, in which case transduction efficiency is determined by counting the number of fluorescing cells via epifluorescence microscopy or fluorescence-activated cell scanner (FACS) (Ao et al. 2008; J. Wu et al. 2010). Other reporters such as *lacZ* (Ao et al. 2008; Hatziioannou et al. 1998; Konishi et al. 2008; McKay et al. 2006) as well as *Gaussia* (Hai et al. 2012) and *Renilla* (Ascione et al. 2009; B. Su et al. 2009) luciferase are also used to a lesser extent in the published PV literature.

See Figure 1.16 for a comparison of published influenza strains used in the production of PV in comparison to the total number of HA sequences in NCBI GenBank. Figure 1.17 shows the various PV production parameters used in the published studies using PV.

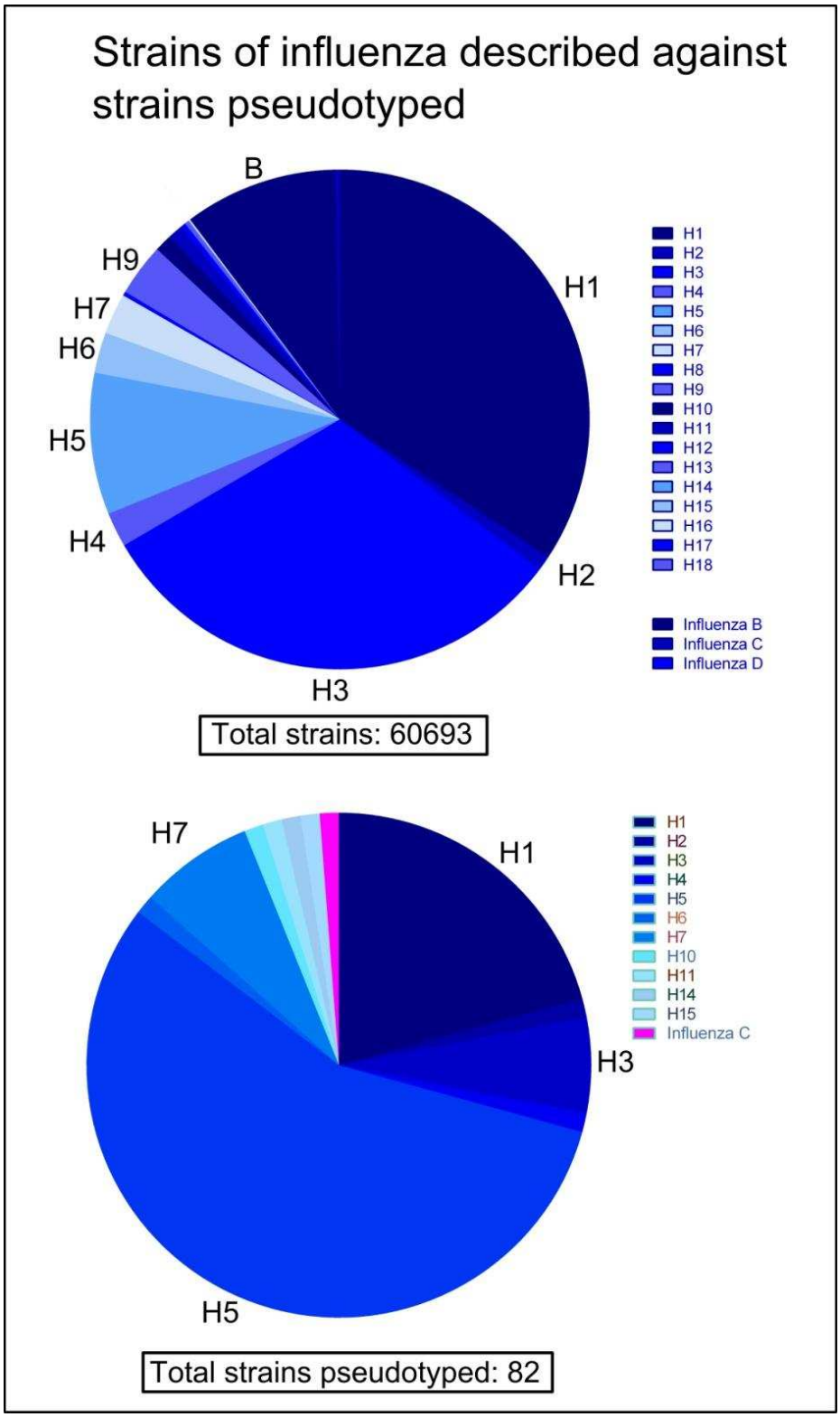

Figure 1.16. Comparison of influenza HA strains described against published HA strains incorporated into PV. Out of a total of 60693 HA sequences extracted from NCBI GenBank, the vast majority come from subtypes H1, H3, H5 and influenza B. Conversely, the current number different subtypes and strains of HA used to produce pseudotypes is 82. The majority of PV strains come from subtypes H1, H3 and especially H5. Figure from (Carnell et al. 2015).

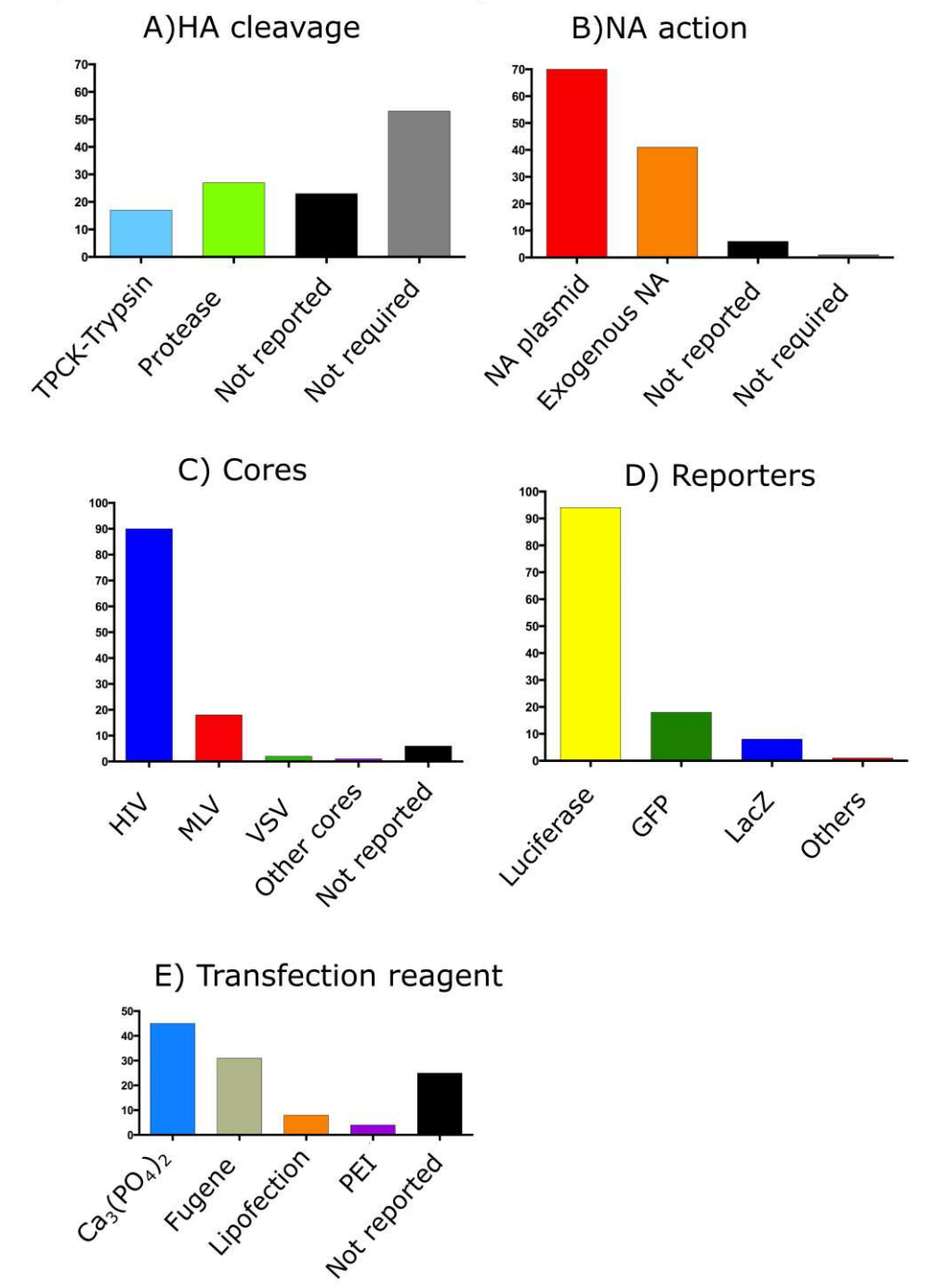

Figure 1.17. Pseudotype production methods. Various parameters including method of HA cleavage (A), PV release (B), retroviral cores used (C), reporter used (D) and transfection reagent used (E) for the production of influenza PV. Figure from (Carnell et al. 2015).

1.21.6 Titration methods

With luciferase reporter PV the RLU can be used as a secondary measure of pseudotype quantity within a sample, but this is dependent on many variables surrounding the cells and the particular luminometer used. Pseudotypes are typically 2-fold serially diluted down or across 96-well plates from a starting 100 µL of harvested supernatant. After an incubation of 48 or 72 hours, RLU can be measured by lysing the transduced cells and adding luciferin (luciferase substrate). This can then be used to calculate the RLU per well and the RLU/ml of the original sample. Reverse transcriptase quantative PCR (RT-qPCR) has also been employed in order to estimate transduced gene copies as well as messenger RNA (mRNA) copies in cells. This method is often used in conjunction with others described in this section in order to have comparative measurements of pseudotype quantity (Wu et al., 2010; Zhang et al., 2010; Du et al., 2010b). In many studies, PV input is normalized via enzyme-linked immunosorbent assay (ELISA) detection of the principal component of the HIV-1 core, p24 (Sawoo et al. 2014; Du et al. 2010; Su et al. 2009; Zhou et al. 2012; Ao et al. 2008; Schmeisser et al. 2013; Wang et al. 2010; Wang, Xie, et al. 2010; Wei et al. 2011; Chaipan et al. 2009; Wang et al. 2008; Zhao et al. 2011; Nefkens et al. 2007; Bosch et al. 2001; Basu et al. 2014). However, as core budding is independent of surface HA, this method will also detect cores lacking envelope glycoproteins as well as cores belonging to replication competent pseudotype viruses. PV HA has also been detected using ELISA and used to normalize pseudotype input (Yang et al. 2014; Wang et al. 2013; Li et al. 2011). Quantification through HI assay has also been used frequently (Hai et al. 2012; Whittle et al. 2014; Yang et al. 2014; Zheng et al. 2012; Zhang et al. 2009; Tisoncik et al. 2011; Zhang et al. 2010; Hultberg et al. 2011; Sawoo et al. 2014; Yang et al. 2007; Wu et al. 2010; Wei et al. 2011). Western blotting is used in some cases to determine the amount of glycoprotein or HIV-1 p24 in a PV sample (Du et al. 2010a; Su et al. 2009; Wang et al. 2011). It is also used in a wider range of studies to ascertain glycoprotein or HIV-1 p24 expression (N. Du et al. 2010; Sawoo et al. 2014; Wei Wang et al. 2008; J. Wu et al. 2010; Y. Zhang et al. 2010).

1.21.7 Cell Input

The vast majority of studies involving neutralisation assays titrate and transduce in 96-well plates with $1x10^4$ cells (HEK293, HEK293T/17 or MDCK) per well. However, the amount of cells can range from $5x10^3$ to $1x10^5$. In some instances, 293A and MDCK-London cells are also used, whereas BHK-21 cells are frequently used for VSV-based pseudotype infection due to their comparative susceptibility (Hanika et al. 2005; Wei et al. 2011; Kong et al. 2006; Ledgerwood et al. 2012; O'Donnell et al. 2012; Ledgerwood et al. 2011; Lin et al. 2009; Rao et al. 2008). Specialised cells over-expressing α2,6-linked sialic acid (MDCK-SIAT) have also been used and compared to parental cells in the presence of soluble HA (Tang et al. 2012).

The importance of pseudotype input in batch to batch variation is highlighted by Garcia et al. 2010, this study suggests that using an RLU input of at least 10^5 per well should be used to ensure that antibody titer is independent of pseudotype input.

1.21.8 Substrates

Steady-Glo and Bright-Glo (Promega) are the most common sources of luciferin, the substrate required by the luciferase enzyme to produce light. Whilst expensive, these two substrates also serve a secondary purpose of lysing cells and releasing any expressed luciferase enzyme.

1.21.9 High-throughput approaches

PVs are amenable to high-throughput approaches and this has been used to evaluate antiviral compound effects on pseudotype transduction, testing a wide range of unique compounds in a single assay performed with 96 or 384-well plates (Wang et al. 2013; Basu et al. 2014). High-throughput assays have also been used for PVs bearing the glycoproteins of different viruses, such as for the identification of HIV-1 inhibitors or other BSL-4 viruses (Basu et al. 2010; Garcia, Gao, et al. 2009; Talekar et al. 2012).

1.21.10 Increased transduction efficiency

Polybrene and polyfect (Qiagen) are used in several studies in order to increase transduction efficiency (Krammer et al. 2012; Hai et al. 2012; Lin & Cannon 2002; McKay et al. 2006; Pica et al. 2012; Sandrin & Cosset 2006; Tsai et al. 2009; Wang et al. 2008; Yang et al. 2014). 1 µg/ml, 8 µg/ml or 16 mg/ml of polybrene is added to virus or virus/antibody mixes before

the addition of cells in titration and neutralisation assays or during incubation. In two studies, spinoculation was used to increase transduction, centrifuging cells and pseudotype at 1250 RPM for 2 hours or 3000 RPM for 1 hour (Cheresiz et al. 2014; Chaipan et al. 2009).

1.22 Pseudotype based neutralisation assays

1.22.1 Protocol

Pseudotype based neutralisation assays (pMN) are usually carried out in 96-well white plates. A measured amount of antibody is incubated with a set amount of quantified virus in a total volume of medium, usually at a 1:1 virus: media ratio. Incubation is carried out at between 20 and 37°C for between 30 minutes to 2 hours (Garcia et al. 2010; Mallajosyula et al. 2014; Schmeisser et al. 2013; Shelton et al. 2013; Temperton et al. 2007; L. Zheng et al. 2011). $1x10^4$ target cells are then added to each well, subsequently the plate is left to incubate at 37°C in 5% CO_2 for 48 or 72 hours. A cell only control as well as known positive and negative sera standards should be used as benchmarks for the neutralisation assay (Wei, Boyington, Dai, et al. 2010; Zhao et al. 2011). See Figure 1.18 for a depiction of the pMN assay.

1.22.2 PV input

The quantities of PV used in neutralisation assays which were normalised based on p24 ELISA ranged from 6.25 to 50 ng/ml (Wei Wang et al. 2008). RLU or RLA values of between 10,000 and 1,000,000 per well (96-well plate) have been used in the influenza PV literature, sometimes in conjunction or normalized with p24 or qPCR methods (Hultberg et al. 2011; Mather et al. 2014; Wei Wang, Xie, et al. 2010). Estimates of copy number per set volume of original viral supernatant can also be used. It is important to note that RLU based values are affected by the make-up of the plasmid bearing the HA gene, as well as a multitude of factors from the luminometer used to cells transduced and substrate added. A further method for quantification of PV involves the dilution expected for the infection of 50% of cells ($TCID_{50}$, Reed and Muench 1938) which can be used with GFP PV.

1.22.3 Serum/antibody dilutions and start points

Antibody input varies depending on availability, especially when taking into account the possibility of repeats and replicates. Antibodies are primarily diluted 2-fold in Dulbecco's

Modified Eagle Medium (DMEM), with or without FBS, across a 96-well plate, with the occasional three, four or five-fold dilution experiment published (Alberini et al. 2009; Cheresiz et al. 2014; Ding et al. 2011; Hai et al. 2012; Mahallawi et al. 2013). Where mentioned, starting concentration of virus and media ranges between 1:4 and 1:40 respectively.

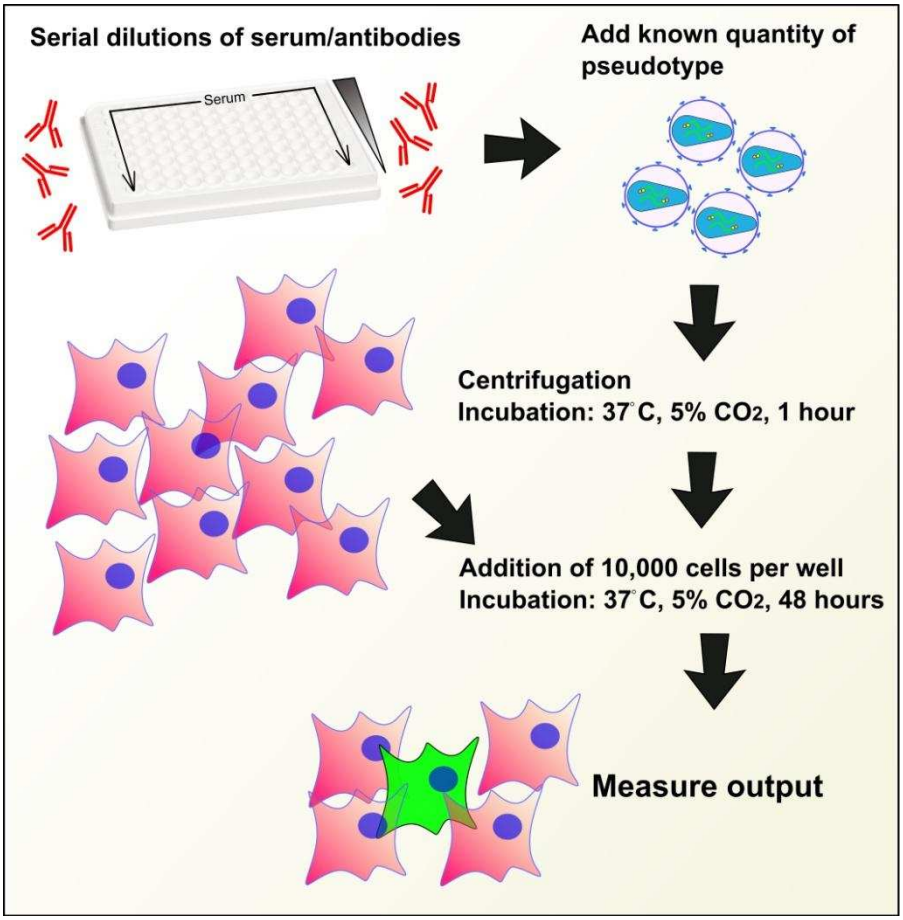

Figure 1.18. Pseudotype based neutralisation assay (pMN). Serial dilutions are carried out down 96-well microtitre plates, whereupon a known quantity of PV is added. Plates are centrifuged to consolidate well contents and incubated for 1h at 37°C, 5% CO_2. Approximately $1x10^4$ HEK293T/17 cells in 50 µl of DMEM are added per well. Plates are incubated for 48h at 37°C, 5% CO_2 before reporter-specific plate readout. Figure from (Carnell et al. 2015).

1.22.4 Incubation times and time periods

When stated, serum inactivation varies from 30 minutes to 1 hour at 56°C (Garcia et al. 2010; Tsai et al. 2009). PV-antibody incubation times are generally consistent between studies, at 37°C for 1 hour. Transduction times vary in 24 hour increments at 24, 48 and 72 hours, after which output is measured. The total length of each neutralisation assays varies, especially regarding measurement methodologies. Output is measured at 48 or 72 hours

post-transduction yet occasionally output is measured 48 or 72 hours after the first wash or medium replenishment.

1.22.5 Controls

Positive sera or specific commercial antibodies are required as positive controls which can be compared to tested sera and used to normalise between assays (see section 1.22.11 on standardisation). Reference sera from the National Institute for Biological Standards and Control (NIBSC), Office International des Epizooties (OIE), Animal and Plant Health Agency (APHA, previously AHVLA) and US Food and Drug Administration (FDA) are regularly used as controls (Hultberg et al. 2011; Molesti et al. 2013; J Sui et al. 2009; Wei Wang et al. 2011; Wei Wang, Castelán-Vega, et al. 2010; Wei Wang, Xie, et al. 2010).

1.22.6 Neutralising antibody titer determination

Antibody effect is displayed using one of many inhibitory concentrations (IC_{50}, IC_{80}, IC_{90}, and IC_{95}). The numerical value relates to the percentage point each particular study is calculating, for example the IC_{50} value can represent the concentration of an antibody that reduces RLU reading by 50%, when compared to 100% and 0% transduction controls (Gorres et al. 2011; Kanekiyo et al. 2013; Rao et al. 2010; Tsai et al. 2009). These controls are essential to the calculation. 100% inhibition can be benchmarked by a cell only control and 0% by incubation of cells and virus in the absence of sera.

1.22.7 HI assay

HI assays using PV utilise the same procedures as with WT virus. Viral samples are diluted in phosphate buffered saline in a 96-well plate, to which 50 µl of a 0.5-1% chick/turkey red blood cell suspension is added. After between 30minutes to 1 hour, the HI plates are scored for agglutination. PV input is adjusted according to WHO guidelines at 4 HI units and sera is treated with receptor destroying enzyme to inactivate nonspecific inhibition of agglutination (Yang et al. 2014; Haynes et al. 2009).

1.22.8 Post-attachment neutralisation assay

The post-attachment neutralisation assay is used to identify antibodies that neutralise HA after it has bound to sialic acid. Oh et al. 2010 modified the post-attachment assays, originally developed by Edwards & Dimmock 2001, to allow WT influenza virus to be

replaced by influenza PV. In this assay, PV are incubated at 4°C with cells to enable the synchronisation of the attachment of virus to sialic acid on the cell surface and to block viral endocytosis. Diluted sera is then added, and following another 4°C incubation, plates are incubated at 37°C to permit transduction (Oh et al. 2010). Transduction is then measured using the same approach as that taken in a neutralisation assay. Antibodies detected by this assay have neutralising activity via their ability to impede the endocytosis step and subsequent HA conformational changes necessary for virus-endosome fusion (Edwards and Dimmock 2001; Hsueh-Ling et al. 2010). Antibodies that have neutralising activity through impeding viral attachment will produce negative results in this assay. The post-attachment assay is useful for evaluating the neutralising capacity of stalk-directed antibodies that do not inhibit viral attachment (Corti et al. 2011; Hsueh-Ling et al. 2010).

1.22.9 Reproducibility

Reproducibility is a major issue in the field of serology. Serum samples are often finite, leading to an inability to reproduce experiments or results in the same context as they were originally published. However, by standardising methods for production, titration and neutralisation and the use of common reference standards it is possible to minimize variation between experiments and research groups. The members within the laboratories of the CONSISE group (section 1.20) have carried out several studies aimed at reducing or at least measuring the amount of variation between laboratories utilising the same techniques. They have also established CONSISE consensus protocols for ELISA and other assays in an effort to further improve inter and intra-laboratory correlation of data generated using these same assays (Laurie et al. 2015; Van Kerkhove et al. 2013). Similar efforts should be made to standardise PV based assays worldwide.

1.22.10 Correlation with other serological assays

Comparisons have been made between pMN assays and traditional serological assays with mixed results. Several articles report increases of between 31.9% and 200% in H5 PV IC_{50} antibody titers in comparison to MN based results with WT virus (Buchy et al. 2010; Garcia, Pepin, et al. 2009). Buchy et al. 2010 show a correlation between H5 PV and MN (spearman 0.79, $p<0.001$), which was also reported by Du et al., 2010a and W. Wang, Xie, et al. 2010, the latter presenting r^2 values of 0.9802 for A/Vietnam/1203/2004, 0.8193 for

A/Anhui/1/2005 and 0.5244 for A/turkey/Turkey/1/2005 strains. Alberini et al. 2009 compared pMN assays to HI, SRH and MN assays using 226 different serum samples. The Pearson correlation test showed significant correlation ($p<0.001$) between the antibody titers calculated from each assay. The correlation coefficients between pMN and HI, SRH and MN assays were 0.73, 0.70 and 0.78 respectively. Furthermore the correlation between H5 and H5 pMN allowed the establishment of a threshold from which pMN titers could be based. pMN data was then analysed based on the threshold which showed protective titers in patients of 38-43%, 54% and 79% after adjuvanted vaccination, second dose and booster respectively (Alberini et al. 2009). Qiu et al. 2012 showed a range of correlations between HI and pMN using different HA subtypes. A/Moscow/10/1999 (H3N2) correlates well ($r=0.8454$, $p<0.0001$), A/Brisbane/59/2007 (H1N1) and A/Japan/305/57 (H2N2) poorly ($r= 0.1171$, $p=0.7472$ and $r=0.1171$, $p=7472$) whereas A/Viet Nam/1203/ 2004 (H5N1) correlates ($r=0.7921$, $p=0.0029$). In an additional study, HI and pMN (IC_{50}) correlate well in Qiu et al. 2013 in the case of A/ Shanghai/4664T/2013 (H7N9) (spearman $r=0.88$, $p<0.0001$) as well as in Whittle et al. 2014 ($r^2=0.6491$, $p<0.0001$). A significant correlation ($p=0.002$) of 65% ($r= 0.65$) was also been reported between SRH and pMN in equine influenza PV and a further study showed the relationship between RLU and HA content (Scott et al. 2012; C. Y. Su et al. 2008).

1.22.11 Approaches towards validation and standardisation

Approaches towards the standardisation of pMN should follow the procedure that was required for MN standardisation. Standardisation of MN in general has focused on the use of pooled serum samples as reference standards. A/California/7/2009 (H1N1) pdm standard was established by the WHO in 2010 with an assignment of potency of 13000 International Units (IU) per ml. A second pooled sera reference standard for H5N1 exists and has successfully been used in a number of studies (Alberini et al. 2009; Stephenson et al. 2009). A cut off value for positive and negative H5N1 neutralising sera exists for this set of H5N1 reference standards (Alberini et al. 2009).

1.22.12 cHA

There has been considerable research into the stalk region of the HA in relation to vaccine design and immunity to influenza. Various stalk-directed mAbs such as CR6261 have been

characterised, opening up the use of cHA to test for the presence of similar antibodies in serum samples (Ekiert et al. 2009; Throsby et al. 2008). Stalk directed antibodies were first identified in 1994 when the cross-reactive C179 mouse monoclonal antibody (mAb) was identified and found to inhibit fusion of several HA subtypes (Okuno et al. 1994). Since then many studies have focused on stalk directed antibodies and their neutralisation of multiple diverse subtypes of influenza (Corti et al. 2010, 2011; Ekiert et al. 2012; Throsby et al. 2008; Wrammert et al. 2011). However this range of heterosubtypic immunity is dependent on the characteristics of the epitope of each antibody tested, which will influence which subtypes, clades and whether they neutralise group 1 or 2 influenza virus HAs. The stalk region of HA is more conserved than the variable globular head, to which the vast majority of neutralising antibodies are directed. While residues in the head mediate attachment of the virus to target cells by binding to sialic acid, the fusion peptide in the stalk of HA is just as crucial to the HA function (Jianhua Sui et al. 2011; Wei, Boyington, McTamney, et al. 2010). In order to test for neutralising stalk antibodies, studies have employed a variety of cHA constructs bearing stalks and heads from different subtypes. The concept behind this revolves around the use of HA heads which are largely non-reactive to the antibodies used in the assay. In this way a neutralising response can be detected in the absence of head directed neutralisation. Classical serological assays are insensitive to the detection of stalk-directed mAbs when compared to pMN. In order to more efficiently test for stalk-neutralising antibodies, some studies have employed a variety of cHA constructs bearing stalks and heads from different subtypes. Several hybrids have been constructed and pseudotyped using HIV-1 cores, these are generally constructed through PCR amplification and incorporation of complimentary restriction sites, allowing ligation of different segments of HA genes together in one plasmid. The presence of a conserved disulfide bond linking cysteines 52 and 277 in influenza A HAs (H3 Aichi numbering), separating the globular head from the stalk region, make production of these cHAs relatively straight forward (Ferrara 2015; Hai et al. 2012). However, when cHAs are produced with influenza B components, the 52-277 delineation is not present, making efforts to produce influenza B cHAs more difficult. One approach successfully swapped cysteines with alanines from a similar location in the influenza B HA (57-366), producing functional cHAs with an influenza B stalk and influenza A head (Ermler et al. 2017). However this study employed the cHA in the production of RG viruses as well as recombinant protein, their use in PV system would require optimisation. A

wider variety of different cHA have been used in reverse genetics approaches towards development of wild type virus bearing cHAs (Krammer et al. 2013; Krammer, Hai, et al. 2014; Krammer, Margine, et al. 2014). These cHA are also promising candidates for 'universal' vaccines, discussed earlier in this chapter. Table 1.1 displays the regions and subtypes used in the construction of cHAs in the listed literature.

Table 1.1 Examples of cHAs originating from divergent subtypes and used for pseudotype production. Article source and composition of cHA are detailed.

Article	Head	Stalk
Hai et al. 2012	H5 A/Vietnam/1203/04	H1 A/Puerto Rico/8/1934
	H1 A/California/04/09	H1 A/Puerto Rico/8/1934
	H7 A/mallard/Alberta/24/01	H3 A/Perth/16/2009
	H5 VN/05 HA	H3 A/Perth/16/2009
Pica et al. 2012	H6 A/mallard/Sweden/86/02	H1 A/Puerto Rico/8/1934
	H9 A/guinea fowl/Hong Kong/WF10/99	H1 A/Puerto Rico/8/1934
	HA1	HA2
Wang et al. 2011	A/Brisbane/59/ 2007	A/New Caledonia/20/1999
	A/New Caledonia/20/1999	A/Brisbane/59/ 2007

1.23 The future of influenza PV

pMN offers the safety of using pseudotypes and the sensitivity of the MN assay. Further validation and standardisation of the assay is required, but once established, this assay should offer a robust and sensitive means of interrogating influenza vaccine trials for head and stalk targeting antibodies. The production of vaccines that elicit stalk-targeting antibodies may in time lead to a universal vaccine, preventing the mortality and morbidity resulting from seasonal influenza and the emergence of pandemic strains, most recently the pH1N1, which caused an estimated 284,500 deaths in its first 12 months of circulation (Dawood et al. 2012). pMN currently offers the opportunity to batch test vaccines or commercialized antibodies in the absence of standardisation. Furthermore, the ability of pMN assay to include PVs bearing cHA, NA and M2 allows the pMN to be used to explain the pathogenicity of seasonal and pandemic influenza strains and perhaps elucidate the antigenic evolution of influenza further. Such information will prove useful for the generation of future vaccines.

1.24 Other uses of influenza PV

1.24.1 Gene therapy

As the field of gene therapy progresses, influenza pseudotyping will benefit from the design of even safer and more effective vectors. As more sophisticated systems are developed they may become more easily standardised and comparable to WT virus. One aspect of gene therapy which may benefit from the field of influenza is the use of viral entry proteins to target delivery of nucleic acids into specific cells. One study used influenza PV to transduce the respiratory epithelial cells of mice after nasal administration with promising results indicating that the method could be used in the treatment of cystic fibrosis (Patel et al. 2013).

1.24.2 PV as Vaccines

PV based vaccines are also becoming more widespread, with several candidates already cited in this thesis. Baculovirus pseudotyped with VSV-G has been used successfully to express HA genes in mammalian cells and provided an efficacious vaccine when tested in chickens and mice (Q. Wu et al. 2009). The VSV-G glycoprotein enabled entry of baculovirus into target cells whereupon the delivered HA gene was expressed. While originally a popular vector for transgene expression in insect cells, VSV-G has been shown to be a useful tool for vaccine production in mammalian cells (Hofmann et al. 1995). In Wu et al. 2009 delivery was achieved through VSV-G incorporation into baculovirus under the effect of the polyhedron promoter and HA under the effect of the CMV promoter in order to achieve expression in insect cells and subsequent infection and expression of HA in mammalian cells. This is an interesting system which could be used as a method for the introduction of PV genes into cells through a VSV-G bearing baculovirus in lieu of cytotoxic transfection reagents. H5 bearing PV have been tested in mice as candidate vaccines, eliciting high levels of anti-HA antibodies as determined by HI. Mice that were vaccinated survived despite weight loss of approximately 12.8–21.1% whereas the non-vaccinated group lost approximately 25.5–26.2% of their bodyweight and died 6 days after H5N1 virus challenge (S. Zhang et al. 2008). A further PV vaccine has been developed which contains a modified HA gene, allowing expression in transduced cells but lacking the viral RNA sequences required for replication. This yields a particle bearing the desired glycoproteins, in this case A/Puerto Rico/8/1934

(H1) that consequently induces a robust T-cell response when given to mice via inhalation. Reduction in the severity of symptoms was also seen in mice infected with a different subtype: H3N2 A-X31 (Powell et al. 2012). Influenza PV could also be used in vaccine design through the use of integrase defective lentiviral vector technology. Defective lentiviral vector technology allows transduction of target cells through maintenance of an episomal reporter construct without integration into the genome. This approach may bring benefits by reducing the chance of interrupting host genes and the eventual dilution of the delivered gene (Banasik and McCray Jr 2010; Farazmandfar et al. 2012).

1.25 Thesis aims and objectives

The aim of the projects reported in this thesis were primarily to make use of HA and NA bearing PV as surrogates for neutralisation assays aimed at the detection of bnAbs. This was to be achieved through the use of panels of human sera as well as mAbs on a library of PV bearing glycoproteins from a range of G1 and G2 influenza subtypes, including divergent subtypes such as H17. Furthermore, the cHA system was to be employed using PV in a comprehensive study in collaboration with the Jenner Institute Laboratories, University of Oxford. This study was aimed at firmly establishing and making use of the pMN cHA system to detect HA stalk-directed antibodies which may be elicited from universal vaccines. Due to the nature of the pMN assay and its requirement of a functional glycoprotein to mediate membrane fusion, this assay should hold advantages over the commonly used ELISA based approaches and pave the way for the detection of binding and neutralising antibodies.

Due to the importance of the viral NA in the viral life cycle and vaccines, efforts were made to establish PV as a source of NA using the ELLA system, allowing comparison of ELLA and pMN data using the same antigen source. The aim of this project was to enable correlation between HA and NA responses detected using PV systems, both of which only provide positive data in the absence of function of the HA and NA proteins: neutralisation of HA or inhibition of NA.

1. **Development of cHA with pandemic H1N1 2009 stalk**
2. **Utilisation of cHA to detect bnAbs in human sera**
3. **Establishment of pELLA**
4. **Correlation of gold standard assays (HI and SRH) with pMN**
5. **Production of H17 bat influenza PV and neutralisation with bnAbs.**

Chapter 2 : Materials and Methods

General materials and methods will be reported in this chapter, with sources, catalogue and accession numbers where necessary. Deviations of these protocols in regards to variables and reagents changed will be detailed in each individual results chapter thereafter.

2.1 DNA Methods

2.1.1 Plasmids, vectors and genes

A variety of different plasmids were used in the projects reported in this thesis, all of them were used for the production of PV and fall within three different types of plasmid. First, eukaryotic expression plasmids were used in order to express relevant influenza genes (HA, NA, M2) for incorporation into PV. Second, lentiviral vectors were used to provide a PV core and genome with desired reporter output. Lastly, accessory plasmids designed to express various different proteases in PV producer cells were used, depending on the requirements of each HA used in PV production. The primary eukaryotic expression plasmid used in this project, pI.18 was derived from influenza DNA vaccine research (Cox et al. 2002). This plasmid contains an hCMV immediate early promoter (IE) and intron A, a CMV enhancer region which enhances expression in eukaryotic cells. This region precedes the multiple cloning site (MCS) which contains sites for DNA cloning via restriction digestion. A CMV terminator sequence is located after the MCS allowing polyadenylation of mRNAs produced from genes expressed at the MCS region. The plasmid also contains a standard pUC origin of replication (Ori) and β-lactamase gene allowing selection of bacteria transformed with this plasmid for molecular biology purposes. The expression of this gene is promoted by a β-lactamase promoter; both of these are antisense to the eukaryotic region containing CMV genes and MCS. The plasmid backbone (Δ insert) is ~4.3 kb in length, depicted in Figure 2.1.

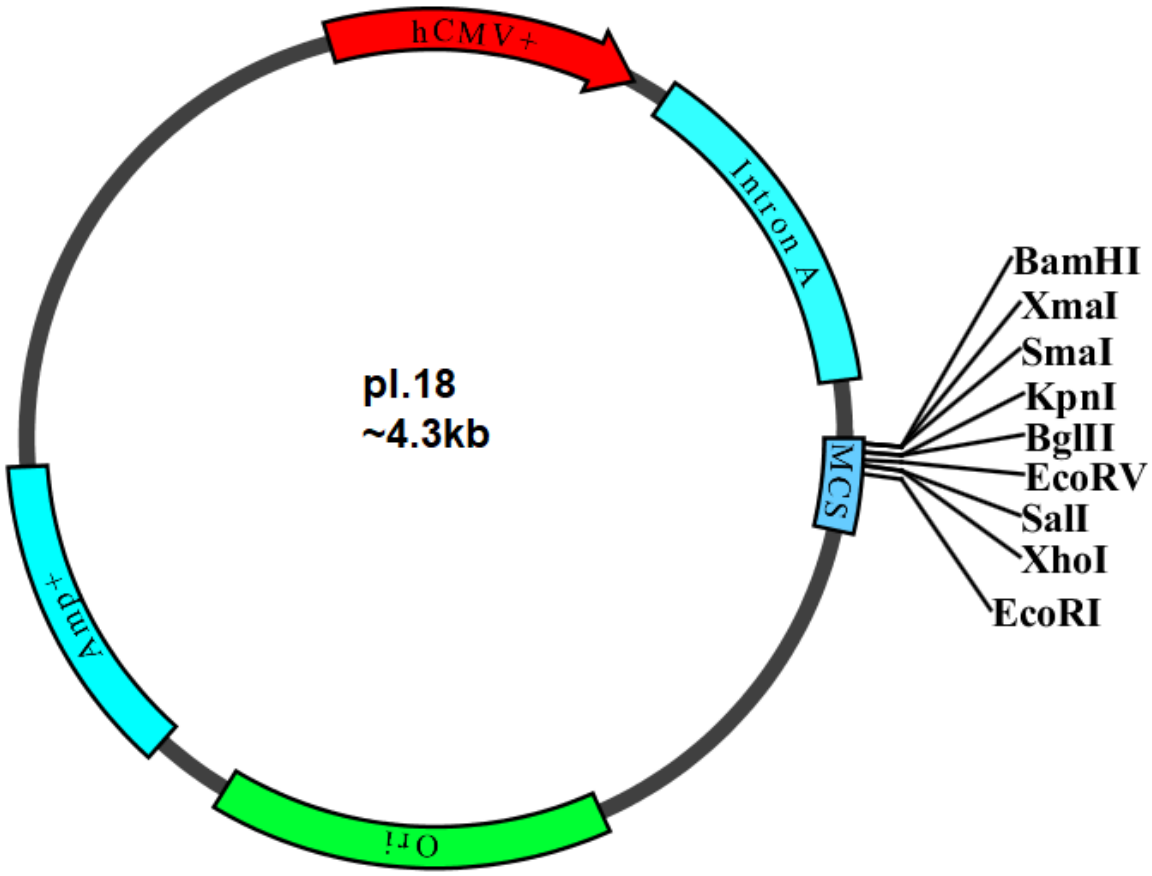

Figure 2.1. Simplified schematic of the eukaryotic expression plasmid pI.18. This plasmid contains a hCMV promoter (hCMV+) alongside the hCMV 'Intron A' enhancer, allowing expression of cloned genes in eukaryotic cells. Bacterial Ori and β-lactamase are also present to allow transformation and selection of bacterial transformants. This Plasmid is ~4,3kb in length.

A second eukaryotic expression plasmid was used, phCMV1. This was used due to the acquisition of a variety of cloned HA genes from Dr Davide Corti at the Institute for Research in Biomedicine, Bellinzona, Switzerland. This plasmid contains a hCMV promoter to drive expression of genes cloned into the MCS, and bacterial transformants can be selected through a kanamycin/neomycin resistance cassette. phCMV1 is also ~4.3kb in length, see Figure 2.2 for a simplified schematic of this plasmid.

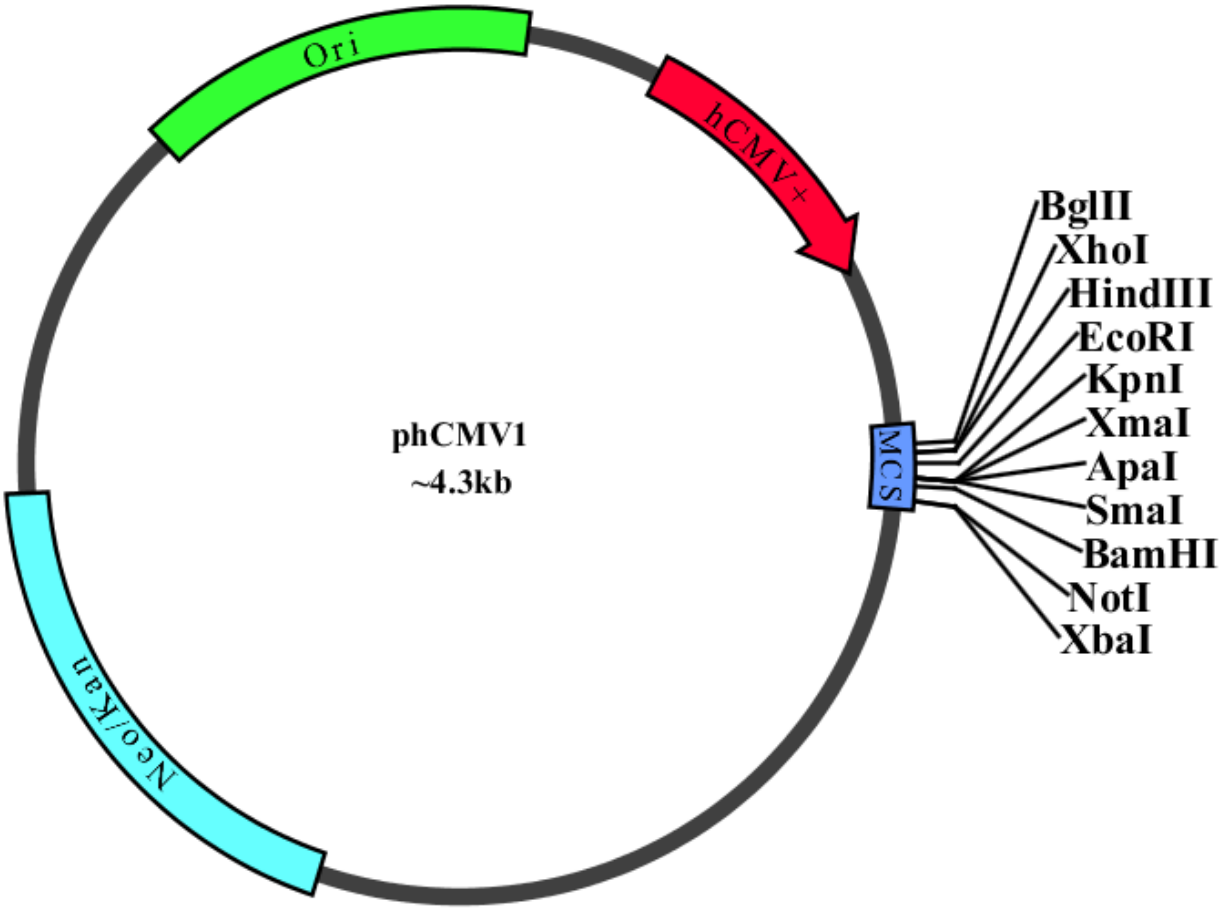

Figure 2.2. Simplified schematic of the eukaryotic expression plasmid phCMV1. This plasmid contains a hCMV+ alongside an Ori for transformation into competent bacteria. Selection of transformants is possible through a Neomycin/Kanamycin resistance cassette.

2.1.2 HIV-1 packaging construct

HIV-1 derived packaging plasmid pCMVΔR8.91 (p8.91) was obtained from Professor Greg Towers, University College London, originating from the laboratory of Dr Didier Trono (Naldini et al. 1996; Zufferey et al. 1997). This lentiviral packaging plasmid contains the relevant genes (*gag, pol, tat,* and *rev*) for the production of HIV-1 packaging proteins required for PV production. These are produced as a single transcript under the control of a hCMV promoter, which will then be exported in various spliced states in an HIV-1 dependent manner. This yields suitable ratios of proteins for the production of particles containing core proteins from *gag* (p17, p24, p7, p6) and enzymes from *pol* (protease, reverse transcriptase, integrase, p15). Other elements included in this plasmid allow replication (Ori) and selection of bacterial transformants (β-lactamase, ampicilin resistance). See Figure 2.3 for a simplified schematic of the p8.91 plasmid.

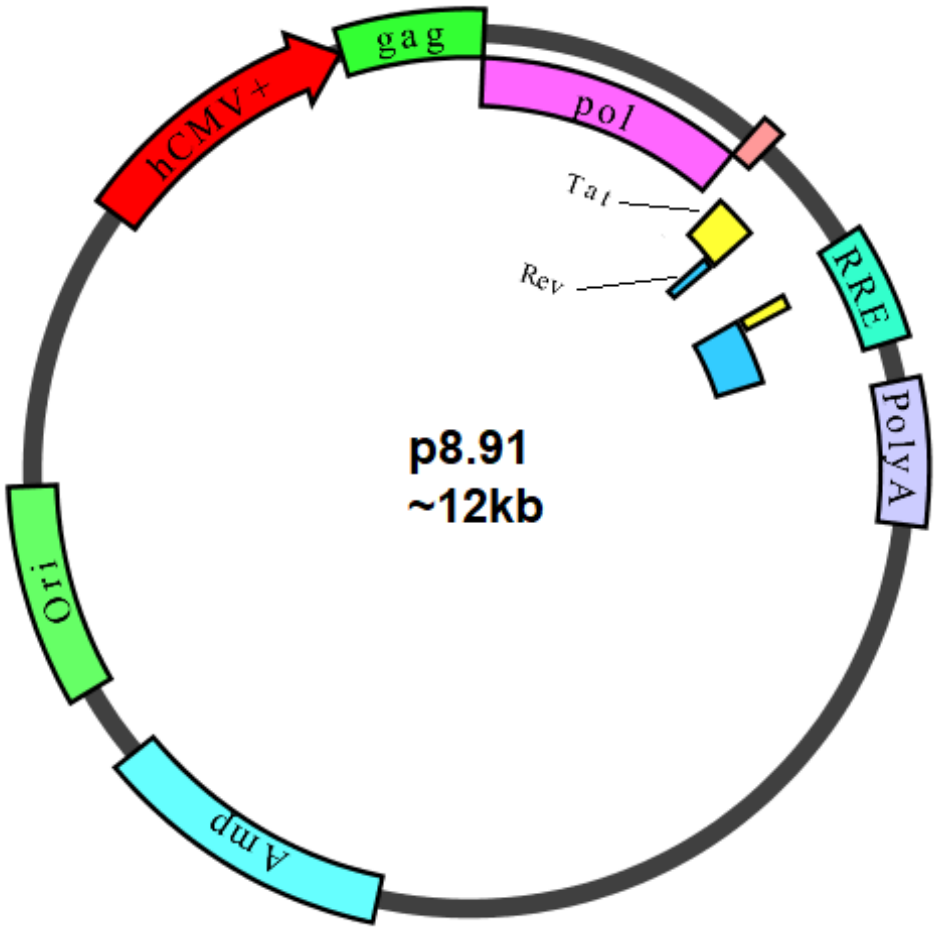

Figure 2.3. Simplified schematic of lentiviral packaging plasmid p8.91. This plasmid contains *gag*, *pol, tat* and *rev* genes, all other HIV-1 genes are disrupted through deletions and/or insertions. HIV-1 genes are under the control of a hCMV promoter (hCMV+) and a polyadenylation site is present downstream to allow stable functional mRNAs to be transcribed. The RRE remains intact in order to allow export of unspliced mRNA from the nucleus. An Ori and β-Lactamase gene are also present for transformation of competent bacteria and ampicillin based selection of transformants.

2.1.3 Luciferase containing vector constructs

A firefly luciferase bearing lentiviral vector was used as a mock genome for incorporation into PVs in order to quantify PV based on RLU. The Plasmid pCSGW (Synonyms pHR'SIN-cPPT-SE & pHR-SIN-CSGW) was obtained from Dr A Thrasher (Institute of Child Health, London, UK) and has been characterised in detail (Demaison et al. 2002). The eGFP gene was replaced with firefly luciferase by Novartis vaccines, Italy, now GlaxoSmithKline, Italy, giving us plasmid pCSFLW. This lentiviral vector contains a truncated HIV-1 genome and is designed to be incorporated into PV via the PSI packaging signal, and to express the firefly luciferase gene after incorporation into the target cell genome after PV mediated transduction. The firefly luciferase gene is under the control of the spleen focus-forming

virus (SFFV) LTR promoter and is enhanced by the Woodchuck hepatitis post-regulatory element (WPRE). LTRs are present with a deletion in the U3 region of the 5' UTR, making this vector 'self-inactivating' in regards to possible replication. Other elements of this plasmid enable replication in bacteria through the Ori and selection through the β-lactamase gene (Amp resistance) and its relevant bacterial promoter. See Figure 2.4.

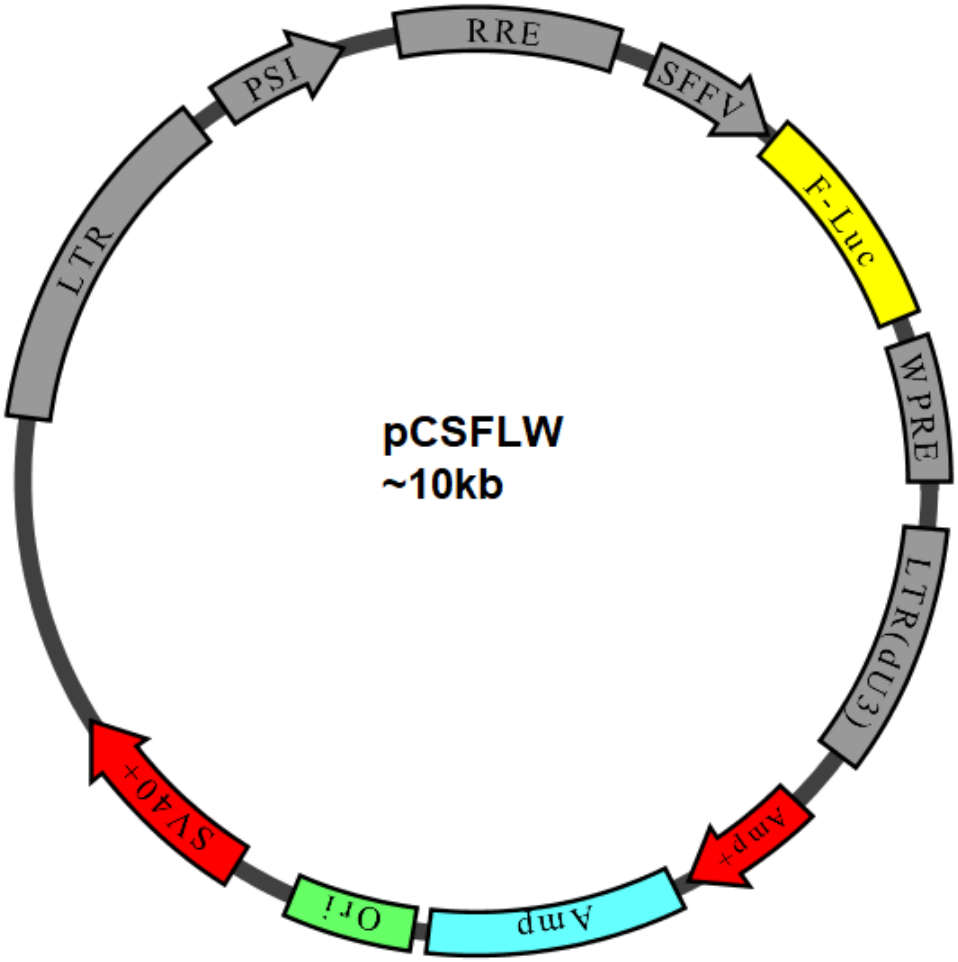

Figure 2.4. Simplified schematic of the lentiviral vector pCSFLW. This construct contains a truncated HIV-1 genome with functional LTRs and firefly luciferase under the control of SFFV LTR promoter and enhanced by the WPRE. Incorporation into PV is enabled by the presence of the packaging signal (PSI).

2.1.4 Protease encoding expression plasmids

In order to mediate maturation of the HA protein, a protease element is required for strains lacking the HPAI polybasic cleavage site. It appears that HEK293T/17 cells do not have adequate proteases or protease concentrations within the cell to mediate this cleavage to a sufficient degree to produce high titre PVs. Therefore, protease-encoding plasmids have been employed in order to mediate maturation of the translated HA0 to HA1 and HA2 subunits, a functional HA protein. Various proteases have been used in PV production and some of this work has been published (Ferrara et al. 2012; Sawoo et al. 2014; Scott et al. 2012; Wei Wang et al. 2008). Type 2 Transmembrane protease, serine 3 (pcDNA3.1 - TMPRSS3) and Type 2 Transmembrane protease, serine 4 (pCMV-Tag3 -TMPRSS4 (ECD) – myc, (Jung et al. 2008) were obtained from Prof. Stefan Pöhlmann (Infection Biology Unit, German Primate Center, Germany). pCAGGS-HAT was obtained from Eva Böttcher-Friebertshäuser, Institute of Virology, Philipps University, Marburg, Germany. The HAT gene was extracted by RT-PCR from 6-week old cell cultures of human airway epithelial cells (Böttcher-Friebertshäuser et al. 2013; Böttcher et al. 2006, 2009). For the sake of simplicity, the pCMV-Tag3 -TMPRSS4 (ECD) – myc plasmid will be referred to as pCMV-TMPRSS4 in the remainder of this thesis.

2.1.5 HA/NA/M2 gene containing plasmids

A library of expression plasmids bearing the HA and NA genes has been established by the Viral Pseudotype Unit for use in the production of PV. Table 2.1 shows the current list of functional plasmids which were used in the projects that form this thesis. This table also includes information such as the accession numbers for each gene, the plasmid in which it has been cloned and the source.

Table 2.1. List of HA, NA and M2 genes used in this thesis, alongside accession numbers, plasmid in which gene has been cloned and source.

Subtype/ Gene	Strain	Accession	Plasmid	Source
H1	A/California/7/2009	CY121680.1	pI.18	Synthesised: Genscript
H1	A/New Caledonia/20/1999	EU103824.1	phCMV1	Dr. Davide Corti
H1	A/Brisbane/59/2007	CY163864.1	pI.18	Dr. Kajia Hoschler
H1	A/South Carolina/1/1918	AF117241.1	phCMV1	Dr. Davide Corti
H1	A/Solomon Islands/3/2006	EU124177.1	pI.18	Prof. Sarah Gilbert
H1	A/Puerto Rico/8/34	AF389118.1	pI.18	Viral Pseudotype Unit
H1	A/Texas/05/2009	GQ457487.1	pI.18	Prof. Sarah Gilbert
H3	A/Texas/50/2012	KC892952.1	pi.18	Synthesised: Genscript
H3	A/Udorn/307/1972	DQ508929.1	pi.18	Viral Pseudotype Unit
H5	A/Vietnam/1194/2004	EF541402	pI.18	Viral Pseudotype Unit
H5	A/gyrfalcon/Washington/41088-6/2014	KP307984	pI.18	Synthesised: Genscript
H7	A/Shanghai/2/2013	KF021597	pI.18	Synthesised: Genscript
H11	A/duck/Memphis/546/1974	AB292779	phCMV1	Dr. Davide Corti
H17	A/Little shouldered bat/Guatemala/060/2011	CY103892.1	pI.18	Synthesised: Genscript
B	B/Bangladesh/3333/2007	CY115255.1	pi.18	Viral Pseudotype Unit
B	B/Brisbane/60/2008	KX058884.1	pi.18	Viral Pseudotype Unit
B	B/Yamagata/16/1988	CY018765.1	phCMV1	Dr. Davide Corti
B	B/Victoria/2/1987	ABL77244.1	phCMV1	Dr. Davide Corti
B	B/Hong Kong/8/1973	K00425	phCMV1	Dr. Davide Corti
B	B/Florida/4/2006	EU515992	phCMV1	Dr. Davide Corti
N1	A/Puerto Rico/8/34	CY033579	pI.18	Viral Pseudotype Unit
N1	A/California/7/2009	KU933487.1	pI.18	Synthesised: Genscript
N2	A/Udorn/307/1972	M879361.1	pI.18	Viral Pseudotype Unit
N2	A/Texas/50/2012	KC892281.1	pI.18	Synthesised: Genscript
N10	A/Little shouldered bat/Guatemala/060/2011	CY103894.1	pI.18	Synthesised: Genscript
M2	A/Hong Kong/156/97	AAC32091.1	pcDNA3	Prof. Wendy Barclay

2.1.6 Nucleic acid quantification and purity

Plasmid concentration and purity data is required prior to transfection of HEK293T/17 cells, production of PV. To this end, purified nucleic acids were analysed using a Nanodrop 2000 (NanoDrop™, Thermo Fisher Scientific), enabling the measurement of concentration (ng/µl) as well as purity via absorbance values at 260/280 and 260/230 nm. The Nanodrop 2000 was first cleaned with 70% ethanol, and then 'blanked' with 1 µl of either dH_2O or EB buffer (Qiagen) depending on plasmid extraction DNA elution solution used. Subsequently, 1 µl of plasmid containing solution (in EB buffer or dH_2O) was pipetted onto the Nanodrop 2000 reader, and nucleic acid concentration and purity measured.

2.1.7 Primers for PCR, mutagenesis, cloning and sequencing

A range of primers were designed and ordered for this study. Project specific primers will be reported within relevant chapters. Generic primers used for sequencing of pI.18 and phCMV1 genes were designed by previous students in the laboratory, located on either side of the MCS site, allowing amplification and sequencing of the gene of interest for each plasmid, regardless of nucleotide differences. These primers are listed in Table 2.2.

Table 2.2. Primers used for the amplification of cloned genes within expression plasmids pI.18 (Int_pI.18 Fwd and Rev) and phCMV1 (phCMV1 Fwd and Rev).

Primer name	Sequence	NT position
Int_pI.18 Fwd	5' TTCTGCAGTCACCGTCCTTGACA 3'	1134-1153
Int_pI.18 Rev	5' GTATACAATAGTGACGTGGG 3'	1430-1449
phCMV1 Fwd	5' TAATACGACTCACTATAGGG 3'	759-778
phCMV1 Rev	5' TATGTTTCAGGTTCAGGG 3'	986-1003

2.1.8 Sanger sequencing

Sequencing was outsourced to GATC Biotech. We utilised their LIGHT run option, using ~ 100ng of target DNA with 10 pmoles of primer. These were sent to their facility and sequences mailed to us or stored on their web server for download. Analysis was carried out using the BioEdit software (Hall 1999), whereupon sequences from forward and reverse reactions were checked and compiled into one gene sequence. Subsequently a BLAST was carried out or alignment using Clustal Omega (S F Altschul et al. 1997; Stephen F. Altschul et al. 1990; Boratyn et al. 2012; Camacho et al. 2009; W. Li et al. 2015; Madden et al. 1996; McWilliam et al. 2013; Morgulis et al. 2008; Sievers et al. 2011; States and Gish 1994; J. Zhang and Madden 1997; Z. Zhang et al. 2000).

2.1.9 Polymerase chain reaction (PCR)

PCR reactions were carried out using several enzymes or kits, depending on availability. Standard PCR was carried out using AccuPrime™ Pfx (Thermo Fisher Scientific). 22.5 µl of AccuPrime™ Pfx SuperMix was added to a microcentrifuge tube with 1 µl of DNA template (~200ng) and forward and reverse primers (200nM final concentration) in a total volume of 25 µl. The microcentrifuge tube was then briefly centrifuged to consolidate the materials at the bottom of the tube. Reactions were then carried out according to the parameters listed in Table 2.3, in a Mastercycler thermal cycler (ep Gradient, Eppendorf).

Table 2.3. Polymerase chain reaction parameters for AccuPrime™ Pfx DNA polymerase.

Step	Temperature	Time period
Initial denaturation	95°C	5 m
35 Cycles	Denaturation: 95°C	15 s
	Annealing: 55-65°C	30 s
	Extension: 68°C	60 s per KB
Samples held at 4°C		

For the production of cHA plasmids Sol CHM and CS CHM, Phusion® High-Fidelity DNA Polymerase (New England Biolabs) was used. In this case, 4 µl of 5X Phusion Buffer, 0.4 µl of 10mM dNTPs, 1 µl of Fwd and Rev primers each, 0.2 µl of Phusion DNA polymerase and ~200ng of template DNA was added to a microcentrifuge tube and made up to 20 µl using dH_2O. The microcentrifuge tube was then briefly centrifuged to consolidate the materials at the bottom of the tube. Reactions were then performed as shown in Table 2.4, in a Mastercycler ep Gradient (Eppendorf) thermal cycler.

Table 2.4. Polymerase chain reaction parameters for Phusion® High-Fidelity DNA Polymerase.

Step	Temperature	Time period
Initial denaturation	98°C	30 s
25-35 Cycles	Denaturation: 98°C	10 s
	Annealing: 45-72°C	30 s
	Extension: 72°C	30 s per KB
Final extension	72°C	5 m
Samples held at 4°C		

Gradient PCR was performed using Phusion® High-Fidelity DNA Polymerase, under the same parameters as listed previously, with one exception. Several microcentrifuge tubes were set-up as previously, and the Mastercycler ep Gradient parameters altered to provide a gradient of annealing temperatures for each tube.

2.1.10 DNA digestion

DNA digestion was carried out using FastDigest restriction endonucleases obtained from ThemoFisher Scientific. PCR products or plasmids were incubated under various parameters listed in Table 2.5. *KpnI, HindIII, EcoRI* and *BamHI* were all used in diagnostic digests for the plasmid pI.18 as well as diagnostic digests for all cHAs produced (Chapter 3). These diagnostic tests were carried out to ensure the correct gene was present in the sample

tested, whether PCR product or existing plasmid after DNA purification. For Plasmid DNA, 1 µl of FastDigest *HindIII* enzyme was mixed with ~1 µg DNA, 2 µl 10X FastDigest Buffer and made up to 20 µl with dH_2O. The reaction was incubated for 15 minutes at 37°C in a Mastercycler thermal cycler and then the enzyme was inactivated at 80°C for 10 m. For PCR products, 0.2 µg DNA was used and *HindIII* digestion carried out for 20 m. For *KpnI* digestion, all parameters remain the same except the digestion time which was 5 m for both plasmid and PCR DNA. *KpnI* was inactivated after digestion at 80°C for 10 m. See Table 2.5 for a table of restriction digestion reaction conditions.

Table 2.5. Parameters for the use of FastDigest enzymes in single digestions of Plasmid or PCR products.

Enzyme	Reaction Temperature	Digestion time (m)	Thermal inactivation
KpnI	37°C	5	80°C, 5 m
HindIII	37°C	Plasmid: 15	80°C, 10 m
		PCR product: 20	
EcoRI	37°C	Plasmid: 15	80°C, 5 m
BamHI	37°C	Plasmid: 5	80°C, 5 m

Double digests were also performed using FastDigest enzymes, Plasmid DNA was incubated with 1 µl of *BamHI* and *EcoRI* each, 4 µl of 10X FastDigest Buffer, 1 µg of plasmid DNA and made up to 40 µl with dH_2O. The mixture was incubated at 37°C for 15 m in a Mastercycler thermal cycler and heat inactivated at 80°C for 5 m.

2.1.11 DNA gel electrophoresis

DNA gel electrophoresis was carried out throughout the DNA phases of each project, in order to determine the size of PCR products and plasmids (digested and in various coiled states). In general, 1% agarose gels were used. These were produced by dissolving agarose powder (Fisher Scientific, cat: BP1356) in 0.5x Tris-Acetate-Ethylenediaminetetraacetic acid EDTA (TAE buffer). This was carried out in a 250 ml conical flask and the mixture was encouraged to form a solution by heating for 1 m intervals in a microwave with mixing in-between heating steps. Once dissolved, the 1% agarose solution was left to cool, whereupon Ethidium Bromide was added to a final concentration of 0.1 µg/ml. In several experiments, SYBR safe DNA gel Stain (Thermo Fisher Scientific, cat: S33102) was used as an alternative, with 5 µl used for every 100 ml of agarose. Gels were cast and allowed to set with appropriate moulds and well inserts as to allow an adequately thin gel to be produced.

DNA samples were loaded into wells after being mixed with 5X loading dye (QIAGEN, Cat: 239901) at a 5:1 ratio. GeneRuler 1kb DNA Ladder Mix (Thermo Fisher Scientific, cat: SM0311) was used to flank sample wells and provide a molecular weight to compare to. For PCR products deemed suitable for DNA extraction, samples were re-run using 1% UltraPure™ Agarose (Invitrogen, cat: 6500-500). Gels were analysed for DNA migration using a transilluminator (UVItec, cat: BXT-26.MX) with G:Box Chemi XT Imaging System (Syngene) and gels were visualised using GeneSnap software (Syngene).

2.1.12 DNA gel extraction

In cases when PCR reactions did not give rise to the desired fragment exclusively, DNA extraction was carried out from excised fragments of agarose gel, using the QIAquick Gel Extraction Kit (cat: 28704). Appropriate segments were excised from agarose gels after gel electrophoresis, ensuring to carry over as little agarose as possible to the DNA extraction step. Excision was performed using a scalpel on a transilliuminator. Each excised fragment was inserted into a pre-weighed 1.5 ml microcentrifuge tube, and weighed. 5 volumes of PB buffer was then added per 100 mg of gel and tubes were incubated at 50°C for 10 m or until agarose was completely dissolved. 1 volume of isopropanol was then added per volume of gel used and the solution passed through a QIAquick column by centrifugation at 13,000 RPM for 1 m. For larger volumes this step was repeated until all of the solution was used up. Flow through was discarded and 0.5ml buffer QG was added. Columns were then centrifuged at 13,000 RPM for 1 m. Subsequently, 0.75 ml of buffer PE was added to each column and they were further centrifuged at 13,000 RPM for 1 m. Flow through was discarded and columns centrifuged again under the same conditions. Finally, DNA was eluted using 50 µl of buffer EB or dH_2O (70°C) by centrifugation. Purified fragments were then used in further gel electrophoresis in order to confirm the correct size fragment was excised, or used in downstream experiments.

2.2 Bacteria methods

2.2.1 Antibiotic stocks, liquid and solid media

Ampicillin (amp) sodium salt (Fisher Scientific, cat: BP1760) and kanamycin (kan) sulphate (Fisher Scientific, cat: BP906) were dissolved in dH2O. Each powder was weighed on a

sensitive scale and made up with dH2O to a concentration of 100 mg/ml (amp) or 10 mg/ml (kan). These were sterile filtered through a 0.45 µm filter (Merk Millipore, cat: SLGP033RS). Amp was used at a concentration of 100 µg/ml in LB broth and 200 µg/ml in LB agar plates. Kan was used at a 50 µg/ml concentration in both applications. Luria Bertani (LB) agar (Fisher Scientific, cat: BP1425), and LB Broth (Fisher Scientific, cat: BP1426) were employed for solid and liquid culture of bacteria respectively. Each reagent, in powder form, was dissolved in dH_20, adhering to manufacturer's guidelines (16g/400 ml agar and 12.5g/500 ml broth) in autoclavable media jars. Super Optimal Broth with Catabolite repression (SOC) medium was obtained from Invitrogen (cat: 15544-034).

2.2.2 Transformation of Escherichia coli (E.coli) cells

Plasmid stocks were produced using the DH5α strain of E. *coli* (Invitrogen, cat: 18265-017). DH5α cells were kept at -80°C in aliquots of 25 µl. Transformation was carried out by addition of ~100 ng of plasmid DNA to 5 µl of DH5α cells with gentle mixing. The mixture was then incubated on ice for 20 minutes whereupon the cells were heat shocked for 30 seconds using an AccuBlock™ Digital Dry Bath (Labnet International, cat: D1100-230 V). Tubes were then incubated on ice for 2 minutes whereupon 200 µl of SOC medium, pre-warmed to room temperature (RT) was added. This mixture was then incubated at 37°C, 225 RPM in a New Brunswick™ Scientific C25KC Incubator Shaker, before 100 µl was removed to be plated onto agar plates with a relevant antibiotic. Plates were then placed in an incubator (Genlab, cat: INC/75) at 37°C overnight, whereupon colonies were assessed and analysed.

2.2.3 Plasmid extraction from bacterial cultures

Plasmid stocks were produced in DH5α E. *coli* and then grown up in liquid broth with relevant antibiotics. Plasmids were extracted using QIAprep spin miniprep kit (Qiagen, cat: 27106) or QIAGEN Plasmid Midi Kit (cat: 12143) using the manufacturer's instructions. The QIAprep spin miniprep kit was used for the majority of plasmids, while the QIAGEN Plasmid Midi Kit was used for production of pCSFLW, HAT, TMPRSS2, TMPRSS4, pI.18 and cHA bearing plasmids pI.18-CS CHM or pI.18-Sol CHM. Bacterial transformants were picked from the agar plates resulting from Section 2.2.2, representing one plasmid clone per colony. One colony was picked and inoculated into 5-10 ml of LB broth with appropriate antibiotic (or

200-500 ml for MIDI prep) using a pipette tip, and incubated overnight at 37°C and 225 RPM. LB broth containing bacterial transformants was then centrifuged at 2500 RPM for 10 minutes in a Sorvall™ Legend™ RT centrifuge in order to form a pellet of bacteria. Subsequently, the manufacturer's instructions were followed. Bacterial pellet was resuspended in buffer P1, then buffer P2 was used to lyse bacteria, and the solution was then neutralised using buffer N3. Solutions were then centrifuged for 10 minutes at 13,000 RPM in a tabletop centrifuge (Thermo Fisher Scientific, cat: 10524723) whereupon the supernatant was decanted into QIAprep 2.0 spin columns. Columns were centrifuged for 60 s at 13,000 RPM and flow through discarded. Buffer PB was then added; tubes centrifuged again for 60 s at 13,000 RPM and flow through discarded. Buffer PE was then added; tubes centrifuged for 60 s at 13,000 RPM and flow through discarded. Finally, tubes were centrifuged for a further 60 s at 13,000 RPM and DNA eluted from the QIA membrane using 50 µl of water at 70°C or EB buffer. Eluted DNA was then analysed using a NanoDrop™ 2000 Spectrophotometer (NanoDrop™ Products, Thermo Fisher Scientific).

2.3 PV methods

2.3.1 PV production

Firefly luciferase PVs were produced by transient co-transfection of HEK293T/17 cells using branched Polyethylenimine (PEI, Sigma, cat: 408727-100ML) in 6-well Nunc™ plates (Fisher Scientific, cat: 10119831). A DNA mix (Table 2.6) comprising of the various plasmids/genes required for each PV was produced depending on the number of wells of a 6-well plate required for transfection. To this, 100 µl of OptiMEM® was added per well, and a further 100 µl added to a separate tube with 17.5 µl of PEI (1 mg/ml) per well. The PEI tube contents were then added to the DNA mix tube whereupon the contents were incubated at RT for 20 minutes with frequent mixing. After incubation, 6-well cell culture media was changed (2 ml/well), and the transfection mix was added drop wise to each well containing 60-80% confluent HEK293T/17 cells seeded the day before (approximately $4x10^5$ cells per well). 6-well plates were lightly swirled to ensure even dispersal of the transfection mix, plates were then incubated at 37°C, 5% CO_2 for 48 h, with media being replaced approximately 12h after transfection to remove traces of PEI. Supernatants were harvested 48 h post transfection using a sterile syringe and 0.45 µm mixed cellulose ester membrane

filter (Fisher Scientific, cat: 10460031). Supernatants were kept at -80°C alongside aliquots for titration in micro centrifuge tubes.

Other transfection reagents were used in this study, including, Endofectin Max and Endofectin Lenti (GeneCopoeia inc, cat: EFM1004-01/02 and EF001/EF002). In both of these cases, transfection was carried out according to manufacturer's guidelines as follows. A DNA mix of the relevant plasmids was prepared (E.g. Table 2.6), and diluted in 200 µl of OptiMEM® per well of a 6-well plate. A second tube was prepared with a further 200 µl of OptiMEM® and 2 µl of Endofectin for every µg of plasmid DNA. Contents of each tube were then mixed, incubated at RT for 25 m and then added to a 60-80% confluent HEK293T/17 monolayer with 10ml of DMEM (In lieu of 8 ml). Supernatants were then harvested 48 h post transfection and filtered using a sterile syringe and 0.45 µm mixed cellulose ester membrane filter to clarify cell debris. Endofectin-Max transfections were performed using antibiotic free medium, with cells cultured in the absence of antibiotics for the passage prior to transfection. Endofectin Lenti transfections were performed with standard DMEM +10% FBS, 1% P/S. The plasmid quantities listed in Table 2.6 represent the general optimised quantities for PV production for all PVs produced. PV bearing glycoproteins requiring different parameters are listed in the relevant chapter methods. NA bearing plasmids can be replaced by the addition of exogenous NA (exNA, Sigma, cat: N2876) after media replacement, 12h post transfection. See Figure 2.5 for a schematic representation of the PV production process.

Table 2.6. DNA mix plasmid quantities. Standard quantities of plasmids required for the production of HA and NA bearing PVs. NA plasmid can be substituted by addition of exogenous NA 12h post transfection.

Plasmid	Plasmid quantity (ng/well)
p8.91	500
pCSFLW	750
pI.18-HA	500
pI.18-NA	250
Protease encoding plasmid	50-500

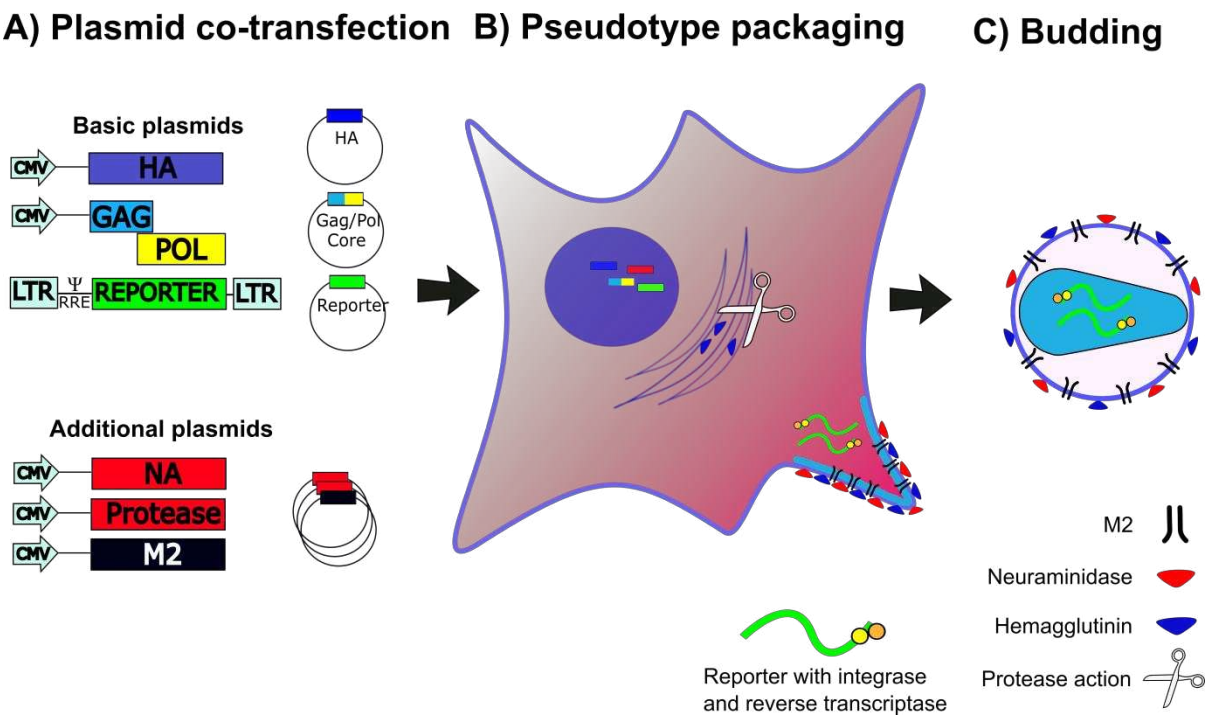

Figure 2.5. Production of influenza PV by co-transfection of multiple expression plasmids into HEK293T/17 cells. Basic plasmids coding for the constituents of the desired PVs are transfected into HEK293T/17 cells alongside additional plasmids, if required. HEK293T/17 cells transcribe and translate the relevant HIV-1 core genes and influenza glycoproteins which are then packaged at the cell surface and bud off in an HIV-1 dependent manner. Particles are released through the NA glycoprotein or exNA added 12h post transfection. Figure from (Carnell et al. 2015).

2.3.2 Pseudotype titration protocol

Titration of firefly luciferase PV was carried out by transduction of susceptible cells (HEK293T/17 for the majority of influenza PV) in 96-well white plates (Thermo Fisher Scientific, cat: 136101). 100 µl of PV containing supernatant is added to row A for each test sample. One row is left empty at this stage for cell only control and one is used for 100 µl of VSV-G PV as a transduction control. 50 µl of DMEM (+10% FBS, 1% P/S) is added to all other wells on the plate, and a 1:2 serial dilution is carried out from row A to row H, with the final 50 µl discarded. This leaves a plate with a dilution series of PV in 50 µl of DMEM, to which $1x10^4$ target cells in a volume of 50 µl are added. Plates are then incubated at 37°C, 5% CO_2 for 48 h. The liquid contents of each well are then removed using a Vacusip portable aspiration system (Integra Biosciences ltd, Surrey, United Kingdom), and 25 µl of a 50:50 mix of Bright-Glo™ Luciferase Assay System and PBS (Pan Biotech, cat: P04-36500) added per well. Plates are then incubated at RT for 5 m whereupon results are recorded using a GloMax 96 Multi detection system luminometer (Promega). Analysis was performed by multiplication of RLU values per well with the corresponding dilution factor, providing a

result in RLU/ml which is used for comparison of RLU titres (Table 2.7). Care is taken at this stage to ensure a linear relationship is present between serial dilution and luminescence output. The effect of multiplication of a non-functional PV preparation can give false positive results due to the nature of the multiplication effect (example shown in yellow, Table 2.7).

In the projects reported in this thesis, titrations were carried out with several controls, to which test variables were compared. VSV-G bearing PV were used as a transduction control, due to their use of a ubiquitous receptor, LDLR (Finkelshtein et al. 2013). VSV-G PV produce very high RLU/ml counts (>$10E^9$) when produced using the standard protocol outlined in section 2.3.1. Testing these alongside other PV allows confidence to be attributed to the results, as a high VSV-G titre shows that cells are correctly producing luciferase and that the substrate is not compromised. Other controls used include PV bearing the HA from A/Vietnam/1194/2004, which is a high titre influenza PV. A negative production control was employed in some instances, where PV were produced using p8.91 and pCSFLW plasmids only, creating Delta Envelope (Δ Env). These PV sometimes succeed in transducing cells to some degree (titres $10E^4$-$10E^5$ RLU/ml), despite a lack of glycoprotein, and can be used as a benchmark for RLU/ml titres.

2.3.3 Pseudotype based microneutralisation assay (pMN)

The pMN assay was the primary assay used in this project and performed in 96-well white plates as in the titration assay. The pMN assay is carried out using 8 and 12 channel multichannel pipettes and plate centrifugation carried out in an ELMI CM-6MT centrifuge with 6M04 rotor. The antibody source (Serum, mAb) is first transferred into the wells of row A at the desired starting quantity/concentration, with rows assigned for virus only, cell only and positive/negative neutralisation controls. Wells containing the antibody source are made up to 100 µl, all other wells (rows B to H) are filled with 50 µl of DMEM (+10% FBS, 1% P/S). Serial 1:2 dilution is then carried out with frequent mixing from row A to row H. The final 50 µl is discarded. This results in a 96-well plate with serial dilutions of test samples at known dilution or concentration; in total volumes of 50 µl. Plates are centrifuged at this point to ensure all samples remain in the liquid portion of each well. Subsequently, the PV of choice for each experiment is diluted in order to give approximately $1x10^6$ RLU per 50 µl, based on previous titration results. 50 µl of this is then added to each well on the 96-well

plate with the exception of cell-only control wells, and plates are centrifuged again to ensure all added virus is present in the liquid portion of each well. The plates are then incubated at 37°C, 5% CO_2 for 1 h in order to allow antibody time to bind to the viral glycoproteins. The final step involves addition of $1x10^4$ target cells per well in a volume of 50 µl. Plates are then incubated at 37°C, 5% CO_2 for 48 h. After this, the liquid contents of each well are then removed using a Vacusip portable aspiration system, and 25 µl of a 50:50 mix of Bright-Glo™ Luciferase Assay System and PBS are added per well. Plates are then incubated at RT for 5 m whereupon results are read using a GloMax 96 Multi detection system luminometer. See Figure 2.6 for a schematic representation of the pMN assay.

Various controls are employed in the pMN assay. First, PV only and cell only wells are assigned per 96-well plate in order to ascertain the actual input (rather than expected input) of PV RLU used in the assay. The cell only wells act as a background value and contamination control. PV only and cell only RLU values represent 0% and 100% neutralisation respectively when data is analysed – wells with serial dilutions of serum are then normalised based upon these 100% and 0% neutralisation thresholds (detailed in section 2.3.4). Each set of experiments will also have positive and negative serum wells acting as controls for the neutralisation of the PV used. Due to the nature of the HA glycoprotein, the most matched antiserum standard or positive serum sample would be used as a positive control, based upon previous experiments. Negative serum used is FBS which is used in a similar quantity to other serum test wells. In some cases, mAbs were used as controls in the absence of a suitable positive serum sample.

Table 2.7. Example data analysis of PV titration results. Raw data luminescence values (RLU) are multiplied up to RLU/ml (highlighted green), and RLU/ml values averaged to give an Average RLU/ml value. Care must be taken to ensure a linear relationship between RLU and PV dilution, as multiplication can lead to high RLU/ml titres which will artificially inflate Average RLU/ml titres (highlighted yellow).

Multiplication factor	H1 PV	VSV-G PV	Virus X
20	5.58E+05	7.17E+08	3.05E+03
40	2.90E+05	5.63E+08	1.10E+03
80	1.43E+05	3.79E+08	6.29E+03
160	6.17E+04	2.16E+08	8.80E+02
320	3.10E+04	1.36E+08	5.43E+03
640	2.41E+04	6.18E+07	3.39E+03
1280	7.15E+03	3.06E+07	1.96E+03
2560	3.62E+03	1.44E+07	3.33E+03
RLU/ml	1.12E+07	1.43E+10	6.11E+04
RLU/ml	1.16E+07	2.25E+10	4.40E+04
RLU/ml	1.14E+07	3.03E+10	5.03E+05
RLU/ml	9.87E+06	3.46E+10	1.41E+05
RLU/ml	9.91E+06	4.35E+10	1.74E+06
RLU/ml	1.54E+07	3.96E+10	2.17E+06
RLU/ml	9.16E+06	3.92E+10	2.51E+06
RLU/ml	9.26E+06	3.69E+10	8.54E+06
Average RLU/ml	1.10E+07	3.26E+10	1.96E+06

2.3.4 pMN analysis

The data collected with the pMN assay was analysed using Graph Pad Prism software (Version 7). Non-linear regression analysis was performed, with each data point normalised between 100% and 0% neutralisation based on cell only and virus only controls, which represent 100% and 0% neutralisation respectively. These normalised values were then plotted alongside their corresponding dilution factor (and log10 dilution factor), which were used to plot a standard curve and extrapolate an IC_{50} (inhibitory concentration 50%) value for the comparison of different serum samples against the same PV. The IC_{50} represents the reciprocal dilution or concentration required for an inhibitor to reduce the PV input ($1x10^6$) to 50% ($5x10^5$). This 50% value is frequently used across the serological field, representing the linear (hill slope) section of a neutralisation curve where the serum is the variable factor. For data generated using serum, dilution factor was used for the analysis, and the hill slope of the generated curves was constrained to be <0. For mAbs/nanobodies at a known concentration, concentration was used for the analysis, hill slopes were then constrained to

>0. Correspondingly, neutralising antibody titres (IC_{50} or other percentile) generated through pMN against serum samples are given as a reciprocal dilution factor (e.g. An IC_{50} of 500 requires a serum sample to be diluted 1:500 to neutralise 50% of the PV used), whereas neutralising antibody titres for mAbs are given in concentration (e.g. An IC_{50} of 500 ng/ml requires a concentration of 50 ng/ml of mAb to neutralise 50% of the PV used.)

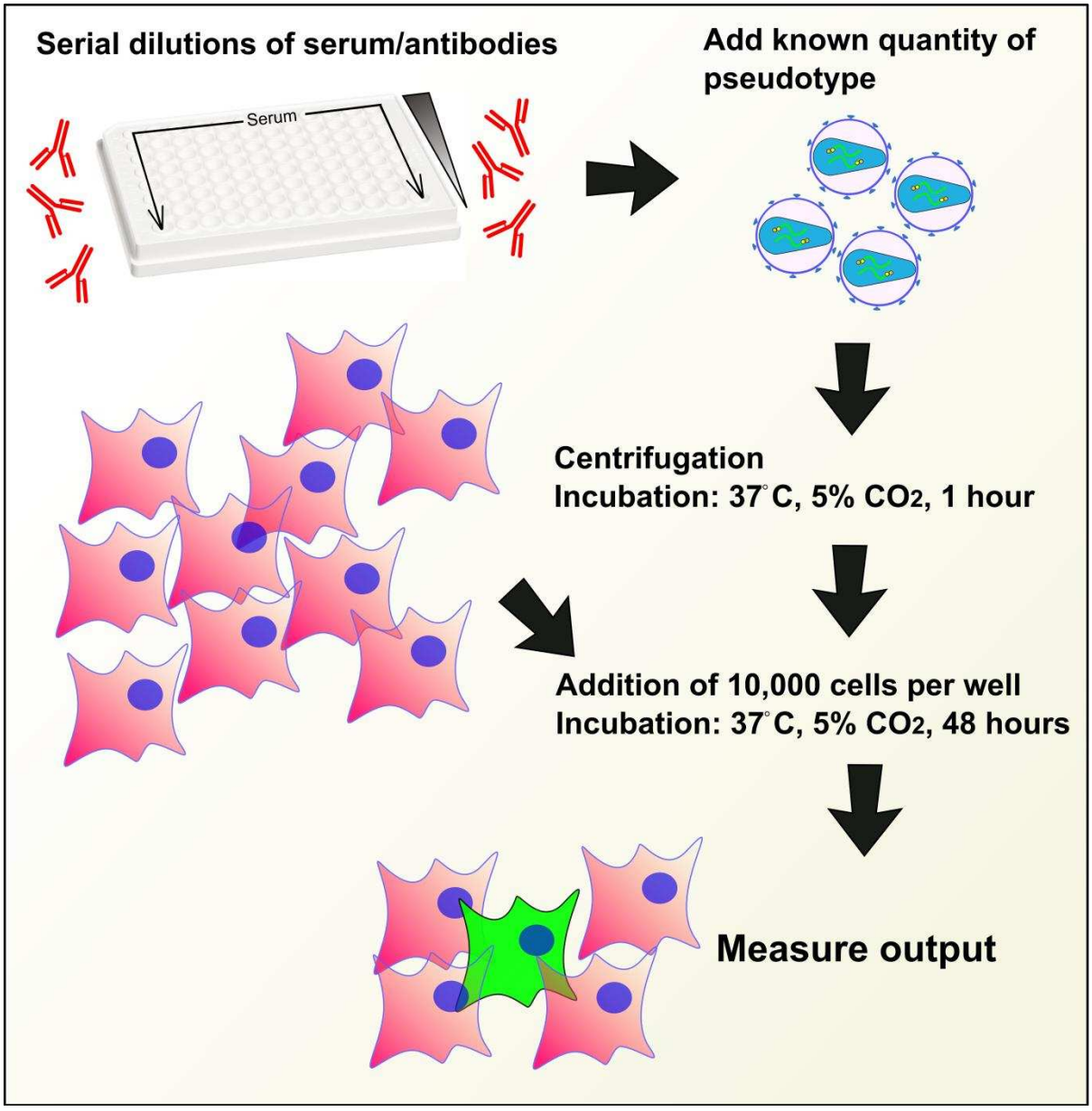

Figure 2.6. Schematic of the Pseudotype based neutralisation assay (pMN). This assay is performed by serial dilution of serum or mAbs in 96-well white plates followed by addition of a known quantity of PV based on previous titration results. Approximately $1x10^4$ HEK293T/17 cells are then added and plates incubated for 48 h at 37°C, 5% CO_2. Data is collected after 48 h depending on the reporter used, in the case of firefly luciferase, cells are lysed and luciferase substrate is added in the form of Bright-Glo™ and results collected using a GloMax 96 luminometer. Figure from (Carnell et al. 2015).

2.3.5 Pseudotype based ELLA

PV based ELLA was performed largely according to standard methods produced and detailed by the CONSISE group (Eichelberger et al. 2016; Gao et al. 2016). PV containing supernatants were serially diluted in 120 µl of sample diluent from a starting well of 240 µl PV supernatant, in clear 96-well plates (Sigma, cat: M9410-1CS). 50 µl of each dilution point was then transferred to 50 µl of sample diluent in a 96-well maxisorp plate (Thermo Fisher Scientific, cat: 439454) previously coated in fetuin (Sigma, cat: F3385), in duplicate. These plates were then incubated for 16-18 h in a humidified incubator at 37°C, 5% CO_2. Subsequently, plates were washed 6 times with wash buffer, then 100 µl of PNA-HRPO (Sigma, cat: L7759) diluted (1:500 or 1:1000) in conjugate buffer was added per well. Plates were incubated at RT in the dark for 2 h whereupon plates were washed 3 times with wash buffer to remove traces of PNA-HRPO. 100 µl of OPD substrate (Sigma, cat: P8287) dissolved in citrate buffer (Sigma, cat: P4922) was then added and plates were incubated at RT in the dark for 10 minutes. Reactions were stopped by the addition of 100 µl 1N H_2SO_4 and plates were read using a Tecan Sunrise (Jencon) ELISA plate reader at 492nm for 0.1sec. Background results were subtracted from sample wells and plotted using PRISM GraphPad.

For inhibition assays, 24 µl of serum (in 240 µl) was diluted across a 96-well clear plate. 50 µl of these dilutions were then transferred to a 96-well maxisorp plate, previously coated in fetuin, in duplicate. A set amount of virus, as calculated from the titration ELLA, yielding a desired OD_{492} per well, was then added and plates left to incubate overnight. The remaining steps are identical to the titration ELLA. Exogenous neuraminidase (exNA) was used as a fetuin digestion control for ELLA titrations. Antisera or positive serum samples suitable for the PV strain used were employed as positive or negative controls in the ELLA inhibition assay.

2.4 Cell work

2.4.1 Cell lines

Multiple cell lines were used in this project for various experiments. In general, HEK293T/17 cells were used for the production of PV as well as a target cell for transduction in titration and pMN assays. MDCK I, MDCK II, rat intestinal epithelial 1495 (RIE 1495) cells were used as target cells for titration and pMN using H17 bearing PV. Human embryo kidney cells

(HEK293T/17) were obtained from Dr Davide Corti, Institute for Research in Biomedicine, Switzerland. MDCK cells used originate from two sources. MDCK I cells were obtained from Prof Sarah Gilbert, University of Oxford. MDCK II and rat intestinal epithelial cells (RIE 1495) were obtained from Dr Martin Schwemmle, Institute of Virology, University of Freiberg, Germany. All cell lines were cultured in DMEM (Pan Biotech, cat: P04-04510) with 10% heat inactivated FBS (Pan Biotech, P40-37500HI) and 1% penicillin/streptomycin (Pan Biotech, cat: P06-07100).

2.4.2 Cell subculture

Cells were subcultured 2-3 times per week depending on project requirements. Cells were diluted in differing volumes dependent on the rate of growth of each cell line. HEK293T/17 Cells were subcultured 1:4 on Mondays and Wednesdays and 1:8 on Fridays in 10 cm^2 Nunc™ dishes (Sigma, cat: 150318). Cell monolayers were washed once with 1 ml Trypsin-EDTA (Pan Biotech, cat: P10-040100) and then incubated with 2 ml Trypsin-EDTA for 5 minutes, allowing the cells to detach. Cells were then resuspended with 6 ml DMEM (+10% FBS, 1% P/S), giving a total volume of 8 ml. Resuspension was performed vigorously in order to ensure the majority of cells were dispersed and not clumped. For the purposes of future cell culture, 1 or 2 ml of the resuspended cells were added to fresh 10cm^2 dishes containing 8 ml of DMEM in order to give 1:4 or 1:8 dilutions of cells for subsequent work. For pseudotype virus production, 200 µl of cell suspension was used per well of a 6-well plate (approx 4x10^5cells). For other cell lines, two washes were performed using PBS in lieu of Trypsin-EDTA.

2.4.3 Freezing/thawing of cell lines

In order to maintain stocks of low passage cells, cells were frozen and stored at -80°C upon acquisition from each stated source. After initial cell culture and several passages in the laboratory, confluent cell monolayers were washed and trypsin was added as in previous cell culture methods. Detached cells were then resuspended, centrifuged (ELMI CM-6MT centrifuge with 6M Rotor, Spectra Services) at 300 rpm for 5 minutes in 15 ml falcon tubes (Greiner Bio-One, cat: 188271) using a 15 ml tube attachment. Media was then decanted, and cell pellets resuspended in FBS with 5% DMSO (VWR International, cat: 282164K). 1 ml of this cell/FBS/DMSO mix was then aliquoted per 1.5ml cryotube (Corning, cat: 430915)

and placed inside a Mr Frosty (Fisher Scientific, cat: 5100-0001) in order to be brought to -80°C at 1°C/minute, minimising cell death during the freezing process. Multiple aliquots of low passage cells were produced for each cell line obtained, around $1x10^6$ cells were frozen per 1 ml. When currently in-use cells had reached a passage number of over 30, aliquots were removed from the -80°C freezer, rapidly thawed by hand and liquids were transferred to a $10cm^2$ dish or T75 flask containing 10 or 15 ml of DMEM +10% FBS 1% P/S. Media was replaced after overnight incubation at 37°C, 5% CO_2 in order to remove traces of DMSO. Cells were subcultured at least two times after this step before being used in PV production or pMN assays.

2.4.4 Justification for use of non standard Bright-Glo quantities

A preliminary test was carried out using the Bright-Glo™ reagent, in order to maximise its use in the projects detailed in this thesis. The Promega Bright-Glo™ manual suggests that addition of 50 µl of Bright-Glo™ directly into the wells of 96-well plates post 48 h incubation. However, due to the difference in DMEM volumes for titration (100 µl final) and pMN (150 µl final), addition of 50 µl of Bright-glo™ leads to a difference in concentration of the luciferase substrate and cell lysis agent between assays. This discrepancy in volumes of media could lead to anomalous results; therefore this preliminary test was carried out in order to evaluate the removal of DMEM from 96-well plates prior to addition of a mix of pre-diluted Bright-Glo™.

Two PV bearing the influenza HA from A/gyrfalcon/Washington/41088-6/2014 (H5, henceforth referred to as Gyr) with WT or human codon optimised (Opt) sequences were tested alongside VSV-G PV and cell only controls. Three 96-well titrations were carried out, with Gyr (WT) and Gyr (Opt) titrated in quadruplicate, alongside VSV-G PV and cell only being titrated once each per plate. Each plate was titrated according to the standard method described in section 2.3.2 with 100 µl of PV containing supernatant diluted 1:2 down a 96-well plate. All three plates were incubated for the standard 48 h at 37°C 5% CO_2 in a humidified incubator, whereupon the contents of each well were removed using a Vacusip. 50 µl of a 50:50 mix of PBS and Bright-Glo™ was added to the wells of plate 1 (T1), 25 µl of the same mix to plate 2 (T2) and a 50 µl of a 25:75 mix of PBS and Bright-Glo™ was added to the third plate (T3). After a 5 minute incubation period, plates were read for luminescence using a Glomax 96 plate reader and results analysed using Microsoft Excel and

Prism Graph Pad. Initial RLU/ml results showed titres in the same range, with a slightly reduced titre recorded for T3 PV which was performed with the lower concentration of Bright-Glo™ (25:75), see Figure 2.7. A Wilcoxon paired, nonparametric T test was carried out between the grouped results from T1, T2 and T3. Results for Gyr (WT) showed effective pairing between all three groups (P=<0.0001), however differences in the median results were only seen between different concentrations of Bright-Glo. T1 and T2 results were not significantly different (P=0.0584), whereas comparing T1/T2 with T3 showed a significant difference in median values (P=0.0078). Similarly, for Gyr (Opt), pairing was effective between T1, T2 and T3 (P=<0.0001) and median values were only significantly different between T1/T2 and T3 results (P=0.0078). T1 and T2 results were not significantly different (P=0.9453). Due to these results, it was decided to carry out the projects in this thesis by removing media from 96-well plates post incubation and then incubating cells with a 50:50 mix of 12.5 µl Bright-Glo and 12.5 µl of PBS. See Figure 2.7 for RLU/ml titres generated in this experiment.

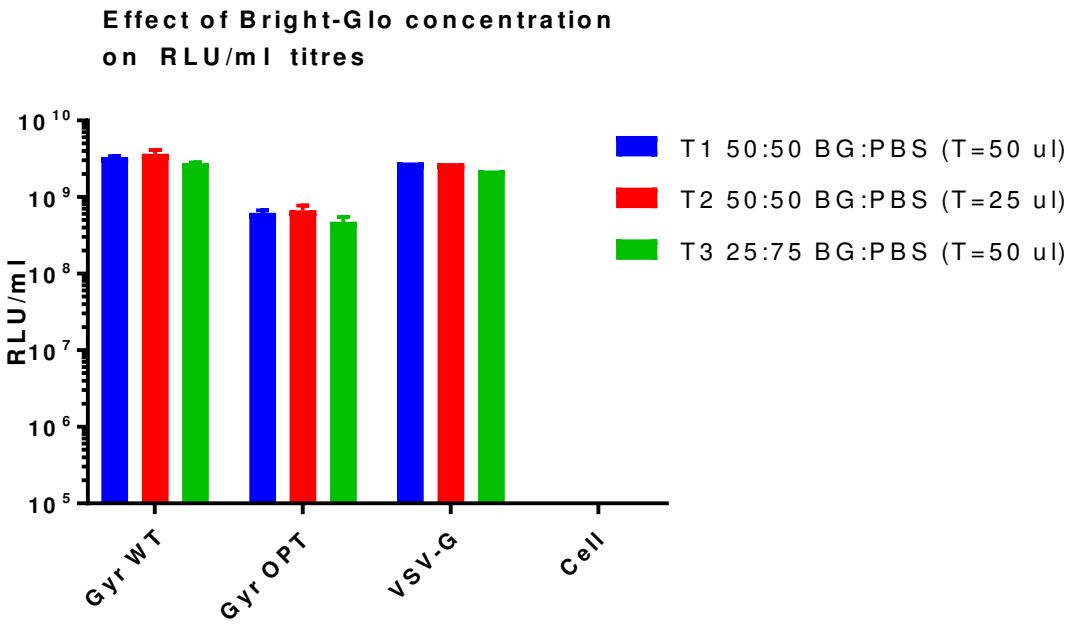

Figure 2.7. Effect of Bright-Glo™ concentration on RLU/ml titres. Reduction in quantity of Bright-Glo™ (T1 to T2) had no significant effect on RLU/ml titres, whereas reduction in concentration (T1/T2 to T3) resulted in reduced RLU/ml outputs. All experiments carried out in quadruplicate with PV bearing three different glycoptoteins (A/gyrfalcon/Washington/41088-6/2014, WT and opt, and VSV-G.

Chapter 3 : Development and utilisation of cHA bearing PV to dissect head and stalk mediated antibody responses from human serum.

3.1 Introduction

3.1.1 Universal vaccines

As described in chapter 1, universal vaccines represent a major avenue for the future of influenza vaccine research. The ability to induce a broadly protective immune response, covering multiple subtypes and persisting for multiple seasons of influenza virus disease is a worthy goal to aim for. Not only would this kind of vaccine reduce costs for administration of vaccines on a yearly basis or through reduced morbidity and mortality, the staggering costs for yearly update of influenza vaccines across the globe could be reduced and better employed.

Various methods have been employed in order to design and test such vaccines, which primarily aim at elicitation of antibodies to the conserved regions of the influenza virus, such as the stalk of the HA trimer or M2. Due to the constraints involved with the functional parts of the HA glycoprotein and its ability to change conformation to allow membrane fusion, this target is less amenable to antigenic drift and therefore likely less able evade a targeted stalk immune response.

One of the most exciting developments in the universal vaccine section of influenza virus research is the progress being made on utilisation chimeric/hybrid cHA based vaccines, reviewed by Kramer and Palese over recent years (Krammer 2016; Krammer and Palese 2013, 2014, 2015). These vaccines employ cHA, originally developed by Pica and colleagues (Hai et al. 2012; Krammer et al. 2013) and developed by this group since 2012 multiple studies have shown this approach's ability to induce broadly neutralising antibodies in mice models, covered in section 1.16 and 1.18. Vaccine immunogenicity for these trials have been tested by pMN assay as well as neutralisation of recombinant cHA bearing influenza viruses by plaque assay (Hai et al. 2012) and ELISA (Krammer et al. 2013).

A second approach has focused on the development of 'headless' HA constructs as protein vaccines allowing the host to produce an immune response against the conserved stalk region in the absence of the immunodominant globular head. This approach has been followed by other groups with varying levels of success (Mallajosyula et al. 2014; Steel et al. 2010; Valkenburg et al. 2016), covered in section 1.16. Immunogenicity data for these projects were tested by HI, ELISA, neutralisation of live virus (Steel et al. 2010) as well as pMN, competition ELISA (Mallajosyula et al. 2014; Valkenburg et al. 2016) and microneutralisation assay (Valkenburg et al. 2016).

3.1.2 Stalk antibody detection

One major obstacle impeding universal vaccine efforts is the inability of gold standard and globally trusted assays to efficiently detect the antibodies being generated by these vaccines. The HI assay, described in section 1.19 is unable to detect stalk binding antibodies as they do not impede the virus' ability to bind to the sialic acid receptor and therefore agglutinate RBCs. This has lead to a variety of approaches for the detection and characterisation of antibody responses elicited from universal vaccines. Among the methods described in section 1.19, ELISA remains the most popular as this assay is flexible and it is possible to use cHA as a substrate, allowing the detection of stalk directed antibodies with this well established system (Nachbagauer, Kinzler, et al. 2016). Other methods used include production of recombinant viruses for use in traditional neutralisation assays (Mallajosyula et al. 2014; Steel et al. 2010) as well as several studies employing reporter-based pseudotype systems such as pMN (Hai et al. 2012; Valkenburg et al. 2016). The benefits of pMN in the ability to detect functional antibodies which neutralise the action of the HA give this assay an advantage which is not apparent in the literature, with this assay still being used in conjunction with gold standard ELISA and MN. The post attachment assay, allowing neutralising antibodies to bind to HA after attachment of the HA to its receptor under cold conditions has been used previously, but is not regularly employed for the evaluation of universal vaccine immunogenicity (Edwards and Dimmock 2001; Hsueh-Ling et al. 2010).

3.1.3 2009 pandemic and stalk antibodies

Multiple studies have demonstrated or re-confirmed an increase in cross-reactive immune responses as a result of pH1N1 infection (Mahallawi et al. 2013; Medina et al. 2010;

Wrammert et al. 2011). Subsequent work has attributed this partly to similarities with the 1918 pandemic virus (Medina et al. 2010) and overall unique origin, it has been shown that sequential immunization with pH1N1 leads to increased cross-reactive neutralising antibody titres when compared to sequential immunization with a drift variant from the original vaccine (Krammer et al. 2012). This data enables us to consider the 2009 pandemic to test our cHA pMN system, as natural infection should boost heterosubtypic immunity. The effect of the 2009 pandemic is discussed in further detail in section 1.11.2.

3.1.4 Project aims

The primary goal of this project was to determine the extent of cross-reactive, stalk directed antibodies elicited by the 2009 influenza pandemic strain, through assay of human sera pre and post 2009. Various parameters render this task difficult, such as the nature of human infection and pre-existing immunity to H1 influenza viruses. Similarly, with the number of serum samples collected, it is difficult to determine the proportion of patients that had actually encountered the pandemic strain. The linked secondary goal of this project was to produce cHA expression plasmids and to employ them in a PV system in order to build up a library of group 1 influenza stalks to which antibodies could be tested. The production of cHA expression plasmids with group 2 (H3) and Influenza B stalks were secondary objectives of this project. While the cHA pMN system has been tested previously in pilot projects, this represents the broadest project undertaken to date using this system.

3.2 Methods

3.2.1 PCR and production of cHA expression plasmids

cHA plasmids were constructed by long distance PCR using oligonucleotide primers spanning two different HAs within their respective expression plasmids pI.18, as shown in Figure 3.1. DNA fragments were amplified from the expression plasmid bearing the HA stalk and HA head of choice using primers listed in Tables 3.1 to 3.3. These PCR fragments were then fused into one plasmid via the In-Fusion or Gibson Assembly methods (Gibson et al. 2009; B. Zhu et al. 2007). The first fragment consisted of the pI.18 sequence and HA stalk sequences, with an overlap of around 10 nucleotides of the target HA head region at the 5’ and 3’ termini. The second fragment consisted of the HA head region of choice, with overlaps of

the HA stalk of choice at the 5' and 3' termini. These two fragments were then incubated together with In-Fusion or Gibson assembly kits, in order to yield the pI.18 expression plasmid bearing a cHA composed of the head region from one HA (H11) and the stalk from another (H1, H3, and Flub). Figure 3.1 shows a schematic of the production process for these cHA expression plasmids.

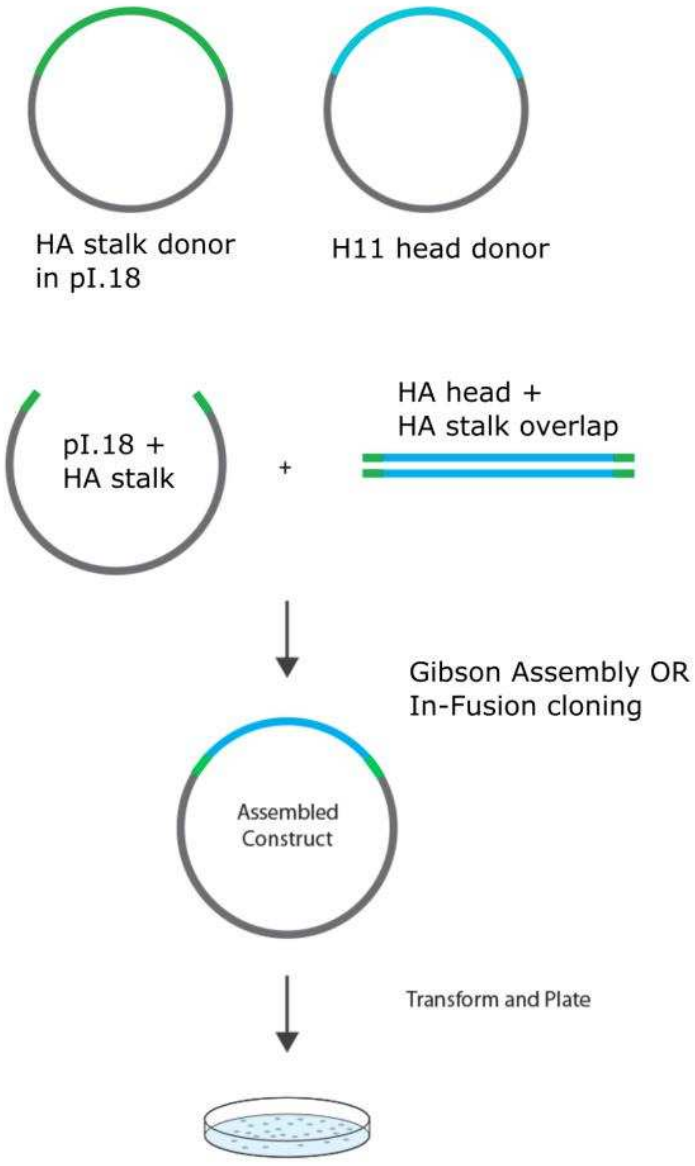

Figure 3.1. cHA expression plasmids were produced using either Gibson Assembly or In-Fusion cloning kits. PCR fragments were produced from plasmids bearing the HA stalk and HA head of interest with complementary overlap regions, leading to a cHA expression plasmid with the head and stalk region from two different plasmids, after assembly.

3.2.2 Cloning methods for the production of cHA plasmids

In-Fusion® HD Cloning system (Clonetech, cat: 639645) was used for the generation of cHA plasmids (B. Zhu et al. 2007). cHAs with stalks from A/Solomon Islands/3/2006 (Sol CHM) and 2009pdm consensus sequence (A/Texas/50/2009 or CS CHM) were produced. Original primers were designed to produce a further cHA bearing the stalk from A/Brisbane/59/2007 (Bris CHM) but this was not used in downstream applications. Briefly, Linearised plasmid (pI.18) containing the stalk from A/Texas/05/2009 or A/Solomon Islands/3/2006 and H11 head overlaps was incubated in a 1:2 ratio with H11 head PCR fragments, themselves containing overlapping sections on 5' and 3' ends complimentary with the A/Texas/05/2009 or A/Solomon Islands/3/2006 stalks. This equated to 100 ng of linearised plasmid and 200 ng of PCR head fragment. To each reaction, 1 µl of In-Fusion enzyme was added after addition of 2 µl 5X In-Fusion reaction buffer, making up the final volume to 10 µl with dH_20. Each reaction was incubated for 15 minutes at 37°C, followed by 15 minutes at 50°C, then placed on ice. The reaction volume was then mixed with 30 µl of TE buffer (pH 8), and then tested via gel electrophoresis or transformed into competent E. *coli.* Gibson Assembly® Master Mix (New England Biolabs, cat: E611S) was used to produce G2 (G2 CHM) and Flu B (Flu B CHM) cHA plasmids (Gibson et al. 2009). Briefly, linearised plasmid (pI.18) containing the stalk from B/Brisbane/60/2008 or A/Udorn/307/1972 with H10 head overlaps was incubated in a 1:2 ratio with H10 head PCR fragments, containing overlapping sections on 5' and 3' ends complimentary with B/Brisbane/60/2008 or A/Udorn/307/1972 stalk sections. This equated to 100 ng of linearised plasmid and 200 ng of PCR head fragment. To this, 10 µl of Gibson Assembly Master Mix (2x) was added, and dH_20 used to make the reaction up to 20 µl. Samples were then incubated at 50°C for 15 minutes and then stored on ice until used in gel electrophoresis or for transformation of competent E. *coli*.

Table 3.1. Primers for the generation of PCR fragments used in the production of cHA expression plasmids Bris CHM, Sol CHM and CS CHM. Forward and Reverse primers bearing the name of the cHA and fragment type (in = head fragment, out = linearised vector fragment) are listed alongside their annealing temperatures (°C).

Primer ID	Sequence	Annealing temperature °C
H11_Bris_in_fwd:	CACAACGGCAAGCTGTGCAGCATCGACGGAAAAG	64.7
H11_Bris_in_rev:	CTGACACTTGGCGTCGCAAGACTCGATATTCAGGTCGC	64.3
H1_Bris_out_fwd:	CGACGCCAAGTGTCAGACC	58.1
H1_Bris_out_rev:	CAGCTTGCCGTTGTGGCT	59.1
H11_CS_in_fwd:	CACAACGGCAAGCTGTGCAGCATCGACGGAAAAG	64.7
H11_CS_in_rev:	CTGACAGGTGGTGTTGCAAGACTCGATATTCAGGTCGC	63.1
H1_CS_out_fwd:	GCAACACCACCTGTCAGACC	57.9
H1_CS_out_rev:	CAGCTTGCCGTTGTGCTT	56.5
H1_CS_fwd:	TCTAGAGTCAAAATGAAGGCTATCCTGGTCGT	58.4
H1_CS_rev:	TCTAGAAATTTAAATACAGATCCGGCACTGC	55.3
H11_sol_out_fwd	CACAACGGCAAGCTGTGCAGCATCGACGGAAAAG	64.7
H11_sol_out_rev	TGACACTTGGCGTCGCAAGACTCGATATTCAGGTCGC	64.4
H1_sol_in_fwd	TGCGACGCCAAGTGTCAGACC	61.3
H1_sol_in_rev	GCACAGCTTGCCGTTGTGGC	62.1

Table 3.2. Primers for the generation of PCR fragments used in the production of cHA expression plasmids for G2 CHM. Forward and Reverse primers bearing the name of the cHA and fragment type (in = head fragment, out = linearised vector fragment) are listed alongside their annealing temperatures (°C).

Primer ID	Sequence	Annealing temperature °C
H10_In_Fwd	5’ CCTCAACGGGGAAAATATGCATGAAAGGAAGAT 3’	58.4
H10_in_Rev	3’ GATGCATTCAGAAATGCAGCTGTTGTCAATCAG 5’	58.1
H3_out_Rev	5’ GATCTTCCTTTCATGCATATTTTCCCCGTTGAGG 3’	58.5
H3_out_Fwd	5’ ATTGACAACAGCTGCATTTCTGAATGCATCACTC 3’	58.5

Table 3.3. Primers for the generation of PCR fragments used in the production of cHA expression plasmids for FluB CHM. Forward and Reverse primers bearing the name of the cHA and fragment type (in = head fragment, out = linearised vector fragment) are listed alongside their annealing temperatures (°C).

Primer ID	Sequence	Annealing temperature °C
H10_in_fwd	CTCAAAGGAACAGAATGCATGAAAGGAAGATCA	56.9
H10_in_rev	CGTATTTTTCGTGGAGGCAGCTGTTGTC	59
B_out_fwd	ATTGACAACAGCTGCCTCCACGAAAAATACG	59.3
B_out_rev	TGATCTTCCTTTCATGCATTCTGTTCCTTTGAG	56.9

3.2.3 Serum information

A panel of sera, designated 'Jenner Sera', was kindly provided by Prof Sarah Gilbert, University of Oxford. This panel consisted of sera taken from clinical trials involving vaccines designed at the Jenner Institute, University of Oxford. Clinical trials were carried out using NP based vaccines, therefore no detected HA response should be attributed to the effect of the vaccine. For the purpose of this study, the serum samples can be considered from the population of Oxford between 29/07/2008 and 26/10/2016. A total of 179 samples were obtained from patients just prior to and in the years following the 2009 influenza pandemic, with 13 samples from 2008, 7 from 2009, 27 from 2010, 13 from 2011 and 118 from 2012-2016. For the purpose of this study, samples were arranged according to the date on which samples were taken and then assigned a number from 1-179 in order to make results easier to analyse. Serum panel information is displayed in appendix X1. These sera were tested using the three virus chimeric pMN system consisting of parental A/duck/Memphis/546/1974 (H11), A/California/7/2009 (H1) and the CS CHM composed of the head from the parental H11 strain and stalk from parental H1 strain.

A second panel of sera, designated 'Sports Science Sera' was also used in this project. This panel consisted of 60 pairs of sera originating from a set of athletes in Scotland. These sera were tested via pMN on A/Brisbane/59/2007 (H1), A/Vietnam/1194/2004 (H5) A/Udorn/307/1972 (H3) and A/Shanghai/2/2013 (H7), representing a human seasonal (H1, H3) as well as pandemic potential avian subtype (H5, H7) per influenza group. This would allow for measurement of pan-group cross-reactive immune responses between the four subtypes tested as published previously but with the addition of human seasonal strains

(Molesti et al. 2014). Serum samples were paired, with a 12 week interval between them per patient. No action or effect was being measured for the 12 week period; samples were taken as part of an unrelated study on the effects of chronic exercise. Antibody standards were used as controls for all pMN assays. These were produced by hyperimmune stimulation, involving the vaccination of sheep multiple times with a HA protein vaccine. This was carried out by the NIBSC.

3.3 Results and discussion

3.3.1 Production of cHA expression plasmids

First, primers listed in tables 3.1-3.3 were used to produce the two components required for the production of cHA expression plasmids. Linear pI.18 DNA including the H1 stalk overlap of choice (A/Texas/05/2009 (H1), A/Brisbane/59/2007 (H1) and A/Solomon Islands/3/2006 (H1)) was produced by PCR, yielding a fragment ~5 kb in length. However the expected 5 kb product was accompanied by various nonspecific bands and smears. A shorter fragment bearing the H11 head and short overlaps for each specific H1 stalk were also produced, yielding a clean band at ~500 bp in length. See Figure 3.2 and 3.3 for the results from duplicate PCR and gel electrophoresis of the fragments generated as described above.

It was decided that gel extraction, rather than PCR optimisation was the most efficacious and cost-effective method to obtain the desired PCR fragment in pure form, due to the size of the desired fragment and lack of flexibility in primer design. Gel extraction was performed (Section 2.1.12) after excision of the bands containing the putative constructs designed in this project: linear H11 head and H1 stalk bearing fragments designed for in-fusion or Gibson assembly. Figure 3.4 shows gel electrophoresis of the purified fragments excised from the gels shown in Figures 3.2 and 3.3.

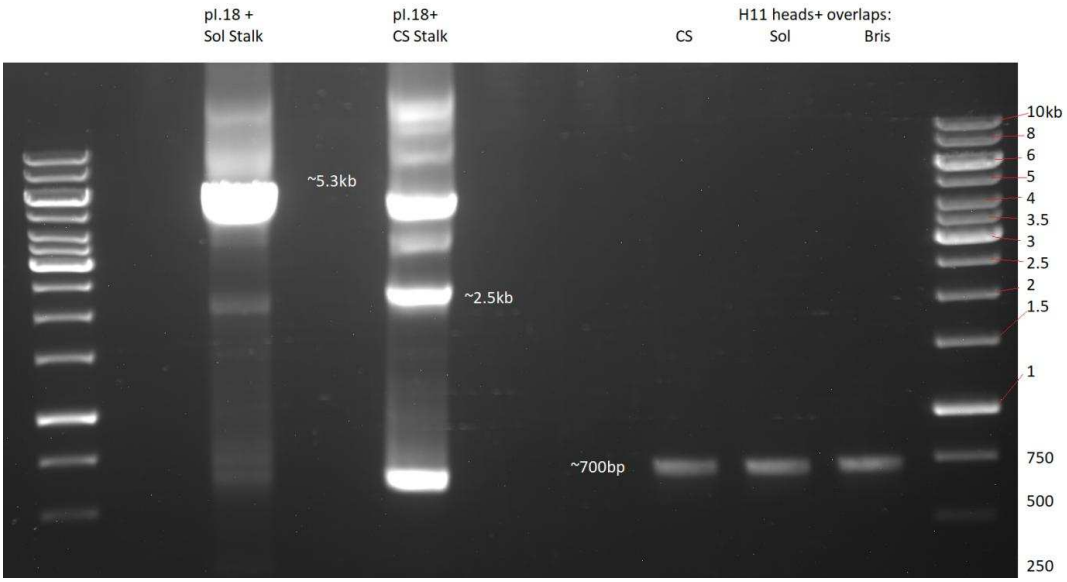

Figure 3.2. Initial attempt at PCR of pI.18 linear vector with H1 stalk overlaps, as well as H11 head DNA fragments with complementary H1 stalk overlaps. Strong bands at the expected 5.3kb mark for pI.18 + H1 stalks and 700bp band for H11 heads are present. Several nonspecific bands present after PCR of pI.18 + stalk combinations, with the strongest nonspecific band at ~2.5kb.

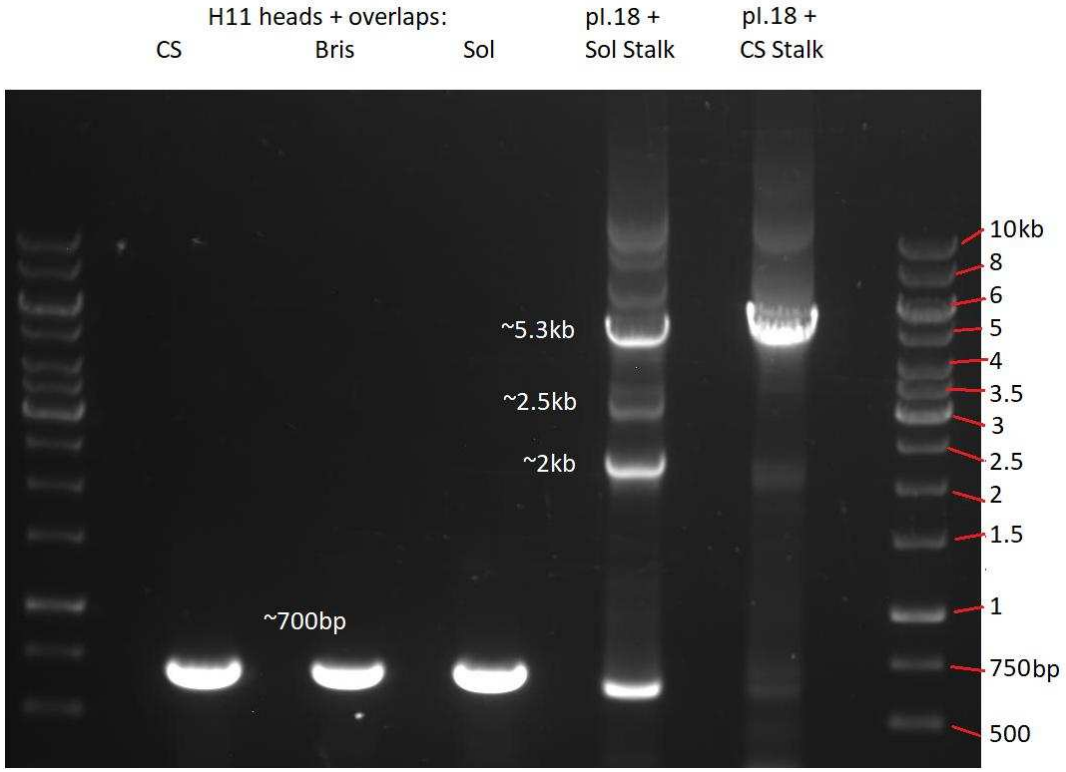

Figure 3.3. Repeat of the Initial attempt at PCR of pI.18 linear vector with H1 stalk overlaps, as well as H11 head DNA fragments with complementary H1 stalk overlaps.

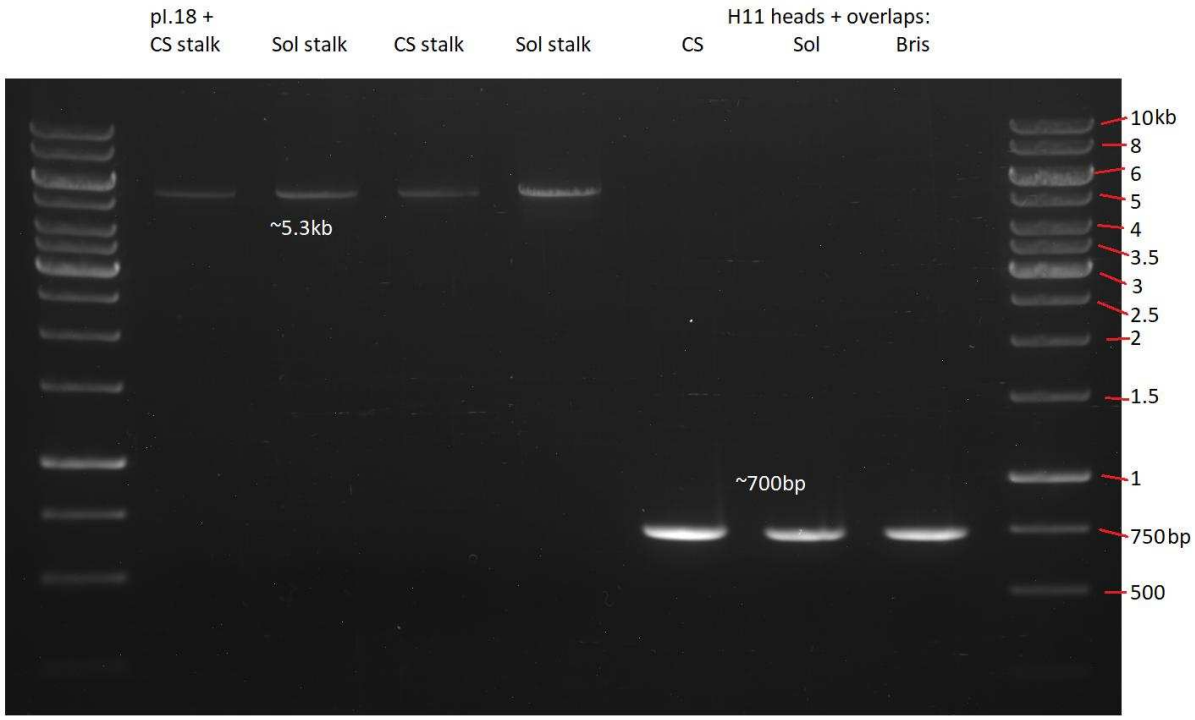

Figure 3.4. Gel electrophoresis of gel extracted PCR products. Left hand side of the figure shows the production of a linear DNA fragment consisting of the pI.18 expression plasmid sequence flanked by H1 stalk sequences. The right side of the graph shows the remaining part of the chimera, linear DNA fragments consisting of the H11 head flanked by H1 stalk sequences.

The first attempt at the production of cHAs via in-fusion was unsuccessful, yielding no band or smear for the Sol CHM when tested directly by gel electrophoresis. This first Sol CHM attempt was run alongside further PCR reactions of H11 heads with CS, Brisbane and Sol overlaps, as well as pI.18 CS and Sol stalks with H11 overlaps (Figure 3.5).

Due to the possibility that cHA plasmids were present in the previous sample, but not detectable by gel-electrophoresis, In-Fusion was then attempted again and the reaction mix was then immediately transformed into competent E. *coli* (section 2.2.2). Colonies were successfully grown overnight in the presence of amp. Four colonies from both CS CHM and Sol CHM plates were picked and grown in LB broth overnight as per section 2.2.2. Of these four clones, three were selected based on the optimal optical density of bacterial growth, plasmids were extracted as per Section 2.1.11 and gel electrophoresis was performed on plasmids resulting from each colony, alongside parental phCMV-H11 (Figure 3.6). Typical plasmid conformation was observed for each clone, at varying strengths, indicating the presence of dsDNA plasmids in various coiled and uncoiled states for both cHA plasmids.

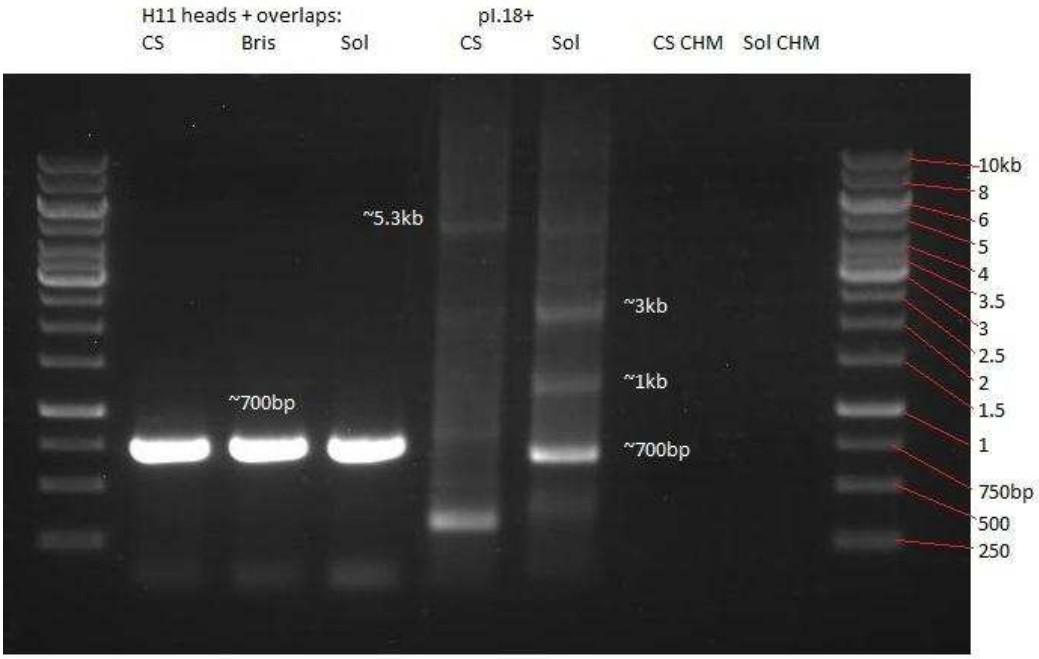

Figure 3.5. Gel electrophoresis of H11 heads with CS, Bris and Sol overlaps, alongside pI.18-CS and pI.18-Sol linearised plasmids with H11 head overlaps. Dark lanes (CS CHM, Sol CHM) show the unsuccessful visualization of 5 µl of cHA expression plasmids after In-Fusion assembly.

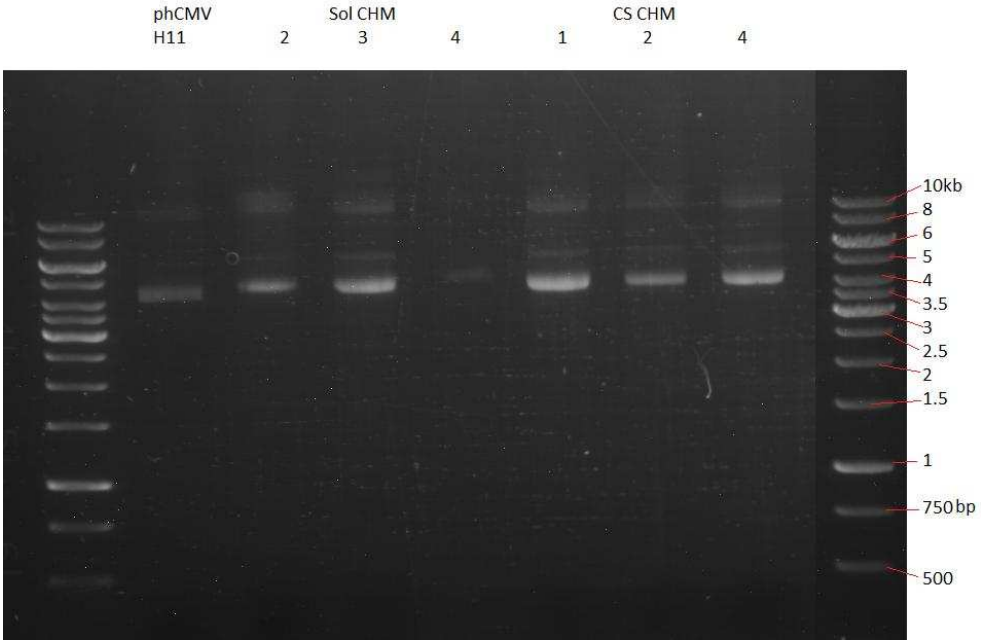

Figure 3.6. Gel electrophoresis of plasmids pI.18 bearing Sol CHM and CS CHM genes, alongside phCMV-H11. Three colonies of bacterial transformants were grown overnight in LB broth and plasmids were extracted. Clones 2, 3 and 4 for Sol CHM and 1, 2 and 4 for CS CHM were run in this gel. Clones were selected based upon the optical density of LB broth after overnight culture.

Each cHA plasmid was then used in PCR using the original 5' and 3' plasmids in order to obtain a full length HA fragment. Results show the presence of a strong band at ~1.7 kb, the

expected length of the cHA gene for both cHA plasmids (Figure 3.7A). Restriction digestion was also performed; plasmids were linearised using KpnI, cutting once at a site within the MCS which should still be present within the cHA plasmids MCS. Results show the presence of one large band at above 5 kb, the expected size for this plasmid being ~6kb (Figure 3.7B). A double digestion was also carried out, with BamHI and EcoRI, two sites flanking the MCS region containing the cHA gene. This yielded two fragments as expected; a ~1.7 kb band composed of the cHA gene, and a ~4 kb band composed of the pI.18 plasmid (Figure 3.7C).

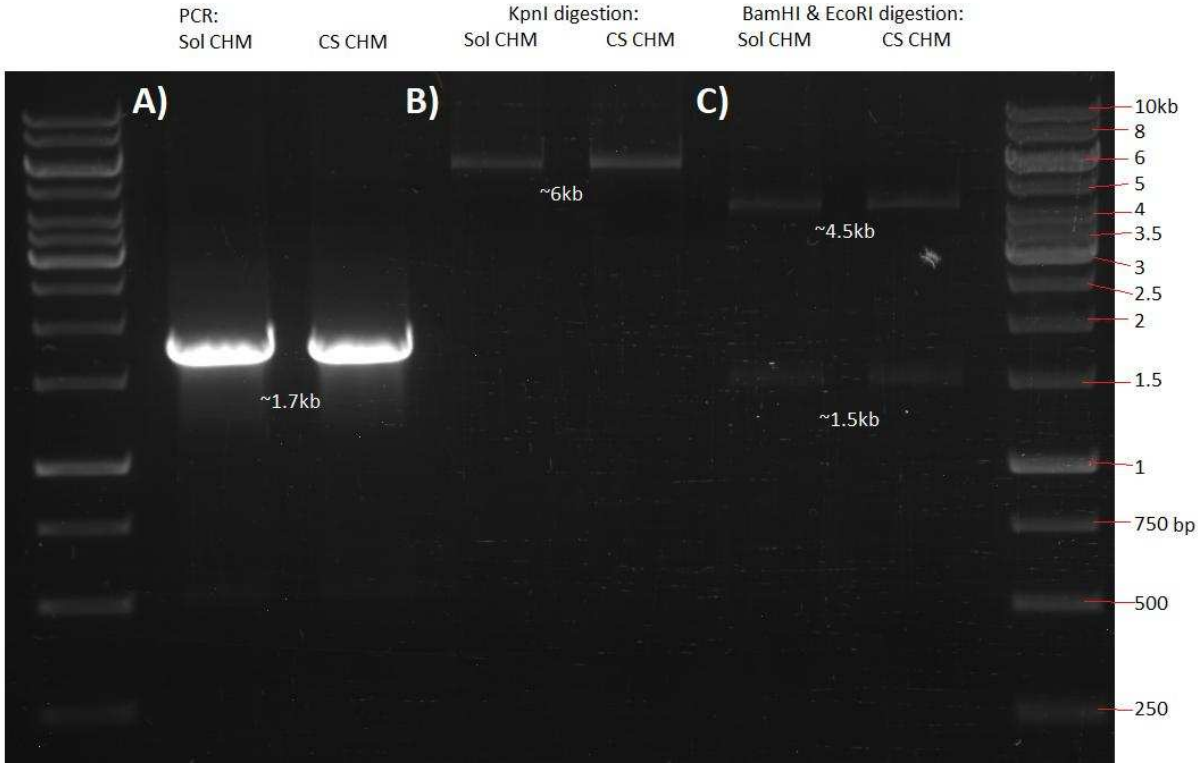

Figure 3.7. Gel Electrophoresis of PCR and restriction digestion of cHA plasmids Sol CHM and CS CHM. A) PCR of Sol CHM and CS CHM plasmids using 5' and 3' terminal primers yields a band at ~1.7 kb, consisting of the cHA gene. B) KpnI digestion of Sol CHM and CS CHM plasmids yields one band at >5 kb consisting of the linearised pI.18 plasmid containing the cHA genes. C) Double digestion of Sol CHM and CS CHM using BamHI and EcoRI yields two bands at ~1.7 kb and ~4 kb, consisting of the cHA genes and linearised pI.18 plasmid respectively.

Sol CHM and CS CHM clones were then sequenced using pI.18 internal primers, yielding sequences which were analysed using BioEdit to ensure the expected sequence and orientation was present in both cHA plasmids, which was the case. Large stocks of each plasmid were then produced using the QIAGEN Plasmid Midi kit (cat: 12125), yielding stocks sufficient for the completion of the project (200 µl at 1-2 µg/µl each). Generation of two further cHA plasmids was attempted during this project. The first was a group 2 (G2) cHA with A/chicken/Germany/N/1949 (H10) head and A/Udorn/307/1972 (H3) stalk. The second

was a Flu B cHA with A/chicken/Germany/N/1949 (H10) head and B/Brisbane/60/2008 stalk. These were produced in a similar fashion to the previous Sol CHM and CS CHM cHA plasmids, with a few differences. These chimeras were produced by Gibson assembly (New England BioLabs, cat: E2611S). Fragments were first generated by PCR, expected fragments were gel extracted as with previous cHAs and run on 1% agarose gels alongside the original PCR products (Figure 3.8). Gibson assembly was then carried out as described previously, 1 µl of the reaction mix was used to transform competent E. *coli* and plasmids were sent off for sanger sequencing alongside being employed for the production of PV. While the production of plasmids bearing G2 and Flu B cHAs was successful, it was not possible to produce PV using these plasmids in subsequent experiments within the scope of this project.

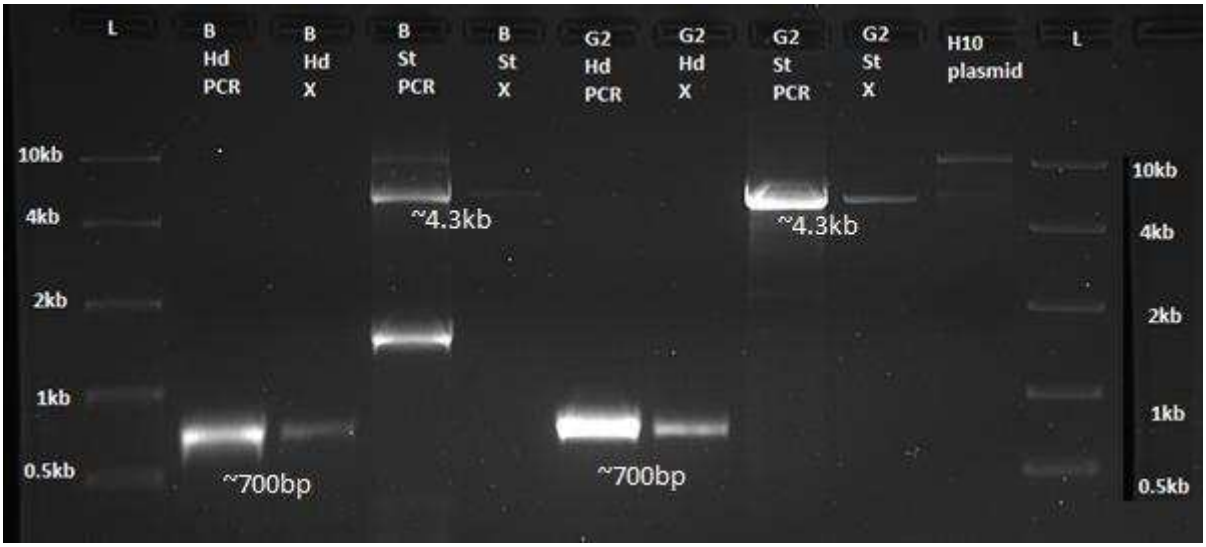

Figure 3.8. Gel electrophoresis of PCR and Gel extracted fragments for Flu B CHM and G2 CHM alongside phCMV1-H10 plasmid. From left to right: 10kb ladder, PCR of H10 head with B/Brisbane/60/2008 overlaps before and after extraction (x). B/Brisbane/60/2008 stalk with H10 head overlaps in pI.18 before and after extraction. H10 head with A/Udorn/307/1972 stalk overlaps, before and after extraction. A/Udorn/307/1972 stalk with H10 head overlaps in phCMV1 before and after extraction. H10 plasmid in phCMV1. 10kb ladder.

3.3.2 Production of cHA bearing PV

A cHA bearing the H11 head and A/South Carolina/1/1918 stalk has previously been produced by a PhD student in the Viral Pseudotype Unit, Dr Francesca Ferrara. This was used in preliminary tests which gave rise to this project. However, this cHA PV was difficult to produce, and only low titre preparations resulted when transducing HEK293T/17 cells

(Figure 3.9). Production was attempted with co-transfection of pCAGGS-HAT in 6-well format, which was found to be the optimal protease for production of this chimera (PhD Thesis, Francesca Ferrara). Due to the success in the production of further chimeras, this plasmid was not used further in this project, and efforts were focused on establishing the CS CHM for use with the Jenner Sera.

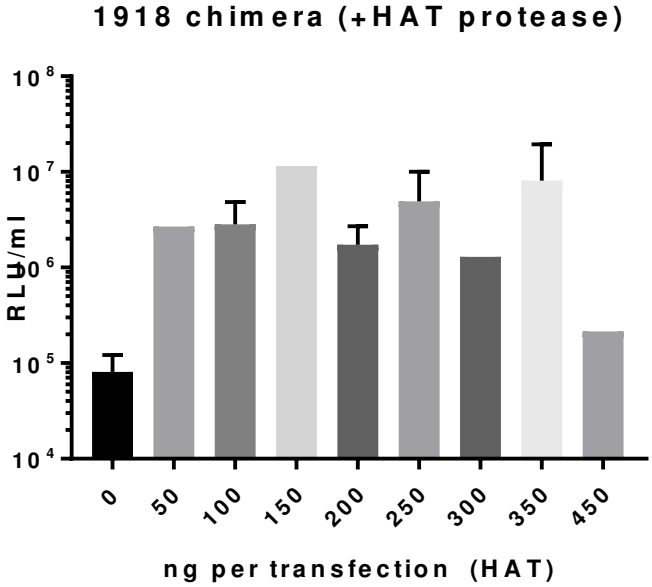

Figure 3.9. Production of cHA bearing stalk from 1918 pandemic influenza. cHA bearing PV with A/South Carolina/1/1918 (H1) stalk and A/duck/Memphis/546/1974 (H11) head), co-transfected with pCAGGS-HAT. Production was attempted using a range of concentrations of pCAGGS-HAT plasmid from 50 to 450 ng per transfected well (6-well format).

3.3.3 Production of pandemic 2009 H1 PVs

Due to the cHA system benefiting from the ability to test the cHA PV alongside its parental subtype strains, it was a requirement for this project to produce a working PV bearing the H1 from the 2009 pandemic. Early efforts to produce PV bearing this 2009 pandemic HA were unsuccessful, employing the A/Texas/05/2009 codon optimised gene (kind gift from Prof Sarah Gilbert, University of Oxford) cloned into plasmid pI.18. A further plasmid expressing the influenza M2 protein from A/Hong Kong/156/97 (H5N1), cloned into pcDNA3.1, was transfected in a final attempt to increase titres of A/Texas/05/2009 PV, after M2 was successfully used by other research groups to the same ends (Figure 3.10) (McKay et al. 2006; Wei Wang, Castelán-Vega, et al. 2010). Initial results were successful and a linear relationship was observed between quantity of M2 expression plasmid added to the

transfection mix and RLU titre (Figure 3.10). However this experiment could not be repeated despite multiple attempts with the same and newly generated reagents.

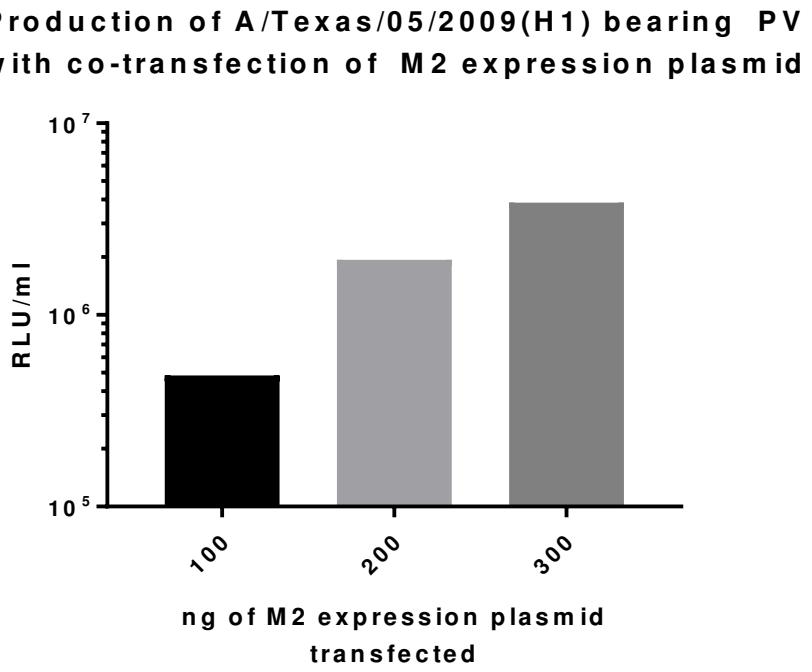

Figure 3.10. Effect of co-transfection of M2 expression plasmid on the RLU titres of PV bearing the A/Texas/05/2009 (H1) glycoprotein. Production was carried out in HEK293T/17 cells with the co-transfection of 100, 200 and 300 ng of M2 expression plasmid. The results from this experiment could not be repeated.

Further attempts at the production of pandemic 2009 HA bearing PV resulted in the commercial synthesis of the WT A/California/7/2009 (H1) (CA/09) gene cloned into plasmid pI.18 by Genscript (Piscataway, New jersey, USA). PVs were then produced in the presence of the previous proteases HAT and TMPRSS4; with results yielding useable titres of virus within the $10E^8$ RLU/ml range (Figures 3.11 and 3.12). Due to the success in production of CA/09 PV above $10E^8$ RLU/ml with both TMPRSS4 and HAT, no further optimisation was carried out and further stocks were produced with co-transfection of 150 ng/well of pCAGGS-HAT in 6-well format. However these titres were not significantly different from production with 50 ng (P=0.306), 250 ng (P=0.166), 300 ng (P=0.365) or 750 ng (p=0.821), but significantly different from 100 ng (P=0.157).

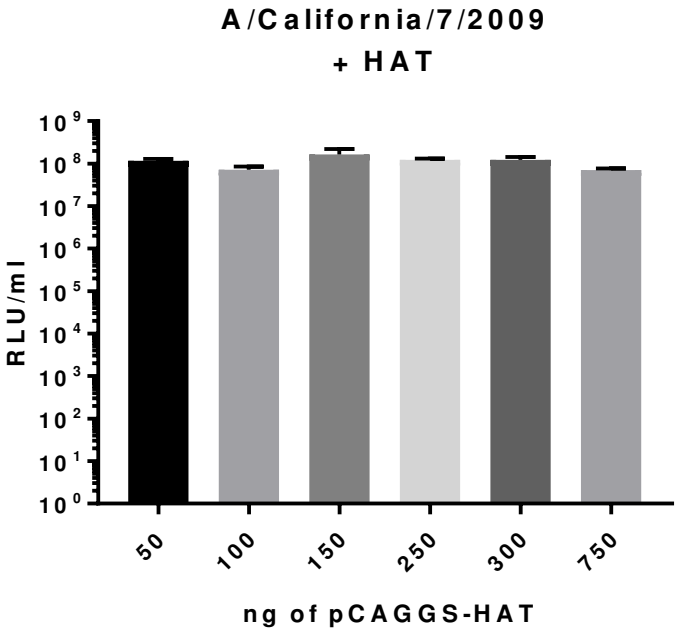

Figure 3.11. RLU/ml titres for the optimisation of A/California/7/2009 (H1) bearing PV with the co-transfection of 50-750ng of pCAGGS-HAT per well. Highest RLU/ml titres were obtained using 150 ng HAT, however this was not significantly different from 50 (P=0.306), 250 (P=0.166), 300 (P=0.365) or 750 (p=0.821), but significantly different from 100 (P=0.157).

For production of CA/09 PV in the presence of TMPRSS4, the highest RLU/ml titres were obtained with 100 ng of pCMV-TMPRSS4, giving an average titre of $1.69E^8$, compared to $9.12E^7$ and $2.75E^7$ for 150 and 250 ng respectively. Differences between 100 and 150 (P=0.0011), 100 and 250 (P=0.0050) as well as 150 and 250 (P=0.225) were all significant.

CA/09 PV produced with 110ng of pCMV-TMPRSS4 was significantly greater than PV produced with 50 ng (P=0.0255), 100 ng (P=0.0007), 250 ng (P=0.0026) and 750 ng (P=0.0030) of pCAGGS-HAT.

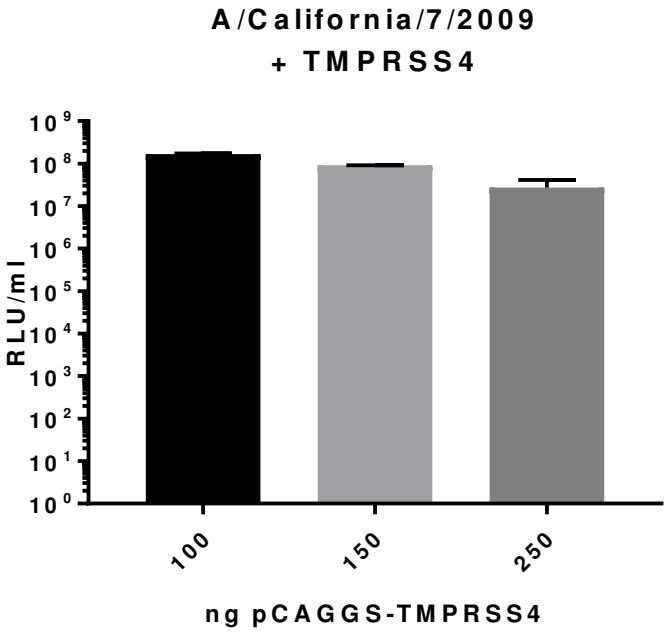

Figure 3.12. RLU/ml titres for the optimisation of A/California/7/2009 (H1) bearing PV with the co-transfection of 100-250ng of pCMV-TMPRSS4 per well. The highest RLU/ml titre was obtained with co-transfection of 100 ng pCMV-TMPRSS4.

Employment of a newly available transfection reagent (Endofectin Max ©) did lead to a further rise in RLU/ml titres, despite this also not being significantly greater than those generated using PEI (P=0.836), see Figure 3.13. PVs transfected using this reagent were incubated in a larger volume of DMEM (10 ml in lieu of 8 ml) without antibiotics, and no medium change was required the day after transfection. These two factors must be considered alongside the transfection reagent to evaluate any further increases in titres when comparing reagents. It is likely that a larger quantity of virus has been produced with Endofectin Max to allow similar titres with a 25% increase in volume of PV containing supernatant. The exact parameters used are listed in section 2.4.1.

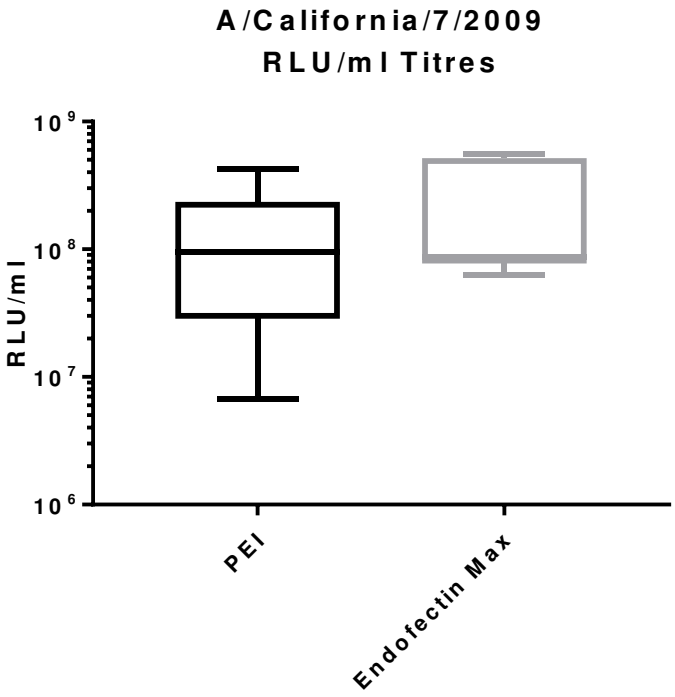

Figure 3.13. RLU/ml titres for various stocks of PV bearing the H1 from A/California/7/2009. Data comparison between production with polyethilynimine and Endofectin Max. There is no significant difference between PEI and Endofectin Max RLU/ml values (p=0.863).

3.3.4 Production of cHA PV

Optimisation of the process for the production of cHA bearing PV was carried out in 6-well format using a range of protease expression plasmids, notably pCAGGS-HAT and pCMV-TMPRSS4. For the Sol CHM, optimal results were obtained when co-transfecting HEK293T/17 cells with 200 ng of pCAGGS-HAT alongside the lentiviral and HA plasmids (Figure 3.14), yielding an RLU titre of over $10E^8$ RLU/ml. Co-transfection of 100 ng or 250 ng pCAGGS-HAT yielded the second highest results with titres just under $10E^8$ RLU/ml. pCMV-TMPRSS4 had little effect when co-transfected under the same conditions, titres remained below $10E^7$ RLU/ml, higher than the Δ protease control ($10E^5$ RLU/ml) but lower than the optimal condition of 200 ng pCAGGS-HAT. See Figures 3.14 and 3.15 for bar charts of RLU/ml titres for Sol CHM PVs produced in the presence of different quantities of pCAGGS-HAT and pCMV-TMPRSS4.

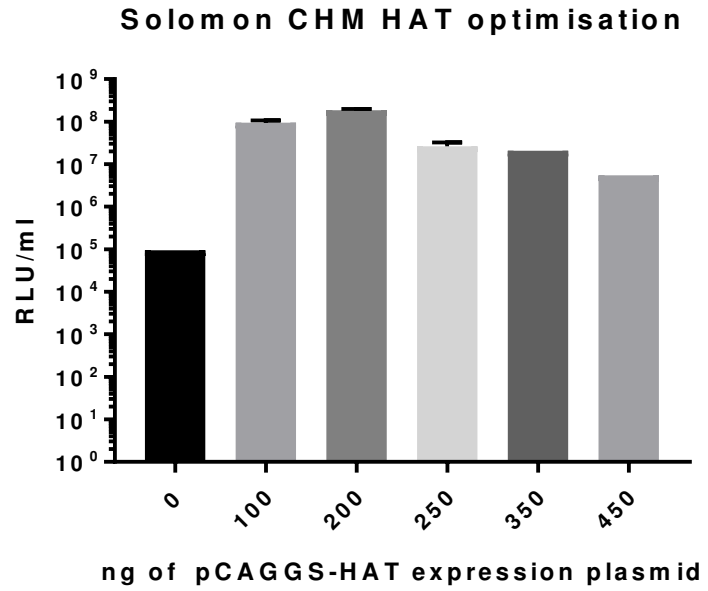

Figure 3.14. Production of Sol CHM PVs with co-transfection of pCAGGS-HAT from 100-450 ng per well (6-well format). Production Δ protease results shown in black (0). 100, 200 and 250 parameters repeated after initial single run. Highest titres obtained with co-transfection of 200 ng pCAGGS-HAT: 10^8 RLU/ml.

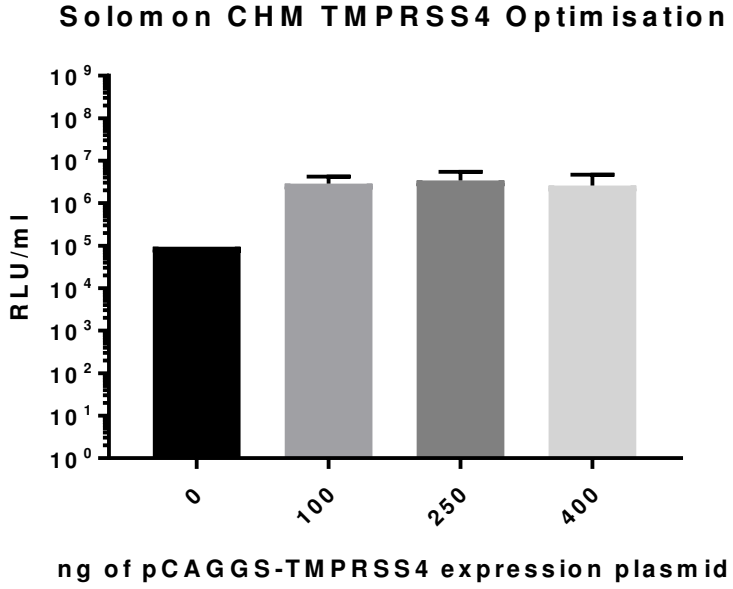

Figure 3.15. Production of Sol CHM PVs with co-transfection of pCMV-TMPRSS4 from 100-400 ng per well (6-well format). Production Δ protease results shown in black (0). Experiment performed in duplicate for 100, 250 and 400 parameters. 100-400 ng of pCMV-TMPRSS4 resulted in similar titres in the 10^6 RLU/ml range.

For the CS CHM cHA, more varied results were obtained when producing PV bearing this glycoprotein with different quantities of the protease expression plasmids pCAGGS-HAT and pCMV-TMPRSS4. Addition of 100-450 ng of pCAGGS-HAT to the transfection mix in 6-well format increased titres of CS CHM several logs higher than the Δ protease control (0). The highest RLU titre is seen with co-transfection of 100 ng pCAGGS-HAT, however there was no significant difference between 100 and 200 (p=0.45), 100 and 250 (p=0.43) or 200 and 250 (p=0.89) titres. See Figure 3.16.

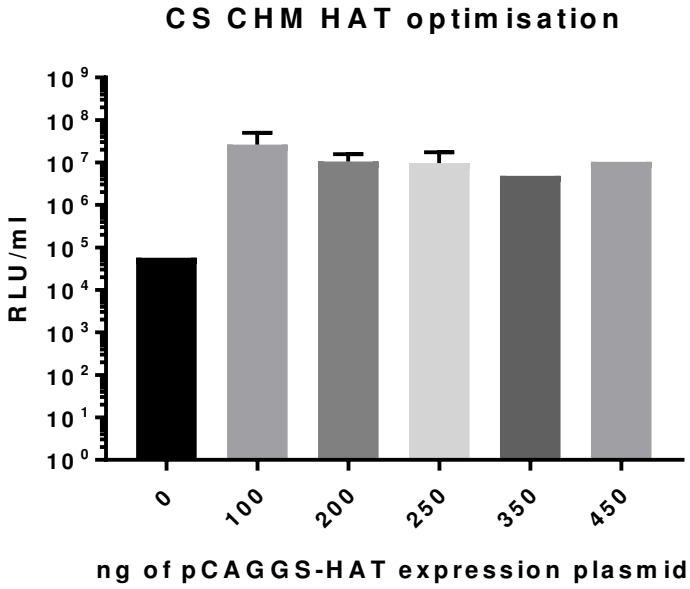

Figure 3.16. Production of CS CHM PVs with co-transfection of pCAGGS-HAT from 100-450 ng per well (6-well format). Production Δ protease results shown in black (0). 100, 200 and 250 ng parameters performed in duplicate. Highest luciferase titres (RLU/ml) are observed with the addition of 100ng pCAGGS-HAT, giving a titre of over 10^7 RLU/ml.

CS CHM bearing PV produced in the presence of pCMV-TMPRSS4 had low RLU/ml titres, with averages around one log higher than the Δ Protease control. The highest RLU/ml value was obtained with co-transfection of 400 ng of pCMV-TMPRSS4 ($7E^7$ RLU/ml). However, as with transfection with pCAGGS-HAT, there was no significant difference between 100 and 250 (p=0.06) 100 and 400 (p=0.63) or 250 and 400 (p=0.43) RLU titres. See Figure 3.17.

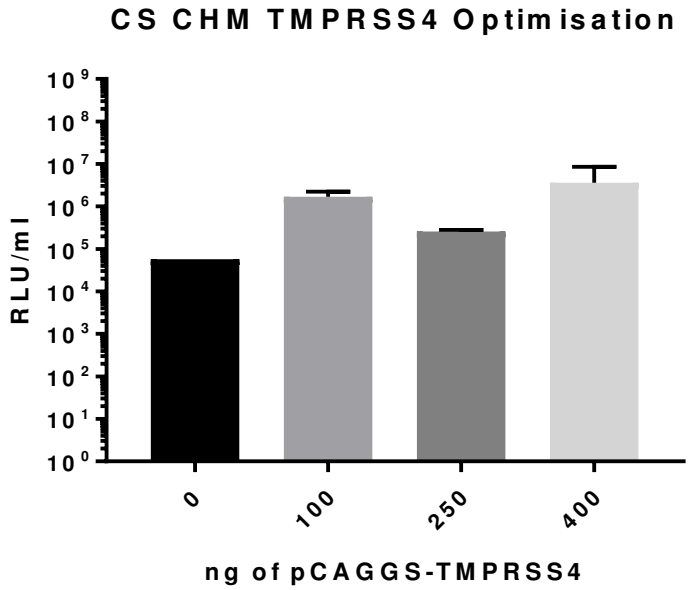

Figure 3.17. Production of CS CHM PVs with co-transfection of pCMV-TMPRSS4 from 100-400 ng per well (6-well format). Production Δ protease results shown in black (0). Experiment performed in duplicate for 100, 250 and 400 parameters. Highest luciferase titres (RLU/ml) are observed with addition of 400 ng pCAGGS-TMPRSS4, followed by 100 ng and 250ng.

Optimal conditions for the production of PV were decided as the lowest concentration of protease encoding plasmid required to obtain the highest RLU/ml titre. For Sol CHM this was 200 ng and for CS CHM 100 of pCAGGs-HAT per well in 6-well format. These parameters were employed with other standard plasmid quantities (500 ng p8.91, 750 ng pCSFLW, 500 ng pI.18-HA per well) in order to produce stocks of each cHA PV. Titres for stocks produced after optimisations are displayed in Figure 3.18.

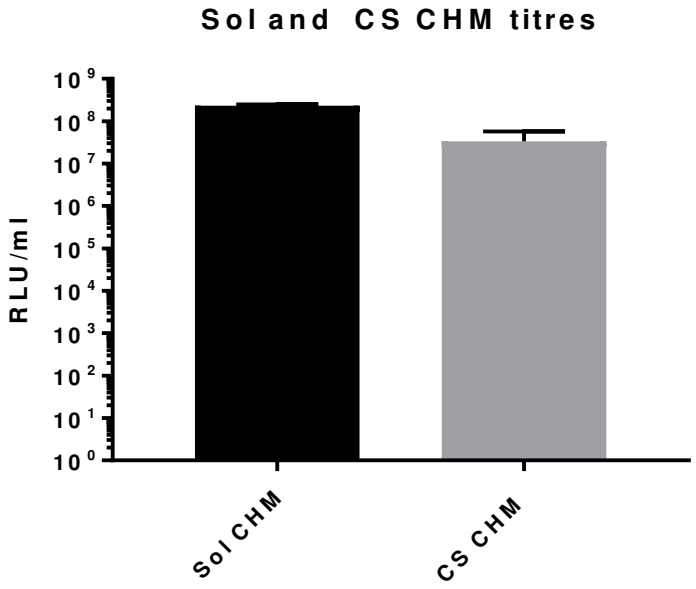

Figure 3.18. Production of Sol CHM and CS CHM bearing PV. RLU/ ml titres for Sol CHM (200 pCAGGS-HAT per well) and CS CHM (100 pCAGGS-HAT per well) produced in bulk after the protease plasmid optimisation process. Sol CHM titres average above 10^8 RLU/ml while CS CHM titres average between 10^7 and 10^8 RLU/ml.

3.3.5 Group 2 and Influenza B cHAs

Attempts to produce PVs bearing cHAs with group 2 and influenza B stalks were unsuccessful. Proteases HAT, TMPRSS2 and TMPRSS4 were tested in an optimisation grid with a range of 50-500ng per well co-transfected alongside 500 ng of p8.91, 750ng pCSFLW and 500ng cHA, as per standard method (section 2.4.1). No effect was seen with any of the proteases as RLU values resembled Δ protease values when each preparation was titrated on HEK293T/17 cells.

3.3.6 pMN of Jenner Sera

The Jenner Sera were assayed in duplicate against the three viruses of the chimeric CS CHM system: Parental H11 PV (A/duck/Memphis/546/1974), Parental H1 PV (A/California/7/2009) and the CS CHM. By utilising the cHA alongside the parental strains, this allowed the CS CHM neutralising antibody titres to be interpreted in the context of the same serum neutralising antibody titres against the parental strains – allowing dissection of the head-only and stalk-only responses seen. Care was taken to reduce variability in this project which involved 179 unique sera, requiring a large quantity of PV stocks and cells to

be produced and pooled in order to ensure the sera could be compared with no variation in PV or cell input. Neutralising antibody titres (IC_{50}) for these experiments are shown in appendix X1. Overall, neutralising antibody titres were higher in the period after the 2009 pandemic than before it, despite a low sample size pre 2009 (n=20). Titres for H11 increased from 12 to 199, CA/09 from 3596 to 5068 and CS CHM from 376 to 1380. See Figure 3.19.

Neutralising antibody titres were bracketed in different ways due to the way in which samples were taken each yearly period. First, neutralising antibody titres were bracketed according to year (Figure 3.20) in order to include all the data collected and provide an overview for the trend in neutralising antibodies against the cHA system PVs between 2008 and 2016. For PV bearing H11, low neutralising antibody titres were recorded for patients in 2008 and 2009. 2010 saw a sharp increase in neutralising antibody titres, with one patient recording an IC_{50} of 1883 against this HA subtype. 2011, 2012 and 2013-2016 (2013+) show an overall increase in neutralising antibody titres against H11 with several patients displaying neutralising antibody titres over 500. For PV bearing the pH1 CA/09 HA, pre 2009 pandemic results were high when compared to H11, with the average IC_{50} reading at 3596. This is most likely due to the nature of H1 infection; conserved epitopes within the pH1 HA are likely to have been encountered in human populations previously, despite the exotic swine nature of this particular strain (Xu et al. 2010). This may explain the relatively high IC_{50} values recorded from sera obtained before the existence of this strain in human populations when considering the sensitivity of pMN over traditional assays (Temperton et al. 2007). However, 2009 sera neutralising antibody titres remained similar to that pre-2009, with just two patients showing increased neutralising antibody titres (7388 and 9274), raising the average IC_{50} for 2009 to 4068. Subsequent years showed a similar trend, with average IC_{50} remaining around 3-4000 but increasing to 5000+ after 2012: 2010 (3878), 2011 (3395), 2012 (5018) and 2013-2016 (5858). While these averages remain similar, it is apparent in Figure 3.20 that some patients have elevated neutralising antibody titres against the pandemic strain in each bracket. For the CS CHM itself, neutralising antibody titres are low pre 2009 and for 2009 itself, with average neutralising antibody titres at 410 for 2008 and 278 for 2009. Average IC_{50} values rise to an average of 1410 for 2010 and remain higher than pre 2010 at 1224 for 2010, 1430 for 2012 and 1386 for 2013-2016. Figure 3.20 shows this data alongside a distinct increase in average and quartile IC_{50} results for the sera against CS CHM.

Second, values were bracketed for the influenza season (September to April) between years, excluding values taken between these times (May to August), shown in Figure 3.21. This data shows a very different profile to the year-bracketed data, with an increase in neutralising antibody titres against H11, CA/09 and CS CHM observed for the 2009-2010 influenza season, the first season for pH1N1. Neutralising antibody titres against H11 are very low for the 2008-2009 season (n=19) and rise sharply in the 2009-2010 (n=9) season due to one patient with an IC_{50} of 1883. Neutralising antibody titres then remain in the 0-500 range with patients in 2010-2011, 2011-2012 and 2014-2015 showing titres higher than 500. For CA/09, neutralising antibody titres remain similar between seasons, with IC_{50} values averaging around 3-5000. There are occasional high data points such as in 2012-2013 (23,954) and 2013-2014 (15,535) seasons which skew the data, and may represent serum being taken from a patient shortly after exposure to a pH1N1 strain after it had replaced previous H1N1s as the dominant seasonal strain. Average neutralising antibody titres seem to increase in the 2013-2014 and 2014-2015 seasons with average IC_{50} values of 6892 and 5711 respectively. For CS CHM, the 2008-2009 season shows the lowest neutralising antibody titres as with H11 and CA/09 PV. The 2009-2010 season sees titres increase as a result of one patient's IC_{50} of 5420. Subsequent seasons show average IC_{50} values remain well above the 393 (mean) of the 2008-2009 seasons, averaging at 1209, 1506, 1455, 1328, 1264 and 1318 for seasons 2009-2010 to 2014-2015. Neutralising antibody titres then drop for the final season in which serum samples were taken in this serum panel, with an average IC_{50} of 750. However, with only two patients in this group, this is most likely not an accurate representation of neutralising antibody titres for this season. See Figure 3.21 for graphic representation of influenza season bracketed neutralising antibody titres described in this paragraph.

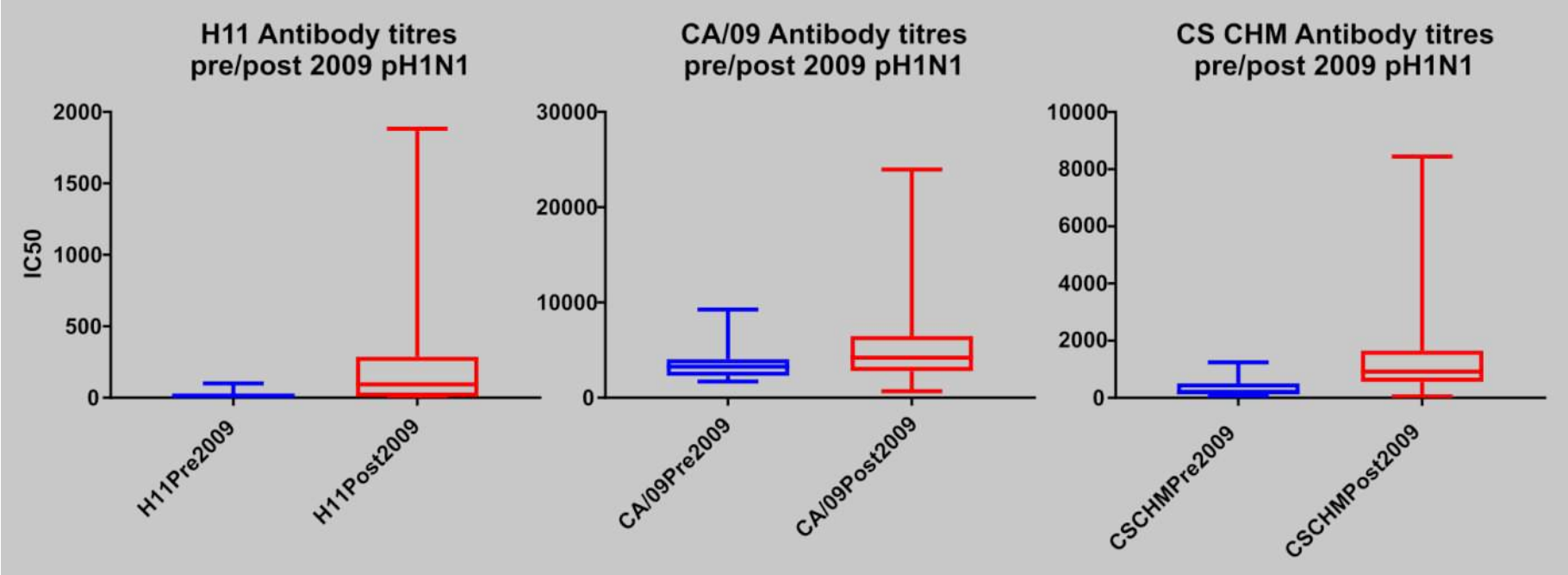

Figure 3.19. Box plots for pMN neutralising antibody titres (IC_{50}) generated by Jenner Sera against A/duck/Memphis/546/1974 (H11), A/California/7/2009 (H1) and CS CHM bearing PV. Neutralising antibody titres for sera are bracketed pre and post pH1N1 pandemic. Elevated antibody titres are observed against all three PVs after the 2009 pandemic. Cross-reactivity is seen through pre 2009 sera neutralising A/California/7/2009. Mean antibody titres are increased due to a small subset of patients with increased titres.

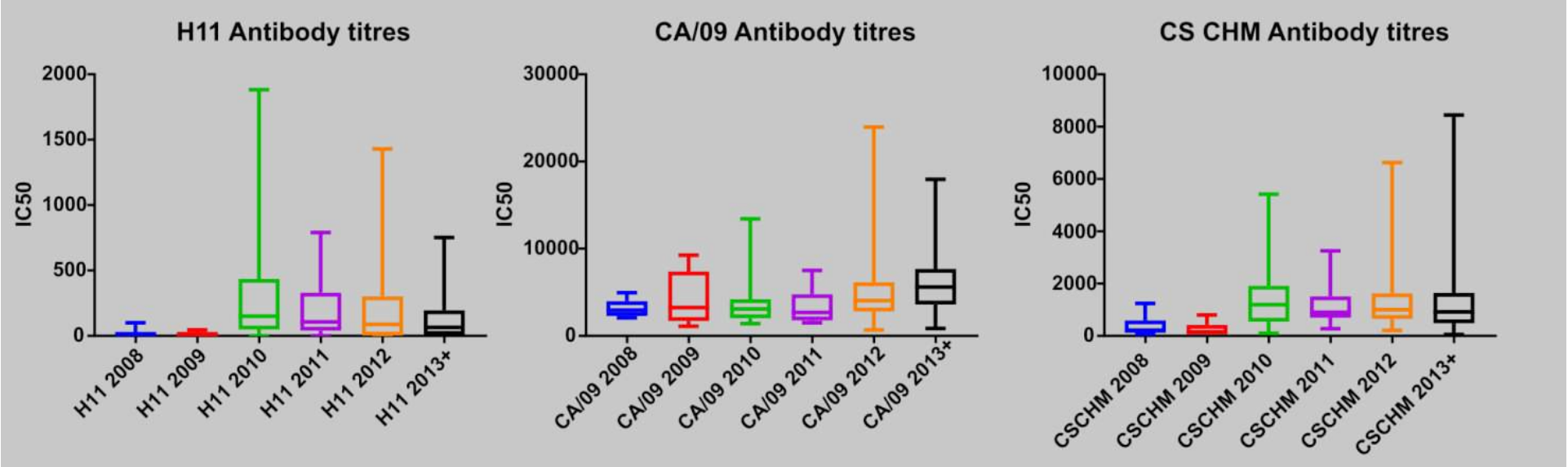

Figure 3.20. Box plots for pMN neutralising antibody titres (IC_{50}) generated by Jenner Sera against A/duck/Memphis/546/1974 (H11), A/California/7/2009 (H1) and CS CHM bearing PV. Neutralising antibody titres bracketed by year of serum collection. Pre 2009 neutralising antibody titres are low for all three PV except for CA/09 PV. Neutralisation of all three PV increases post 2009 when considering average IC_{50}, this is driven by a small group of patients having raised neutralising antibody titres, displayed as whiskers. NB: 20 samples between 2008 and 2009.

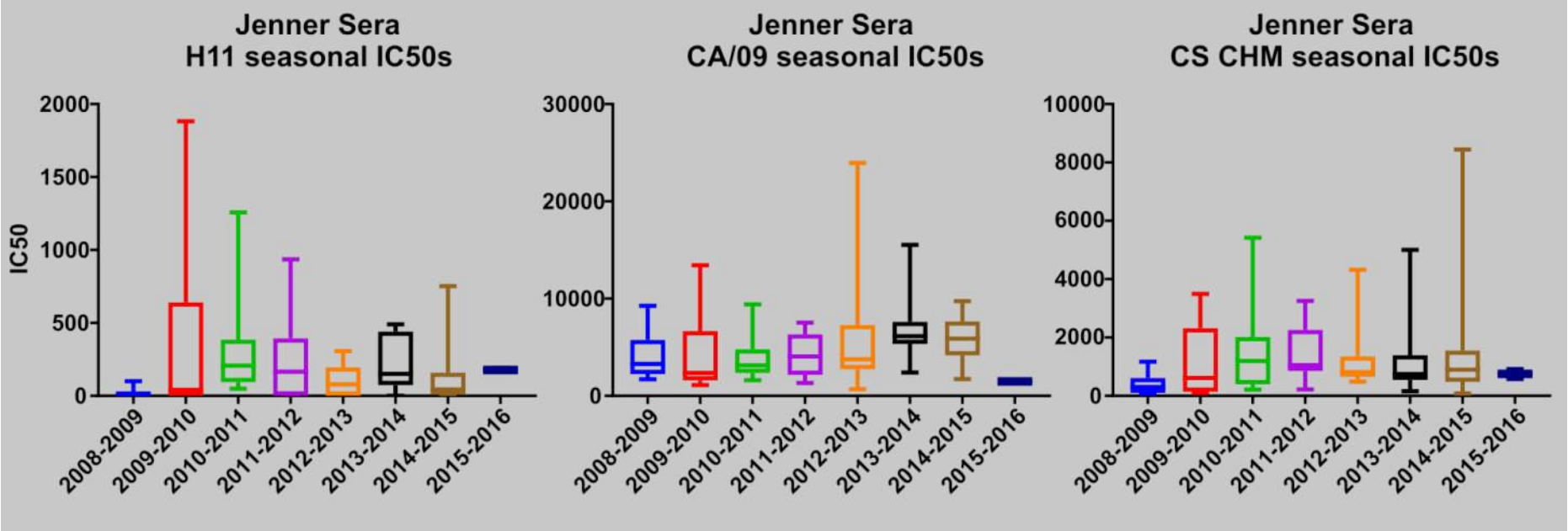

Figure 3.21. Box plots for pMN neutralising antibody titres (IC_{50}) generated by Jenner Sera against A/duck/Memphis/546/1974 (H11), A/California/7/2009(H1) and CS CHM bearing PV. Neutralising antibody titres are bracketed by influenza season (September-April) for sera collected between 2008 and 2016. Mean neutralising antibody titres are similar for all seasons for H11 PV, with several high titres observed in the 2009 pandemic season. Mean titres against CA/09 fluctuate, with a slight increase seen in the 2013-2014 and 2014-2015 seasons. Antibody titres against CS CHM increase after the 2008-2009 season with a small dip observed after the 2011-2012 season. Sera with high titres are observed against all three PV, shown by distinct whiskers rising above the 75% quartiles. NB: only 2 patients fall within the 2015-2016 season.

Finally, neutralising antibody titres were bracketed by age to observe the extent to which immunity is dictated by age and previous exposure amongst the group of Jenner Institute patients (Figure 3.22). One of the aims of this project was to use the cHA system via PV to detect increases in stalk-directed antibodies elicited by natural infection with the pH1N1 pandemic (Wrammert et al. 2011). However, due to the serum set being spread over multiple years and the lack of data regarding the infection history of each patient, it is difficult to distinguish whether high responders against the chimera have stalk directed antibodies as a result of pH1N1 or previous strains. Nevertheless, when bracketing neutralising antibody titres by age group, CA/09 titres match the infection data for pH1N1, with young adults being one of the hardest hit groups (Karageorgopoulos et al. 2011; Shrestha et al. 2011). Despite this, the 40-50 and 50+ age groups show an increased ability to neutralise CS CHM as well as the heterologous H11 PV, which is consistent with other studies showing an increase in broadly neutralising antibodies in the elderly after repeated exposure to influenza viruses throughout their lifetime (Nachbagauer et al. 2016). One drawback of this bracketing is the spread of ages within the panel patients, with 67 patients in their 20s, 7 in their 30s, 11 in their 40s and 67 in the 50+ group.

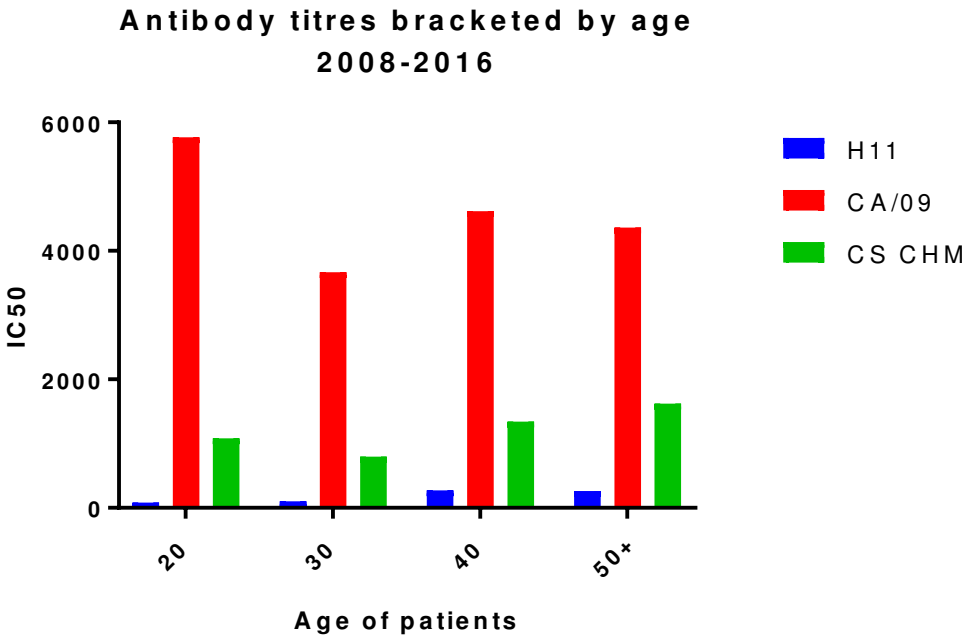

Figure 3.22. Average neutralising antibody titres (IC_{50}) bracketed by age group between 2008 and 2016 against PV bearing A/duck/Memphis/546/1974 (H11), A/California/7/2009 (H1) and CS CHM glycoproteins. Neutralising antibody titres to H11 are highest in the 40 and 50+ age groups whereas for CA/09 the 20 and 40 age groups show the highest titres. The highest titres for CS CHM are seen in 40 and 50+ age groups.

3.3.7 Sports Science sera

Aside from the cHA system, it is also possible to test for heterosubtypic immunity by testing the same sera against a range of PV bearing HAs of different subtypes or strains. It was decided that utilising this alternative approach with a separate set of sera (Sports Science Sera) could serve as a useful comparison between currently available and novel systems. This serum set was used as this approach requires considerable quantities of serum in order for the same sample to be assayed using multiple PV bearing different HAs. The samples originate from a group of athletes studied in a chronic exercise study, taken from patients in their morning resting states at baseline (0 weeks, V1) and after a 12 week interval (V2).

The Sports Science Sera were tested on a wide range of influenza A PV (H1, H5, H3, H7) in order to assess heterosubtypic responses per patient against a wide range of unrelated virus HAs. This experiment was carried out foremost to evaluate the level of heterosubtypic responses obtainable from the testing of different influenza viruses using the same serum sample. Data generated in this way shows a snapshot of the immune repertoire of the patient at the time the sample was taken, which can be employed in our PV system to determine whether exposure to H1 or H3 seasonal strains have boosted H5 or H7 group specific immunity, or cross group immunity.

Predictably, neutralising antibody titres generated by assay of serum samples on the above listed PV using pMN generated high values for human seasonal subtypes (H1, H3) and lower values for the exotic avian subtypes of pandemic potential (H5, H7). Mean IC_{50} values for sera against H1 were 7407 (median 4014), while the H5 IC_{50} mean was 647 (median 385). For group 2 influenza PV, the mean IC_{50} for H3 and H7 were 4384 and 557 respectively (median 3095 and 400 respectively). This data is shown in Figure 3.23.

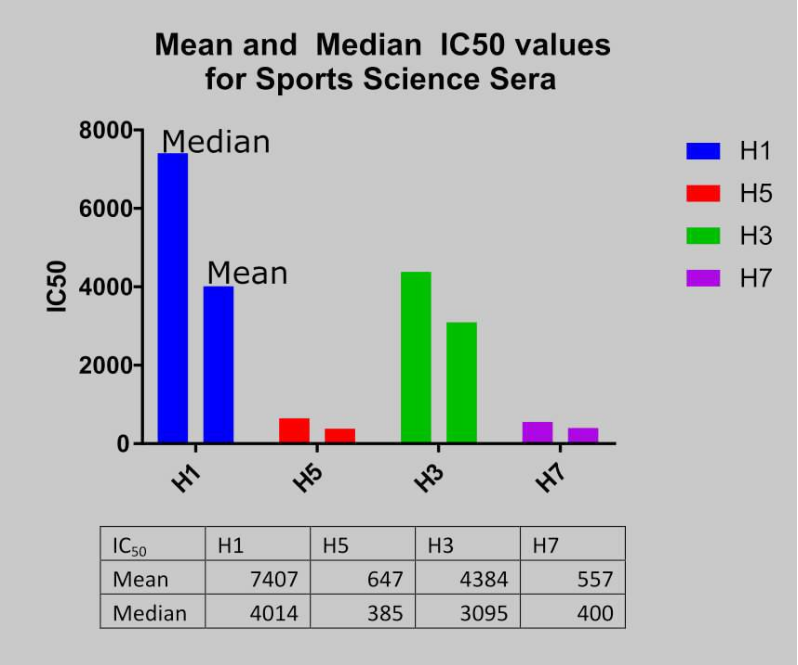

IC_{50}	H1	H5	H3	H7
Mean	7407	647	4384	557
Median	4014	385	3095	400

Figure 3.23. Neutralising antibody titre (IC_{50}) for the 60 pairs of Sports Science Sera assayed against A/Brisbane/59/2007 (H1), A/Vietnam/1194/2004 (H5), A/Udorn/307/1972 (H3) and A/Shanghai/2/2013. Median and mean IC_{50} values are displayed in bar graph and tabular format.

Due to the lack of definitive thresholds for positive or negative results in the pMN assay, it is difficult to determine the level of cross-reactivity between subtypes, and especially whether these cross-reactive responses would result in immunity or reduced morbidity in case of challenge. These problems can only be addressed by challenge experiments, in a suitable model, which will be required for the further development of this assay and its more widespread use. The resources, expertise and ethical requirements for such an experiment were not available during the length of this studentship and therefore objectives were focused on the interpretation of data obtained and comparisons between these generated datasets. Within the data summarized in Table 3.4, 10 patients with high neutralising antibody titres against H1 showed correspondingly high IC_{50} values against H5. 8 patients with high IC_{50} against H3 showed high IC_{50} against H7 (Table 4). Within this subset, a further two patients (serum ID: 9 and 41) neutralised H1, H5, H3 and H7 PV.

Table 3.4. Sera that strongly neutralised group 1 (H1, H5) or group 2 (H3, H7) influenza PV tested. Sera 9 and 41 (bold) showed high neutralising antibody titres against all PV tested

Group:	Serum ID									
1	5	7	8	**9**	15	23	35	**41**	45	49
2	3	-	-	**9**	12	26	28	**41**	57	58

This method for the detection of heterosubtypic immunity is laborious and costly in terms of reagents and materials. Due to the nature of serum and its (lack of) availability, this method is perhaps not suitable for analysis of vaccine immunogenicity in terms of broadly neutralising antibodies. This is especially true when mouse models are used, as these unfortunately do not yield high volumes of serum. Furthermore, due to the fact that each PV used will represent just one strain and one subtype of influenza virus, vast amounts of serum will be required to use a system such as this and obtain comprehensive results taking into account drift between currently circulating strains of the same subtype.

3.3.8 ELLA data

Six serum samples were selected from the Jenner Sera which displayed a range of neutralising antibody titres against H1 CA/09 in order to test these samples against the matched strain NA using ELLA. These were tested using various parameters investigated further in chapter 5. H11N1 and N1 bearing PVs were tested using serum samples 20, 31 and 23 which were all low positives against H1 (CA/09) HA PV via pMN, having average neutralising antibody titres of 1115, 1492 and 2033 respectively. High positives, determined in the same fashion, were samples 34, 91 and 59. These displayed neutralising antibody titres against CA/09 HA in pMN of 3868, 3769 and 6219 respectively. Negative controls included influenza anti-A/California/7/2009 and anti-B/Brisbane/60/2008 HA serum (NIBSC). exNA from Clostridium *perfringens* was used as a digestion control to determine the maximum digestion possible per well (data not shown). Results correlated strongly with IC_{50} values generated against H1 (CA/09) PV, with HP and LP samples acting as low and high positives against N1 as well as the original H1. LP samples 20, 31 and 23 gave IC_{50} values of 0, 30 and 14 with a OD90% input, with the OD2.0 input, IC_{50} values were 0, 341 and 150. For HP samples, 34, 91 and 59 IC_{50} values were 91, 153 and 209 respectively at OD90%, and 629, 1288 and 1613 for OD2.0. Negative controls all gave values of zero except B/Brisbane antiserum which had an IC_{50} of 4 at OD2.0. Despite this, negative samples are clearly

grouped at the negative end of the spectrum of results. However, the curves generated are slightly elevated when using an input of OD2.0, inhibition starting between 20-40% at starting dilution compared to below 5% with an OD90% input. See Figure 3.24 for inhibition curves generated by ELLA using these Jenner Sera samples. Correlation between neutralising antibody titres against the CA/09 HA (pMN) and the CA/09 NA (ELLA) was very strong, pMN and ELLA (OD90%) correlated with a Pearsons r of 0.95 (P=0.0031) and with ELLA (OD2.0) with a Pearsons r of 0.92 (P=0.0089). Both ELLA parameters tested using the same sera also correlated very strongly with each other (Pearsons r= 0.99, <0.0001). See Figure 3.25 for correlation graphs.

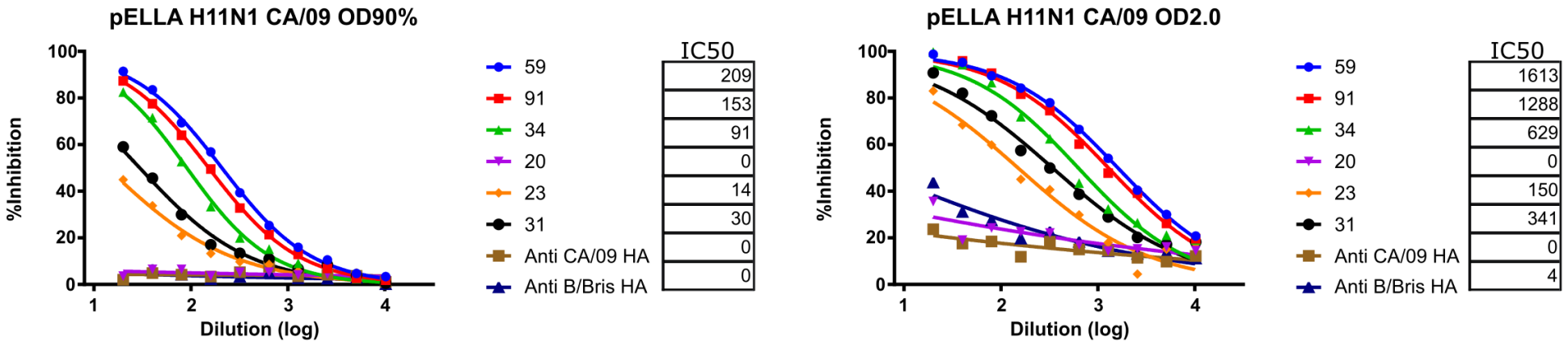

Figure 3.24. ELLA inhibition curves generated using Jenner Institute sera against H11N1 bearing PV (N1 A/California/7/2009). High positive (34, 91 and 59) and low positive (20, 31 and 23) sera based upon pMN IC_{50} values against A/California/7/2009 HA PV were tested against the matched N1. Serum sample 59 showed the strongest inhibition of N1, followed by 91 and 34, all three high positives. The low positive sera neutralised the least, with 31 and 23 neutralising weakly and serum 20 not at all. Negative controls include anti-A/California/7/2009 and anti-B/Brisbane/60/2008 HA serum (NIBSC). This experiment was carried out in duplicate with an input virus of OD_{492} 90% or 2.0.

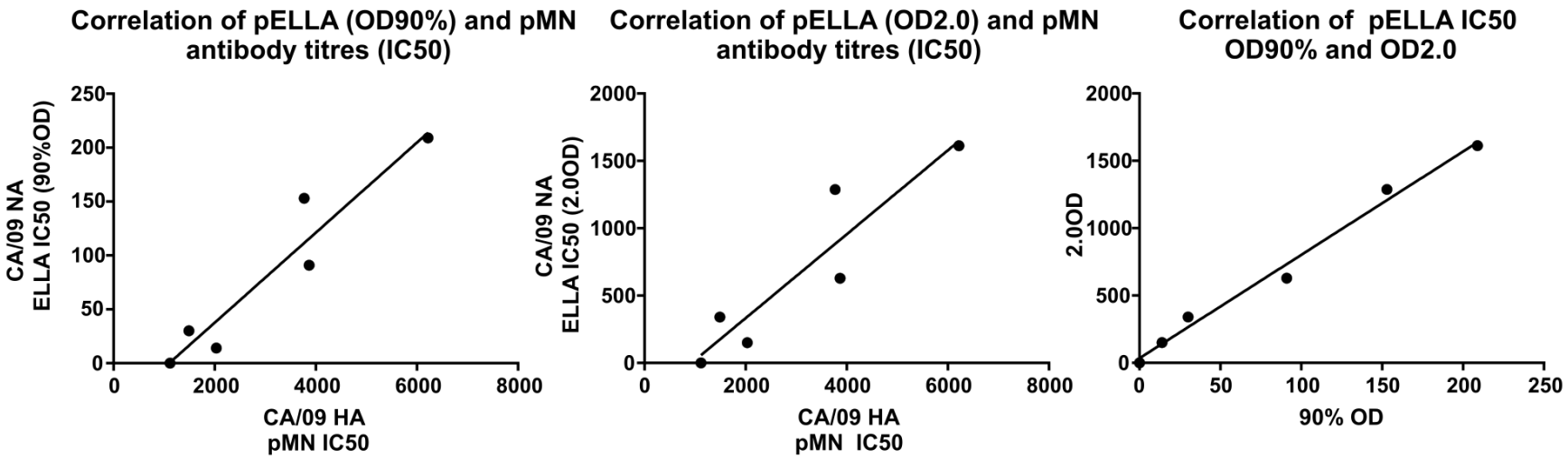

Figure 3.25. Correlation of neutralising antibody titres against the HA and NA of A/California/7/2009. pMN IC_{50} values generated against the HA of CA/09 are compared with ELLA IC_{50} values against the NA of CA/09. ELLA (OD90%) neutralising antibody titres and pMN neutralising antibody titres correlate strongly (Pearsons r= 0.95). ELLA (OD2.0) neutralising antibody titres and pMN neutralising antibody titres also correlate strongly (Pearsons r=0.92). ELLA neutralising antibody titres for OD90% and OD2.0 inputs show an almost perfect correlation, Pearsons r=0.99).

3.4 Discussion and conclusions

This project has been successful in that novel cHAs have been produced, optimised and tested against a large serum panel. While PV luciferase titres are not optimal for the CS CHM, they are still useable, further efforts can be made to improve titres using new transfection reagents as they become available. While the Gibson/In-Fusion assembly methods are laborious, they are excellent tools for the creation of cHA expression plasmids at relatively low cost (Gibson et al. 2009; B. Zhu et al. 2007). Unexpectedly high neutralising antibody titres were recorded against the CA/09 PV in the year prior to its existence, despite the exotic swine nature of this HA (Figure 3.21). While this is partly explained due to shared epitopes as mentioned previously (Xu et al. 2010), it renders efforts to interpret the cHA data more difficult. Interpretation of the cHA pMN system works by comparison of the CS CHM with each parental PV, H11 and CA/09. The premise is that H11 responses should only be present in the form of anti-stalk antibodies due to conserved epitopes within the group 1 influenza stalk – and not the exotic H11 head which is dissimilar to that of CA/09. Alongside this, the CA/09 chimera gives us an overall idea of the potency of antibodies in the serum at neutralising CA/09 at the globular head and stalk regions. As for the CS CHM, which is composed of the H11 head and CA/09 stalk, this PV should only be neutralised by stalk directed antibodies which have neutralised CA/09 or H11, but should be unaffected by antibodies targeting the HA head of CA/09, thus allowing dissection of the head response and focus on those stalk-reactive antibodies that are relevant to universal vaccine design. This has been achieved as the sera has less of an effect on the CS CHM than the parental CA/09 PV, but correlation is still observed in that high responders against CS CHM are likely to have high neutralising antibody titres against CA/09 and the H11 parental strain, both having a conserved group 1 stalk (Figure 3.19).

In regards to the Sports Science sera, a larger quantity of reagents was required to perform the assays against multiple different subtypes. However, the data generated did give an excellent overview on the immune repertoire of each patient at the point in time that the serum was collected. It was possible to determine some cross-reactive responses in patients when assaying the same sera against different subtypes within the same group of influenza A (Table 3.4), however, great care must be taken in the choice of strains used as this method remains intensive in the quantity of serum used.

Unfortunately it was not possible to troubleshoot the lack of success in the production of group 2 or influenza B PV. The problems are most likely due to incompatibility issues between the H10 (group 2) head and H3 (group2) or influenza B stalks used. Sanger sequencing showed that each gene was as designed and theoretically should have formed a polyprotein with distinct head and stalk regions post cleavage. However, for reasons which were not further investigated in this project, these two cHA expression plasmids did not give rise to working PV. This could be due to the stability of the protein, expression of the gene, toxicity issues with the cells and the pI.18-HA or phCMV-HA constructs, or lack of compatibility with the three proteases tested as well as those presently expressed in HEK293T/17 cells. While attempts to produce these cHAs failed, other research groups have successfully produced and tested similar systems (Ermler et al. 2017). Further time and investment is required to assess and overcome the problems which lead to these negative results, for the sake of this project it was decided that the CS CHM and its matched CA/09 parental strain would be the most suitable for pMN testing of the Jenner Sera, and to thus proceed with it.

The use of ELLA in conjunction with pMN using the chimera system gave rise to a further subset of data (Figure 3.24), possibly proving that certain patients had or had not been infected with the pH1N1 strain. By testing high positive and low positive samples (determined by pMN) using ELLA, we were able to show that the same strength of antibody response was present against the matched NA of this virus. This is very useful as there are currently no thresholds in pMN for positive or negative samples, especially as the sensitivity of pMN can often lead to strong neutralisation from human sera when regarding H1 PV, as seen with CA/09 neutralising antibody titres in sera collected prior to 2009 (Figure 3.19). In the ELLA results, low positive samples with HA neutralising antibody titres at or below 2000 tested low or negative in ELLA, whereas the high positives with titres above 3000 all tested positive (Figure 3.24). This was even more apparent when using a viral input of 2.0 OD, with increased values for high positive samples. Furthermore, correlation between pMN neutralising antibody titres and ELLA antibody tires was excellent (Figure 3.25), further proof that this relationship between NA and HA antibody titres is present as would be expected after infection with pH1N1.

3.5 Further work

Within the specific aims of this project, ideally the CS CHM system should be tested on a further set of sera, ideally from a larger group of patients pre and post the 2009 pandemic with accompanied metadata detailing infection status in regards to the 2009 strain. One of the major limitations of this project was the availability of sera pre 2009 as well as the majority of sera sourced in the 2012-2016 period. Further work should also focus on solving the issues surrounding the group 2 and Flu B chimeras, and after efforts have been made to produce working PV, more recent strains of H3 as well as Victoria and Yamagata influenza B stalks should be incorporated into this system.

Chapter 4 : Correlating SRH, HI and pMN using influenza B HA bearing PV

4.1 Introduction

4.1.1 Influenza B Virus classification and disease

Influenza B viruses comprise two co-circulating, antigenically distinct lineages that diverged from their progenitor, strain B/Hong Kong/8/1973, into the 'Yamagata like' (B/Yamagata/16/1988 type) and 'Victoria like' (B/Victoria/2/1987 type) lineages (Rota et al. 1990). This human virus causes a significant proportion (20-30%) of global morbidity associated with influenza virus disease, due to its global distribution and unpredictable switches in the predominating lineage circulating (Ambrose and Levin 2012; Glezen et al. 2013; Mccullers et al. 2004). The WHO vaccine recommendations include an up to date strain from both lineages for quadrivalent vaccines but only one for trivalent ones. Should the circulating lineage not match the predicted lineage there is an inevitable drop in coverage against influenza B linked disease (Ambrose and Levin 2012; Belshe 2010; Heikkinen et al. 2014; WHO 2016). In the United States, multiple quadrivalent vaccines have been approved and are in use (Weir and Gruber 2016).

4.1.2 Assays for influenza and the B type

Single radial immuno-diffusion (SRID) has been one of the mainstays for the identification and characterisation of inactivated influenza vaccines, correlating with immunogenicity and clinical benefit/protection (Cate et al. 1983; Hobson et al. 1972; La Montagne et al. 1983; M. S. Williams 1993; M. S. Williams et al. 1980; T. G. Wise et al. 1977; Wood et al. 1977; P. F. Wright et al. 1983). HI has been used for many decades as the tool used for detection of influenza antibodies (section 1.19) (Hirst 1941). These assays, in combination with ELISA (Lambré and Kasturi 1979) and single radial haemolysis (Schild et al. 1975) form the gold standard assays for detection of influenza virus antibodies, and are generally applicable to the B type. However, more recent work has highlighted the shortcomings of the traditional assays, focusing on the development of novel assays utilising various different technologies

(Bodle et al. 2013; Estmer Nilsson et al. 2010; Hashem et al. 2013; Khurana et al. 2014; Kuck et al. 2014; Pierce et al. 2011; Schmeisser et al. 2014; Temperton et al. 2007; Trombetta et al. 2014; Wen et al. 2015).

In this chapter, determining the correlation of the gold standard assays of HI and SRH with the recently Flu-B adapted pMN assay is the goal, as HI detects primarily RBS proximal antibodies while SRH detects IgG1, IgG3 and IgM class antibodies which are compatible with the complement cascade. pMN detects HA neutralising antibodies. As with SRH, HI has been correlated with protection against influenza, with titres at or above 40 linked to 50% or greater protection from infection in adults (Al-Khayatt et al. 1984; Cox 2013; Hobson et al. 1972; Potter and Oxford 1979). Linking either of these assays with pMN, despite the detection of different types of antibody, would allow more confidence to be attributed to the results generated using this assay, despite it actually detecting neutralisation of the function of the influenza HA glycoprotein.

Ether treatment has been employed for influenza B viruses, prior to HI experiments, raising the efficacy of the HI test to that of the complement fixation (CF) test (Kendal and Cate 1983; Monto and Maassab 1981; Pyhälä et al. 1985). This technique was developed due to the lack of reactivity of certain strains of influenza with RBCs, as well as the B type. Alongside the adaptation of SRID to influenza B resulting in SRH, ether treatment was found to increase sensitivity but reduces specificity of HI during assay of serum samples against influenza B (Chakraverty 1980; Julkunen et al. 1985; Kendal and Cate 1983; Monto and Maassab 1981; Oxford et al. 1982; Schild et al. 1975; Turner et al. 1982).

4.1.3 mAbs and camelid derived antibodies

mAbs are increasingly being used in influenza research, whether for development of standards to complement or validate assays or more directly to evaluate HA epitopes targeted through vaccination or as a therapy, as seen in the semi-recent Ebola outbreak (Davey et al. 2016; X. Qiu et al. 2014). The mAbs employed in this chapter were developed as an antibody-based alternative for influenza B identity (Yamagata or Victoria lineages) and potency assays (Verma et al. 2017).

Nanobodies are single domain antibodies derived from camelids which lack light chains and are able to bind to one single epitope. These have been developed and used in a wide range

of experiments ranging from use as crystallography chaperones, diagnostic tools and therapeutics (Muyldermans 2013).

4.1.4 Project aims

Correlation data between assays is important for in depth interpretation of immunogenicity data, especially when correlation is determined with an assay that has been used for *in vivo* or challenge studies, establishing a correlate of protection. By inter-comparison of assays utilising different approaches, the scientific community can make more informed decisions on the future direction of vaccine design and testing. To date, no experiment of this sort has been performed using influenza B, with efforts focusing more on the predominant A type. As a major contributor to morbidity and mortality, it is essential to interrogate the correlations and relationships between data produced for influenza B. This is especially important as this type is lacking a definitive reservoir and circulates yearly as part of two lineages. In this project, influenza B PVs will be interrogated using a defined set of mAbs and a panel of sera, to put this resource to use in the correlation of pMN, SRH and HI.

4.2 Methods

4.2.1 Plasmids

Expression plasmid phCMV1 bearing the HA gene for B/Hong Kong/8/1973, B/Yamagata/16/1988 and B/Florida/4/2006 were obtained from Dr Davide Corti, Institute for Research in Biomedicine, Bellinzona, Switzerland. B/Victoria/60/2008, B/Brisbane/60/2008 and B/Bangladesh/3333/2007 HA genes were sub cloned into plasmid pI.18 at the Viral Pseudotype Unit, University of Kent by Dr Francesca Ferrara.

Plasmids p8.91 and pCSFLW are described in section 2.1.2 and 2.1.3 respectively. Protease encoding plasmids used are detailed below in Table 1, alongside other information regarding the strains of influenza B used in this project (Accession #, Lineage, optimal protease for production). These optimal values for co-transfection of proteases were derived from previous work, and scaled down (50%) to 6-well format from 10cm^2 dish format (Ferrara 2015).

Table 4.1. Influenza B strains, accession numbers, lineage, protease type and quantity required for production in 6-well format are displayed.

Strain	Accession #	Lineage	Protease	ng per 6-well
B/Hong Kong/8/1973	K00425	Pre-split	HAT	125
B/Victoria/2/1987	FJ766840	Victoria	HAT	125
B/Brisbane/60/2008	KX058884	Victoria	TMPRSS4	125
B/Yamagata/16/1988	CY018765	Yamagata	HAT	125
B/Florida/4/2006	EU515992	Yamagata	HAT	125
B/Bangladesh/3333/2007	CY115255	Yamagata	HAT	250

4.2.2 Serum samples

One serum set was used per lineage of influenza B, consisting of samples taken pre and post seasonal vaccination. Paired low and high responders (according to HI results) were chosen by Dr Claudia Trombetta, University of Siena, Italy. In total, 41 pairs of sera were assayed against B/Brisbane/60/2009 and 43 pairs against B/Florida/04/2006. Due to anonymity laws in Italy regarding the collection and use of human sera, no further data is available regarding these samples.

4.2.3 HI assay

This experiment was carried out by Dr Claudia Trombetta, University of Siena, Italy. The influenza viruses used in the HI were B/Brisbane/06/2008 (15/146) and B/Florida/04/2006 (08/138) obtained from the NIBSC, United Kingdom. Serum samples were pre-treated with receptor destroying enzyme (RDE) from Vibrio *cholerae* (Sigma Aldrich) at 1:6 ratio for 18 h at 37°C in a water bath and then heat-inactivated for 1 hour at 56°C in a water bath with 8% sodium citrate at a 1:5 ratio. Turkey erythrocytes (Emozoo S.N.C, Invorio, Italy) were centrifuged twice, washed with a saline solution (0.9%) and adjusted to a final dilution of 0.35%. RDE-treated serum samples were diluted two fold with saline solution (0.9%) in a 96-well plate, starting from an initial dilution of 1:10. 25 µl of influenza virus was added to each well and the mixture was incubated at room temperature for 1 h. At the end of the incubation, erythrocytes were added and the plates were evaluated for the inhibition of agglutination after 1 h at R.T.

The neutralising antibody titre was expressed as the reciprocal of the highest serum dilution showing complete inhibition of agglutination. Since the starting dilution was 1:10, the lower limit of detectable neutralising antibody titre was 10. When the titre was below the detectable threshold, the results were conventionally expressed as 5 for calculation purposes, half the lowest detection threshold. Geometric mean titers were calculated from experimental repeats.

4.2.4 SRH assay

This experiment was carried out by Dr Claudia Trombetta, University of Siena, Italy. The influenza viruses B/Brisbane/06/2008 (15/146) and B/Florida/04/2006 (08/138) were obtained from the NIBSC. Serum samples were heat-inactivated at 56°C for 30 min in a water bath. Turkey erythrocytes (Emozoo S.N.C.) were centrifuged twice and washed with phosphate buffered saline (PBS). Diluted virus was added to the erythrocyte suspension at a concentration of 2000 haemagglutination units (HAU) per ml. The erythrocyte - virus suspension was incubated at 4°C for 20 minutes and subsequently, a solution of 2,5 mM Chromium Chloride ($CrCl_3$) was added to the suspension and it was incubated at R.T for 10 minutes. The suspension was then carefully mixed once and then centrifuged. A stock solution, consisting of 1.5% agarose in PBS containing 0.1% sodium azide and 0.5% low gelling agarose was prepared. This agarose stock solution was maintained at 45°C in a water bath. The final suspension of erythrocytes, virus and guinea pig complement was vigorously shaken and evenly spread onto each plate. Plates were incubated at room temperature for 30 minutes and then stored at 4°C for 30 - 90 minutes. Holes were introduced into each plate with a calibrated punch and 6 µl of each serum sample was dispensed into each hole. The plates were stored in a humid box and incubated at 4°C for 16 – 18 hours in the dark. Subsequently, plates were incubated in a water bath at 37°C for 90 minutes; diameters of the areas of haemolysis were then read in mm with a calibrating viewer (Schild et al. 1975).

4.2.5 mAbs, nanobodies and controls

mAbs were obtained from Dr Jerry Weir, Food and Drug Administration (FDA), U.S.A. These were produced by immunization of BALB/c mice with mammalian-derived VLP containing the HA glycoprotein of a relevant influenza B strain. When antibody titres for HA VLP ELISA were above 1:50,000, respective spleen cells were fused with a myeloma cell line.

Hybridomas were then titrated, selected and expanded for further testing, whereupon the clones in the following table were derived (Table 4.2). mAb specificity was determined by ELISA (Verma et al. 2017). A panel of nanobodies was obtained from the NIBSC as part of a joint project to determine their ability to neutralise PV bearing HAs from various influenza strains, including influenza B PV. These were produced in-house by the NIBSC team led by Dr Simon Hufton, Dr Walter Ramage and Dr Tiziano Gaiotto. Specificity of nanobodies was determined by yeast display and binding, these specificities are listed in Table 4.3.

Anti-B/Brisbane/60/2008 HA serum (11/136) was obtained from the NIBSC and employed against all strains of influenza B as a serum positive control. This antiserum had previously been tested in our laboratory by Dr Francesca Ferrara, showing that it was capable of neutralising all available strains of influenza B (table 4.1) to varying degrees, with the highest potency against the matched B/Brisbane/60/2008 strain.

Table 4.2. mAbs obtained from Dr Jerry Weir, FDA, U.S.A. Five total mAbs, two specific for each lineage of influenza B and one binding to an epitope conserved between both lineages (cross).

mAb	2F11	3E8	1H4	8E12	5A1
Target lineage	Cross	Yamagata	Yamagata	Victoria	Victoria

Table 4.3. Panel of llama derived nanobodies obtained from the NIBSC. 14 different nanobodies with specificity to epitopes which are shared between influenza B lineages (Cross) or confined to one lineage (B Victoria or B Yamagata). Specificity determined through yeast display and binding experiments.

Assigned ID #	Antibody	specificity
60	1b-6	cross
61	2a-6	B vic
62	2a-20	cross
63	2b-3	cross
64	2a-10	cross
65	Yam 2c-24	B yam
66	Vic 1b-10	cross
67	Yam 2b-9	cross
68	Yam 1a-4	B Yam
69	Yam 2b-2	cross
70	NGS#1	B Yam
71	Yam 1b-9	cross
72	Yam 2a-1	cross
73	Yam 2c-16	cross
74	Vic 2c-8	cross

4.2.6 Statistical analysis

The final neutralising antibody titres for each serum sample were averaged between replicates and these averages were compared between assays. This resulted in a table of results which could be compared. This comparison was carried out in Prism Graph pad where a two tailed Pearson's correlation was performed on pairs of data sets which were plotted against each other. A line of best fit was used in order to show the general trend of correlation between data sets. Analysis was performed between pre vaccination (V1), post vaccination (V2) and V1 to V2 fold change data sets. pMN data consisted of both IC_{50} and IC_{90} values, and further analysis was carried out on transformed (log10) V2 data.

4.3 Results

4.3.1 Production of influenza B PV

Prior to starting this project, large stocks of influenza B PV were produced in order to reduce batch to batch variation between repeated experiments. Titres were more variable for strains in the Victoria lineage; many attempts were made to produce high titre preparations which could span the length of each project. Later attempts succeeded in producing high titre B/Brisbane/60/2008 with titres exceeding $1x10^9$ RLU/ml, thus sufficient for the length of the project. Yamagata lineage preparations were less variable, and all production attempts yielded virus with titres exceeding $1x10^8$ RLU/ml. Viral titres for influenza B PV produced during the duration of this project are shown in Figure 4.1, with VSV-G positive transduction control as an example of maximum titres achievable.

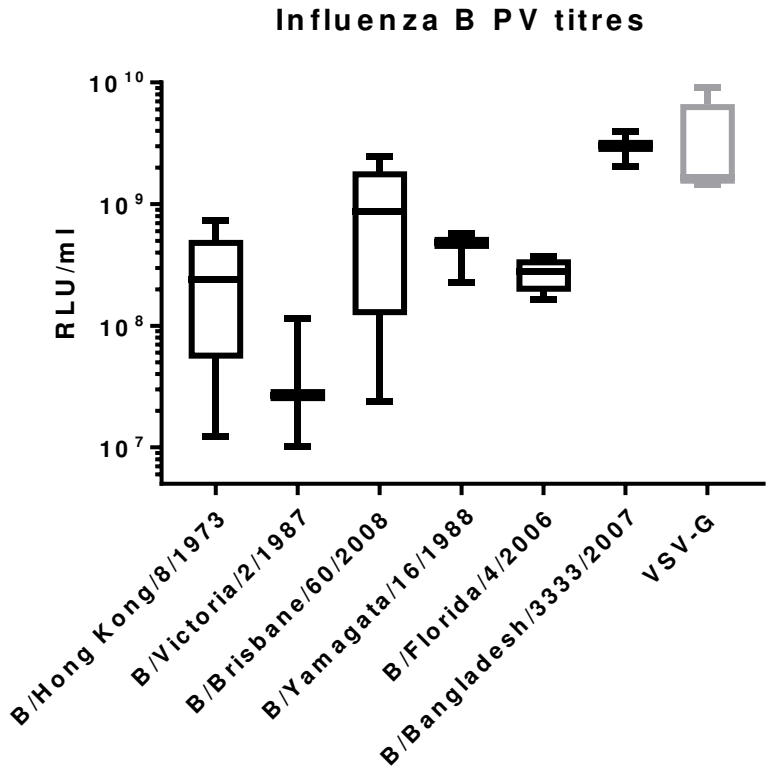

Figure 4.1. Titres (in RLU/ml) for all influenza B HA bearing PV produced prior to the start of this project. VSV-G titres titrated alongside influenza B PV displayed as a maximal transduction/luciferase production signal for comparison.

4.3.2 Lineage specific and cross-reacting mAbs neutralise influenza B PV

Lineage specific mAbs functioned as expected against all PV except B/Brisbane/60/2008 which was not susceptible (Figure 4.3). This PV was unaffected by either the Victoria specific mAbs, or the 2F11 cross-lineage mAb. This is also despite the anti-B/Brisbane/60/2008 HA serum (NIBSC) having the greatest effect on its matched PV strain (IC_{50} >256,000), Figure 4.5. The 2F11 mAb neutralised Yamagata lineage strains the strongest (IC_{50}: 2-4 ng/ml), followed by the pre lineage strain B/Hong Kong/8/1973 (IC_{50}: 8 ng/ml) and finally the Victoria strain B/Victoria/2/1987 (IC_{50}: 160). The Yamagata specific mAbs 3E8 and 1H4 only had an effect on Yamagata PVs, neutralising B/Bangladesh the strongest (IC_{50}: 3 and 4 ng/ml respectively), followed by B/Florida (IC_{50}: 21 and 3 ng/ml) and B/Yamagata (IC_{50}: 34 and 6 ng/ml). Victoria specific mAbs 8E12 and 5A1 neutralised B/Hong Kong the strongest (IC_{50}: 2 and 4 ng/ml respectively) followed by B/Victoria (IC_{50}: 47 and 22). See Table 4.4 for list of IC_{50} values for each mAb.

Table 4.4. IC_{50} values in ng/ml for the neutralisation of 6 strains of influenza B HA-PV by mAbs. Yamagata and Victoria lineages highlighted in pink and blue respectively. With the exception of B/Brisbane, the cross lineage mAb 2F11 acts as expected, neutralising all influenza B PV. Yamagata specific mAbs neutralise PV bearing HAs from Yamagata lineage strains while Victoria specific mAbs neutralise PV bearing HAs from Victoria lineage strains. The pre-lineage split strain B/Hong Kong is neutralised in a Victoria like manner, by 2F11 and Victoria lineage specific mAbs 8E12 and 5A1.

mAb	Target	B/Hong Kong	B/ Yamagata	B/Florida	B/Bangladesh	B/Victoria	B/Brisbane
2F11	Cross	8	3	2	4	160	-
3E8	Yamagata	-	34	21	3	-	-
1H4	Yamagata	-	6	3	4	-	-
8E12	Victoria	2	-	-	-	47	-
5A1	Victoria	4	-	-	-	22	-

The data for the Victoria lineage viruses show reduced antibody potency, with IC_{50} values up to 20 times higher. Also, Victoria epitope targeting mAbs neutralise B/Victoria and the Hong Kong precursor. Neutralisation curves for the above data are shown in Figures 4.2, 4.3 and 4.4.

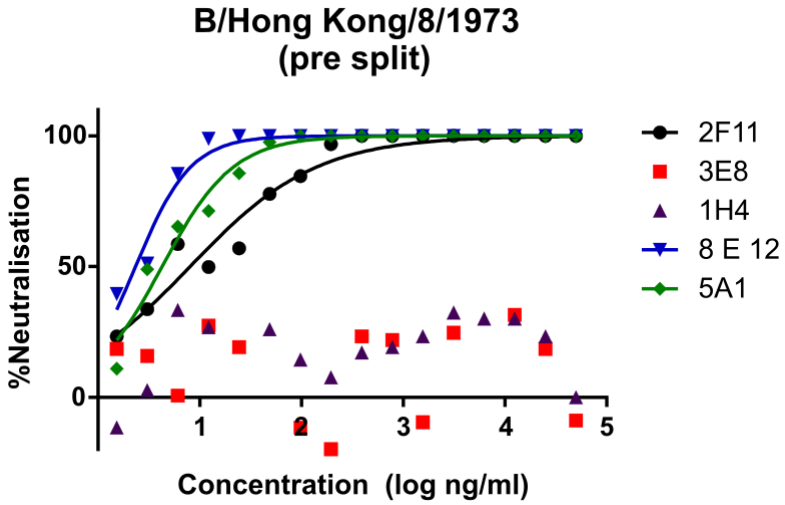

Figure 4.2. pMN neutralisation curves for FDA mAbs 2F11, 3E8, 1H4, 8E12 and 5A1 against PV bearing the HA glycoprotein from the influenza B pre-lineage split strain, B/Hong Kong/8/1973. This PV is neutralised in a Victoria like manner, knocked down strongly by Victoria specific mAbs 5A1, 8E12 and cross-lineage mAb 2F11 but not Yamagata specific mAbs 3E8 or 1H4.

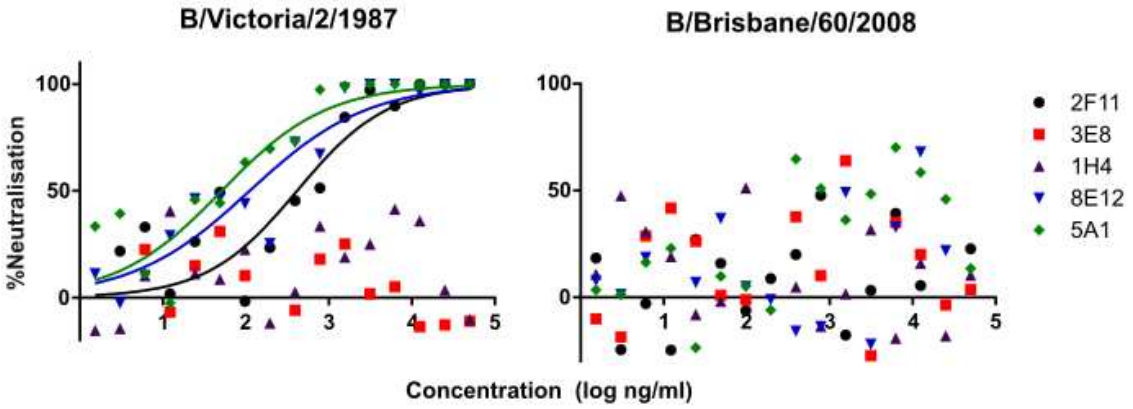

Figure 4.3. pMN neutralisation curves for FDA mAbs 2F11, 3E8, 1H4, 8E12 and 5A1 against PV bearing HA glycoproteins from Victoria lineage strains B/Victoria/2/1987 and B/Brisbane/60/2008. Victoria lineage PV are not neutralised by Yamagata specific mAbs 3E8 or 1H4. A/Victoria/2/1987 PV acts as expected, being neutralised by Victoria lineage specific mAbs 5A1, 8E12 and cross-lineage mAb 2F11. B/Brisbane/60/2008 PV are not neutralised by any of the mAbs tested, including Victoria lineage and cross-lineage mAbs.

Anti B/Brisbane/60/2008 polyclonal sheep serum was used as an anti-influenza B control in all of these experiments and for all strains of influenza B PV due to its polyclonal nature and therefore ability to cross-react. This antiserum neutralises the matched strain B/Brisbane/60/2008 and the other Victoria lineage strain B/Victoria/2/1987 the highest (Figure 4.5), 100% neutralisation is seen from the starting dilution point of 1:200 up to the penultimate point 1:128,000.

4.3.3 Llama derived antibody neutralisation of Victoria and Yamagata lineages.

Varying results were seen when the NIBSC panel of llama derived antibodies (subsequently referred to as nanobodies) was tested on the type strains of the Victoria and Yamagata lineages. Nanobodies targeting the conserved epitopes shared between both lineages did neutralise them (samples 60, 63, 66, 67, 71, 72, and 74). However, B/Victoria specific nanobody 61 neutralised both lineage strains whereas Yamagata specific nanobodies were unable to neutralise either PV. Figure 4.6 shows the IC_{50} values for nanobodies assayed against B/Victoria and B/Yamagata PV, as well as specificity determined by yeast epitope display at the NIBSC.

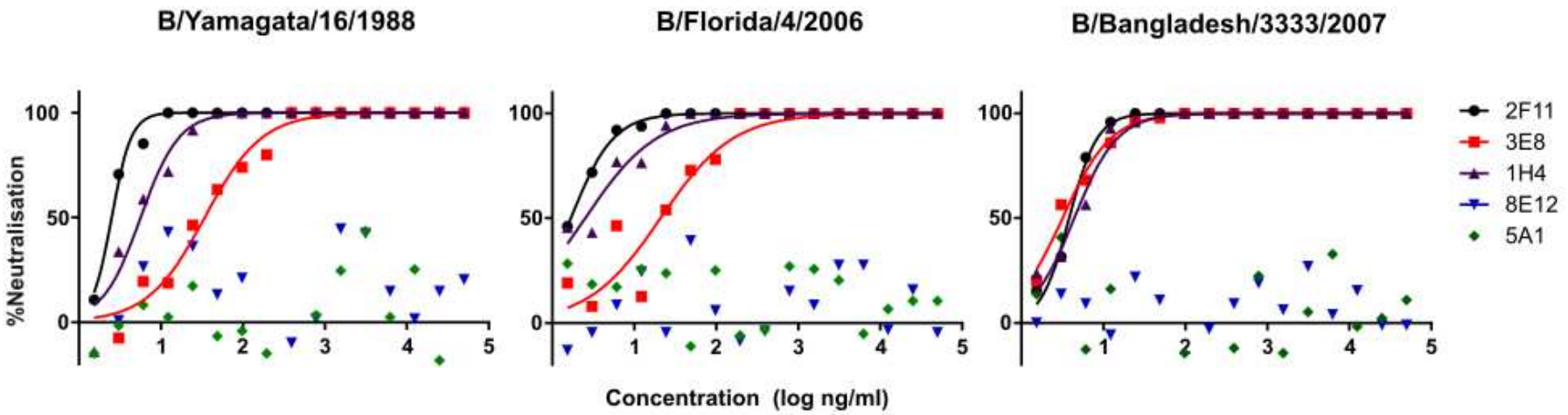

Figure 4.4. pMN neutralisation curves for FDA mAbs 2F11, 3E8, 1H4, 8E12 and 5A1 against PV bearing HA glycoproteins from Yamagata lineage strains B/Yamagata/16/1988, B/Florida/4/2006 and B/Bangladesh/3333/2007. Strong neutralisation is observed by Yamagata specific mAbs 3E8 and 1H4, and by cross-lineage 2F11. No neutralisation is observed for Victoria specific mAbs 8E12 and 5A1.

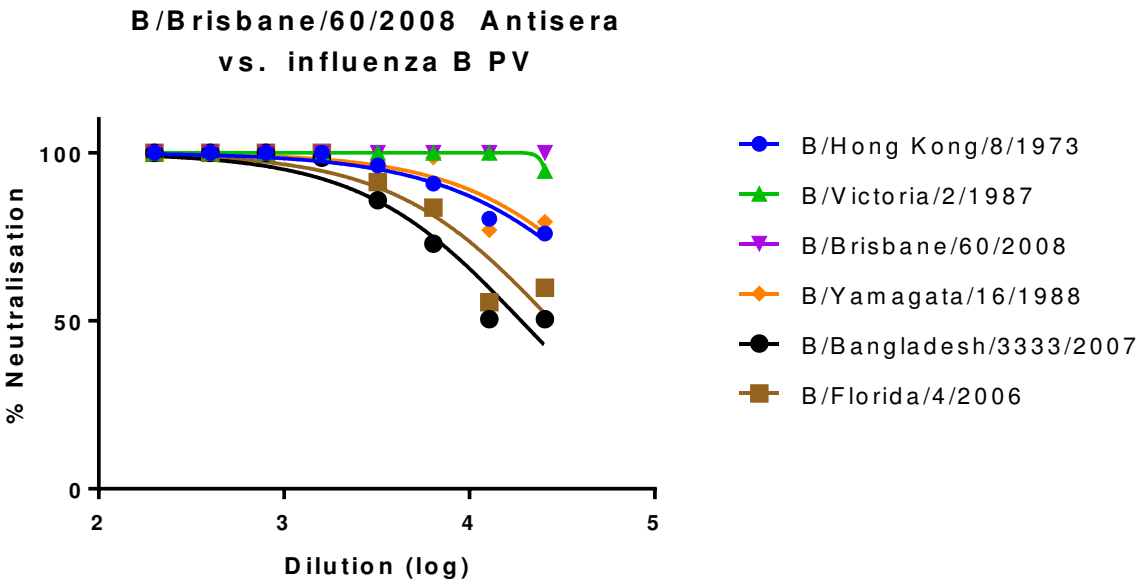

Figure 4.5. Anti-B/Brisbane/60/2008 HA serum (11/136) neutralises matched and related strains B/Brisbane/60/2008 and B/Victoria/2/1987 the strongest, but also neutralises Yamagata lineage strains and the B/Hong Kong/7/1973 precursor to a lesser extent.

4.3.4 Correlation of SRH, HI, pMN

Completion of pMN, SRH and HI on B/Florida/04/2006 and B/Brisbane/60/2008 experiments yielded neutralising antibody titres for all three assays which could then be compared and contrasted. Endpoint titres for high responders (V2) are displayed in Figure 4.7. The titre profiles of each serum set are very similar between the two viruses, when considering each virus has its own unique set of sera. HI values range from 5 to 1280 for both B/Brisbane/60/2008 and B/Florida/04/2006, with arithmetic means at 156 and 270 respectively. SRH values range from 37 to 106 and 38 to 99 mm^2 for B/Brisbane/60/2008 and B/Florida/04/2006 respectively. Arithmetic means were 58 and 57 mm^2. pMN (IC_{50}) values ranged from 4594 to 209,395 for B/Brisbane/60/2008 and 3349 to 31,954 for B/Florida/04/2006. Arithmetic mean pMN titre means were 41,613 and 11,740 respectively.

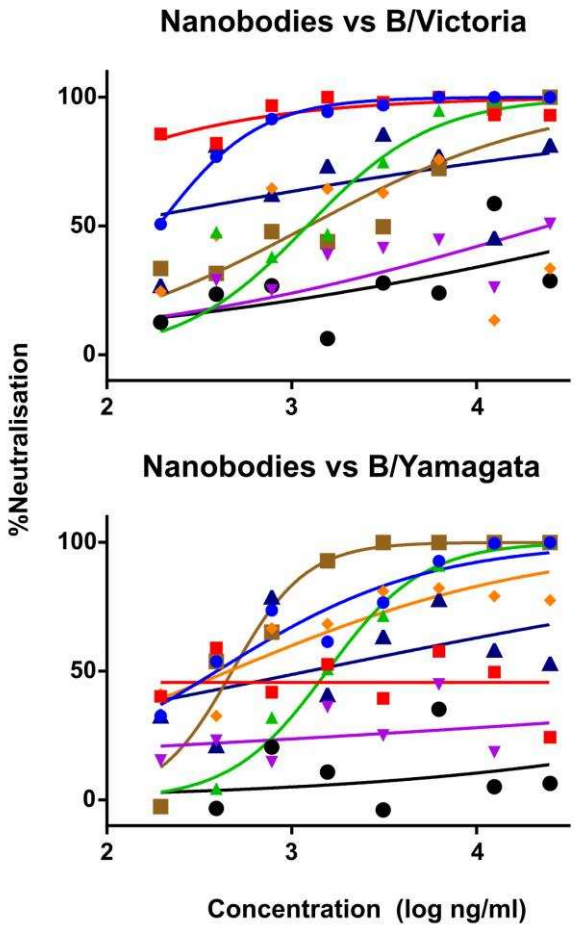

		IC50	
	Specificity	Victoria	Yam
60	Cross	189	393
61	Victoria	2380	4722
62	Cross	17	N/A
63	Cross	1213	1554
64	Cross	24178	N/A
65	Yamagata	21373	N/A
66	Cross	233	3
67	Cross	N/A	456
68	Yamagata	N/A	20588
69	Cross	1703	N/A
70	Yamagata	102628	N/A
71	Cross	1227	476
72	Cross	90	1227
74	Cross	3420	3037

Figure 4.6. pMN assay carried out using a panel of llama derived nanobodies on original lineage specific influenza B strain PV, B/Victoria/2/1987 and B/Yamagata/16/1988. Neutralisation curves for a subset of samples, and IC_{50} values in ng/ml for all nanobodies tested. Nanobody information is shown in table 4.3.

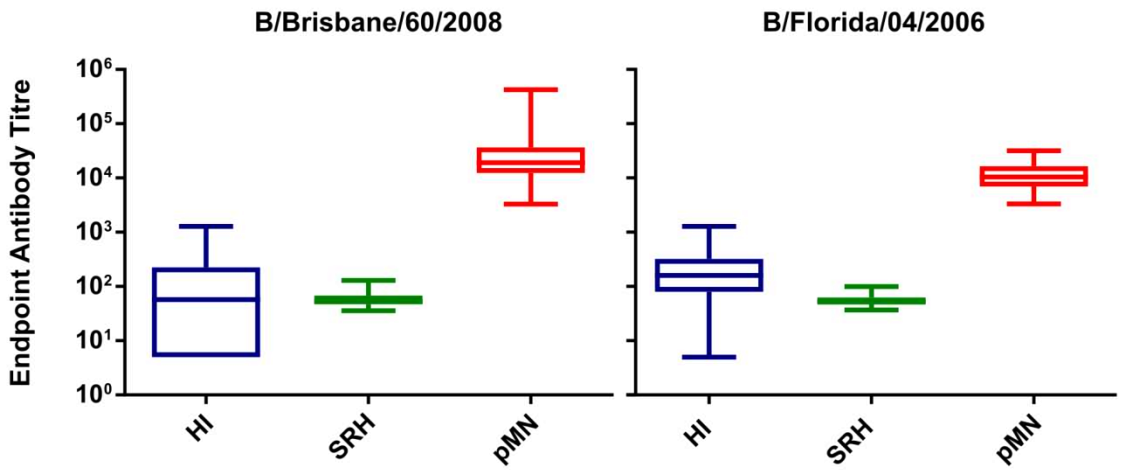

Figure 4.7. HI, SRH and pMN endpoint titres (IC_{50}) for high responders (V2, based on previous HI assay) against B/Brisbane/60/2008 and B/Florida/04/2006. Titres displayed show similar profiles for each strain tested, with a broader range of pMN IC_{50} values for B/Brisbane/60/2008.

4.3.5 Correlation of data: B/Brisbane/60/2008 IC_{50}

Correlation was evaluated between all three assays: pMN, SRH and HI. Three different sets of values for each assay were correlated, V1 data (pre-vaccination low responders), V2 data (post-vaccination high responders) and fold change between V1 and V2. For B/Brisbane/60/2008, no correlation was observed between pMN and the other assays, with Pearson's r values ranging from -0.07 to -0.08 (P = 0.13 to 0.9). SRH and HI correlated when fold changes were compared (r= 0.224, P=0.1539), and much more so after the removal of two outliers (r= 0.60, P= >0.0001). V1 results weakly correlated (r=0.32, P=0.0375) for SRH and HI, and more so for V2 results (r=0.39, P=0.0123). See Figures 4.8, 4.9 and 4.10 for correlation graphs and data.

4.3.6 Correlation of data: B/Brisbane IC_{90} and transformed data

Upon transformation of the V2 data to a logarithmic (log10) scale, correlation is still not seen between pMN and SRH or HI, with weak correlation between the latter two (r=0.35, P=0.0189). pMN IC_{90} data correlated weakly with HI and SRH (r= 0.37 and 0.45, P= 0.00188 and 0.0026 respectively). The correlation seen was reduced by transformation of IC_{90} data and comparison on a log scale (r= 0.23 and 0.32, P= 0.132 and 0.0372 respectively). See Figures 4.11, 4.12 and 4.13.

4.3.7 Correlation of data: B/Florida IC_{50}

In the same fashion as the B/Brisbane results, V1, V2 and fold change (V1 –V2) data sets were correlated between pMN, SRH and HI. In contrast to the results for B/Brisbane, pMN data correlated well with SRH and HI. For the fold change data, pMN correlated with HI and SRH (r= 0.66 and 0.56, P= <0.0001). SRH and HI correlated strongly (r= 072, P= <0.0001), see Figure 4.16. V1 data predictably showed very little, if any, correlation, with r values from -0.07 to 0.33 across the three assays, see Figure 4.14. For V2 data, pMN correlated well with SRH (r=0.46, P=0.0023), HI (r=0.61, P= >0.0001). V2 SRH and HI correlated strongly (r=0.79, P=<0.0001), see Figures 4.15 and 4.16.

4.3.8 Correlation of data: B/Florida IC_{90} and transformed data

Transformation to a log10 scale caused a slight reduction in the significance attributed to the correlation between pMN and SRH or HI (r= 0.57 or 0.30, P= 0.0002 or 0.0555), but correlation remained strong between all three assays. IC_{90} data correlated very well between pMN and SRH or HI (r= 0.85 and 0.65, P= <0.0001) and this was maintained when data was transformed to the log10 scale (r= 0.78 and 0.62, P= <0.0001). See Figures 4.17, 4.18 and 4.19.

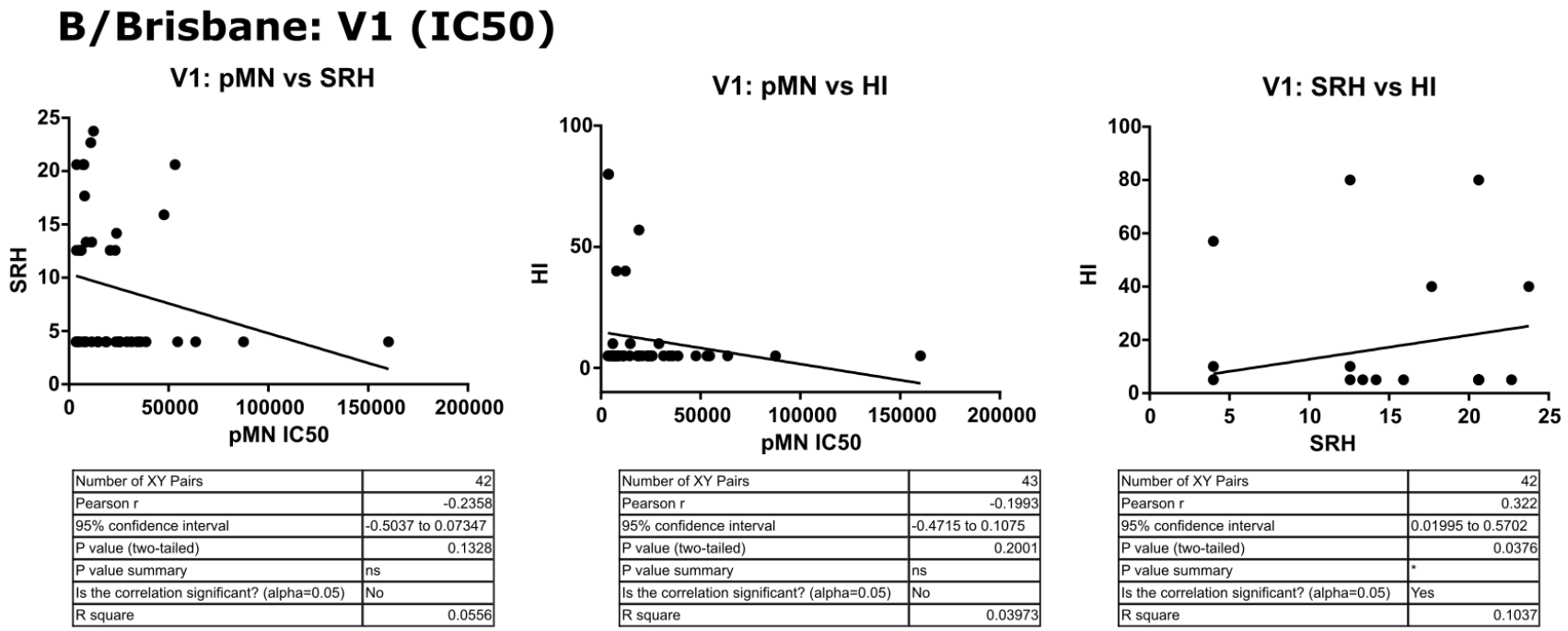

Number of XY Pairs	42
Pearson r	-0.2358
95% confidence interval	-0.5037 to 0.07347
P value (two-tailed)	0.1328
P value summary	ns
Is the correlation significant? (alpha=0.05)	No
R square	0.0556

Number of XY Pairs	43
Pearson r	-0.1993
95% confidence interval	-0.4715 to 0.1075
P value (two-tailed)	0.2001
P value summary	ns
Is the correlation significant? (alpha=0.05)	No
R square	0.03973

Number of XY Pairs	42
Pearson r	0.322
95% confidence interval	0.01995 to 0.5702
P value (two-tailed)	0.0376
P value summary	*
Is the correlation significant? (alpha=0.05)	Yes
R square	0.1037

Figure 4.8. Correlation of SRH, HI and pMN (IC_{50}) mean V1 values assayed against B/Brisbane/60/2008 PV. Pearson's two tailed analysis performed using prism Graph Pad. No correlation was observed between IC_{50} neutralising antibody titres and SRH or HI (Pearsons r = -0.23 and -0.19 respectively). Weak correlation was observed between SRH and HI for these V1 sera (Pearsons r = 0.32).

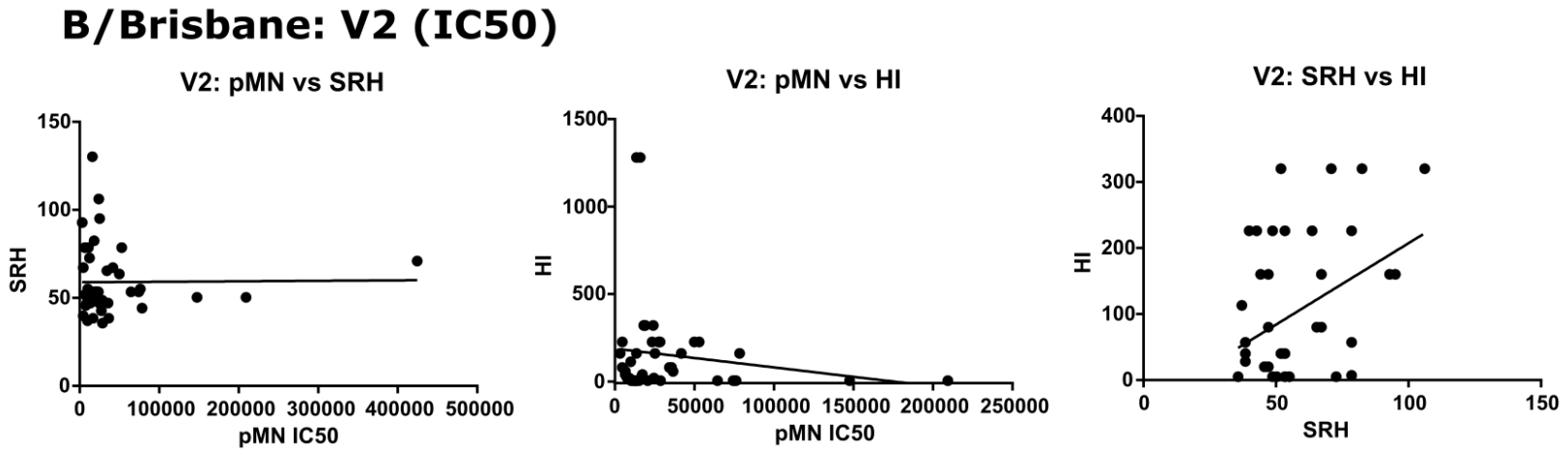

Number of XY Pairs	42
Pearson r	0.009791
95% confidence interval	-0.2951 to 0.3129
P value (two-tailed)	0.9509
P value summary	ns
Is the correlation significant? (alpha=0.05)	No
R square	0.00009586

Number of XY Pairs	42
Pearson r	-0.1529
95% confidence interval	-0.4366 to 0.1585
P value (two-tailed)	0.3338
P value summary	ns
Is the correlation significant? (alpha=0.05)	No
R square	0.02337

Number of XY Pairs	41
Pearson r	0.3874
95% confidence interval	0.09047 to 0.6211
P value (two-tailed)	0.0123
P value summary	*
Is the correlation significant? (alpha=0.05)	Yes
R square	0.1501

Figure 4.9. Correlation of SRH, HI and pMN (IC_{50}) mean V2 values assayed against B/Brisbane/60/2008 PV. Pearson's two tailed analysis performed using prism Graph Pad. No correlation was observed between IC_{50} neutralising antibody titres and SRH or HI (Pearsons r = 0.009 and -0.152 respectively). SRH and HI values correlated (Pearsons r = 0.38).

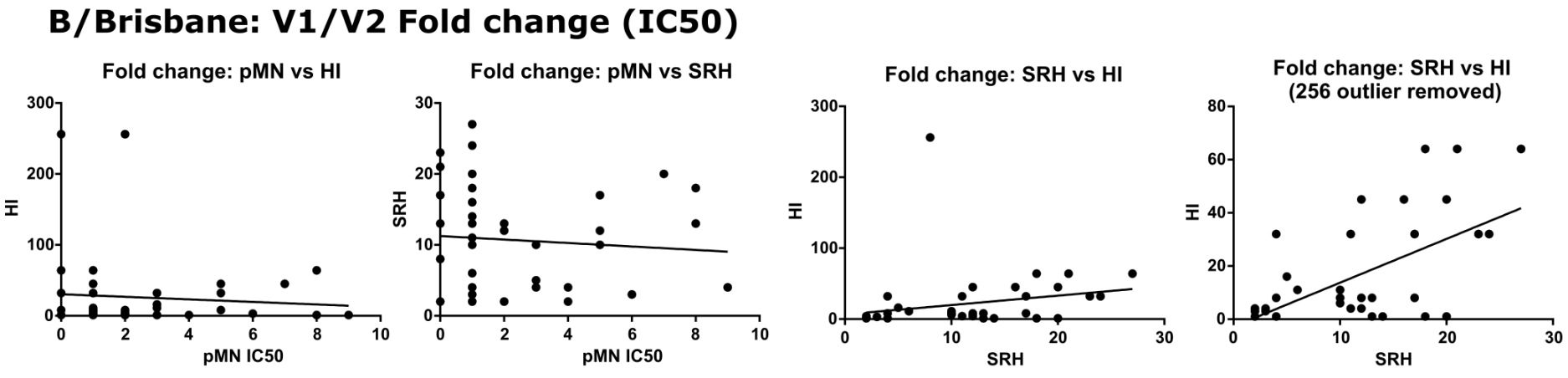

Number of XY Pairs	43
Pearson r	-0.07783
95% confidence interval	-0.3696 to 0.2279
P value (two-tailed)	0.6198
P value summary	ns
Is the correlation significant? (alpha=0.05)	No
R square	0.006057

Number of XY Pairs	42
Pearson r	-0.08294
95% confidence interval	-0.3774 to 0.2268
P value (two-tailed)	0.6015
P value summary	ns
Is the correlation significant? (alpha=0.05)	No
R square	0.006879

Number of XY Pairs	42
Pearson r	0.224
95% confidence interval	-0.08589 to 0.4943
P value (two-tailed)	0.1539
P value summary	ns
Is the correlation significant? (alpha=0.05)	No
R square	0.05016

Number of XY Pairs	41
Pearson r	0.6019
95% confidence interval	0.3610 to 0.7675
P value (two-tailed)	< 0.0001
P value summary	****
Is the correlation significant? (alpha=0.05)	Yes
R square	0.3623

Figure 4.10. Correlation of SRH, HI and pMN (IC_{50}) V1 to V2 fold change values assayed against B/Brisbane/60/2008 PV. Pearson's two tailed analysis performed using prism Graph Pad. No correlation was observed between IC_{50} neutralising antibody titres and HI or SRH (Pearsons r = -0.07 and -0.08 respectively). Weak correlation was observed between SRH and HI (Pearsons r = 0.22), which was improved after removal of outlying HI value (Pearsons r = 0.60).

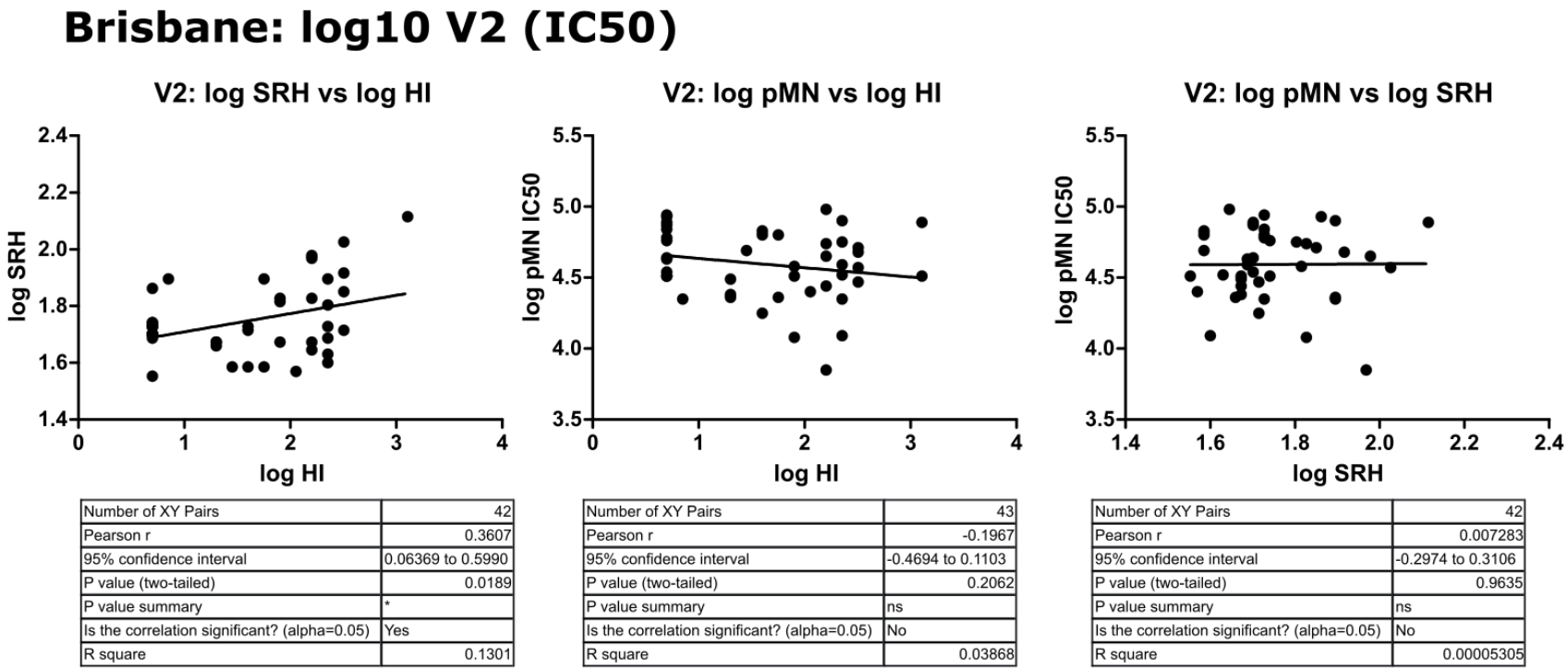

Number of XY Pairs	42
Pearson r	0.3607
95% confidence interval	0.06369 to 0.5990
P value (two-tailed)	0.0189
P value summary	*
Is the correlation significant? (alpha=0.05)	Yes
R square	0.1301

Number of XY Pairs	43
Pearson r	-0.1967
95% confidence interval	-0.4694 to 0.1103
P value (two-tailed)	0.2062
P value summary	ns
Is the correlation significant? (alpha=0.05)	No
R square	0.03868

Number of XY Pairs	42
Pearson r	0.007283
95% confidence interval	-0.2974 to 0.3106
P value (two-tailed)	0.9635
P value summary	ns
Is the correlation significant? (alpha=0.05)	No
R square	0.00005305

Figure 4.11. Correlation of transformed (log10) SRH, HI and pMN (IC_{50}) mean V2 values assayed against B/Brisbane/60/2008 PV. Pearson's two tailed analysis performed using prism Graph Pad. Weak correlation is observed between log SRH and HI values (Pearsons r =0.36). No correlation is observed between log IC_{50} neutralising antibody titres and log HI or SRH values (Pearsons r = -0.196 and 0.007 respectively)

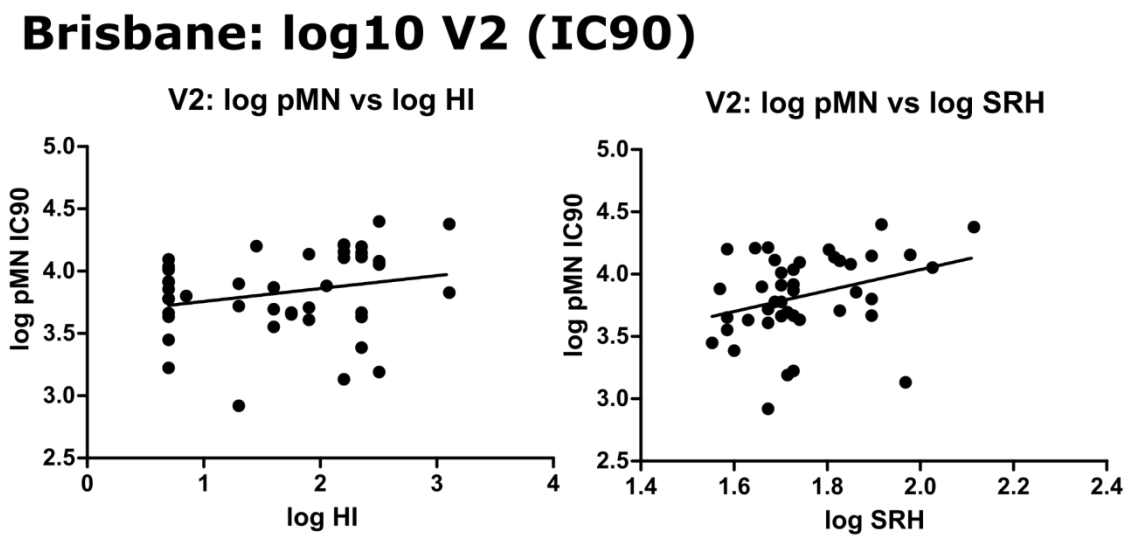

Number of XY Pairs	43
Pearson r	0.2334
95% confidence interval	-0.07209 to 0.4988
P value (two-tailed)	0.132
P value summary	ns
Is the correlation significant? (alpha=0.05)	No
R square	0.05446

Number of XY Pairs	42
Pearson r	0.3226
95% confidence interval	0.02058 to 0.5706
P value (two-tailed)	0.0372
P value summary	*
Is the correlation significant? (alpha=0.05)	Yes
R square	0.104

Figure 4.12. Correlation of transformed (log10) data for pMN (IC_{90}) with HI and SRH using mean V2 values for sera assayed against B/Brisbane/60/2008 PV. Pearson's two tailed analysis performed using prism Graph Pad. Weak correlation is observed between log IC_{90} neutralising antibody titres and log HI or SRH values (Pearsons r = 0.23 and 0.32 respectively).

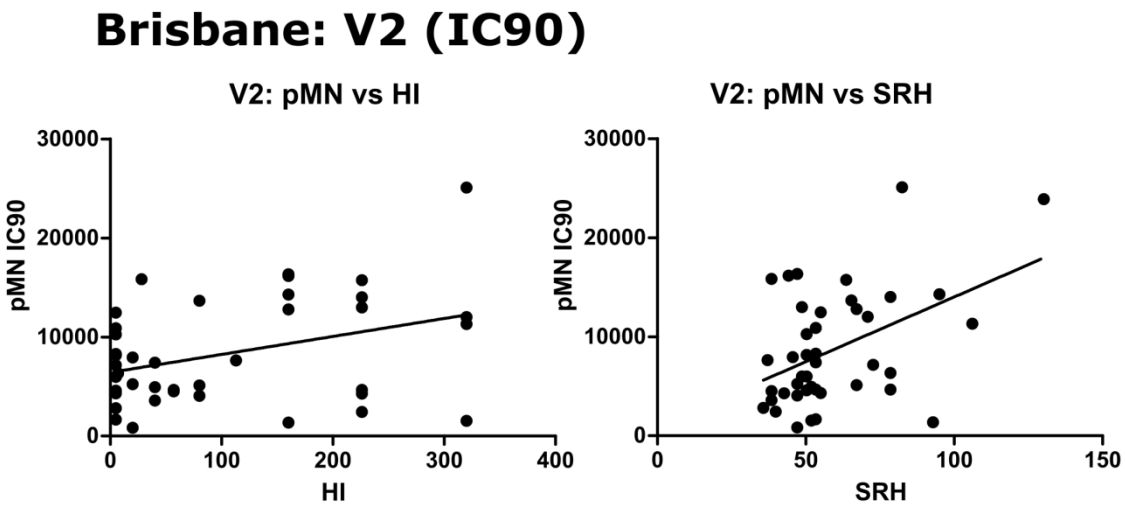

Number of XY Pairs	41
Pearson r	0.3654
95% confidence interval	0.06499 to 0.6051
P value (two-tailed)	0.0188
P value summary	*
Is the correlation significant? (alpha=0.05)	Yes
R square	0.1335
Notes: removed 1280 HAI result (SI05 and SI43)	

Number of XY Pairs	42
Pearson r	0.4535
95% confidence interval	0.1735 to 0.6657
P value (two-tailed)	0.0026
P value summary	**
Is the correlation significant? (alpha=0.05)	Yes
R square	0.2057

Figure 4.13. Correlation of pMN (IC_{90}) with HI and SRH using mean V2 values for sera assayed against B/Brisbane/60/2008 PV. Pearson's two tailed analysis performed using prism Graph Pad. Weak correlation is observed between IC_{90} neutralising antibody titres and HI (Pearsons r = 0.36). IC_{90} values correlate well with SRH values (Pearsons r =0.45).

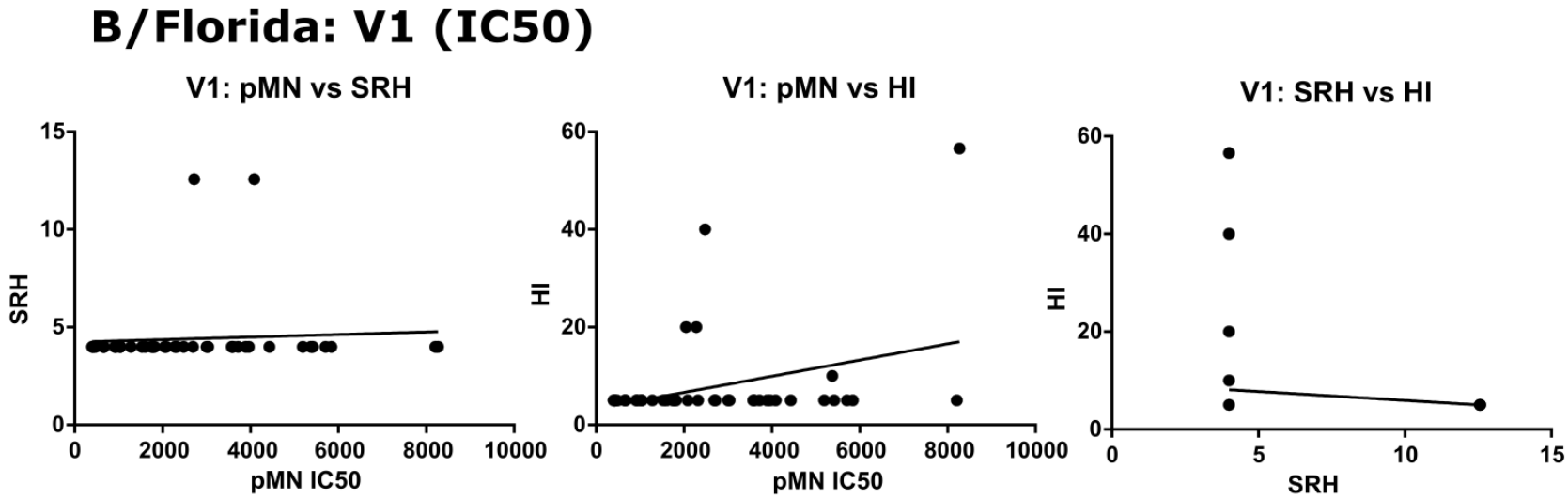

Number of XY Pairs	41
Pearson r	0.06942
95% confidence interval	-0.2435 to 0.3693
P value (two-tailed)	0.6663
P value summary	ns
Is the correlation significant? (alpha=0.05)	No
R square	0.004819

Number of XY Pairs	41
Pearson r	0.3311
95% confidence interval	0.02607 to 0.5798
P value (two-tailed)	0.0344
P value summary	*
Is the correlation significant? (alpha=0.05)	Yes
R square	0.1097

Number of XY Pairs	41
Pearson r	-0.06799
95% confidence interval	-0.3680 to 0.2449
P value (two-tailed)	0.6728
P value summary	ns
Is the correlation significant? (alpha=0.05)	No
R square	0.004623

Figure 4.14. Correlation of SRH, HI and pMN (IC_{50}) mean V1 values assayed against B/Florida/4/2006 PV. Pearson's two tailed analysis performed using prism Graph Pad. No correlation is seen between IC_{50} neutralising antibody titres and SRH (Pearsons r=0.06), or between SRH and HI (Pearsons r= -0.06). Weak correlation is observed between IC_{50} values and HI (Pearsons r = 0.33)

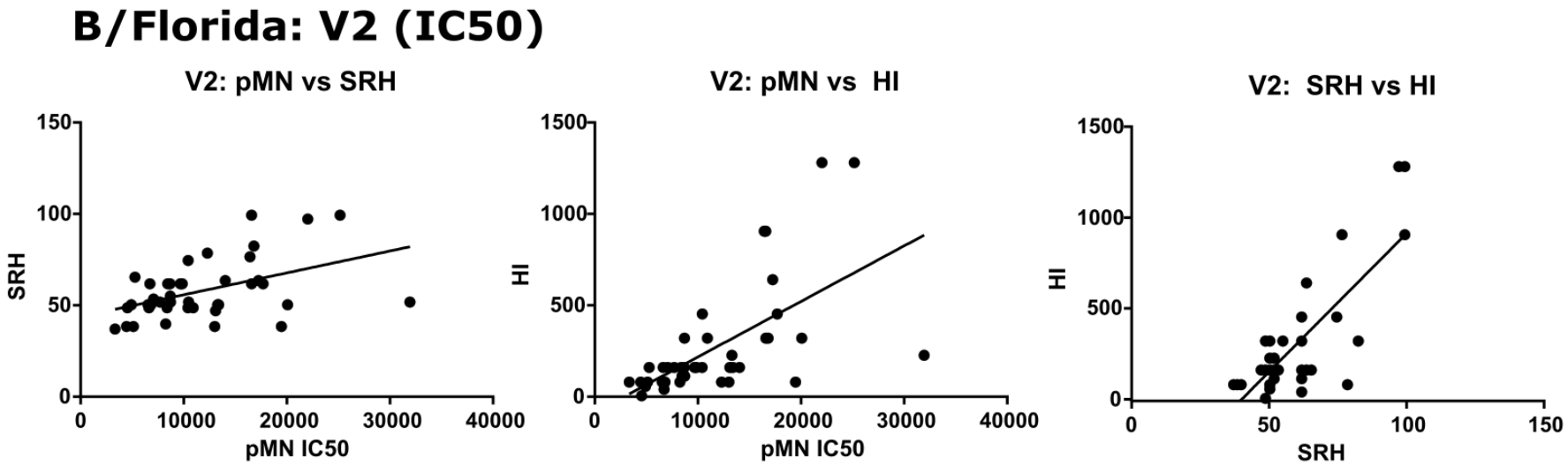

Number of XY Pairs	41
Pearson r	0.4624
95% confidence interval	0.1804 to 0.6742
P value (two-tailed)	0.0023
P value summary	**
Is the correlation significant? (alpha=0.05)	Yes
R square	0.2138

Number of XY Pairs	41
Pearson r	0.6108
95% confidence interval	0.3732 to 0.7732
P value (two-tailed)	< 0.0001
P value summary	****
Is the correlation significant? (alpha=0.05)	Yes
R square	0.373

Number of XY Pairs	41
Pearson r	0.7929
95% confidence interval	0.6417 to 0.8847
P value (two-tailed)	< 0.0001
P value summary	****
Is the correlation significant? (alpha=0.05)	Yes
R square	0.6287

Figure 4.15. Correlation of SRH, HI and pMN (IC_{50}) mean V2 values assayed against B/Florida/4/2006 PV. Pearson's two tailed analysis performed using prism Graph Pad. Weak correlation is observed between IC_{50} neutralising antibody titres and SRH (Pearsons r= 0.46). Strong correlation is observed between IC_{50} antibody titres and HI (Pearsons r=0.61), as well as between SRH and HI (Pearsons r =0.79) for the V2 data tested.

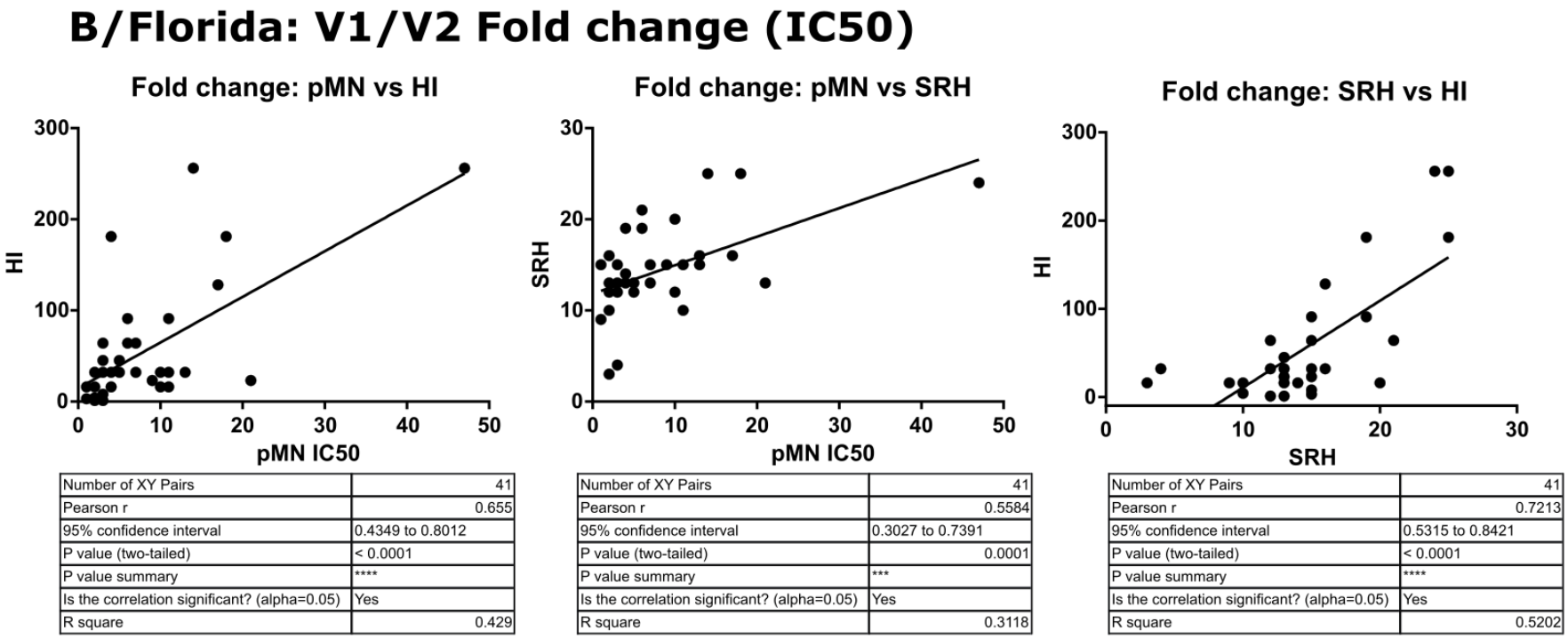

Figure 4.16. Correlation of SRH, HI and pMN (IC_{50}) V1 to V2 fold change values assayed against B/Florida/4/2006 PV. Pearson's two tailed analysis performed using prism Graph Pad. Strong correlation is seen between fold change in pMN and HI values between V1 and V2 neutralising antibody titres (IC_{50}), Pearsons r = 0.65. pMN and SRH V1/V2 fold changes correlate well, Pearsons r = 0.55, and strong correlation is observed for V1/V2 fold change for antibody titres of SRH and HI (Pearsons r= 0.72).

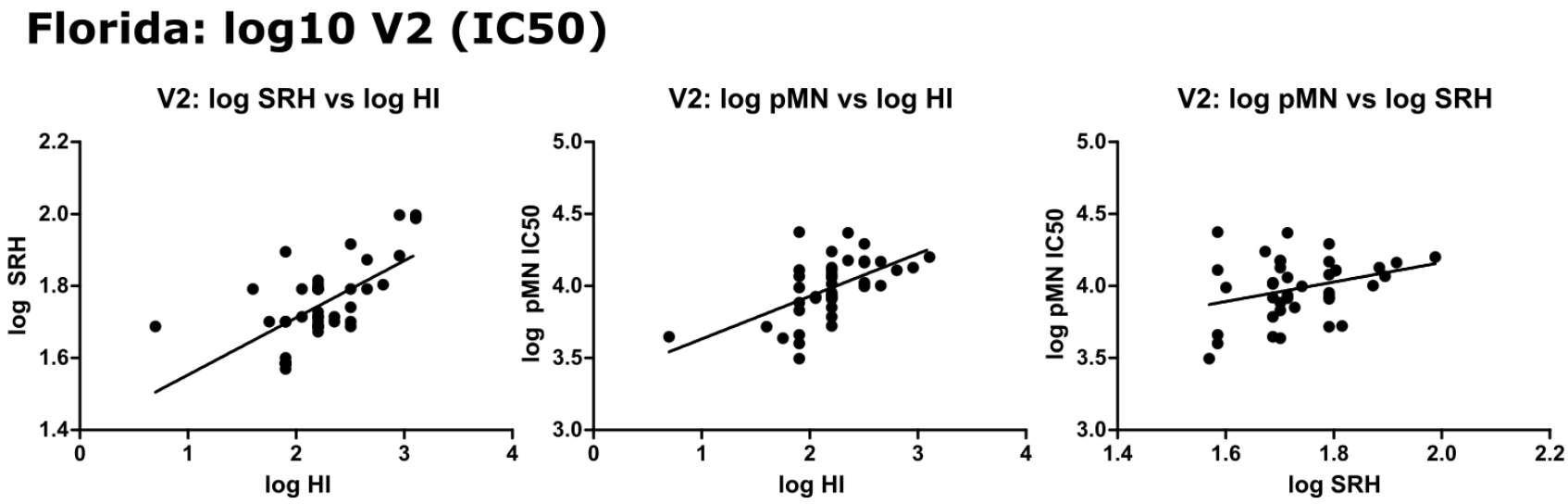

Number of XY Pairs	41
Pearson r	0.6278
95% confidence interval	0.3967 to 0.7840
P value (two-tailed)	< 0.0001
P value summary	****
Is the correlation significant? (alpha=0.05)	Yes
R square	0.3941

Number of XY Pairs	39
Pearson r	0.5654
95% confidence interval	0.3041 to 0.7476
P value (two-tailed)	0.0002
P value summary	***
Is the correlation significant? (alpha=0.05)	Yes
R square	0.3197

Number of XY Pairs	39
Pearson r	0.3091
95% confidence interval	-0.007192 to 0.56
P value (two-tailed)	0.0555
P value summary	ns
Is the correlation significant? (alpha=0.05)	No
R square	0.09554

Figure 4.17. Correlation of transformed (log10) SRH, HI and pMN (IC_{50}) mean V2 values assayed against B/Florida/4/2006 PV. Pearson's two tailed analysis performed using prism Graph Pad. Strong correlation is observed between log SRH and HI (Pearsons r = 0.62. log pMN and log HI correlate well (Pearsons r= 0.56) and weak correlation is seen between log pMN and log SRH (Pearsons r= 0.30).

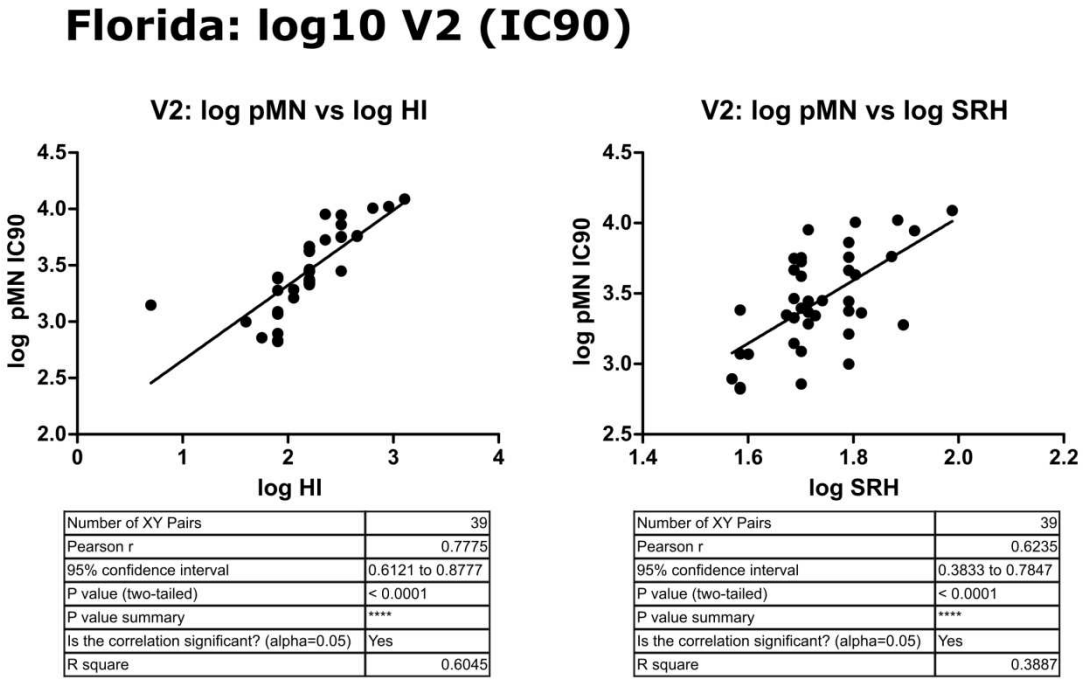

Number of XY Pairs	39
Pearson r	0.7775
95% confidence interval	0.6121 to 0.8777
P value (two-tailed)	< 0.0001
P value summary	****
Is the correlation significant? (alpha=0.05)	Yes
R square	0.6045

Number of XY Pairs	39
Pearson r	0.6235
95% confidence interval	0.3833 to 0.7847
P value (two-tailed)	< 0.0001
P value summary	****
Is the correlation significant? (alpha=0.05)	Yes
R square	0.3887

Figure 4.18. Correlation of transformed (log10) data for pMN (IC_{90}) with SRH and HI mean V2 values, assayed against B/Florida/4/2006 PV. Pearson's two tailed analysis performed using prism Graph Pad. Strong correlation is observed between log IC_{90} neutralising antibody titres and log HI or SRH values, with Pearsons r values of 0.77 and 0.62 respectively.

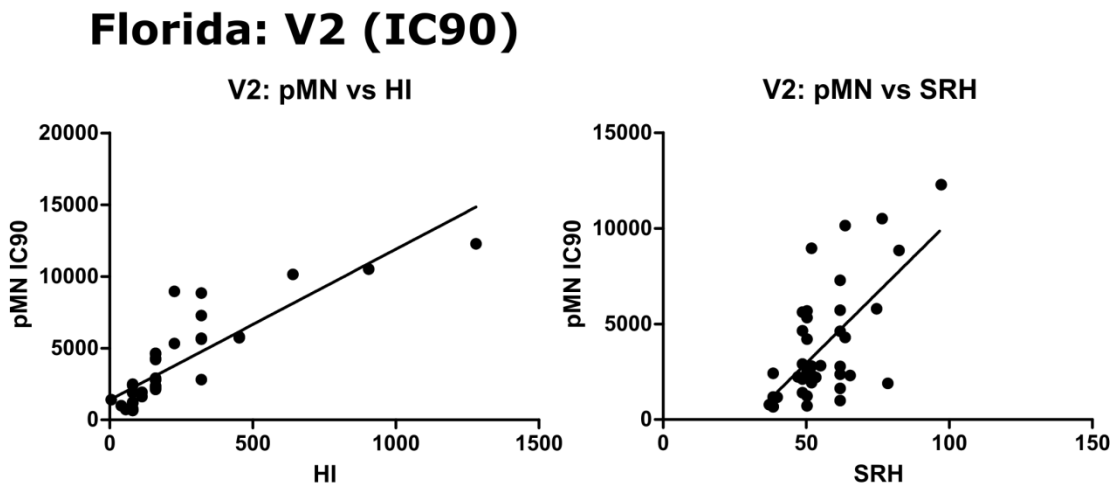

Number of XY Pairs	39
Pearson r	0.852
95% confidence interval	0.7338 to 0.9202
P value (two-tailed)	< 0.0001
P value summary	****
Is the correlation significant? (alpha=0.05)	Yes
R square	0.726

Number of XY Pairs	39
Pearson r	0.6469
95% confidence interval	0.4163 to 0.7993
P value (two-tailed)	< 0.0001
P value summary	****
Is the correlation significant? (alpha=0.05)	Yes
R square	0.4184

Figure 4.19. Correlation between pMN (IC_{90}) with SRH and HI mean V2 values, assayed against B/Florida/4/2006 PV. Pearson's two tailed analysis performed using prism Graph Pad. Strong correlation is observed between IC_{90} neutralising antibody titres and HI or SRH, with Pearsons r values of 0.85 and 0.64 respectively.

4.4 Discussion

Neutralisation of influenza B bearing PV with influenza B specific mAbs was consistent, with the exception of B/Brisbane/60/2008 results. Victoria lineage specific mAbs neutralised the type B/Victoria/2/1987 PV while Yamagata lineage specific mAbs neutralised Yamagata lineage strains (Figures 4.3 and 4.4). The cross-lineage specific mAb 2F11 neutralised both lineages as well as the pre-lineage split strain B/Hong Kong/8/1973. Similar results were obtained for the nanobodies tested on influenza B PV, with the majority of data matching specificities determined by yeast epitope display by project collaborators at the NIBSC (Figure 4.6). However, this project is still ongoing with further work required before conclusions can be drawn about their efficacy in comparison with the mAbs tested in this project. Discordant correlation was seen between Victoria and Yamagata lineages, with the former correlating well between pMN, SRH and HI and the latter only correlating between SRH and HI.

4.4.1 Neutralisation by influenza B mAbs

While the majority of influenza B mAbs generated by the FDA neutralised the expected strains in the pMN assay, neutralisation was not seen for B/Brisbane/60/2008 by Victoria specific mAbs, in contrast to data in the originally published article (Verma et al. 2017).

One possible explanation for this is N-linked glycosylation masking epitopes on the HA surface. The presence or absence of a glycosylated residue would drastically alter results when neutralising with a mAb which targets one specific epitope. In this project, a WT B/Brisbane/60/2008 gene was used to produce PV for use in pMN, while B/Victoria/2/1987 was human codon optimised. HI and SRH conducted by Dr Claudia Trombetta made use of inactivated antigen produced in bacteria whereas Verma and colleagues used a combination of ELISA using inactivated antigen and PV assays. For the latter assay, it is very likely that the B/Brisbane/60/2008 gene used was human codon optimised, as this research group employs this practice regularly (Personal communication with Dr. Jerry Weir, FDA). There is research to suggest differences in N-linked glycosylation between WT and human codon optimised genes in the HIV-1 glycoprotein gp120, with optimised sequences showing a reduction in glycosylation frequency (Ebrahimi and West 2014). Studies on egg-adaptation of influenza B viruses have characterised mutations within the 190 helix loop of the RBD which lead to significant change in antigenicity of the HA (Robertson et al. 1985; Shaw et al.

2001), due to the loss of an N-linked glycosylation site (Saito et al. 2004). Despite the lack of neutralisation shown against B/Brisbane/60/2008 by the Victoria specific mAbs, polyclonal hyperimmune antisera produced against the same HA subtype was the most effective at neutralising it (Figure 4.5), suggesting that the HA itself is antigenically 'correct' and that the problem lies in the specific epitopes targeted by 8E12 and 5A1. These mAbs were reported to bind to the amino acid residues 241 and 203 respectively which are within or close to the 190 helix which spans from residue 195 to 235 (Ni et al. 2013; Verma et al. 2017).

The fact that mAbs specific for the Victoria lineage also neutralised the pre-lineage split strain (Figure 4.2) is not surprising, as fewer structural differences have been reported between these than between the pre lineage strain and the Yamagata lineage. The positions of escape mutations generated against the Victoria lineage specific mAbs 8E12 and 5A1 presented in their characterisation were P241Q and K203R respectively (Verma et al. 2017). These are present within the 190 helix (RBD) of Victoria strains which is very similar in amino acid composition to the 190 helix of the pre lineage split strain B/Hong Kong/8/1973 (Ni et al. 2013).

4.4.2 Correlation between SRH and HI

Overall, SRH and HI correlated the strongest across both lineages, except for in V1 samples which were predictably very low due to the lower sensitivity of these assays (Figure 4.8 and 4.14). As most of the V1 samples are negative in terms of HI and SRH data, they are clustered around the respective titres of 5 and 4 mm^2, which lead to a lack of correlation when analysed. Fold change and V2 samples correlated for both Victoria and Yamagata lineages (Figures 4.8-4.13 and 4.15-4.19), indicating that increases in antibody are being detected in a similar fashion between these two assays.

4.4.3 Correlation between pMN and SRH

pMN correlated well with SRH for the Yamagata lineage strain B/Florida (Figure 4.15-4.19), correlation was observed for all analyses apart from V1 samples (Figure 4.14), which could be attributed to the same reasons for the lack of correlation in this set of samples between SRH and HI. As many of these samples would be classed as negative in SRH, the data is skewed towards the $4mm^2$ SRH data, while pMN is detecting a much larger breadth of responses from each so-called negative sample. This suggests that pMN would be a better

assay for evaluation of low-response samples, as its sensitivity offers an advantage over SRH. For B/Brisbane however, the only correlation observed was between IC_{90} values (transformed and raw data). Despite this, Pearson's r was still below 0.5 in each case. This is most likely due to the same problem as discussed in section 4.4.1 regarding the source of HA antigen used in each assay.

4.4.4 Correlation between pMN and HI

As with pMN and SRH, good correlation is seen for the Yamagata strain (Figures 4.15-4.19) but not the Victoria strain (Figures 4.8-4.12), once again, B/Brisbane/60/2008 is only poorly correlating when analysis is performed using IC_{90} values (Figure 4.13). B/Brisbane/60/2008 IC_{50} neutralising antibody titres are not correlating with SRH or HI when using either fold change or V2 serum data, transformed or raw.

4.5 Conclusions

The results discussed in this section, while discordant in regards to B/Brisbane/60/2008 PV, still represent the first comprehensive study correlating HI, SRH and pMN assays on this less well studied influenza type. Future work should focus on the Victoria lineage serum samples which should either be assayed against a codon optimised B/Brisbane/60/2008 PV, or all experiments regarding this lineage should be performed on a different strain within the same lineage, in order to evaluate whether the problem lies in the B/Brisbane/60/2008 protein itself or within the whole of the Victoria lineage. Ideally this project would be carried out on the lineage type strains B/Victoria/2/1987, B/Yamagata/16/1988 and the pre-lineage strain B/Hong Kong/8/1973.

Chapter 5 : Development and use of ELLA for detection of sialidase activity and inhibitory antibodies against NA bearing PV.

5.1 Introduction

5.1.1 ELLA

ELLA is a safe and reproducible system for the detection of sialidase activity (or its inhibition) in a 96-well format (Couzens et al. 2014; Lambré et al. 1991; Westgeest et al. 2015). This assay has taken over from the traditional thiobarbituric acid (TBA) assay (Sandbulte et al. 2009; Warren 1959), and is used regularly to detect NA activity or for follow-on experiments such as inhibition assays (Cate et al. 2010; Couzens et al. 2014). Using this assay, antiviral compounds in addition to antibodies (monoclonal, polyclonal or serum based) can be tested against different subtypes and strains of NA in the context of its intrinsic activity rather than simple binding as would be measured by ELISA. This allows investigators to evaluate any increases in NA inhibiting antibodies as a result of vaccination, whether these are protective and the extent to which the evolution of the protein escapes antibody based enzyme inhibition (Hassantoufighi et al. 2010; Kilbourne 1976). This assay employs the lectin from the species Arachis *hypogaea* (peanut), conjugated to horseradish peroxidase (PNA-HRPO). This lectin binds to galactose, which is exposed after sialidase activity on the carbohydrate fetuin. Fetuin is therefore used to coat 96-well plates in the ELLA assay, with PNA-HRPO used to quantify NA activity through detection of digested fetuin (Figure 5.1).

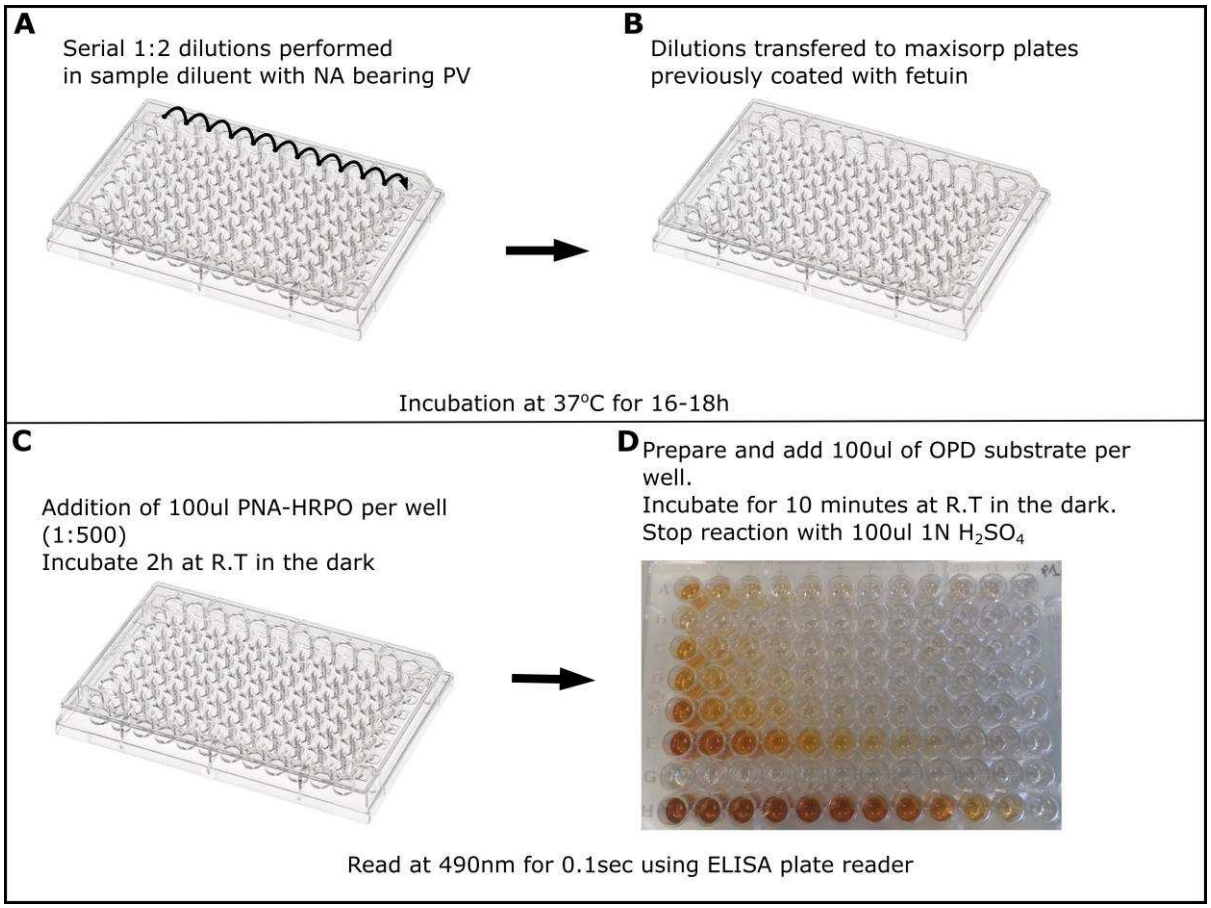

Figure 5.1. A schematic for the enzyme-linked lectin assay (ELLA). PV samples are diluted 1:2 across a 96-well clear plate (A), before being transferred to a maxisorp plate coated in fetuin (B). After incubation (C), PNA-HRPO is added and plates incubated, before OPD substrate is added and plates read at an optical density of 492nm (D). Typical results of an ELLA titration are shown in panel D.

Alternative assays are available and utilised in other studies, such as MUNANA, named after the chemical substrate used: 2'-(4-methylumbelliferyl)-a-D-N-acetylneuraminic acid (Potier et al. 1979), and a chemiluminescence assay, originally devised by (Buxton et al. 2000) and compared to MUNANA by (Wetherall et al. 2003).

ELLA is being increasingly used and developed further towards the goal of validating it to measure antibody responses elicited by vaccination (Changsom et al. 2016; EMA 2010; Fritz et al. 2012; Sandbulte et al. 2016). There are however issues surrounding the instability of NA in commercial vaccines, with reported variances in NA activity post vaccine production (Kendal et al. 1980; Trombetta et al. 2014). Irrespective of these issues, the elicitation of NA antibodies through vaccination and the detection of such antibodies is of growing interest to the influenza community (Wohlbold and Krammer 2014).

Further issues have been reported in the form of HA stalk-directed antibodies, which have been shown to interfere with the activity of NA in the ELLA assay for 2009pdm H1N1 (Rajendran et al. 2017). Despite this interference, it seems that NA antibody responses match those against HA, with immunity against a primary infection being boosted through original antigenic sin after infection by subsequent strains (Rajendran et al. 2017). The data presented in this study showed that N1 titres tended to be low in the groups studied, in comparison to N2 or influenza B NA titres, which was postulated to be due to lower antigenicity of the N1.

5.1.2 CONSISE study

The CONSISE group, described in chapter 1, published a position piece aimed at standardisation of ELLA across different laboratories worldwide, by comparing data generated using the same reagents (Couzens et al. 2014; Eichelberger et al. 2016). N1 and N2 antigens were used to measure antibodies targeting these proteins from a panel of 12 sera in three different assays and in 23 different laboratories worldwide. These serum samples (8 of the original 12) and their attributes are shown in Table 5.1. Each serum sample was tested against reassortant H6N1 and H6N2 influenza viruses (inactivated virus), providing neutralising antibody titres against each NA. These were compared between labs, showing differences in titres between labs remained below 4-fold (n=15/23 and 16/23 for H6N1 and H6N2 respectively). The study identified the crucial factors involved in ELLA such as background signal and viral input, of which it was decided to evaluate the latter with PVs as a source of NA instead of the traditional use of WT virus.

5.1.3 Study aims

The aim of this project was to establish and make use of the ELLA system with available reagents, making use of and measuring NA activity of PVs. Until now, the Viral Pseudotype Unit had only incorporated NA into PVs in order to measure its activity (or lack of) through the increase or decrease in PV production titre in comparison with exogenous NA or no source of NA at all. Essentially, NA had only previously been tested through its ability to allow influenza PV to bud from the producer cell surface. The ultimate desired goal of this project was to be able to measure immune responses inhibiting the action of NA. After producing stocks of NA PVs and titrating them using ELLA, efforts were made to produce

high titre, reproducible stocks to employ in inhibition assays. It was also decided to fully evaluate this assay by challenging the standard operating conditions used when utilising WT virus, including the concentrations of materials (PNA-HRPO) and input quantities (PV). The traditional pMN assay benefits from the ability to produce HA only PV, enabling neutralising or inhibiting compounds to be measured against only one protein. Addition of NA to the PVs allows steric hindrance of HA binding by NA-antibody complexes, preventing certainty that a detected inhibition response is due to HA directed antibodies. Similarly, the goal of this project was to evaluate whether production of NA only PVs was possible in order to measure clean inhibition titres against this enzyme in the absence of HA and its ability to interfere via steric hindrance.

Table 5.1. Panel of sera obtained from the CONSISE group via the NIBSC. A total of 8 samples were tested in this project. High positive samples S1 and S2 derive from purified human IVIG and Transgenic bovine plasma (vaccinated with TIV 2012/2013). Sample S3 is pooled human sera and samples S4-S8 individual human sera vaccinated post 2009/2010.

Sample I D	Description
S1	Human purified IVIG, chosen from HP HI neutralising antibody titres in 2013 (Source: Baxter Biomedical Research)
S2	Transgenic bovine plasma (TIV 2012/2013) (Source: Sanford Research)
S3	Pooled human sera (Source: Lonza Pharma & Biotech)
S4-S8	Human sera, post 2009/2010 Influenza vaccination (Source: Accelovance, Contract Research Organisation)

5.2 Methods

The ELLA protocol detailed in this chapter was initially derived from Couzens et al. 2014, several variations in the parameters used in this protocol were used in order to examine the system using PVs as a source of NA. PNA-HRPO was used at both 1:500 and 1:1000 dilutions during the galactose-binding step. In the inhibition assay (Section 5.2.5), PV input and dilution was varied in order to give ranges from OD2.0 to OD3.5, the latter being equivalent to 90% of the maximal signal obtained in the ELLA NA titration (Section 5.2.4).

5.2.1 Alignment of NAs

Amino acid sequences for A/Brisbane/59/2007 (Accession: AHG96686.1) and A/California/7/2009 (Accession: ACQ63272.1) NA genes were aligned using the PROMALS3D online tool, accessible at http://prodata.swmed.edu/promals3d/promals3d.php (Pei et al. 2008).

5.2.2 Production of HA/NA bearing VLPs

In parallel to PVs produced bearing HA/NA or NA only detailed in section 5.2.3, VLPs were produced, essentially composed of PVs bearing HA/NA or NA glycoproteins but lacking the lentiviral reporter, core or both. A schematic diagram for the types of PV or VLP used in this chapter is presented in Figure 5.2.

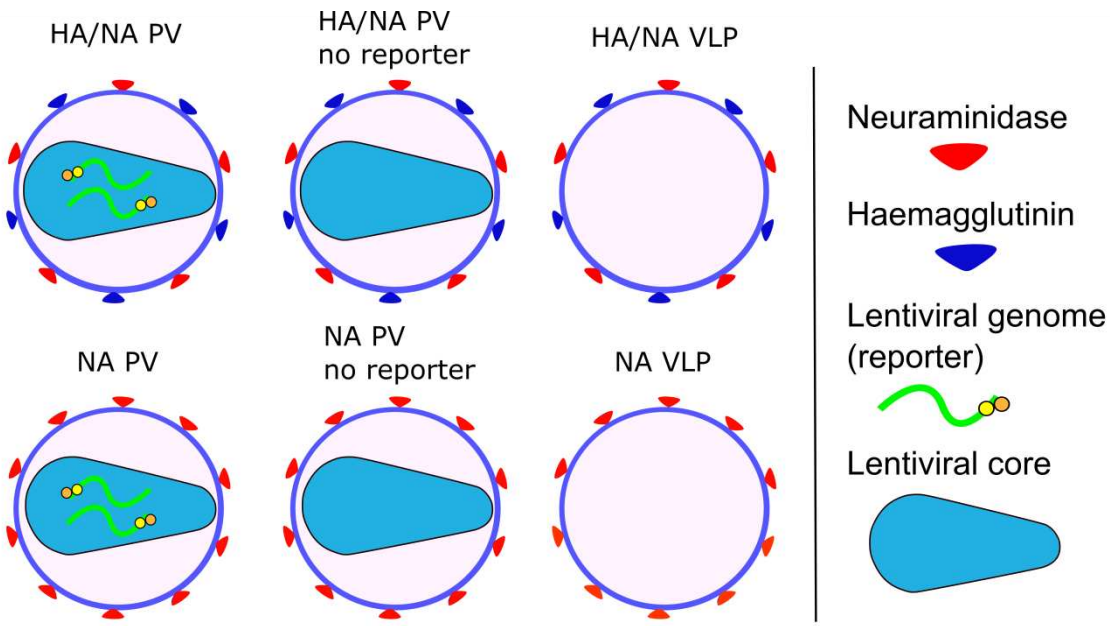

Figure 5.2. Different NA bearing particles produced and tested during this chapter. PVs bearing HA/NA or NA only were produced alongside the same particles lacking the lentiviral reporter or lacking both the lentiviral reporter and core (designated VLPs).

5.2.3 Production of HA/NA and NA only PV

HA/NA and NA only PV were produced by PEI mediated co-transfection of HEK293T/17 cells, as described in chapter 2. However, various different plasmid inputs and combinations were tested during the optimisation of ELLA using PV, which are detailed in each respective

results data section. Further deviances from the previously described method include harvesting of PV 72 h post transfection in lieu of 48h.

5.2.4 ELLA (Titration)

The standard ELLA protocols used in this chapter are detailed in chapter 2, deriving from the CONSISE protocol described by (Couzens et al. 2014). Titrations were originally carried out with a starting volume of 24 µl of sample diluted in a total of 240 µl sample diluent (1:20 starting dilution after transfer to maxisorp plate). Due to the lower activity observed from PV preparations in comparison with available CONSISE concentrated inactivated virus samples, it was decided to use 120-240 µl of PV in the first well, giving a starting dilution of 1:2 when transferred to fetuin coated maxisorp plates.

5.2.5 ELLA (Inhibition assay)

Serum inputs remained the same as previously described in chapter 2; at 24 µl in 240 µl (1:10 start). exNA (sources from Sigma and Roche) were originally tested from 1:240 (1 µl) and 1:48 (5 µl) starting dilutions, eventually 1:240 was deemed suitable for control purposes due to the very high activity seen from these commercial bacterial preparations.

5.3 Results

5.3.1 Initial testing & controls

Initially, ELLA was performed with a set of standard reagents, kindly provided by CONSISE through the NIBSC as part of a collaborative study which was carried out as part of efforts to standardise ELLA across laboratories worldwide (Eichelberger et al. 2016). These reagents included inactivated reverse genetics (RG) influenza viruses bearing the H6 HA and either N1: A/Brisbane/59/2007 (H1N1) and A/California/7/2009 (H1N1) or N2: A/Uruguay/716/2007 (H3N2), while internal genes were derived from A/Puerto Rico/8/38 (H1N1). A set of serum samples was also included, detailed in the cited article and Table 5.1. In parallel to testing of the CONSISE virus samples, two sources of bacterial exNA were employed as controls in the initial tests, from Sigma (Clostridium *perfrigens*, cat: N2876) and Roche (Vibrio *cholerae*, cat: 000000011080725001). These exNAs of bacterial origin (both genes and method of production) were highly potent in terms of NA activity (Figure 5.3). The first titration of these exNAs was carried out at 1:48 (5 µl, 0.05 Units) and 1:240 (1 µl,

0.01 Units) starting dilutions, Figure 5.3. High absorbance values were observed along the length of the dilution series, with the only drop in attributed to the Clostridium *perfringens* origin exNA after dilution past 1:10,000. The other dilution series tested in this experiment remained at OD_{492} values of between 3 and 4 with no decrease in absorbance detected despite increasing serial dilutions.

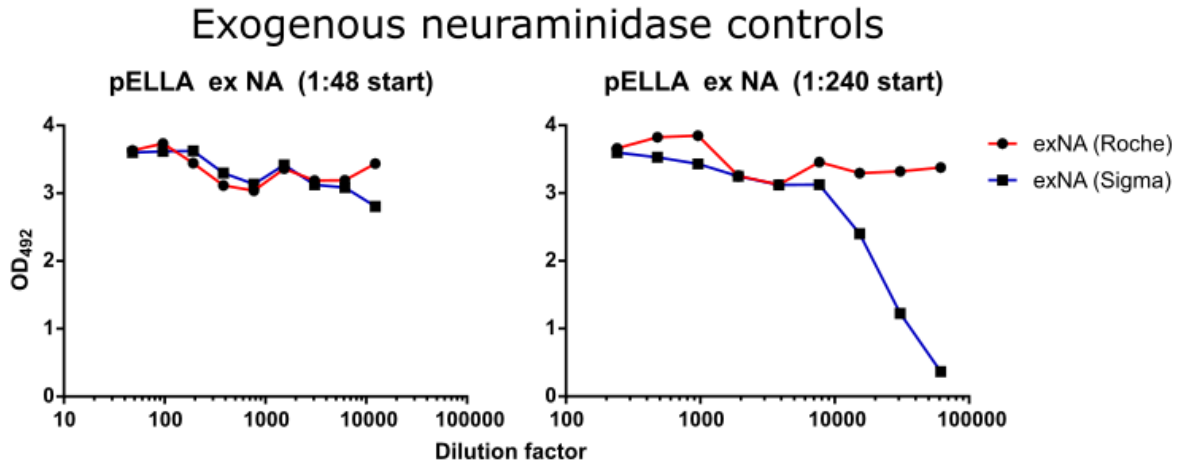

Figure 5.3. exNA was tested for use as a positive control in the ELLA assay. Two exNAs from different sources were tested. exNA Roche from Vibrio *cholerae* and exNA Sigma from Clostridium *perfringens*. Digestion of the fetuin coated plates, exposing galactose which could then be detected by PNA-HRPO is variable but consistently high across the diution series, with 1:48 and 1:240 starting dilutions. Only one test sample was titrated to the point where reduced digestion was seen with increased dilution of the sample (exNA Sigma 1:240).

CONSISE reverse genetics viruses H6N1 and H6N2 displayed high titres (OD_{492} >3.0) even when diluted past 1:1000, in the same range as exNA (see Figure 5.4). These results provided a benchmark to which PV NA titres could be compared to in subsequent experiments. It was decided to produce of a panel of PVs by transfecting expression plasmids coding for different combinations of HA/NA subtype glycoproteins, in order broaden the likelihood for positive results, and to detect NA activity where possible which could then be built upon.

5.3.2 Use of VLPs as a source of NA

Initial experiments did not utilise lentiviral packaging or vector plasmids, only HA or NA genes were transfected, as they had previously been shown to bud independently of other proteins (B. J. Chen et al. 2007). Due to HA and NA's ability to form particles independently, it was first decided to use these VLPs bearing only the N1 of A/Puerto Rico/8/1934 or the N2

of A/Udorn/307/1972, both of which were from characterised and widely used laboratory strains of influenza (Figure 5.5). In parallel, VLPs bearing H11 (A/duck/Memphis/546/1974) in combination with the N1 from A/California/7/2009 or N2 of A/Texas/50/2012 were also produced (H11N1, H11N2), which were acquired for this project by commercial gene synthesis from Genscript (USA). This was also repeated with H5 from A/Vietnam/1194/2004 (H5N1, H5N2). Finally, H1N1 (A/California/7/2012) and H3N2 (A/Texas/50/2012) matched HA/NA VLPs were produced and titrated by ELLA. For ELLA titration data for all of the above NA bearing VLPs, see Figures 5.3-5.6. High absorbance values were observed for all reassortant RG viruses, with high values seen past the 1:100 dilution point (Figure 5.4). Poor or no NA activity was detected from N1 (PR8) and N2 (Udorn) VLPs tested, with results at 1:10 dilution yielding absorbance values of just over 1 for VLPs bearing N2 Udorn produced using 1.5 µg of NA plasmid (Figure 5.5). For the A/California/7/2009 N1 however, high absorbance values were measured, providing an OD_{492} readout near 4.0, while other glycoprotein combinations of H11N2, H5N1, H5N2 or the matched H1N1/H3N2 showed lower NA activity (<3.0). Figure 5.6 shows this data, including exogenous NA control.

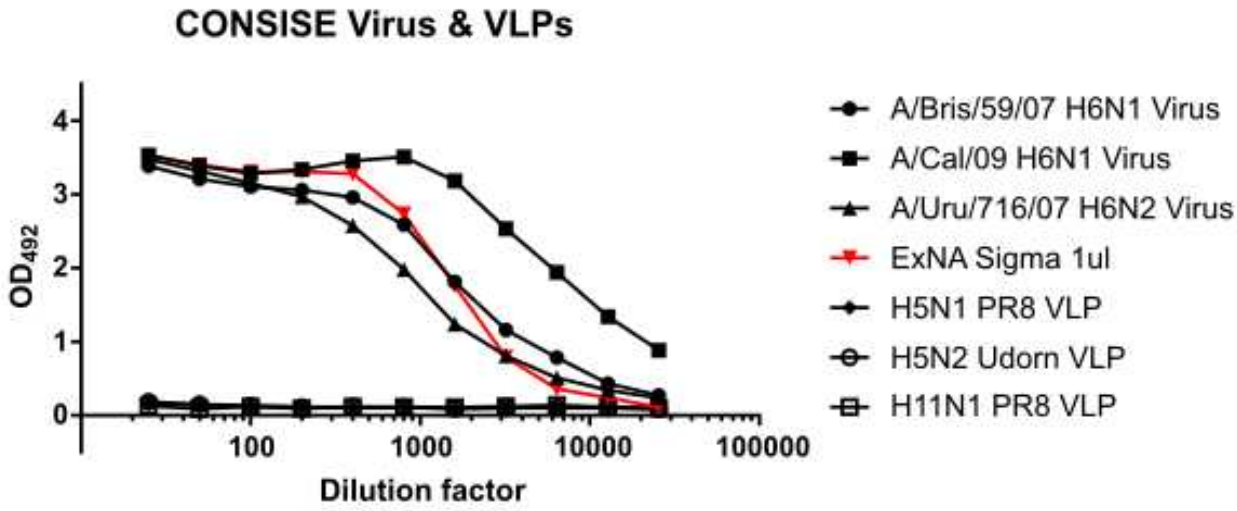

Figure 5.4. ELLA titration data for the CONSISE viruses (H6N1 A/Brisbane/57/2007 and A/California/7/2009, H6N2 A/Uruguay/716/2007) and three different PV (H5N1and H11N1 A/Puerto Rico/8/1934 and H5N2 A/Udorn/307/1972. High titres above OD_{492} of 3.0 are observed for all three viruses, while VLPs bearing N1 from A/Puerto Rico/8/1934 (PR8) or A/Udorn/307/1972 (Udorn) show no activity.

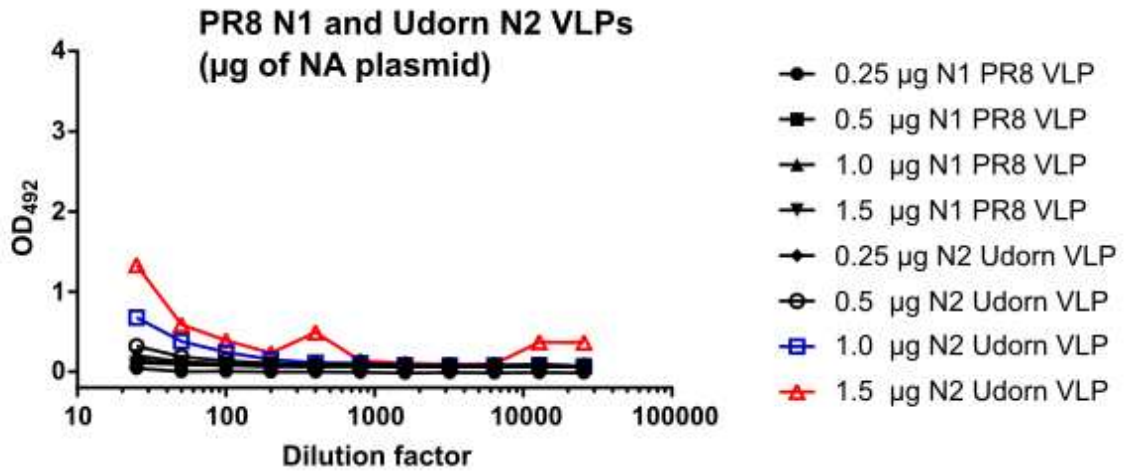

Figure 5.5. ELLA titration data for VLPs bearing N1 from A/Puerto Rico/8/1934 (PR8) and N2 from A/Udorn/307/1972 (Udorn) glycoproteins. Production inputs of NA plasmids listed, from 0.25 µg to 1.5 µg. Low NA activity is observed for the starting dilutions of N2 Udorn produced with 1.0 or 1.5 µg of NA plasmid.

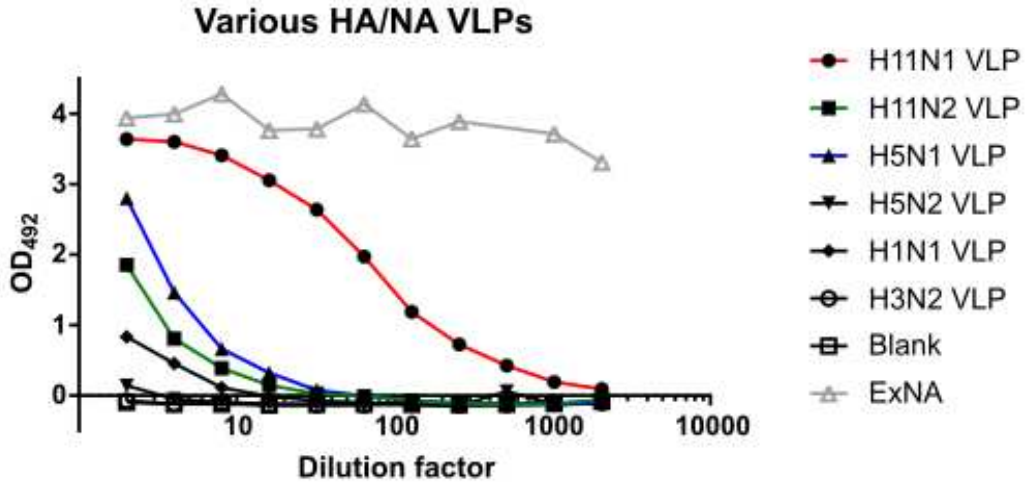

Figure 5.6. ELLA titration data for various different NA bearing VLPs. NAs from A/California/7/2009 (N1), A/Texas/50/2012 (N2) in combination with different HAs (H11, H5, H1 and H3). High NA activity is observed for the H11N1 VLP, followed by weaker activity for H5N1, H11N2 and H1N1.

In parallel with the previously described experiment, an attempt was made to produce N1 and N2 bearing VLPs with the same H3 from A/Texas/50/2012, producing each VLP in 6-well format with differing quantities of NA plasmid (Figure 5.7 A). This was carried out with addition of 0.1 µg, 0.25 µg, 0,5 µg, 1 µg, 1.5 µg and 3 µg of N1 plasmid. A further experiment was carried out with the H3 from A/Texas/50/2012 and 500ng of matched N2 per well, this time supplementing the transfection mix with pCMV-TMPRSS4 protease. However, these experiments were unsuccessful and no NA activity was observed for any of the different preparations when compared to positive results or exNA (Figure 5.7 B).

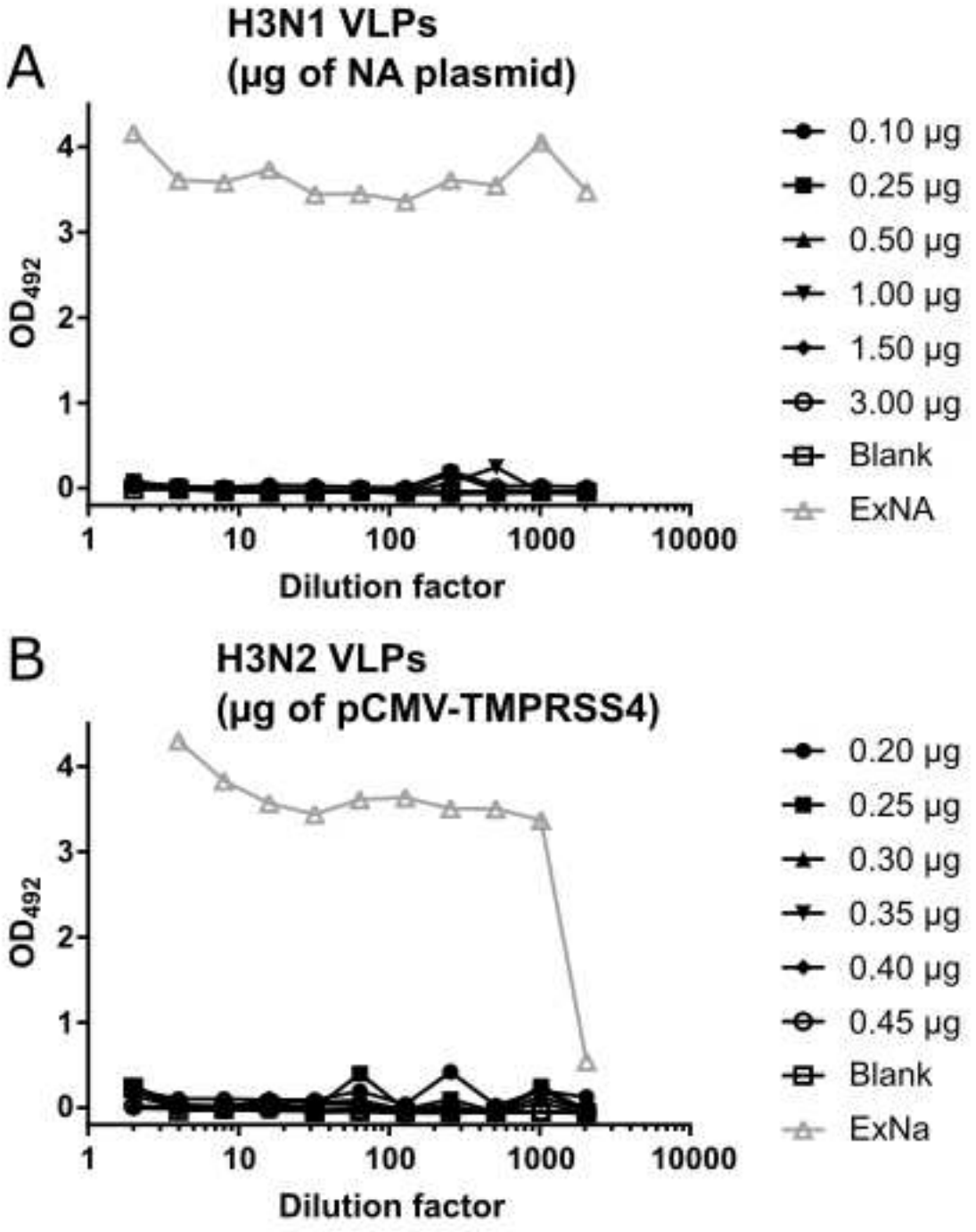

Figure 5.7. ELLA of VLPs bearing H3 (A/Texas/50/2012) and either N1 (A/California/7/2009) or N2 (A/Texas/50/2012). A) H3N1 VLPs produced with between 0.1 and 3.0 µg of NA per well. B) H3N2 VLPs produced with 0.5 µg of NA and between 0.2 and 0.45 µg of pCMV-TMPRSS4 per well. No NA activity is observed for any of the above listed VLPs.

5.3.3 Detection of N1 activity, addition of lentiviral core/reporters

Following these results, it was decided to then test whether the addition of plasmid p8.91 to the transfection mix would influence subsequent NA activity from our produced PVs, thinking that this could ameliorate the budding of particles bearing the glycoproteins whose action were being measured. The N1 (A/California/7/2009) or N2 (A/Texas/50/2012) expression plasmids were transfected into HEK293T/17 cells, supplementing the lowest and highest test wells with plasmid p8.91 in order to assess its influence on the budding of particles and subsequent NA activity. As shown by the data in Figure 5.8 A, the addition of higher quantities of NA plasmid and addition of p8.91 increases N1 titres. This was not reproduced with N2 (A/Texas/50/2012), however, the lack of any detected NA activity suggests a different problem in this instance (Figure 5.8 B).

From this point forwards, p8.91 and pCSFLW were always used to produce HA/NA PV, rather than HA/NA bearing VLPs. This was decided in order to not only reduce the amount of variables in this experiment, but by the strong suggestion from this data that the presence of p8.91 and pCSFLW in the production process enables higher NA titres from resulting PV containing supernatants.

5.3.4 Production of PVs with high NA activity

Upon use of p8.91 and pCSFLW plasmids in the production process, higher NA titres were observed, as seen in Figure 5.9 where N1 and N2 PV were produced with both lentiviral plasmids. As observed in previous experiments, increasing NA plasmid quantity lead to increased activity from the same input of PV containing supernatant, with 1 µg of NA plasmid per 6-well well giving the highest absorbance values and therefore highest NA activity (Figure 5.9). We repeated these results with H1 in addition to N1, observing a similar trend in the data, with the exception that lower NA quantities produced detectable NA activity when expressed on the surface of PV alongside H1 (Figure 5.10). N2 (A/Texas/50/2012) activity was still not detected in this experiment, titres being below an OD_{492} of 1.0 (Figures 5.9 and 5.10).

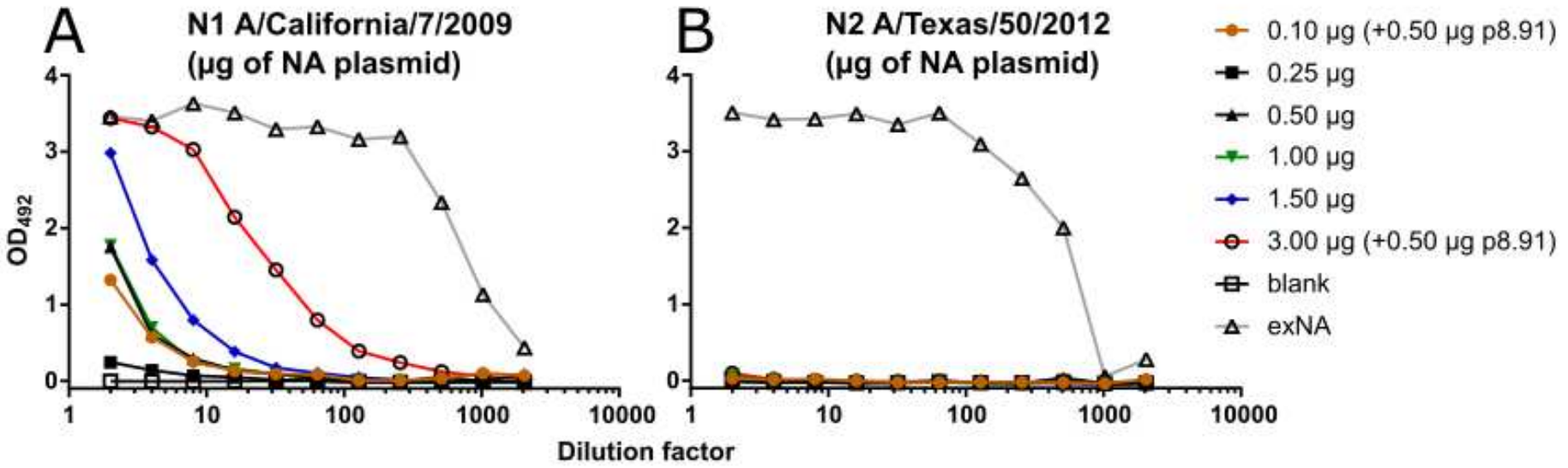

Figure 5.8. ELLA of VLPs bearing N1 (A/California/7/2009) or N2 (A/Texas/50/2012). A) Increasing the quantity of NA plasmid (shown in µg) leads to an increase in NA activity, with 3.0 µg yielding the highest activity in this experiment for VLPs. Addition of 0.5 µg of plasmid p8.91 (HIV-1 packaging plasmid) leads to an increase in NA activity alongside increased quantities of NA plasmid. VLPs produced with 0.10 µg of NA and 0.5 µg of p8.91 show increased activity compared to 0.25 µg NA with no p8.91 plasmid. Addition of 3.0 µg of NA plasmid alongside 0.5 µg p8.91 plasmid lead to the highest NA activity detected to date in these experiments. B) No NA activity is detected for N2 bearing VLPs, shown alongside exogenous NA control.

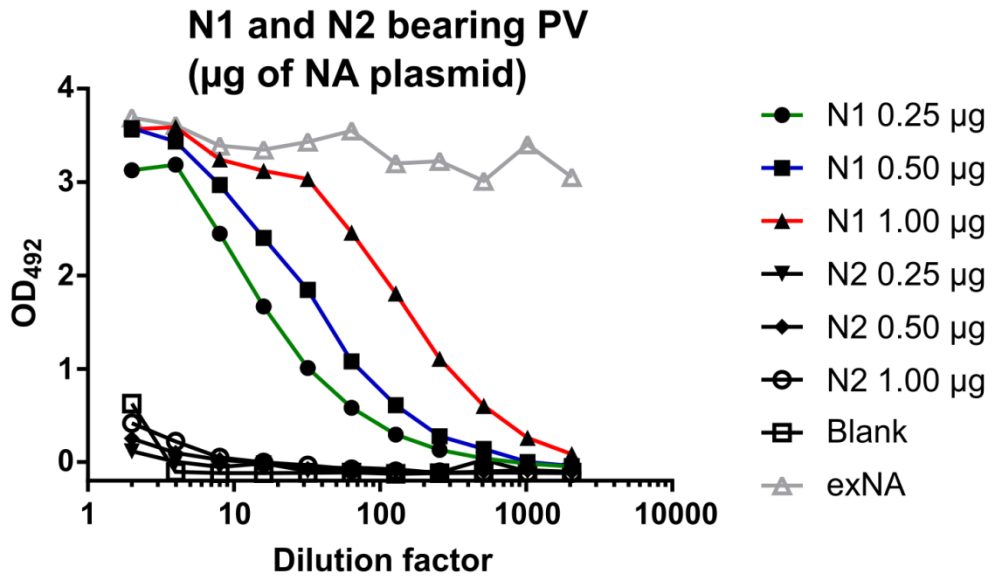

Figure 5.9. ELLA of lentiviral PVs bearing N1 (A/California/7/2009) and N2 (A/Texas/50/2012) glycoproteins, produced with p8.91 and pCSFLW lentiviral core and reporter plasmids. Increasing input of NA plasmid in the production stage leads to increased activity in ELLA. Poor or no NA activity detected for N2 PVs.

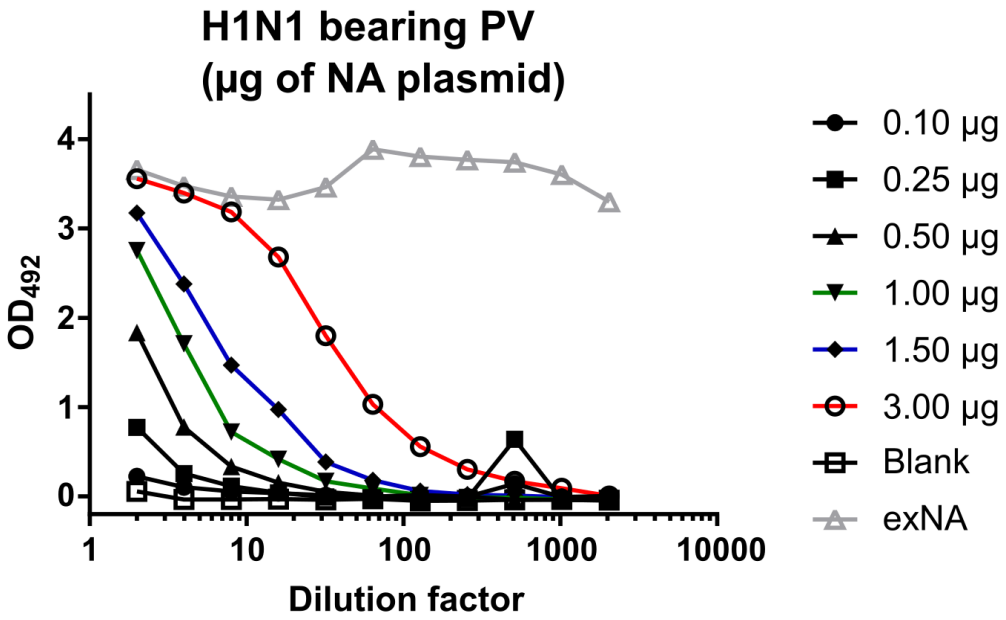

Figure 5.10. ELLA of lentiviral PVs bearing H1 and N1 (A/California/7/2009) glycoproteins, produced with p8.91 and pCSFLW lentiviral core and reporter plasmids. Increasing input of NA plasmid in the production stage leads to increased activity in ELLA. Addition of H1 to PVs increases NA activity of PVs produced with lower quantities of NA plasmid.

5.3.5 Addition of exotic HA (H11) to NA bearing PVs

Having successfully produced matched H1N1 PV with NA activity was a significant step, as the same PV could thus be used to detect NA and HA mediated antibody responses through ELLA and pMN respectively, using the same batch of PV. One of the benefits of the pMN assay is the ability to produce PVs with only HA on the surface, releasing particles with exogenous NA and enabling a 'clean' reading of antibody activity against HA. In a similar fashion, the rational in this case was to produce an analogous system for ELLA in the production of NA only PVs as described in Prevato et al. 2015. However, it was decided to additionally attempt the production of HA/NA PVs with a mismatched, exotic HA, that from H11 (A/Shear Water/Western Australia/2576/1979 (H11N9)) alongside the tested NAs in order to determine the effect on NA inhibiting antibody titres. Due to the avian nature of H11, as with the H6 used in RG virus production, few neutralising antibodies should be present in human serum samples due to the presence of different head epitopes humans have not encountered, though this is still an assumption. This would allow for a more even platform for comparison between H11NX PVs and H6NX RG viruses in ELLA. At the time these experiments were carried out, no H6 expressing plasmid was available in our laboratory. H11 was chosen due to its previous use in cHA experiments as a non-reactive glycoprotein, as well as its overall lack of reactivity with previously used human serum samples (chapter 3).

5.3.6 PV bearing exotic H11 and NA

The final attempts at producing high titre NA activity PV preparations were carried out through the use of H11 plasmid in conjunction with p8.91, pCSFLW and the NA plasmid of choice (Figure 5.11). This yielded PVs bearing both N1 (A/California/7/2009) and N2 (A/Texas/50/2012) in sufficient quantities to perform multiple titrations and progress to the inhibition phase of this ELLA project. Having these PVs with high NA activity also allowed us to test the concentration of PNA-HRPO required to reach the digestion ceiling for this assay, a variable within the two studies which we based this project upon (Eichelberger et al. 2016; Prevato et al. 2015). It was suggested in the CONSISE protocol that each batch of PNA-HRPO should be titrated with a known NA source in order to determine the optimal concentration to detect full digestion of the fetuin coat, saving on costs associated with this expensive reagent and increasing the number of assays which could be performed per batch.

Therefore it was decided to test the same PV preparations with 1:500 and 1:1000 dilutions of PNA-HRPO. H11N1, H11N2 and N1 only PV all produced with p8.91 and pCSFLW and harvested 72 h post transfection were titrated (1:1000 PNA-HRPO) in duplicate (Figure 5.11). Subsequently, the same titration was carried out using 1:500 and 1:1000 PNA-HRPO dilutions in parallel (Figure 5.12). As shown by this data, there is a clear increase in the detection of NA activity when using more concentrated (1:500) PNA-HRPO and this is more evident for the lower titre PVs N1 (only) and H11N2 at lower dilution points of PV. The exNA control was the least affected by the change in PNA-HRPO dilution, with values only marginally lower when halving the PNA-HRPO concentration.

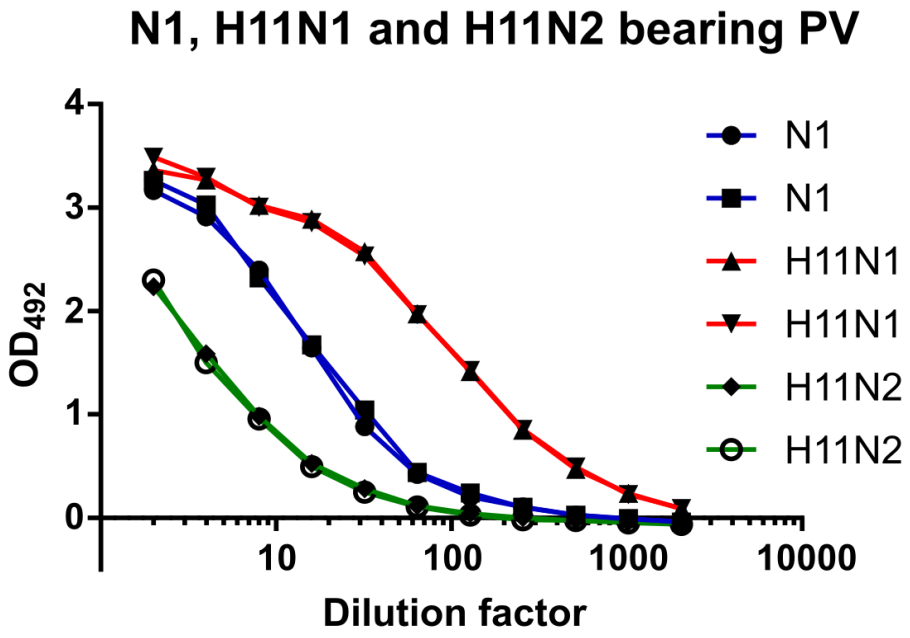

Figure 5.11. ELLA of lentiviral PVs bearing only N1 (A/California/7/2009) or H11 (A/duck/Memphis/546/1974) and N1 or N2 (A/Texas/50/2012) glycoproteins. 3 µg of NA plasmid per well alongside standard quantities of HA, p8.91 and pCSFLW. H11N1 NA activity is higher than N1 only activity while both show high NA activity at early dilution points. H11N2 activity is low in comparison with N1 and H11N1 PVs.

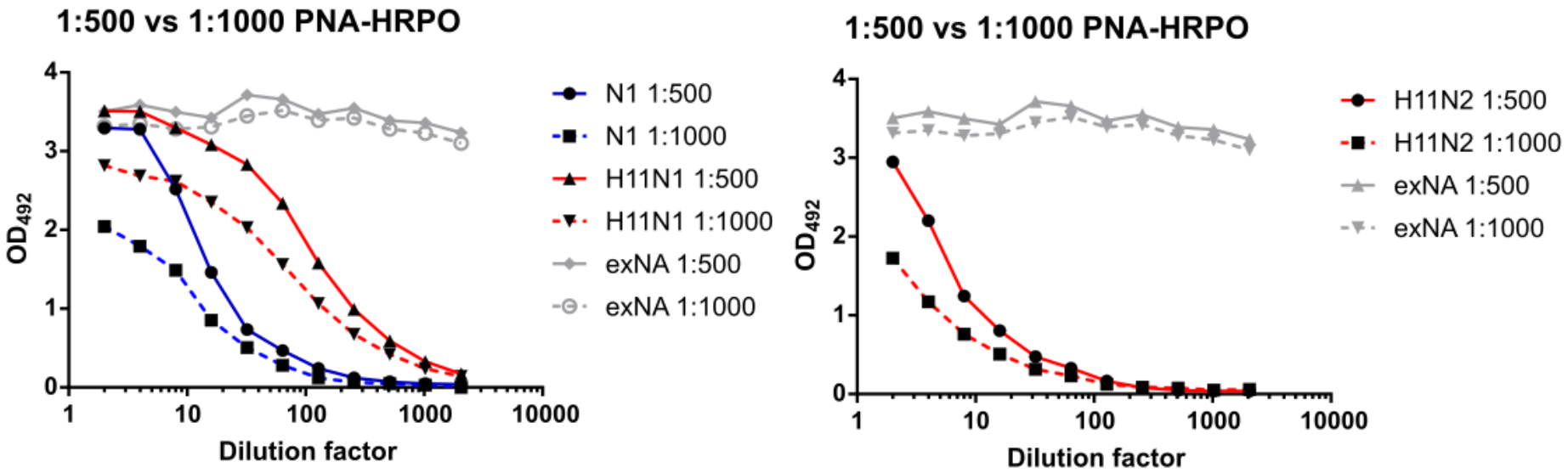

Figure 5.12. ELLA Titration of N1, H11N1 (A/California/7/2009) and H11N2 (A/Texas/50/2012) with 1:500 and 1:1000 dilution of PNA-HRPO. exNA controls shown in grey. Increases in PNA-HRPO concentration lead to increased NA titres detected for N1, H11N1, H11N2 and exNA sources of NA tested. The largest increase was seen with N1 PV, increasing from OD_{492} of 2.0 to 3.2. Increased titres were more apparent at higher concentrations of NA source, suggesting that 1:1000 dilution of PNA-HRPO is not sufficient to detect all available galactose with theses sources of NA.

Eichelberger et al. 2016 detailed that an absorbance value ranging between 1.7 to 4, in the linear phase of the titration curve, should not give rise to any differences in geometric mean antibody titres (GMT) when used as an input for inhibition ELLA (Eichelberger et al. 2016). This suggests that even low titre PVs produced in the previously detailed experiments could be used in inhibition ELLA and give comparable antibody titres to the same experiment carried out with a higher PV input. The article from which the ELLA protocol used was obtained, utilised an OD_{492} input of 2, within the 1.7-4 range (Prevato et al. 2015). In order to test these arguments in conjunction with the PV system in ELLA, it was decided to perform inhibition assays with the same panel of sera, using different viral inputs as well different PNA-HRPO dilutions.

5.3.7 Inhibition ELLA with CONSISE sera

After the successful production of H11N1 and N1 preparations with NA activity titres at an OD_{492} >3, it was decided to employ the set of CONSISE sera shown in Table 5.1. To begin with, inhibition assays were carried out using a viral input of 90% of the maximal titre obtained, as described by (Couzens et al. 2014). Due to the constraints of the 12 row by 8 column plates used for ELLA, we opted to assay 8 sera in duplicate across the plate, using 6 post vaccination human sera (2009/2010 TIV), purified human IVIG from patients immunized against H1N1 strain A/Brisbane/59/2007 (2009/2010 TIV) and finally transgenic (humanised IG) bovine plasma immunized with the 2012/2013 vaccine strain (including A/California/7/2009 (H1N1)). The latter sample, vaccinated with strain A/California/7/2009 acts as a positive control in this experiment.

These sera were assayed against both H11N1 and N1, providing inhibitory IC_{50} results. Increased inhibition titres were observed for N1 only pseudotypes (Figure 5.14). As expected, S2, the transgenic bovine plasma immunized with the matched CA/09 virus showed the highest titres against H11N1 or N1. The second highest titres were observed for S1, the purified human IVIG from 2009/2010 TIV vaccinated patients. The NA of the strain used in this vaccine (A/Brisbane/59/2007) is dissimilar to Eurasian swine CA/09 NA, with 88 amino acid changes or insertions/deletions (Figure 5.13).

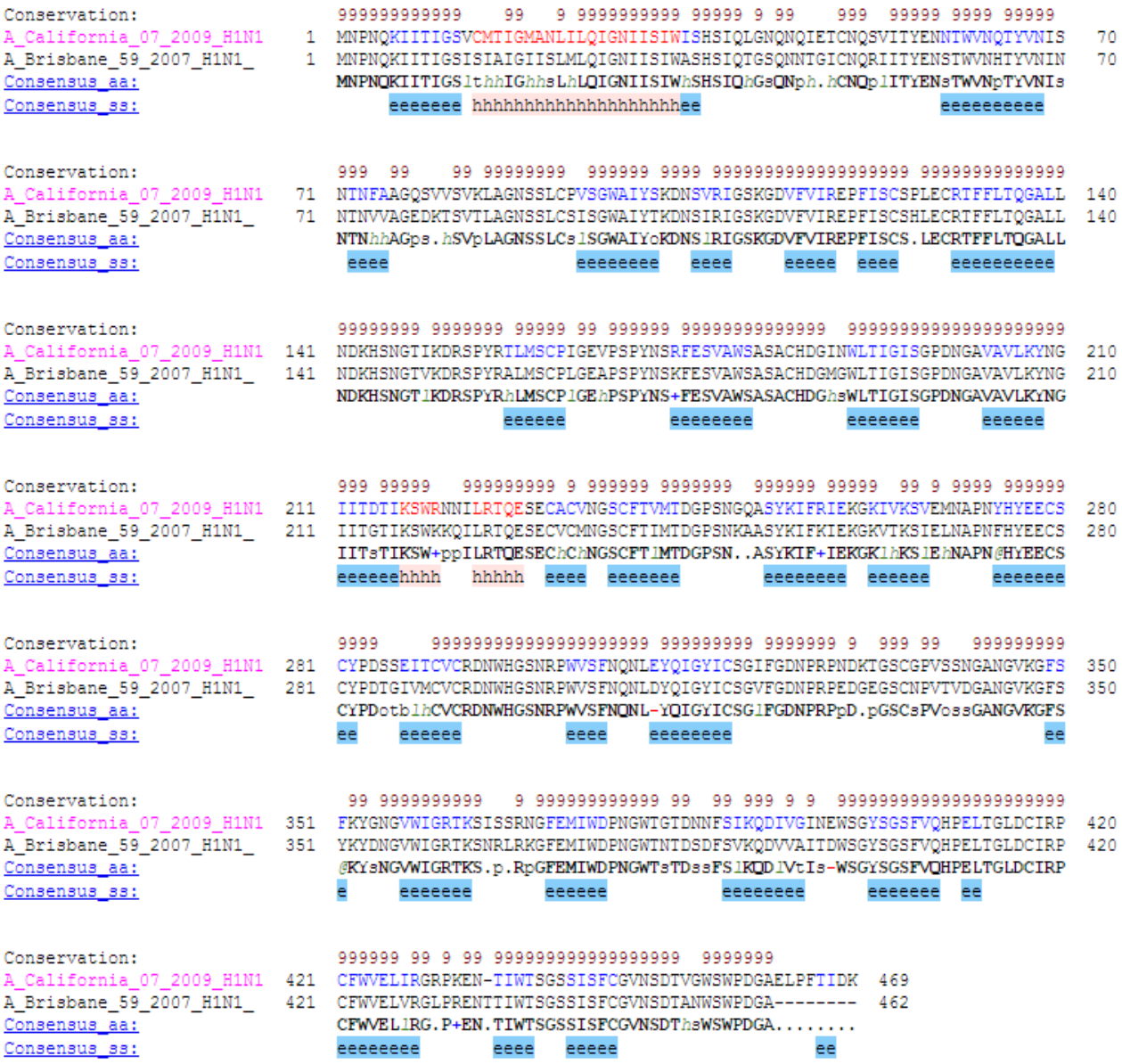

Figure 5.13. Amino acid alignment of the NA gene from A/Brisbane/59/2007 (Accession: AHG96686.1) and A/California/7/2009 (Accession: ACQ63272.1). Predicted consensus secondary structure denoted by chains of "h" for alpha helices and "e" for beta sheets. 2D and 3D alignment generated using amino acid sequences in the PROMALS3D tool. (Pei et al. 2008)

5.3.8 Inhibition of N1 by CONSISE sera

The human serum samples (S3-S8) inhibited the N1 to varying degrees and higher titres may indicate previous infection with a virus bearing a similar N1 or better reaction/presence of antibodies to the 2009/2010 vaccine strain. Data in Figure 5.14 shows two sets of repeats for each experiment, Figure 5.15 shows datasets merged and corresponding differences in IC_{50} values which are small. Inhibitory titres against N1 were higher compared to those

against H11N1, despite the same input of serum and PV. IC_{50} values increased 5 to 35 fold when using the 'clean' NA only PV (Figure 5.14 & 5.15).

Upon testing the same panel of sera on H11N2 PV, higher IC_{50} values were seen, as well as a different neutralising profile for samples S3-S8. S1 and S2 behaved as against the CA/09 NA, S1 showed an IC_{50} of 2627, 3-fold higher than against H11N1. S2 was again the strongest inhibitor, with IC_{50} of above 5120 and 100% neutralisation throughout the dilution series. Samples S3-S8 showed different inhibitory profiles against H11N2 than H11N1. Samples S3 and S4 showed higher titres against H11N2 (IC_{50}: 286 & 385) in comparison to H11N1 (IC_{50}: 83 & 68). S5 was more inhibitory than the previous two samples against H11N2 (IC_{50}: 407) and H11N1 (IC_{50}: 287) while S6 and S7 were weak inhibitors of both H11N1 and H11N2 (IC_{50}: 109 & 117 for H11N2 and 5 & 101 for H11N1). Interestingly, sample S8 very strongly inhibited H11N2 (IC_{50}: 1130) but not H11N1 (IC_{50}: 9), see Figure 5.16 for H11N2 CONSISE sera ELLA data.

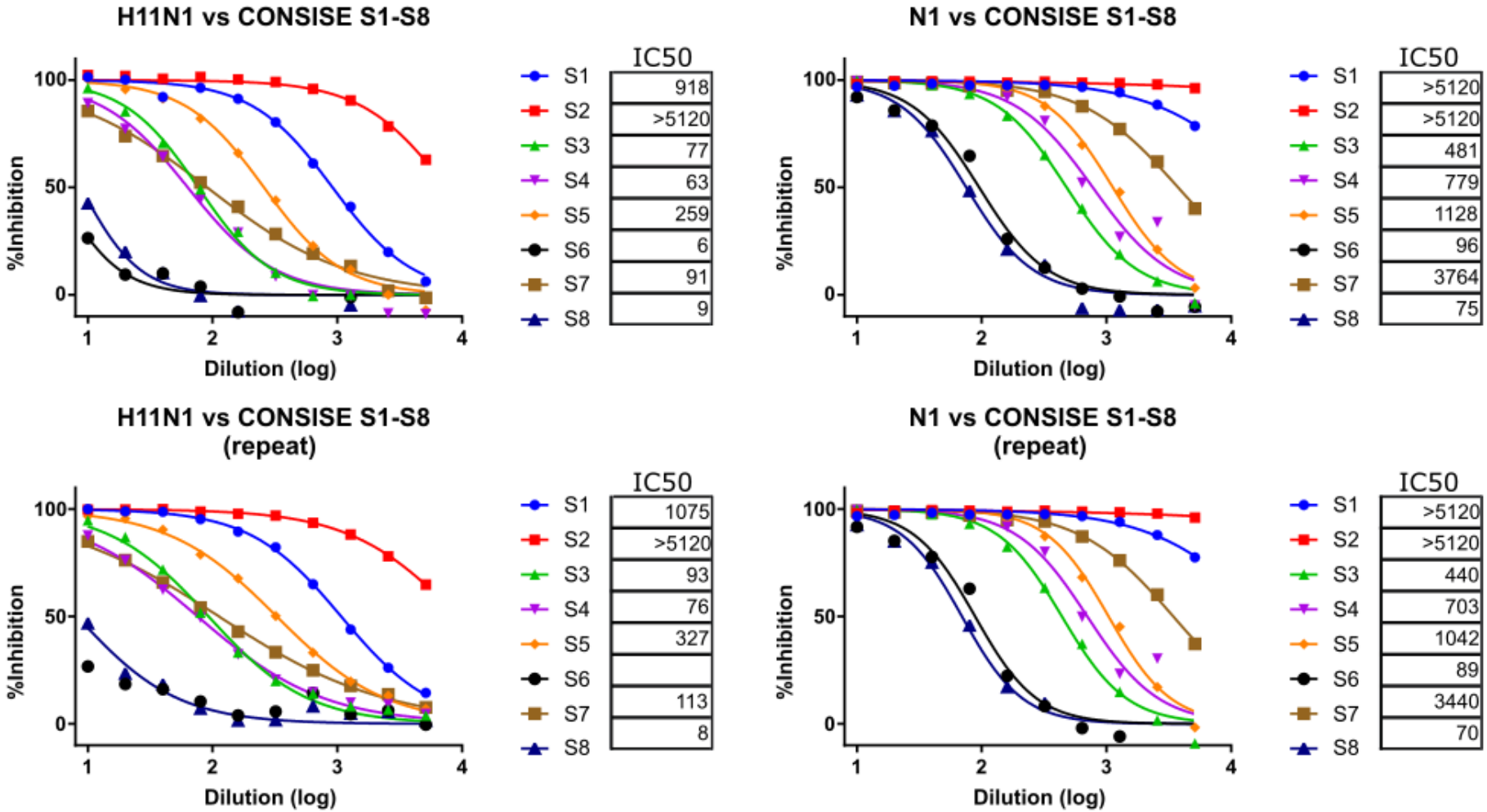

Figure 5.14. ELLA Inhibition curves for CONSISE serum samples S1-S8 assayed against H11N1 and N1 PV using ELLA. The top and bottom graphs on the left are replicates for H11N1 PV whereas the top and bottom graphs on the right are replicates for N1 PV. IC_{50} values for each serum sample are shown adjacent to the key. Replicates show near identical inhibition curves and antibody titres (IC_{50}). Replicate values are merged together to produce Figure 5.15.

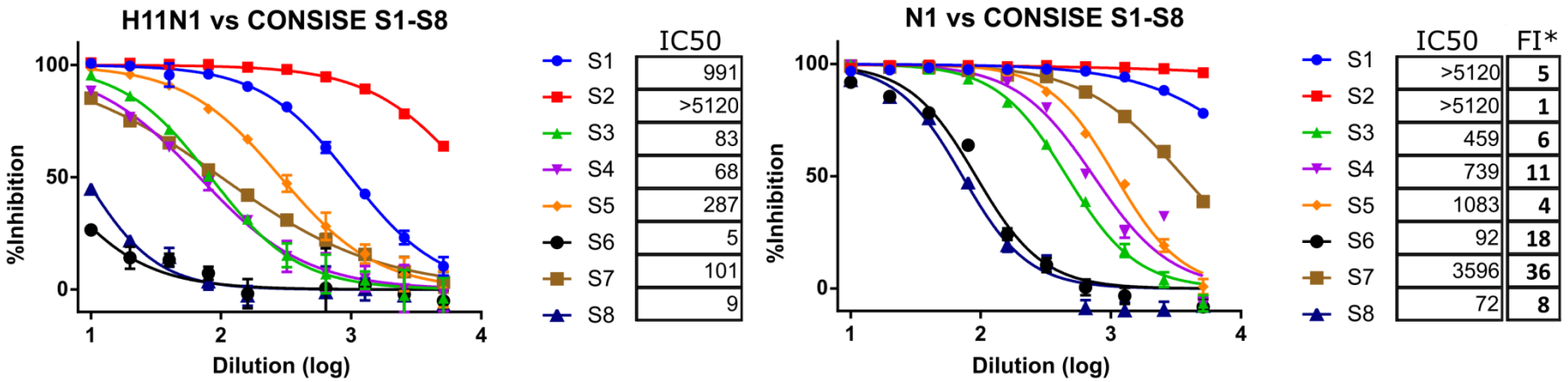

Figure 5.15. ELLA inhibition curves for CONSISE serum samples S1-S8 assayed against H11N1 and N1 PV, including error bars and average IC_{50} values. Fold increase in IC_{50} values from H11N1 to N1 shown in the column titled FI*. Inhibition profiles are similar between H11N1 and N1 PV, with sera S2 and S1 showing the strongest inhibition and sera S6 and S6 the weakest inhibition. Changing from H11N1 to N1 only PV leads to an increase of 1-36 fold difference in antibody titre (IC_{50}).

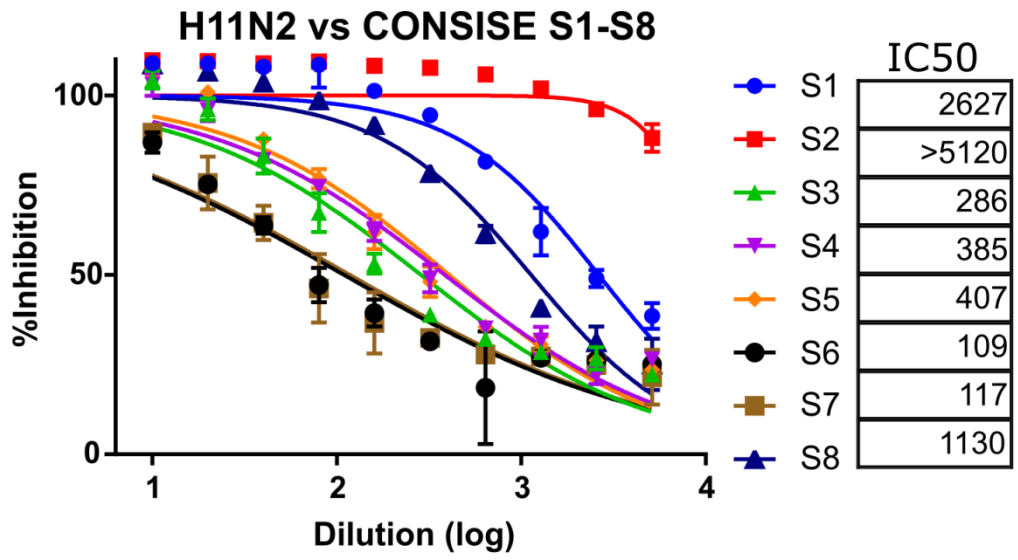

Figure 5.16. ELLA inhibition curves for CONSISE serum samples S1-S8 assayed against H11N2 PV, including error bars and average IC_{50} values. Sera S2 followed by S1 and S8 show the highest levels of inhibition of N2 activity, followed by S5, S4, S3, S7 and S6 in descending order.

5.3.9 Evaluation of PNA-HRPO and Viral input factors on antibody titres

In order to test the difference in results obtained from using different concentrations of PNA-HRPO, it was decided to perform a set of experiments comparing 1:500 and 1:1000 dilutions. As previously mentioned, it was suggested that each NA source should be titrated with differing dilutions of PNA-HRPO, in order to determine the digestion ceiling for each virus and adapt the dilution for subsequent experiments, saving on reagents where possible. The aims for this part of the project were to test its effect on the generation of inhibitory IC_{50} data and whether any changes occurred as a result of the PNA-HRPO dilution variable. This test was also duplicated while using two different PV inputs, 90% of the maximal titration and an input of OD2.0, as calculated from the titration results listed previously. This variable, as mentioned earlier, was stated to not influence inhibitory titres between OD_{492} inputs of 1.7-4 (Eichelberger et al. 2016), and experiments in the published literature report varying inputs (Prevato et al. 2015).

We decided to test these variables with H11N1 PVs and one high (HP) and one low (LP) positive serum sample, as determined by previous pMN experiments (chapter 3), run in duplicate. All the data for these experiments are displayed in Figures 5.17 and 5.18 with inhibition curves alongside IC_{50} values. All data points represent mean values of two data points with variation depicted through whiskers. Changing the dilution of PNA-HRPO had a strong effect on IC_{50} values recorded, whether inputs were OD90% or OD2.0. OD90% input

IC_{50} values increased when dilution was increased from 1:500 to 1:1000. The HP sample increased from 908 to 1511 and the LP sample from 1 to 2. With a 2.0 input the HP sample increased from 8125 to 9524 and the LP from 55 to 228. To compare 90% and 2.0 inputs (Figure 5.17), IC_{50} values increased noticeably when moving from 90% to 2.0 inputs, the HP sample increased from 1511 to 9524, LP from 2 to 110 when using 1:1000. For 1:500 PNA-HRPO, the HP sample IC_{50} increased from 908 to 8125, and the LP from 1 to 41.

5.3.10 Jenner sera ELLA

After evaluating the ELLA system and deciding to use 1:500 PNA-HRPO as well as an OD_{492} of 90% where possible, it was decided to field test this assay on relevant serum samples in order to produce some useful and interesting data, as opposed to assaying samples which have been previously tested and published. We selected six serum samples from the Jenner Sera panel, obtained from Prof. Sarah Gilbert, Jenner Institute Laboratories, University of Oxford, which are detailed in more depth in chapter 3 (and appendix X1). This section of this chapter represents a preliminary study on these serum samples. The decision was made to continue the OD90% vs. 2.0 experiments using these serum samples to determine the effect this variable has on negative controls which weren't incorporated into our previous experiments. H11N1 PVs were tested using serum samples 20, 31 and 23 which were all low positives against H1 (A/California/7/2009) HA PV (Figure 5.19). High positives, determined in the same fashion, were 34, 59 and 60. Negative controls anti-A/California/7/2009 HA serum as well as anti-B/Brisbane/60/2008 HA serum (NIBSC). exNA was used as a digestion/positive control as seen previously.

Results correlated well with IC_{50} values generated against H1 (CA/09) PV as seen in chapter 3 (Figure 3.25), with HP and LP samples acting as low and high positives against N1 as well as the original H1. LP samples 20, 23 and 31 gave IC_{50} values of 0, 30 and 14 with a 90% OD input. With the OD input of 2.0, IC_{50}s were 0, 341 and 150. For HP samples, 34, 59, and 60 IC_{50} values were 91, 209 and 153 respectively at OD90%, and 629, 1613 and 1288 for OD2.0. Negative controls all resulted in values of zero except B/Brisbane antiserum which had an IC_{50} of 4 at OD2.0. Despite this, negative samples are clearly grouped at the negative end of the spectrum of results. However, the curves generated are elevated when using an input of OD2.0, inhibition starting between 20-40% at the starting dilution compared to below 5% with an OD input of 90%.

A further set of serum samples were assayed against H11N2 (A/Texas/50/2012), originating from the sports science sera project collected in the United Kingdom (chapter 3, serum IDs in appendix X2), see Figure 5.20. Five serum samples (3 HP and 2 LP), as determined through pMN carried out against A/Udorn/307/1972 in Chapter 3 were tested against H11N2 PV in ELLA. Three HP samples were 9 0V (IC_{50} 8170), 21 12V (IC_{50} 11279) and 39 0V (IC_{50} 12763), and two low positive samples were 33 12V (no IC_{50}) and 50 12V (IC_{50} 957). Controls used include the same negative controls as used previously, with added antiserum generated against inactivated H3N2 (A/Udorn/307/1972) virus, despite this virus being very different to the PV strain utilised (A/Texas/50/2012). Due to the low titre/activity of H11N2 preparations, they were used without dilution, which generated an OD of 2.2 per well (50 µl). This was not optimal based on previous results comparing higher ODs to 2.0. Serum sample 50 had a matched IC_{50} with the Anti H3N2 control at 33. 39 generated an IC_{50} of 89 and other samples were more positive, 9, 21 and 33, giving IC_{50} values of 137, 103 and 225 respectively. Negative control antisera for A/California/7/2009 and B/Brisbane/60/2008 were once again elevated, as seen in Figure 5.19 with H11N2 and a 2.0 viral input.

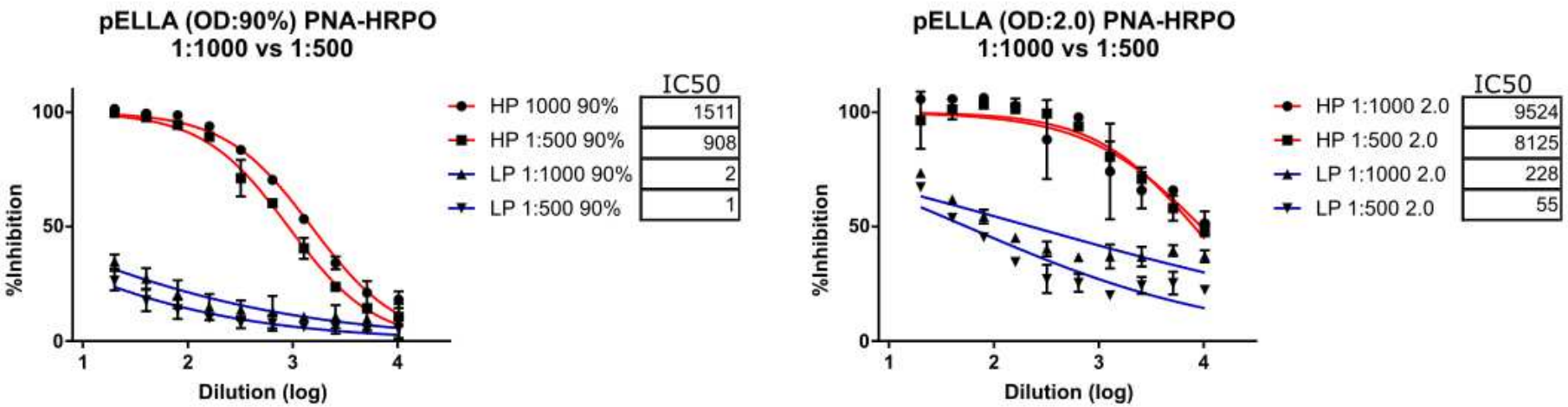

Figure 5.17. Analysis of multiple variables in ELLA. Two graphs comparing H11N1 PV input on neutralisation of PVs by high positive (red) and low positive (blue) serum samples. The left graph compares neutralisation with 1:500 or 1:1000 PNA-HRPO and an OD90% input. The right graph compares the same with an OD2.0 input. Similar neutralisation profiles are seen for the same serum samples in ELLA performed with 1:500 or 1:500 PNA-HRPO concentration, with a drop in NA activity signal observed for 1:1000 PNA-HRPO data points.

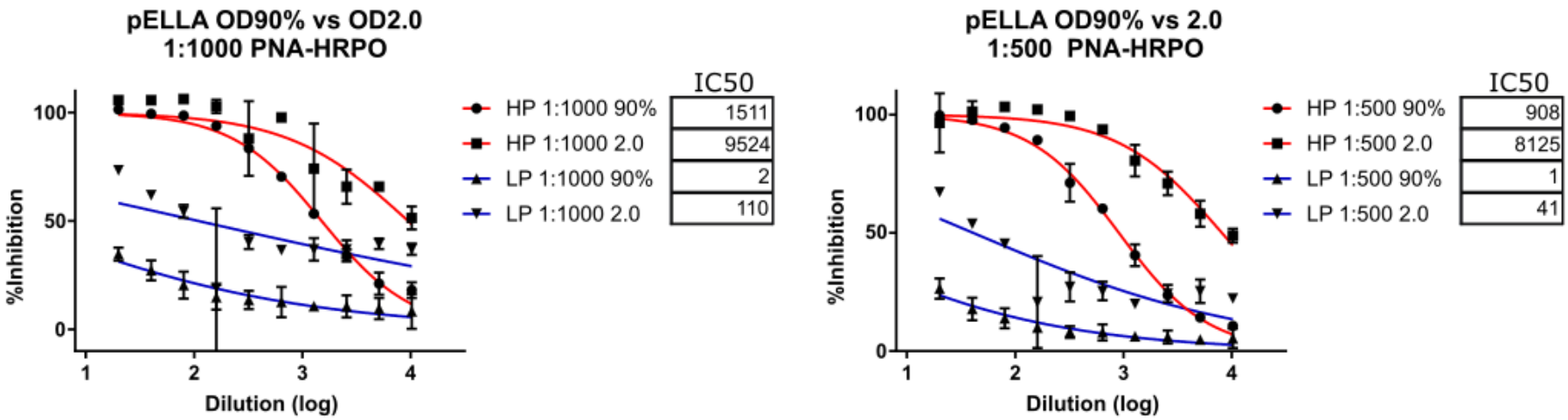

Figure 5.18. Analysis of multiple variables in ELLA. Two graphs comparing the dilution of PNA-HRPO on neutralisation of H11N1 by high positive (red) and low positive (blue) serum samples. The left graph compares HP and LP samples with OD90% and OD2.0 inputs at 1:1000 PNA-HRPO. The right graph compares the same variables at 1:500 PNA-HRPO. Neutralisation of N1 activity is reduced when changing from 1:500 PNA-HRPO to 1:1000 as well as when using a higher viral input (OD90% rather than OD2.0). Different neutralisation profiles are seen for HP samples when reducing viral input from OD90% to OD2.0.

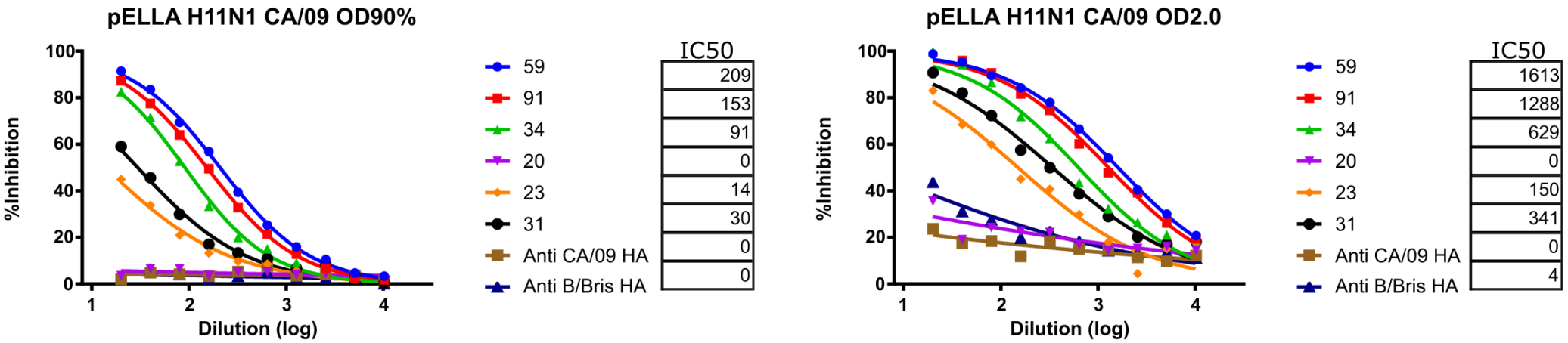

Figure 5.19. ELLA inhibition assay testing serum samples from the Jenner institute, University of Oxford on H11N1 PV. Six sera were tested against H11N1, representing three high positive (S245, S236 and S221) and three low positive samples (S004, S214 and S086) based upon results against A/California/7/2009 HA PV. Similar results are obtained against the N1, showing distinct positive and negative samples against H1 as against N1. Negative controls include anti-A/California/7/2009 and anti-B/Brisbane/60/2008 HA serum (NIBSC). Experiment carried out in duplicate with an input virus of OD_{492} 90% or 2.0.

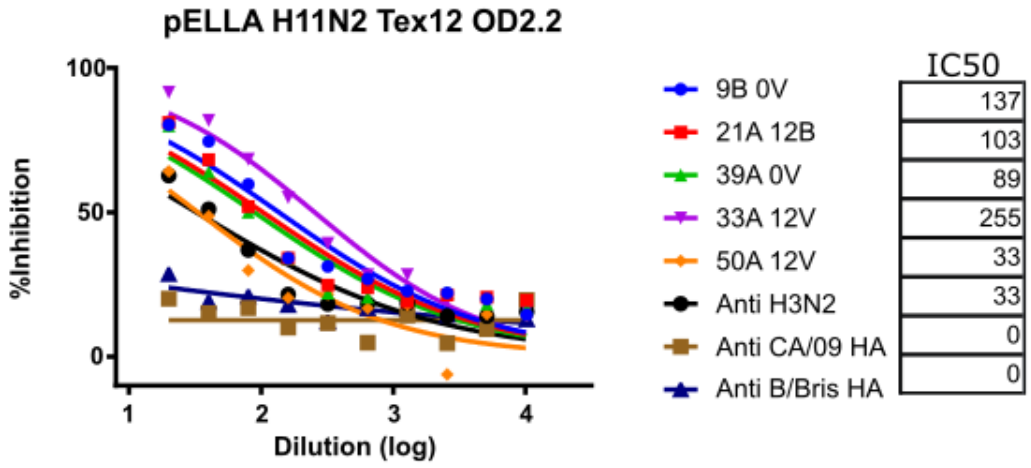

Figure 5.20. ELLA inhibition assay testing Sports Science Serum samples obtained from Dr. Glen Davison, University of Kent on H11N2 PV with an OD_{492} 2.2 input. Negative controls include anti-A/California/7/2009 and anti-B/Brisbane/60/2008 HA serum (NIBSC). A PV positive control from H3N2 positive antiserum against A/Udorn/307/1972 is also included (Anti H3N2).

5.4 Discussion and conclusions

In general, this project has been successful in A) setting up the ELLA assay with PV and B) employing it in a project involving available sera. The CONSISE protocol was employed and after initial unsuccessful attempts, PVs with high titre NA activity were produced, enough so to perform various experiments interrogating the other parameters of the assay (Viral input & PNA-HRPO concentration). The ability to produce these high NA titre PVs at relatively little expense and effort is very useful in terms of the future for generation of inhibition data against influenza NAs. Interestingly, it seems that the ability to induce budding from the cell surface is one of the largest factors influencing the titre of the NA PV, as production with the addition of HIV-1 core genes and HA increases titres (Figure 5.8). The latter point is most likely due to the HA ability to induce membrane curvature with NA (B. J. Chen et al. 2007). The increases in NA titres when using lentiviral vector and packaging plasmids are most likely due to an increase in particles exiting the cell, taking influenza glycoproteins present on the cell membrane, with them. The combination of HA and lentiviral plasmids lead to the highest NA titres recorded and enabled subsequent ELLA inhibition assays with a single batch of PV. The addition of lentiviral plasmids most likely increased titres by increasing the number of PV coming off the surface of the HEK293T/17 producer cells, taking with them the NA glycoproteins present on the cell membrane. The ability of *gag* and HIV core proteins to induce budding has been reviewed in extensive detail (Sundquist and Kräusslich 2012).

When using exNA throughout the experiments in this chapter, the typical data was variable, with many data spikes or troughs, as opposed to a typical 100% cut-off line that we would have expected from fully digested fetuin (Figure 5.3). This may be due to the concentrated nature of this reagent in combination with inadequate or insufficient mixing during the dilution steps. Another explanation would be possible discrepancies in the coating of wells in the maxisorp plates, leading to slight differences in the amount of galactose exposed upon full digestion of the fetuin. This would explain how NA activity seems to drop after three dilution points, but then rises back up after 6 dilution points. PVs tended to present differently, with much smoother titration curves observed.

The data generated using H11N1 and N1 only PV was interesting, due to the fact that H11 should have no or little influence on the inhibition of the NA enzyme. A large increase (1 to 36 fold increase) in antibody titres was seen from H11N1 to N1 PV, suggesting that the presence of HA is having a dampening effect on available antibodies (Figure 5.15). One possible explanation is steric hindrance caused by the presence of the HA, which may mask certain sites on the NA as seen in other published articles (Rajendran et al. 2017). This phenomenon is matched in the results we see in the pMN assay, with 'clean' HA only PV easier to neutralise than HA/NA PV using the same serum. It is possible that the presence of HA allows binding of PV to the fetuin coated walls of the 96-well plates, possibly immobilizing PVs and preventing access to other PVs to the substrate.

H11N1 tests against the CONSISE serum samples showed the use of ELLA in detection of cross-neutralising responses against NA. Serum sample S1, consisting of pooled human serum vaccinated with the 2009/2010 TIV neutralised N2 higher than N1, which is expected due to the relationship between PV strains and vaccine strains. The A/California/7/2009 N1 originated from Eurasian swine in this triple reassortant virus, the A/Texas/50/2012 strain represents a drift mutant from the 2009/2010 vaccine strains, therefore sharing a greater similarity. Nevertheless, the decreased viral input for H11N2 of OD2.2 compared to the OD90% (>3.0) for H11N1 is another possible explanation for the increased antibody titre of S2 against H11N2 in comparison to H11N1 (Figure 5.16).

These data reinforce previous concerns about input of virus and use of differing concentrations of reagents. We have shown that using lower viral inputs leads to an inflation of IC_{50} values; including those for negative controls which are a cause for concern

when data is generated using these lower inputs (Figures 5.17 and 5.18). We have also shown that use of N1 only vs. H11N1 PVs leads to an inflation of IC_{50}, most likely due to HA directed antibodies hindering the ability of NA. This previous point could be interrogated by the use of NA only antisera or a panel of mAbs, which could be tested on H11N1 and N1 PV. This highlights the problem posed by the use of human sera in serology, each sample is from an individual with an unknown number of exposures to various subtypes of influenza virus, the interplay between HA and NA mediated antibodies lead to discrepancies in results. These discrepancies would be better explained with the aid of such a study.

Poor NA titres were observed for N2 bearing PV produced during this project, representing a problem which must be solved in order to make full use of this assay (Figure 5.12). Issues leading to these low titres may involve the optimal conditions required for this enzyme to function in the assay. Quantities of NA present on the surface of PV may also be involved, through the lower expression of NA proteins in HEK293T/17 cells. However there is no evidence for this and WT viruses (H1N1, H3N2 and influenza B) have been reported to have no statistically significant differences in the content of NA (Tanimoto et al. 2005).

The results presented in this chapter are encouraging in the respect that over a short time period, PV based ELLA has very rapidly been employed using relevant subtypes of NA, and these have been used in inhibition assays. ELLA is a useful tool, as future circulating or vaccine strains could be produced at short notice and useful data generated. This project saw two previous vaccine strain NAs synthesized (A/California/7/2009 and A/Texas/50/2012), alongside their matched HAs, providing the ability to produce H1N1, H1 or N1 PVs. While these strains are no longer matched to current vaccine or circulating strains, they are still relevant as the majority of sera obtained will have been exposed to the H1N1 pandemic, or the H3N2 seasonal strain. By keeping a PV library with current strains and updating it, we can perform archeo-serology and scan backwards through circulating strains using the same serum sample to estimate a person's infection history.

Chapter 6 : Development and use of H17 and H17N10 PV

6.1 H17N10 and H18N11

The bat derived influenza viruses H17N10 and H18N11 were discovered recently in fruit bats using consensus-degenerate RT-PCR in Guatemala and Peru respectively (Tong et al. 2012, 2013). Both viruses contain eight gene segments in the standard IAV conformation. A marked sequence divergence in the genetic material of both of these viruses is seen when compared to other IAV subtypes. However, this chapter will focus on H17N10 due to the availability of H17 and N10 genes.

6.1.1 H17N10 genes and proteins

The H17 HA can be placed within group 1 of Influenza A (Tong et al. 2012). Studies have shown that it is not capable of agglutinating red blood cells in a standard HI assay and it has been suggested that "haemagglutinin-like 17, HL17" be a more fitting designation (Ma et al. 2015). Trypsin-like and TMPRSS2 mediated cleavage has been demonstrated for H17, and as with other IAVs, it is required for proteolytic activation and fusion competence (M. Hoffmann et al. 2016; Maruyama et al. 2016). However, the dynamics surrounding activation and fusion mediated by H17 are under question due to its instability at 37°C (50% unfolded), ability to trigger at high pH (8.0), and it's high trypsin susceptibility (Sun et al. 2013). The H17 trimer does not bind to traditional (2,6 or 2,3) linked sialic acid as its receptor, as do other IAVs - according to surface plasmon resonance (SPR), MDCK cell binding and glycan microarray assays (Sun et al. 2013). Either the binding of this glycoprotein cannot be detected by currently available assays or it utilises a different receptor entirely. Interestingly, the fusion peptide of H17 is highly conserved when compared to other IAV strains, especially those in group 1. Figure 6.1 shows an amino acid alignment carried out using the web tool Clustal Omega (Sievers et al. 2011). Here the C-terminal region of the HA protein shows high conservation in the fusion peptide (starting residues highlighted by a red box) alongside recent H1 (group 1) and H3 (group 2) vaccine strains (A/California/7/2009 and A/Texas/50/2012).

```
H3_Texas_2012       KCKSECITPNGSIPNDKPFQNVNRITYGACPRYVKQSTLKLATGMRNVPEKQTRGIFGAI 351
H1_CA/09            DCNTTCQTPKGAINTSLPFQNIHPITIGKCPKYVKSTKLRLATGLRNIPSIQSRGLFGAI 350
H17                 DCSTKCQTPLGALNSTLPFQNVHQQTIGNCPKYVKATSLMLATGLRNNPQMEGRGLFGAI 348
                    .*.: * ** *:: .  ****::  * * **:*** :.* ****:** *. : **:****

H3_Texas_2012       AGFIENGWEGMVDGWYGFRHQNSEGRGQAAD
H1_CA/09            AGFIEGGWTGMVDGWYGYHHQNEQGSGYAAD
H17                 AGFIEGGWQGMIDGWYGYHHENQEGSGYAAD
                    *****.** **:*****::*:*.:* * ***
```

Figure 6.1. HA C-terminal amino acid sequence alignment of influenza A strains A/little yellow shouldered bat/Guatemala/060/2010 (H17), A/Texas/50/2012 (H3) and A/California/5/2009 (H1pdm). Starting residues of the fusion peptide highlighted by a red box. Alignment carried out using Clustal Omega.

The internal genes (PB1, PB2, PA, NP, M, and NS) sequences are related to Influenza A and B according to phylogenetic analysis, but do not cluster within either group. The polymerase complex has been shown to be functional via genome mini reporter assay, and all other genes have been shown to function *in vitro* when HA and NA genes are used from surrogate non-bat influenza A viruses. These replicative synthetic viruses produced with the H17 internal genes also infected mice with high disease severity (Tefsen et al. 2014; Tong et al. 2012; B. Zhou et al. 2014). The NA gene is more greatly diverged, and sits outside either A or B types (Tong et al. 2012), possibly originating from an extinct or as-yet unknown type (Q. Li et al. 2012). No sialidase activity has been detected from this enzyme which shares overall structural features with other NAs, but displays differences in crucial conserved amino acids attributed to the function of previously described NAs – sialic acid binding and enzymatic cleavage (Colman et al. 1983; García-Sastre 2012; Q. Li et al. 2012; X Zhu et al. 2012). Despite this, N10 has a typical canonical NA fold as well as calcium binding site, and shares overall structure when superimposed onto other NAs. The putative active site has a wider binding site pocket with an open pseudo-active site which has unfavourable electrostatic potential, making it a poor candidate for sialic acid binding and cleavage (Q. Li et al. 2012; X Zhu et al. 2012; Xueyong Zhu et al. 2013).

6.1.2 Culture of H17N10 influenza virus

Initial attempts at culture or rescue of WT H17N10 virus failed (Tong et al. 2012, 2013). However, other groups have since succeeded in producing H17 bearing particles pseudotyped with H17 and N10 glycoproteins (M. Hoffmann et al. 2016; Maruyama et al. 2016). In both the previously cited articles, a rhabdoviral (VSV) system was used to

characterise H17 and N10. Hoffmann et al. managed to show infection of the bat derived cell lines EidNi/41, HypNi/1.1, EpoNi/22.1, but not traditional IAV or other cell lines (MDCK, HEK293T, and Vero). Maruyama et al. 2016 published similar results, successfully infecting bat derived cell lines (IndFSPT1, YubFKT1, and SuBK12-08), and interestingly, managed to infect the MDCK cell line used. A more recent study succeeded in using a VSV system to infect a variety of human or other mammalian derived cells including MDCK II and RIE 1495, also succeeding in producing competent H17N10 and H18N11 which were propagated in the same cell lines in the presence of trypsin (Moreira et al. 2016). The fact that some research groups have had success with MDCKs while others have not is a problem compounded by the nature of this cell line designation. MDCK cells are often used in influenza research and there are a great variety of 'strains' available including MDCK I and MDCK II which were used in this project. Differences in results between laboratories could be accounted for by lack of correct information about the strains used. This problem is discussed comprehensively by Dukes et al. 2011. These studies on the H17 and N10 genes, combined with the characterisation of internal gene segments by Juozapaitis et al. 2014 , are evidence that H17N10 is a functional virus to which we have only just started to culture as a full viral entity (Moreira et al. 2016).

6.1.3 Zoonotic potential

Due to the nature of influenza A and the risk posed to human and livestock populations from reassortant strains with epidemic/pandemic potential, the discovery of novel and significantly divergent subtypes of influenza virus was worrying to the influenza community. This was reinforced after the publicity surrounding the bat-suspected Ebola outbreak in 2014. Efforts are now being made to discover whether bats represent a true reservoir for influenza viruses, and if there remain further subtypes to be characterised. Due to the large diversity in, and widespread nature of bat populations, further studies are required to determine the risk of crossover and host susceptibility (Serra-Cobo and López-Roig 2016). To further support the importance of this point, a recent study identified influenza H9 cross-reactive antibodies in a large proportion (30%) of bats in Ghana (Freidl et al. 2015). This serological approach may represent a solution, as antibodies may be detectable for longer periods post infection than vRNA through consensus RT-PCR. While similar studies to the original H17N10 and H18N11 articles (Tong et al. 2012, 2013) have been carried out in

Europe on central European bats (Fereidouni et al. 2015; Sonntag et al. 2009), no evidence of influenza virus was detected through consensus RT-PCR. Efforts must be made to reproduce these studies worldwide using PCR and serology to map the extent of cross-reactive immunity and influenza prevalence in bats. Further work on H17 and N10 suggests that receptor specificity is not only impeding attempts to study the WT virus, but also acting as a major limiting factor for infection due to receptor presence or abundance on different cell types (B. Zhou et al. 2014). Zhou et al. 2014 found that the bat viruses were incompatible with influenza A or B on a genetic and protein level, reducing the risk of reassortment with influenza A or B viruses and subsequently reducing the pandemic potential of these viruses.

6.2 Methods

6.2.1 Plasmids, Cells and reagents

The eukaryotic expression plasmid pI.18 (Cox et al. 2002) was used as a backbone for H17 and N10 (A/little yellow shouldered bat/Guatemala/060/2010) expression plasmids, both genes of which were subcloned into pI.18 by a previous student, Dr Francesca Ferrara, at the Viral Pseudotype Unit, Medway School of Pharmacy.

Multiple cell lines were used in this project. Human embryo kidney cells (HEK293T/17) were obtained from Dr Davide Corti, Institute for Research In Biomedicine, Switzerland and were used for production of PV as well as in titration and neutralisation assays. MDCK cells used originate from two sources. MDCK I cells were obtained from Prof Sarah Gilbert, University of Oxford. MDCK II, alongside rat intestinal epithelial cells (RIE 1495) were obtained from Dr Martin Schwemmle, Institute of Virology, University of Freiberg, Germany. MDCK I, II and RIE 1495 cells were utilised in titration and neutralisation assays. mAbs used include CR6261 (Friesen et al. 2010), CR9114 (Dreyfus et al. 2013) as well as F16-nt and F16-chol which were originally described by Corti et al. 2011 and reproduced from the published sequence by Lacek et al. 2014.

Four human sera were used in this project. These were kindly provided by Prof. Sarah Gilbert, Jenner Institute Laboratories, University of Oxford. Samples were taken from adult human volunteers during an influenza vaccine clinical trial (NP vaccine) in the Oxford area, United Kingdom. Two high positive and two low positive (based on pMN neutralising

antibody titre to CS CHM cHA PV, see chapter 3) were selected from a panel of sera in order to interrogate H17N10 PVs, using MDCK II and RIE 1495 as target cells in the neutralisation assay.

6.2.2 Cell culture

MDCK I, MDCK II and RIE 1495 cells were cultured in T25 or T75 flasks (Thermo Fisher Scientific, cat: 156367, 156499). Cells were subcultured 1:5 on Mondays and Wednesdays, 1:10 on Fridays. Cell monolayers were washed twice with PBS (without Calcium/Magnesium, Pan Biotech, cat: P04-36500) before addition of 2 ml (T25) or 4 ml (T75) Trypsin 0.05 % EDTA (Pan Biotech, cat: P10-040100) and incubation for 10-20 minutes at 37°C, 5% CO_2. Cells were resuspended in a total volume of 5 ml (T25) or 10 ml (T75) whereupon they were diluted for use in titration/pMN assays or seeded for future use.

6.2.3 Production of luciferase PV using H17 and N10 glycoproteins

Luciferase PVs were produced as in chapter 2, section 2.3.1. Standard reagents were used for the production of H17 and H17N10 PV, plasmid quantities are listed in Table 6.1.

Table 6.1. DNA mix plasmid quantities. H17N10 PV were produced by co-transfection of HEK293T/17 cells with the following quantities of plasmid per well of a 6-well plate.

Plasmid	Concentration (ng/well)
p8.91	500
pCSFLW	750
pI.18-H17	500
pI.18-N10	250
Protease encoding plasmid	125

NA-only PV produced for ELLA were produced in a similar fashion to other PV, with the exception that supernatants were harvested 72 h post transfection, in lieu of the traditional 48 h. Table 6.2 lists plasmid quantities for each preparation of N10-only PV produced. Other viruses used in the ELLA were produced previously and using standard methods. These were quantified by RLU/luminescence and used in the ELLA as controls (N1-N9) or to determine N10 activity (H17N10, H5N10).

Table 6.2. List of plasmid quantities used for N10, H5N10 and H17N10 PV production. Production was carried out in 6-well plates, values represent ng per well. Plasmid IDs are shown alongside the exact quantities (per well of a 6-well plate) of plasmid used in the transfection mix when producing PV.

		PV ID							
		N10 500	**N10 750**	**N10 1000**	**N10 1500**	**N10 2000**	**N10 3000**	**H5N10**	**H17N10**
Plasmid	**N10**	500	750	1000	1500	2000	3000	250	250
	HA	-	-	-	-	-	-	500	500
	p8.91	500	500	500	500	500	500	500	500
	pCSFLW	750	750	750	750	750	750	750	750

6.2.4 Titration of H17 and H17N10 on various cell lines

H17 and H17N10 bearing PV were titrated as described in chapter 2 (section 2.3.2). Multiple cell lines were used as targets for these PV: MDCK I, MDCK II, RIE 1495 as well as HEK293T/17.

6.2.5 pMN of H17 and H17N10

bnmAbs were employed using the pMN assay. Input quantity used was 5000 ng, giving a concentration gradient of 5000 to 40 ng after 1:2 serial dilutions, across which the mAbs neutralising capacity was measured. mAbs CR9114, F16-nt and F16-chol were tested. A subset of samples from the Jenner institute laboratories, University of Oxford (detailed in chapter 3 and appendix X1) were also tested on H17N10 PV.

6.2.6 ELLA using N10

The ELLA is described in further detail in sections 2.3.5 and 5.2.4. ELLA titration was carried out using N10 PV produced under various parameters (Table 6.2) as well as H5N10, H17N10 and other IAVs (H3N1, H3N3, H3N4, H3N8, H3N9) produced using standard parameters (Table 2.6).

6.3 Results

6.3.1 Titration of PV preparations using newly acquired cell lines: MDCK II and RIE 1495.

The H17 and N10 glycoproteins were obtained through a gene synthesis service (Genscript, USA) and cloned into vector pI.18. These genes were then used to produce H17 and H17N10 bearing PV. However, the original cell lines tested were not permissive to these PV. Only

one positive result was obtained which could not be repeated. H17 bearing the pCSGW GFP reporter was successfully used to transduce U87 cells after having been produced in the presence of TMPRSS2 and HAT proteases. This work was carried out by Dr Stuart Mather (Figure 6.2).

The lack of results with a luciferase reporter and lack of reproducibility with GFP lead to cessation of this project until further reagents became available, the starting point of this chapter. Upon evaluation of some of these initial preparations on the newly available cell lines MDCK II and RIE 1495, a positive signal was obtained (Figure 6.3) for one preparation of H17N10 produced with 125 ng of HAT protease encoding plasmid in a 6-well dish format by Dr Keith Grehan. This initial positive result provided a starting point for further experiments.

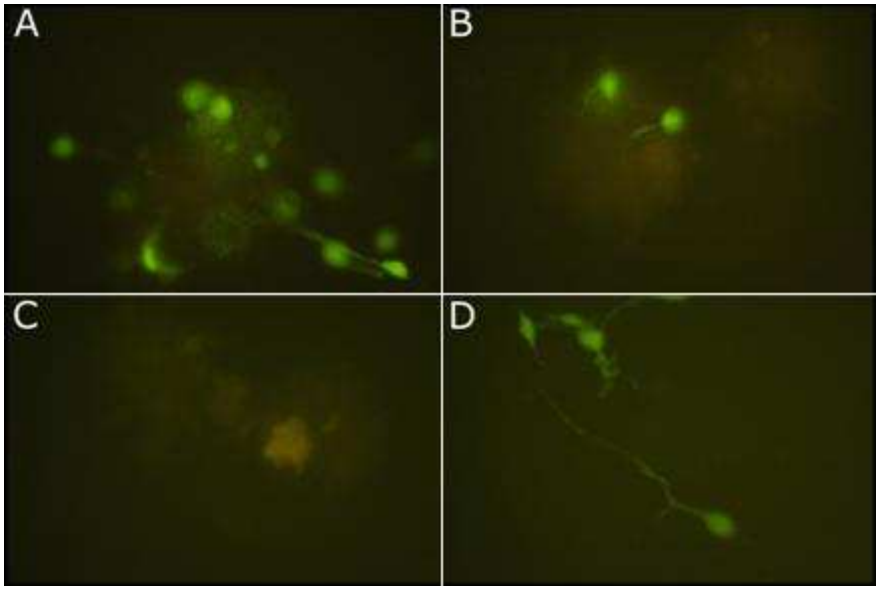

Figure 6.2. Transduction of U87 cells by influenza GFP PV. A) H17 produced using pCAGGS-HAT. B) H17 PV produced using pCAGGS-TMPRSS2. C) Cell only control. D) H5 (A/Viet Nam/1194/2004) PV positive control. Immunofluorescence carried out by Dr Stuart Mather.

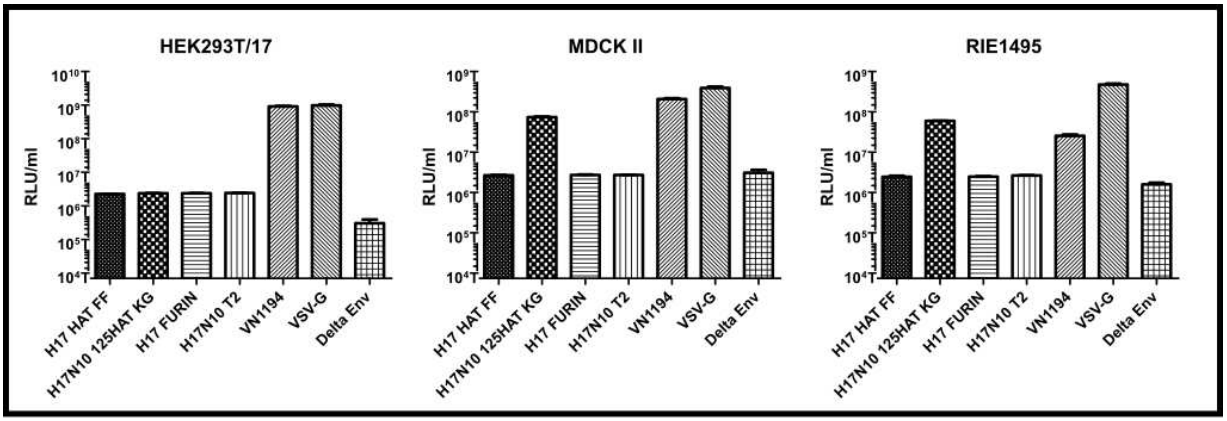

Figure 6.3. Titration of initial H17 based PV preparations on HEK293T/17 as well as newly acquired cell lines MDCK II and RIE 1495. No positive RLU/ml signal is observed for H17 based PV titrated on HEK293T/17 cells when compared to Delta Envelope negative control and A/Vietnam/1194/2003 (VN1194) and VSV-G positive controls. When using MDCK II and RIE 1495 cells, a positive signal is observed for one H17 PV preparation: H17N10 produced with 125ng HAT by Dr Keith Grehan.

6.3.2 H17 and H17N10 are activated by proteases HAT, TMPRSS2 and TMPRSS4.

Further experiments were planned and carried out to repeat the previous results under the same production parameters, and also to produce H17 and H17N10 bearing PV in the presence of other proteases available in the laboratory. All experiments from this point forward were carried out with co-transfection of 125 ng of protease encoding plasmid per 6-well plate well, in addition to pI.18-H17, p8.91, and pCSFLW plasmids (+ pI.18-N10 for H17N10 PV). It was decided that this plasmid quantity was sufficient for the detection of an increased PV titre, based on experiments with other influenza luciferase PV. Our results show that TMPRSS2, TMPRSS4 and HAT significantly increase the titres of H17 and H17N10 PV, titres being several logs higher than baseline cell or delta envelope controls in both MDCK II and RIE 1495 cells. There is a disparity between the results obtained between H17 and H17N10 on MDCK II cells, with H17N10 titres approximately one log higher. Titres obtained when transducing RIE 1495 cells were consistently the highest within this set of data. VSV-G PVs were used as a cell transduction control, providing us with a maximum transduction value due to the fact that this glycoprotein mediates entry with a highly ubiquitous LDLR receptor (Finkelshtein et al. 2013). VSV-G PV titres were lower than H17 titrated on MDCK II, and H17 and H17N10 titrated on RIE1495, possibly indicating that the H17 receptor is in greater abundance than LDLR. H17 and H17N10 PV were also able to transduce MDCK I cells after activation via HAT (Figures 6.4 and 6.5).

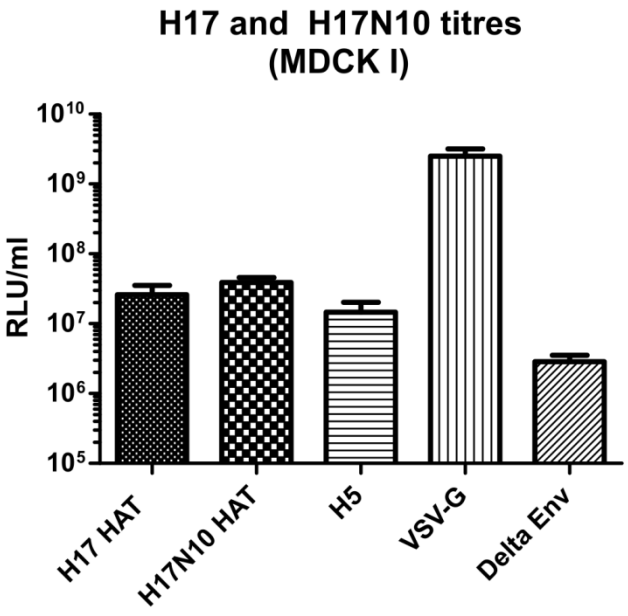

Figure 6.4.Transduction of MDCK I cells by H17 and H17N10 PV produced in the presence of HAT. H5 (A/Vietnam/1194/2004), VSV-G and Delta Envelope PV used as controls. H17 and H17N10 PV both show RLU/ml values higher than H5 which is not significantly higher for H17 (p=0.3496) but significantly higher for H17N10 (p= 0.0240). H17 and H17N10 titres were both significantly higher than Delta Env titres (P=0.0326 and 0.0003 respectively).

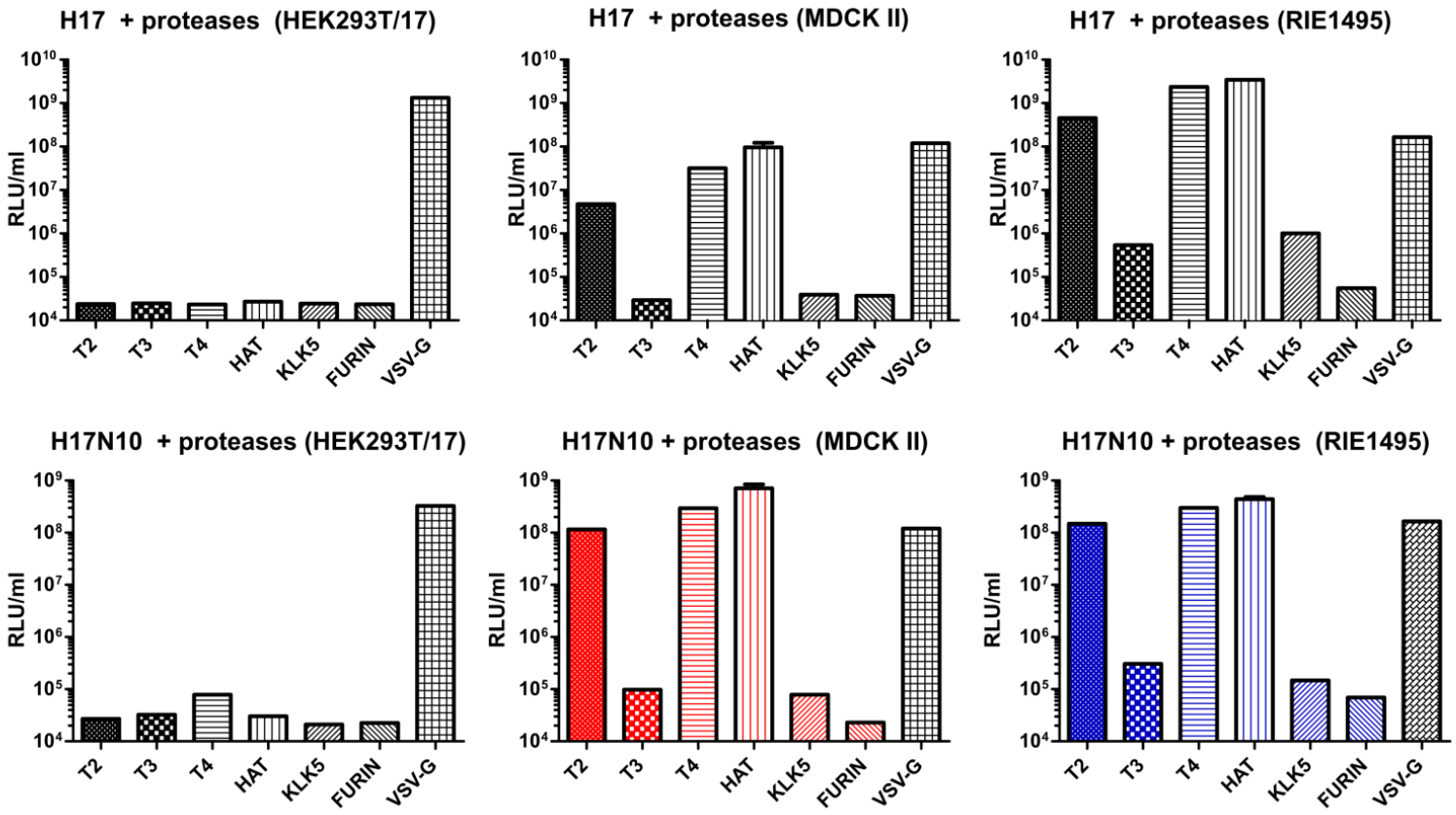

Figure 6.5. Luciferase based titration of H17 and H17N10 PV produced in the presence of proteases TMPRSS2 (T2), TMPRSS3 (T3), TMPRSS4 (T4), HAT, KLK5, and Furin. Values in RLU/ml. VSV-G bearing PV used as transduction control for high titre PV. Proteases T2, T4 and HAT included in the production stage of H17 and H17N10 PV lead to high titre PV due to proteolytic activation of the H17 glycoprotein, with the highest titres observed in RIE 1495 cells.

6.3.3 N10 mediates release of group 1 and group 2 influenza PV.

Production of PV bearing H5 HA (A/Vietnam/1194/2004) or H7 HA (A/Shanghai/2/2013) and the N10 (A/little shouldered bat/Guatemala/060/2010) lead to an increase in RLU/ml titre for both PVs when compared to H5-only and H7-only PV produced in the absence of a source of NA (Figure 6.6). PV produced without an envelope glycoprotein produced a luciferase signal approximately 1-2 logs lower than H5/H7 PV produced without an NA source present.

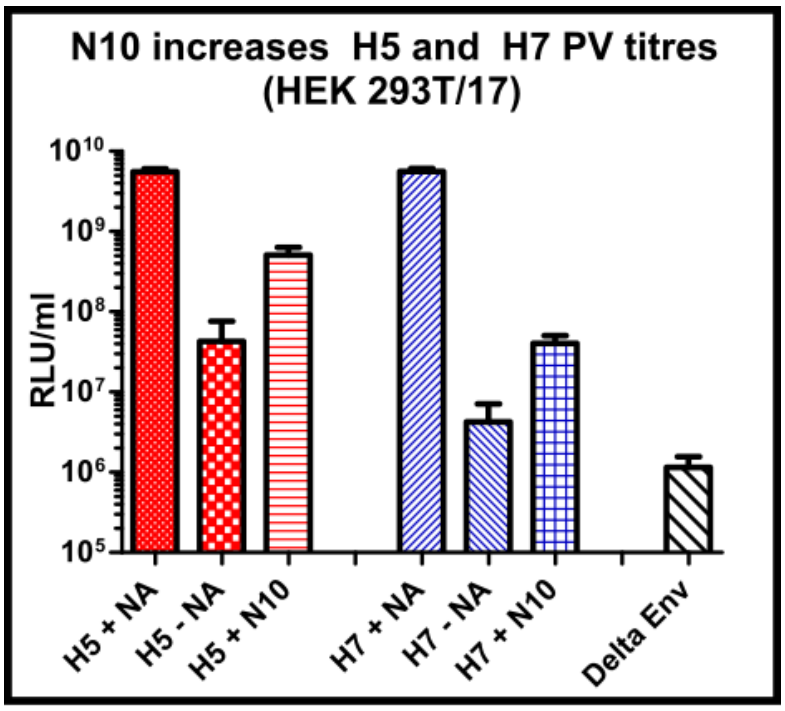

Figure 6.6. N10 releases group 1 (H5) and group 2 (H7) bearing PV. RLU/ml titres for H5 (A/Vietnam/1194/2004) and H7 (A/Shanghai/2/2013) released with exogenous NA (+ NA), N10 (+N10) or produced in the absence of NA (-NA). Delta envelope control represents a baseline RLU/ml value.

Subsequently, results for multiple different preparations of N10 as well as H17N10 and H5N10 bearing PV (Table 6.2) produced negative results in the ELLA. In contrast, control H3 PVs bearing N1, N3, N4 and N9 were positive for sialidase activity to varying degrees (Figure 6.7). Control PV (H3NX) produced by Rebecca Kinsley and Martin Mayora-Neto.

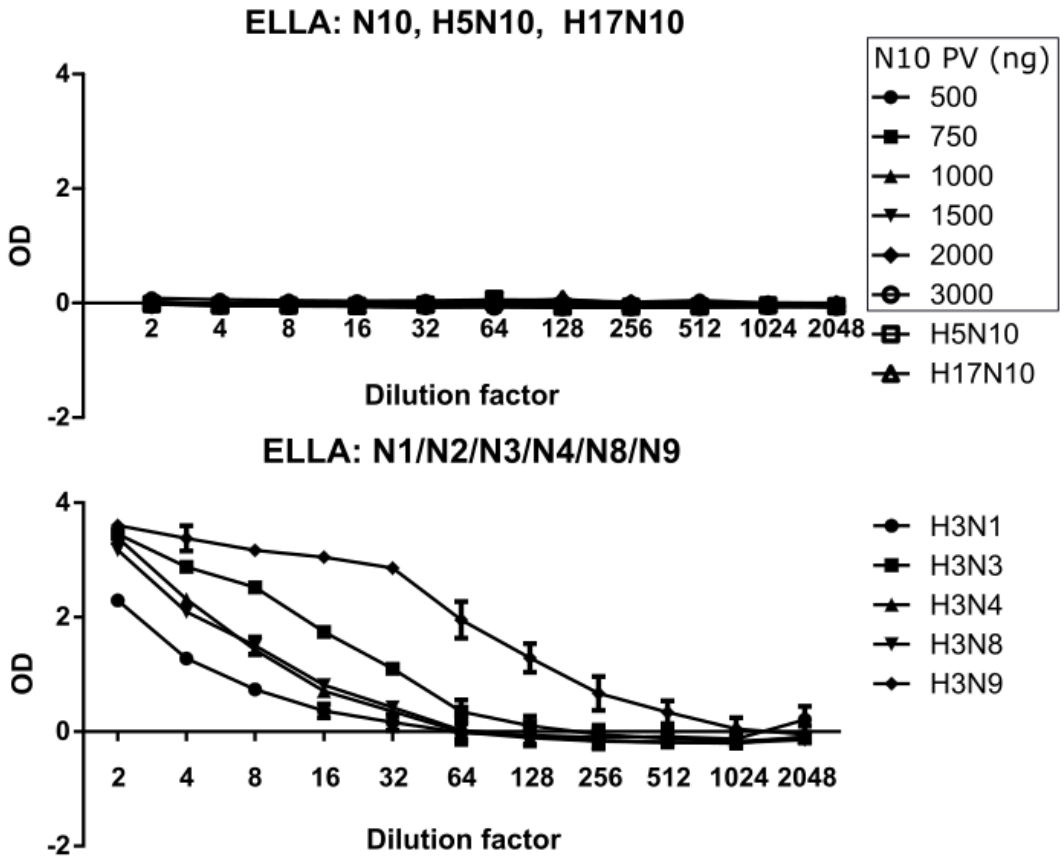

Figure 6.7. ELLA for PVs bearing N10, H5N10, H17N10 and H3NX (N1, N3, N4, N8, N9) glycoproteins. No NA activity is observed for any N10 bearing PV. NA activity is detected for N9, N3, N4, N8 and N1 PV alongside the H3 glycoprotein (ordered from strongest to weakest NA activity).

6.3.4 H17 is neutralised by bnmAbs targeting the conserved stalk region.

bnmAb CR9114 strongly neutralised H17N10, giving IC_{50} neutralising antibody titres of 61.18 ng/ml on MDCK II cells and 66.41 ng/ml on RIE 1495 (Figure 6.8). F16-nt also neutralised H17 and H17N10, giving neutralising antibody titres of 12 μg/ml (MDCK II) and 68 μg/ml (RIE 1495) (Figure 6.9). F16 conjugated to cholesterol (F16-Chol) was much less neutralising, antibody titres were 191 μg/ml (MDCK II) and 997 ug/ml (RIE 1495) (Figure 6.10). CR6261 did not neutralise H17N10 at any concentration attempted (maximum 100 μg/ml starting concentration).

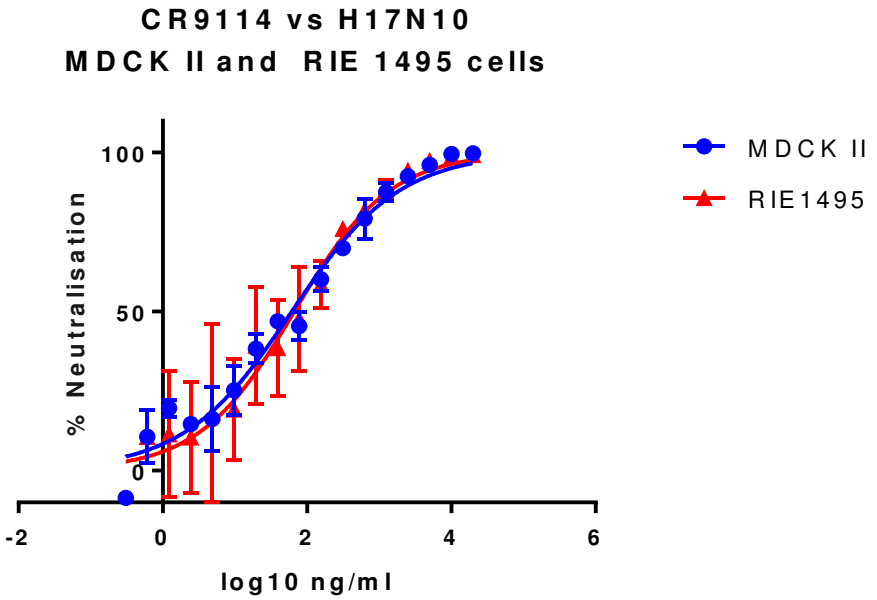

Figure 6.8. Neutralisation of H17N10 by mAb CR9114 when transducing MDCK II and RIE 1495 cells. CR9114 neutralises H17N10 PV when using both MDCK II and RIE 1495 in the pMN assay. Neutralising antibody titres (IC_{50}) for CR9114 on MDCK II and RIE1495 cells were 61.18 and 66.41 ng/ml respectively. mAbs were tested in duplicate with more consistent neutralisation seen when using MDCK II cells in the pMN assay.

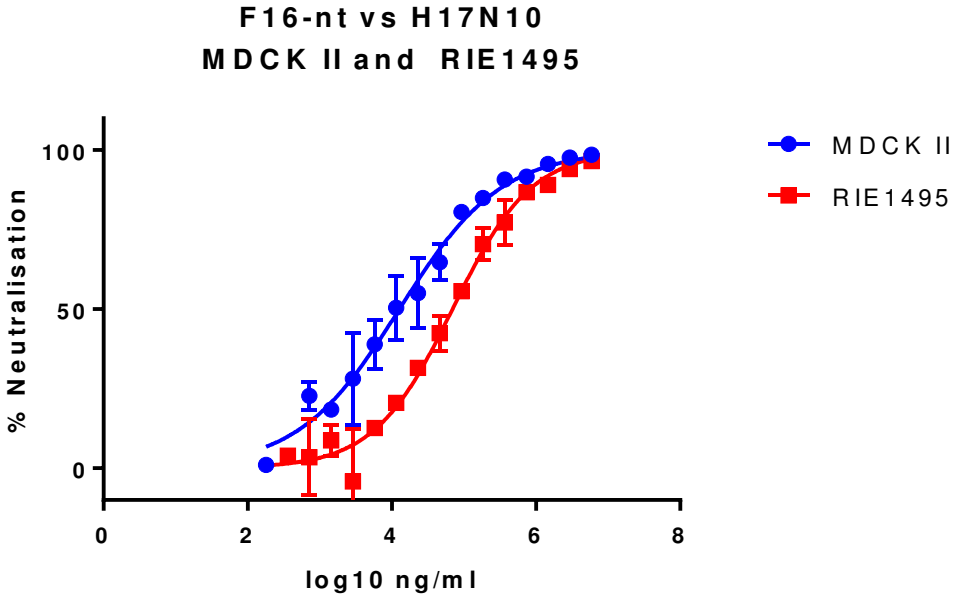

Figure 6.9. Neutralisation of H17N10 PV by mAb F16-nt when transducing MDCK II and RIE 1495 cells. F16-nt neutralises H17N10 PV when using both MDCK II and RIE 1495 in the pMN assay. Neutralising antibody titres (IC_{50}) for F16-nt on MDCK II and RIE1495 cells were 12 and 68 µg/ml respectively. mAbs were tested in duplicate with consistent neutralisation seen when using both MDCK II and RIE1495 cells in the pMN assay.

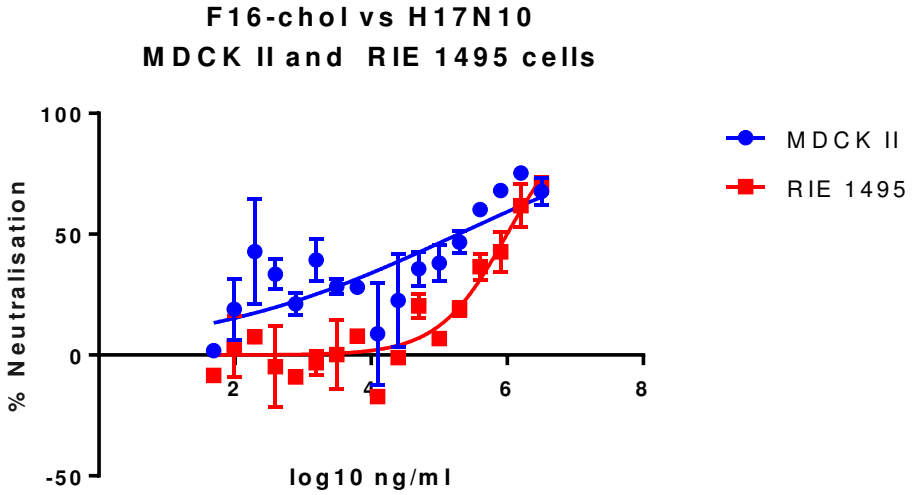

Figure 6.10. Neutralisation of H17N10 PV by mAb F16-chol when transducing MDCK II and RIE 1495 cells. F16-chol poorly neutralises H17N10 PV, using both MDCK II and RIE 1495 in the pMN assay. Neutralising antibody titres (IC_{50}) for F16-chol on MDCK II and RIE1495 cells were 191 and 997 µg/ml respectively. mAbs were tested in duplicate with more consistent results observed when using RIE 1495 cells.

6.3.5 Human sera show neutralising activity against H17N10.

The subset of human serum samples used in pMN assays on H17N10 PV showed varying neutralising titres; titres for sera were between 24 and 289, representing the reciprocal dilution point for inhibition of 50% of the RLU input signal. Neutralisation curves are displayed in Figure 6.11 and IC_{50} values recorded in Table 6.3. The most consistent neutralisation curves were generated when PVs were used to transduce RIE 1495 cells in the presence of serum J136 (IC_{50}: 289). Other sera show a trend towards decreasing neutralisation as serum is diluted, but no distinctive curve is produced by nonlinear regression analysis, reducing the confidence which can be attributed to these results. Nevertheless, neutralisation is observed when compared to negative serum control (FBS).

Table 6.3. IC_{50} values for subset of Oxford serum samples assayed against H17N10 PV. Samples J136 and J56 were chosen as high positive samples while J50 and J170 were chosen as low positive samples, based on pMN against CS CHM PV. High and Low positive serum samples behave similarly against H17N10 PV.

Serum ID	**IC_{50} (MDCK II)**	**IC_{50} (RIE1495)**
J136	137	289
J50	3	78
J56	191	176
J170	24	47

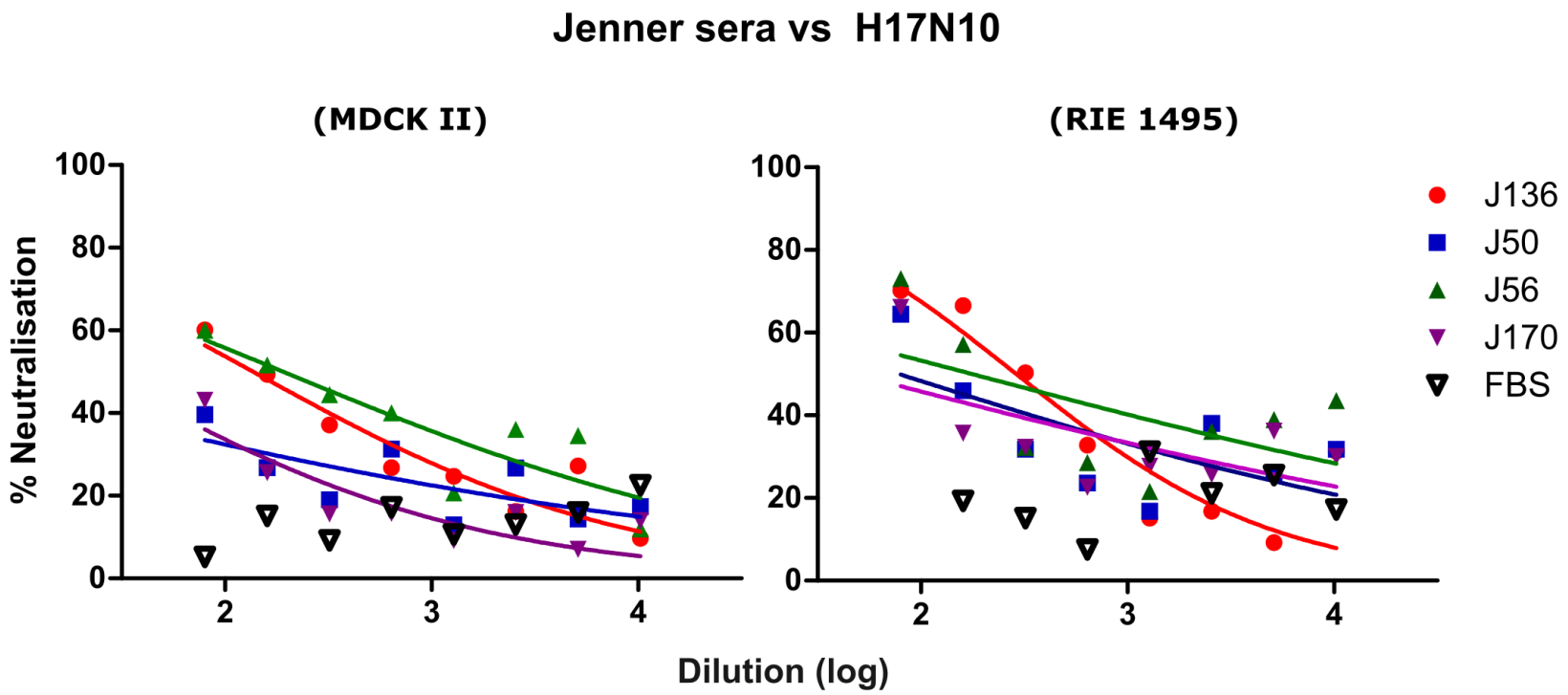

Figure 6.11. Neutralisation of H17N10 PV by Jenner Sera samples (J#). Two high positive (J136 and J56) and two low positive (J50 and J170) as determined by pMN vs. CS CHM bearing PV. Serum samples were picked and assayed against H17N10 luciferase PV on both MDCK II and RIE 1495. Neutralisation was observed, with high positive samples more efficiently neutralising H17N10 PV than low positive samples when compared to the negative serum control FBS.

6.4 Discussion

6.4.1 H17 PV transduce MDCK I, MDCK II and RIE 1495 cells

By acquiring and employing the new cell lines MDCK II and RIE 1495, an H17 dependent luciferase signal from the transduction of these cells by our PV was produced (Figure 6.3). This allowed us to study this HA as well as the effect of its matched NA in neutralisation and inhibition assays. Our data reinforces the utility of MDCK II and RIE 1495 cell lines in characterisation or study of bat influenza viruses (Moreira et al. 2016). After successfully performing experiments on MDCK II and RIE 1495 cells (Figure 6.5), Experiments were repeated with the MDCK I line, showing successful transduction by H17N10 and H17 luciferase PV, despite previous lack of results with this cell line (Figure 6.4).

6.4.2 H17 HA cleaved by proteases

We have reproduced work showing that TMPRSS2 and trypsin like proteases can activate H17, adding to the list HAT and TMPRSS4 which are frequently used for the activation of other IAV HAs in the PV production process (Figure 6.5) (Ferrara et al. 2012; M. Hoffmann et al. 2016). While we have shown that TMPRSS3, Furin and KLK5 have little to no effect on H17 activation in our PV system, it is possible that these proteases are not compatible with the current PV production system, they may be incorrectly localised within the cell and therefore not have an effect. There is a great deal of further work which could be carried out to further understand the susceptibility of H17 to different proteases as well as the extent to which these types of proteases are present in the cells susceptible to infection by this virus.

6.4.3 N10 releases group 1 (H5) and group 2 (H7) influenza PV

ELLA was negative for all N10 bearing PV, despite the production of multiple different batches with increasing quantities of the pI.18-N10 expression plasmid, in addition to H17N10 and H5N10 which functioned in viral entry assays (Figure 6.7, section 6.3.3). The fact is that N10 is not acting as an IAV like sialidase (García-Sastre 2012), the ELLA assay is not suitable for detection of N10 enzymatic activity, or that it is unable to detect it. However, we have shown that N10 mediates release of group 1 and 2 HA influenza bearing PV in the absence of another source of NA (Figure 6.6). This intriguing finding shows that the

enzyme is acting in an influenza specific manner, but does not help to characterise its interactions with the matched H17 glycoprotein. It is possible that the N10 is cleaving further down the carbohydrate chain, leaving behind residues that do not allow for HA binding, preventing build-up of viral particles on the cell surface and crucially resulting in a negative result in ELLA. It is also possible that NA is mediating increased budding of influenza PV, leading to the increase in titre observed in this fashion (Barman et al. 2004; B. J. Chen et al. 2007; Jin et al. 1997).

6.4.4 H17 PV neutralised by bnmAbs

Despite the undecided nature of the pandemic threat posed by exotic viruses such as H17N10 (or its related bat virus H18N11), it is encouraging to know that stalk-binding bnmAbs are effective at neutralising the H17 glycoprotein (Figures 6.8-6.10). With the ever growing number of research groups attempting to produce universal vaccines that elicit production of similar stalk-targeting antibodies, any breakthrough and subsequent use in vaccination programs or trials should elicit immune responses which cross-react with bat influenza viruses, reducing severity of disease and risks of H17 spreading in naïve human populations.

6.4.5 Further work

In order to strengthen these results, further sets of MDCK derived cell lines should be obtained and tested alongside MDCK I and MDCK II cells. This will help to interrogate the discrepancy in results seen in the published literature and our work (Maruyama et al. 2014; Moreira et al. 2016). This could also encourage stakeholders to further investigate the MDCK cell types they use and increase the reproducibility and accuracy of MDCK derived results. Also, comparison of the MDCK II, RIE 1495 and HEK293T proteome may help characterisation of the H17 receptor and direct future experiments. Much work is required on discovery of the H17 receptor as well as the substrate required for N10 activity. It is unclear whether H17 requires N10 for viral egress through its action or other effects, such as the binding attributes seen in some H3N2 strains (Y. P. Lin et al. 2010). Nevertheless, N10 is shown to be a functional enzyme having a clear impact on egress and production titres of H17 bearing PVs, it would be interesting to discover the substrate in order to be able to adapt ELLA to detect its activity and allow further work to be carried out.

Chapter 7 : Discussion and conclusions

In this thesis, several objectives were achieved using PV bearing influenza glycoproteins. First, a cHA bearing the stalk from the 2009 H1N1pdm strain was produced alongside the parental strains and employed in a serological collaboration towards the detection of heterosubtypic/broadly neutralising antibodies in human sera. This not only confirmed the increase in bnAbs post H1N1pdm, but represents a useful tool for the further dissection of stalk antibody responses from those against the head of future strains through the employment of cHA bearing PV. Second, gold standard serological assays (HI, SRH) were compared to the pMN assay using two defined sets of sera against both lineages of influenza B, showing correlation between assays for the Yamagata but not Victoria lineages. Third, the ELLA assay was adapted to the use of PV and optimisation was carried out with currently relevant strains towards the generation of high ELLA titre PV preparations as well as the generation of reliable and highly reproducible data. Fourth, PV bearing the bat influenza H17 glycoprotein were successfully used to transduce cell lines MDCK I, MDCK II and RIE 1495, and it was shown that this exotic strain was neutralised by characterised bnAbs CR9114 and F16 as well as human sera with high stalk neutralising properties. Subsequently it was shown that the bat influenza N10 glycoprotein, while unable to cleave FBS derived fetuin in the ELLA assay, was still able to mediate the release of group 1 and 2 influenza PV in the absence of another source of NA.

7.1 Chapter 3

The cHA PV system allowed the generation of large amounts of neutralisation data, especially so due to each serum sample being tested on three different HA bearing PV. This resulted in data against an exotic group 1 strain (H11), a pandemic strain (H1 CA/09) and the chimera, allowing the interpretation of heterosubtypic immunity in each of nearly 200 patient samples. Serum samples spanned from 2008 to 2016 but unfortunately only 20 samples were collected from patients prior to the pandemic H1N1 start. Ideally, samples would have been obtained in groups pre and post 2009 with known HI data against the pandemic strain, allowing the confirmation of bnAb increases due to CA/09 infection. However, this was not possible due to the rarity of serum samples which were very kindly provided by the Jenner Institute Laboratories. The three virus system is time and resource

consuming, which is not ideal when low volumes of serum are available. Despite the lack of serum samples pre 2009, the available panel performed as expected, with low neutralising antibody titres against H11, typical cross-reactive titres against CA/09 and relatively low titres against the cHA (Figure 3.19). When bracketed by year (Figure 3.20), an interesting pattern is seen in that after 2009 various spikes in neutralising antibody titres are observed, raising the average titres for each year respectively. When bracketed by influenza season, an even more prominent peak is seen for the 2009 season against all three PV, indicating an increase in heterosubtypic immunity in the first pH1N1 influenza season (Figure 3.21). Each season following 2009-2010 showed increased neutralising antibody titres against the CS CHM. This confirms that circulation of the pH1N1 strain corresponds with increases in heterosubtypic immunity. Age bracketing of neutralising antibody titres generated using the cHA system (Figure 3.22) showed an increase in bnAbs in the elderly and the younger age group (20s) which was hit the hardest by the 2009 pandemic (Dawood et al. 2012; Shrestha et al. 2011). The Sports Science Sera evaluated against various different group 1 and group 2 influenza bearing PV generated interesting data on heterosubtypic protection. Expectedly, high neutralising antibody titres were observed against H1 and H3 seasonal strains and lower titres against exotic H5 and H7 subtypes (Figure 3.23). However, the data generated allowed the pairing of data for high responders against multiple subtypes, enabling us to identify the patients in Table 3.4 who display high titres within a group or between groups. While this system is also resource heavy, this approach could suit a small scale project using a defined set of HA bearing PV. Interestingly, the use of serum samples in ELLA based upon their performance in pMN yielded data which correlated remarkably well between the two assays (Figure 3.25). This is incredibly useful data when considering that infection with pH1N1 will generate an immune footprint against both the HA and NA glycoproteins used in these assays. Having near perfect correlation between antibody titres against each glycoprotein using influenza PV makes these two assays an excellent choice for future projects determining HA and NA directed antibody responses.

The next step for cHA bearing PV is to troubleshoot the problems with the production of group 2 and influenza B cHAs. A starting point could be recreation of successfully published cHAs, using this as a platform for the creation of further cHAs through site directed mutagenesis or seamless cloning. Following this, further large scale projects should be attempted, ideally with serum from universal vaccine candidates which are also being tested

for immunogenicity by traditional means (ELISA). To this end, RLU titres must be improved for cHAs bearing the CA/09 stalk, which has been difficult to produce in high enough titres to perform neutralisation assays. Finally, a larger scale project involving CA/09, CS CHM and ELLA on a defined serum panel from patients known to be positive/negative to CA/09 would be an excellent project to learn more about the strengths and weaknesses of this system.

7.2 Chapter 4

Interesting data on the neutralisation of influenza B PV was generated in the projects listed in chapter 4. First, a panel of recently characterised mAbs was evaluated against the available influenza B PV library, consisting of strains from Yamagata and Victoria lineages as well as the pre-lineage strain (Table 4.4). The results with B/Brisbane/60/2008 were unexpected (Figure 4.3), as the original article in which the mAbs were characterised showed that they were susceptible to Victoria specific mAbs (Verma et al. 2017). The evaluation of pMN alongside widely used assays HI and SRH raised some interesting questions on the nature of serological assays and influenza virus. Two strains, each from a different lineage of influenza B were assayed by HI, SRH and pMN, generating IC_{50} and IC_{90} data for the latter. mAbs behaved as expected for the Yamagata lineage, but not for Victoria in the case of B/Brisbane/60/2008 (Figures 4.3 and 4.4). Interestingly, the pre-lineage strain was neutralised in a similar manner to the Victoria lineage, being susceptible to mAbs generated against cross-lineage epitopes as well as Victoria specific epitopes. The fact that in two different cases discordant results have been attributed to B/Brisbane/60/2008 bearing PV is a cause for concern. Sequencing of this gene revealed no deletions or insertions, PVs were functional and fully able to transduce cells through HA based entry of the lentivirus, and B/Brisbane/60/2008 antiserum neutralised B/Brisbane with a higher potency than other influenza B PVs based on pMN assay (Figure 4.5). It is important to note that the B/Florida/4/2006 gene used was human codon optimised whereas the gene for B/Brisbane/60/2008 was WT. This could lead to differences in glycosylation patterns, masking the target epitopes of the 8E12 or 5A1 mAbs in comparison to the original published paper by Verma and colleagues. This is further reinforced by this groups frequent use of human codon optimised synthesized genes (personal communications with Dr Jerry Weir), and previous work showing the effect of codon optimisation on N-linked glycosylation (Ebrahimi and West 2014). Troubleshooting this problem would be facilitated

by generation of a codon optimised gene for B/Brisbane/60/2008, in order to reduce the number of variables between strains of influenza B PV. Testing WT and codon optimised B/Brisbane PV side by side would yield interesting data on the effect of codon optimisation on influenza HA N-linked glycosylation and whether this causes masking or unmasking of epitopes, leading to the results reported in this chapter. Despite the discordant data with Victoria lineage strain B/Brisbane/60/2008 (Figures 4.8-4.13), pMN, HI and SRH assays correlated well for the Yamagata lineage strain B/Florida/4/2006 (Figures 4.14-4.19). This experiment should be repeated in the future with a further set of PV from each influenza B lineage. First, this would provide further data to determine whether Victoria lineage strains do not correlate well between assays or whether the problem lies in B/Brisbane/60/2008. Second, this would allow the establishment of a correlate of protection of pMN data generated using influenza B PV, which would lend greater value to future projects involving these PV.

7.3 Chapter 5

The data presented in chapter 5 represent the establishment and optimisation of ELLA using PV as a source of NA in the Viral Pseudotype Unit laboratories. This assay adds a further aspect to the use of PV in serology, expanding PV utility in the measurement of immunogenicity of vaccines involving an NA component, and enables the user to perform experiments against novel NA inhibitors designed to reduce morbidity following infection with influenza viruses. Interesting factors affecting the result outputs were tested, such as ELLA viral input (OD_{492} of 2.0 or 90% of titration input) and concentration of PNA-HRPO (Figures 5.2 and 5.17-5.18). These two variables, when diluted gave rise to reduced NA titres or increased antibody titres (Figures 5.17 and 5.18). Also, we succeeded in producing high titre NA only PVs which performed well in ELLA, despite being more easily neutralised than PV bearing HA and NA (Figure 5.11). These PVs provide a platform which, alongside HA only PVs in the pMN assay, offer a clean measure of antibody potency against the glycoprotein of choice – eliminating the effect of steric hindrance from reported antibody titres. The data generated with the various parameters suggested that using more concentrated PNA-HRPO (1:500) and a higher viral input resulted in optimal data. Reduction in viral input lead to increased values for negative controls, and reduction in concentration resulted in higher antibody titres for low positive samples (Figures 5.18 and 5.19). Both of these scenarios

would be best avoided in future projects using ELLA. The next step for ELLA is utilisation in a wide ranging project, alongside pMN values against matched HA bearing PVs. The combination of clean HA/NA responses with high correlation observed between the same pH1 and pN1 assays in chapter 3 (Figure 3.25), show that these two assays work well when carried out side by side, providing a wealth of data which aid interpretation on immunity generated against both glycoproteins, without the risk of data being misinterpreted due to the effect of steric hindrance.

7.4 Chapter 6

In chapter 6 we reported the success in production of H17 an H17N10 bearing PV, and their neutralisation by bnAbs (Figures 6.8-6.10). This exotic HA which has yet to be discovered in virus form in the wild is nevertheless important in the context of the history of influenza viruses and their ability to cross over into humans and contribute to a pandemic. Recent work has shown that the risk is low for H17 and H18 bat influenza viruses, due to incompatibility between these viruses and traditional strains (B. Zhou et al. 2014). We have confirmed that H17 mediates entry though PV based transduction (Figures 6.3-6.5) and also shown that N10 is able to act in a NA-like manner in mediating the release of PV bearing HA from group 1 and 2 influenza (Figure 6.6). While various research groups have studied the N10 protein and concluded that it is not an NA, these results show that it does have a similar action which warrants further investigation. Future work on N10 will include the testing of different sources of fetuin as it is possible that the N10 utilises a different substrate which is not in abundance in the ELLA assay. Attempts must also be made to optimise the ELLA environment to the N10 activity, N10 may not function in the same conditions as avian or human NAs. Finally it would be worth titrating N1 CA/09 in wells previously exposed to N10, to determine whether N10 cleaves fetuin in a manner which releases sialic acid but does not expose galactose, the PNA substrate, thus leading to negative ELLA results.

7.5 Vaccines, future of PV in serology/vaccines

While the focus of this thesis is the production and utilisation of PV in a serological setting, the technique remains poorly represented among influenza laboratories and published articles, giving way to traditional techniques such as HI, ELISA and SRH. This is unfortunate as PV based assays have many strengths over these assays, they are safe, sensitive, easily manipulated and only work with functional glycoproteins, opening avenues for the detection of antibodies or inhibitors not located at the RBS. Some of the problems with the use of PVs surround the fact that they only contain influenza glycoproteins and are effectively a lentivirus gaining entry to cells in a HA mediated fashion. Also, the issue of glycosylation, raised in chapter 4 is an issue, as PVs are exclusively produced in cells originating from the human kidney, whereas batches of inactivated virus used in traditional assays would have originated from other sources, whether cell or egg grown. As with all areas of biology, the idea of standardisation is the goal to be aiming for, and the development of consensus protocols and standard reagents in the future would facilitate the comparison of results between assays as well as between laboratories.

References

Ahmed, M. S., Jacques, L. C., Mahallawi, W. H., Ferrara, F., Temperton, N. J., Upile, N., et al. (2015). Cross-reactive immunity against influenza viruses in children and adults following 2009 pandemic H1N1 infection. *Antiviral Research*, *114*, 106–112. doi:10.1016/j.antiviral.2014.12.008

Akarsu, H., Burmeister, W. P., Petosa, C., Petit, I., Mu, C. W., & Ruigrok, R. W. H. (2003). Crystal structure of the M1 protein-binding domain of the in influenza A virus nuclear export protein (NEP / NS2). *EMBO Journal*, *22*(18).

Akira, S., Uematsu, S., & Takeuchi, O. (2006). Pathogen Recognition and Innate Immunity. *Cell*, *124*(4), 783–801. doi:10.1016/j.cell.2006.02.015

Al-Khayatt, R., Jennings, R., & Potter, C. W. (1984). Interpretation of responses and protective levels of antibody against attenuated influenza A viruses using single radial haemolysis. *The Journal of hygiene*, *93*(2), 301–12. doi:10.1017/S0022172400064834

Alamgir, A. S. M., Matsuzaki, Y., Hongo, S., Tsuchiya, E., Sugawara, K., Muraki, Y., & Nakamura, K. (2000). Phylogenetic analysis of influenza C virus nonstructural (NS) protein genes and identification of the NS2 protein. *Journal of General Virology*, *81*(8), 1933–1940. doi:10.1099/0022-1317-81-8-1933

Alberini, I., Del Tordello, E., Fasolo, A., Temperton, N. J., Galli, G., Gentile, C., et al. (2009). Pseudoparticle neutralization is a reliable assay to measure immunity and cross-reactivity to H5N1 influenza viruses. *Vaccine*, *27*(43), 5998–6003. doi:10.1016/j.vaccine.2009.07.079

Alexopoulou, L., Holt, A. C., Medzhitov, R., & Flavell, R. A. (2001). Recognition of double-stranded RNA and activation of NF-κB by Toll-like receptor 3. *Nature*, *413*(6857), 732–738. doi:10.1038/35099560

Altschul, S. F., Gish, W., Miller, W., Myers, E. W., & Lipman, D. J. (1990). Basic local alignment search tool. *Journal of Molecular Biology*, *215*(3), 403–410. doi:10.1016/S0022-2836(05)80360-2

Altschul, S. F., Madden, T. L., Schäffer, A. A., Zhang, J., Zhang, Z., Miller, W., & Lipman, D. J. (1997). Gapped BLAST and PSI-BLAST: a new generation of protein database search programs. *Nucleic acids research*, *25*(17), 3389–402. http://www.ncbi.nlm.nih.gov/pubmed/9254694. Accessed 17 August 2017

Ambrose, C. S., & Levin, M. J. (2012). The rationale for quadrivalent influenza vaccines. *Human Vaccines and Immunotherapeutics*, *8*(1), 81–88. doi:10.4161/hv.8.1.17623

Ao, Z., Patel, A., Tran, K., He, X., Fowke, K., Coombs, K., et al. (2008). Characterization of a trypsin-

dependent avian influenza H5N1-pseudotyped HIV vector system for high throughput screening of inhibitory molecules. *Antiviral Research*, *79*(1), 12–18. doi:10.1016/j.antiviral.2008.02.001

Area, E., Martin-Benito, J., Gastaminza, P., Torreira, E., Valpuesta, J. M., Carrascosa, J. L., & Ortin, J. (2004). 3D structure of the influenza virus polymerase complex: Localization of subunit domains. *Proceedings of the National Academy of Sciences*, *101*(1), 308–313. doi:10.1073/pnas.0307127101

Ascione, A., Capecchi, B., Campitelli, L., Imperiale, V., Flego, M., Zamboni, S., et al. (2009). Human monoclonal antibodies in single chain fragment variable format with potent neutralization activity against influenza virus H5N1. *Antiviral Research*, *83*(3), 238–244. doi:10.1016/j.antiviral.2009.05.005

Balachandran, S., Roberts, P. C., Brown, L. E., Truong, H., Pattnaik, A. K., Archer, D. R., & Barber, G. N. (2000). Essential role for the dsRNA-dependent protein kinase PKR in innate immunity to viral infection. *Immunity*, *13*(1), 129–41. http://www.ncbi.nlm.nih.gov/pubmed/10933401. Accessed 26 September 2017

Banasik, M. B., & McCray Jr, P. B. (2010). Integrase-defective lentiviral vectors: Progress and applications. *Gene Therapy*, *17*(2), 150–157. doi:10.1038/gt.2009.135

Barman, S., Adhikary, L., Chakrabarti, A. K., Bernas, C., Kawaoka, Y., & Nayak, D. P. (2004). Role of transmembrane domain and cytoplasmic tail amino acid sequences of influenza a virus neuraminidase in raft association and virus budding. *Journal of virology*, *78*(10), 5258–69. doi:10.1128/JVI.78.10.5258

Basu, A., Antanasijevic, A., Wang, M., Li, B., Mills, D. M., Ames, J. a, et al. (2013). New Small Molecule Entry Inhibitors Targeting Hemagglutinin-mediated Influenza A Virus Fusion. *Journal of virology*, *88*(3), 1447–1460. doi:10.1128/JVI.01225-13

Basu, A., Mills, D. M., & Bowlin, T. L. (2010). High-Throughput Screening of Viral Entry Inhibitors Using Pseudotyped Virus. In *Current Protocols in Pharmacology* (Vol. Chapter 13, p. 13B.3.1-13B.3.17). Hoboken, NJ, USA: John Wiley & Sons, Inc. doi:10.1002/0471141755.ph13b03s51

Baum, A., Sachidanandam, R., & García-Sastre, A. (2010). Preference of RIG-I for short viral RNA molecules in infected cells revealed by next-generation sequencing. *Proceedings of the National Academy of Sciences*, *107*(37), 16303–16308. doi:10.1073/pnas.1005077107

Belshe, R. B. (2010). The need for quadrivalent vaccine against seasonal influenza. *Vaccine*, *28*(SUPPL. 4), D45–D53. doi:10.1016/j.vaccine.2010.08.028

Benfield, C. T. O., Smith, S. E., Wright, E., Wash, R. S., Ferrara, F., Temperton, N. J., & Kellam, P.

(2015). Bat and pig IFN-induced transmembrane protein 3 restrict cell entry by influenza virus and lyssaviruses. *Journal of General Virology*, *96*(5), 991–1005. doi:10.1099/vir.0.000058

Berthoud, T. K., Hamill, M., Lillie, P. J., Hwenda, L., Collins, K. A., Ewer, K. J., et al. (2011). Potent CD8+ T-cell immunogenicity in humans of a novel heterosubtypic influenza a vaccine, MVA-NP+M1. *Clinical Infectious Diseases*, *52*(1), 1–7. doi:10.1093/cid/ciq015

Bertram, S., Glowacka, I., Blazejewska, P., Soilleux, E. J., Allen, P., Danisch, S., et al. (2010). TMPRSS2 and TMPRSS4 facilitate trypsin-independent spread of influenza virus in Caco-2 cells. *J Virol*, *84*(19), 10016–10025. doi:10.1128/JVI.00239-10

Bertram, S., Heurich, A., Lavender, H., Gierer, S., Danisch, S., Perin, P., et al. (2012). Influenza and SARS-coronavirus activating proteases TMPRSS2 and HAT are expressed at multiple sites in human respiratory and gastrointestinal tracts. *PLoS ONE*, *7*(4), 1–8. doi:10.1371/journal.pone.0035876

Biswas, S. K., Boutz, P. L., & Nayak, D. P. (1998). Influenza virus nucleoprotein interacts with influenza virus polymerase proteins. *Journal of virology*, *72*(7), 5493–501. http://www.ncbi.nlm.nih.gov/pubmed/9621005. Accessed 25 September 2017

Blesch, A. (2004). Lentiviral and MLV based retroviral vectors for ex vivo and in vivo gene transfer. *Methods*, *33*(2), 164–172. doi:10.1016/j.ymeth.2003.11.005

Blumenkrantz, D., Roberts, K. L., Shelton, H., Lycett, S. J., & Barclay, W. S. (2013). The short stalk length of highly pathogenic avian influenza H5N1 virus neuraminidase limits transmission of pandemic H1N1 virus in ferrets. *Journal of virology*, *87*(19), 10539–51. doi:10.1128/JVI.00967-13

Bock, M., Bishop, K. N., Towers, G. J., & Stoye, J. P. (2000). Use of a transient assay for studying the genetic determinants of Fv1 restriction. *Journal of virology*, *74*(16), 7422–30. doi:10.1128/JVI.74.16.7422-7430.2000

Bodle, J., Verity, E. E., Ong, C., Vandenberg, K., Shaw, R., Barr, I. G., & Rockman, S. (2013). Development of an enzyme-linked immunoassay for the quantitation of influenza haemagglutinin: An alternative method to single radial immunodiffusion. *Influenza and other Respiratory Viruses*, *7*(2), 191–200. doi:10.1111/j.1750-2659.2012.00375.x

Boratyn, G. M., Schäffer, A. A., Agarwala, R., Altschul, S. F., Lipman, D. J., & Madden, T. L. (2012). Domain enhanced lookup time accelerated BLAST. *Biology Direct*, *7*(1), 12. doi:10.1186/1745-6150-7-12

Bosch, V., Kramer, B., Pfeiffer, T., Stärck, L., & Steinhauer, D. A. (2001). Inhibition of release of lentivirus particles with incorporated human influenza virus haemagglutinin by binding to sialic

acid-containing cellular receptors. *Journal of General Virology*, *82*(10), 2485–2494.

Böttcher-Friebertshäuser, E., Klenk, H.-D., & Garten, W. (2013). Activation of influenza viruses by proteases from host cells and bacteria in the human airway epithelium. *Pathogens and disease*, *69*(2), 87–100. doi:10.1111/2049-632X.12053

Böttcher, E., Freuer, C., Steinmetzer, T., Klenk, H.-D., & Garten, W. (2009). MDCK cells that express proteases TMPRSS2 and HAT provide a cell system to propagate influenza viruses in the absence of trypsin and to study cleavage of HA and its inhibition. *Vaccine*, *27*(45), 6324–6329. doi:10.1016/j.vaccine.2009.03.029

Böttcher, E., Matrosovich, T. Y., Beyerle, M., Klenk, H.-D., Garten, W., & Matrosovich, M. N. (2006). Proteolytic activation of influenza viruses by serine proteases TMPRSS2 and HAT from human airway epithelium. *Journal of virology*, *80*(19), 9896–8. doi:10.1128/JVI.01118-06

Braakman, I., Hoover-Litty, H., Wagner, K. R., & Helenius, A. (1991). Folding of influenza hemagglutinin in the endoplasmic reticulum. *Journal of Cell Biology*, *114*(3), 401–411. doi:10.1083/jcb.114.3.401

Brandenburg, B., Koudstaal, W., Goudsmit, J., Klaren, V., Tang, C., Bujny, M. V., et al. (2013). Mechanisms of hemagglutinin targeted influenza virus neutralization. *PLoS ONE*, *8*(12), e80034. doi:10.1371/journal.pone.0080034

Brass, A. L., Huang, I. C., Benita, Y., John, S. P., Krishnan, M. N., Feeley, E. M., et al. (2009). The IFITM Proteins Mediate Cellular Resistance to Influenza A H1N1 Virus, West Nile Virus, and Dengue Virus. *Cell*, *139*(7), 1243–1254. doi:10.1016/j.cell.2009.12.017

Brownlee, G. G., & Fodor, E. (2001). The predicted antigenicity of the haemagglutinin of the 1918 spanish influenza pandemic suggests an avian origin. *Philosophical transactions of the Royal Society B*, *356*(1416), 1871–1876. doi:10.1098/rstb.2001.1001

Buchy, P., Vong, S., Chu, S., Garcia, J. M., Hien, T. T., Hien, V. M., et al. (2010). Kinetics of neutralizing antibodies in patients naturally infected by H5N1 virus. *PloS one*, *5*(5), e10864. doi:10.1371/journal.pone.0010864

Bui, M., Wills, E. G., Helenius, A., & Whittaker, G. R. (2000). Role of the influenza virus M1 protein in nuclear export of viral ribonucleoproteins. *Journal of virology*, *74*(4), 1781–6. doi:10.1128/JVI.74.4.1781-1786.2000

Buxton, R. C., Edwards, B., Juo, R. R., Voyta, J. C., Tisdale, M., & Bethell, R. C. (2000). Development of a Sensitive Chemiluminescent Neuraminidase Assay for the Determination of Influenza Virus Susceptibility to Zanamivir. *Analytical Biochemistry*, *280*(2), 291–300. doi:10.1006/abio.2000.4517

Camacho, C., Coulouris, G., Avagyan, V., Ma, N., Papadopoulos, J., Bealer, K., & Madden, T. L. (2009). BLAST+: architecture and applications. *BMC Bioinformatics*, *10*(1), 421. doi:10.1186/1471-2105-10-421

Carnell, G. W., Ferrara, F., Grehan, K., Thompson, C. P., & Temperton, N. J. (2015). Pseudotype-based neutralization assays for influenza: A systematic analysis. *Frontiers in Immunology*, *6*(MAR), 1–17. doi:10.3389/fimmu.2015.00161

Carragher, D. M., Kaminski, D. A., Moquin, A., Hartson, L., & Randall, T. D. (2008). A novel role for non-neutralizing antibodies against nucleoprotein in facilitating resistance to influenza virus. *Journal of immunology (Baltimore, Md. : 1950)*, *181*(6), 4168–76. http://www.ncbi.nlm.nih.gov/pubmed/18768874. Accessed 26 September 2017

Carrat, F., Vergu, E., Ferguson, N. M., Lemaitre, M., Cauchemez, S., Leach, S., & Valleron, A. J. (2008). Time lines of infection and disease in human influenza: A review of volunteer challenge studies. *American Journal of Epidemiology*, *167*(7), 775–785. doi:10.1093/aje/kwm375

Cate, T. R., Couch, R. B., Parker, D., & Baxter, B. (1983). Reactogenicity, immunogenicity, and antibody persistence in adults given inactivated influenza virus vaccines - 1978. *Reviews of infectious diseases*, *5*(4), 737–47. http://www.ncbi.nlm.nih.gov/pubmed/6622888. Accessed 24 April 2017

Cate, T. R., Rayford, Y., Nino, D., Winokur, P., Brady, R., Belshe, R. B., et al. (2010). A High Dosage Influenza Vaccine Induced Significantly More Neuraminidase Antibody than Standard Vaccine among Elderly Subjects, *28*(9), 2076–2079. doi:10.1038/nm1636.Mutational

Caton, A. J., Brownlee, G. G., Yewdell, J. W., & Gerhard, W. (1982). The antigenic structure of the influenza virus A/PR/8/34 hemagglutinin (H1 subtype). *Cell*, *31*(2 PART 1), 417–427. doi:10.1016/0092-8674(82)90135-0

Cauldwell, A. V., Long, J. S., Moncorgé, O., & Barclay, W. S. (2014). Viral determinants of influenza A virus host range. *Journal of General Virology*, *95*(Pt_6), 1193–1210. doi:10.1099/vir.0.062836-0

Cerwenka, A., Morgan, T. M., & Dutton, R. W. (1999). Naive, effector, and memory CD8 T cells in protection against pulmonary influenza virus infection: homing properties rather than initial frequencies are crucial. *Journal of immunology (Baltimore, Md. : 1950)*, *163*(10), 5535–43. http://www.ncbi.nlm.nih.gov/pubmed/10553081. Accessed 26 September 2017

Chaipan, C., Kobasa, D., Bertram, S., Glowacka, I., Steffen, I., Tsegaye, T. S., et al. (2009). Proteolytic activation of the 1918 influenza virus hemagglutinin. *Journal of virology*, *83*(7), 3200–11. doi:10.1128/JVI.02205-08

Chakraverty, P. (1980). Comparison of haemagglutination-inhibition and single-radial-haemolysis

techniques for detection of antibodies to influenza B virus. *Archives of virology*, *63*(3–4), 285–9. http://www.ncbi.nlm.nih.gov/pubmed/6986861. Accessed 27 June 2017

Changsom, D., Lerdsamran, H., Wiriyarat, W., Chakritbudsabong, W., Siridechadilok, B., Prasertsopon, J., et al. (2016). Influenza Neuraminidase Subtype N1: Immunobiological Properties and Functional Assays for Specific Antibody Response. *PLOS ONE*, *11*(4), e0153183. doi:10.1371/journal.pone.0153183

Chen, B. J., Leser, G. P., Jackson, D., & Lamb, R. A. (2008). The Influenza Virus M2 Protein Cytoplasmic Tail Interacts with the M1 Protein and Influences Virus Assembly at the Site of Virus Budding. *Journal of Virology*, *82*(20), 10059–10070. doi:10.1128/JVI.01184-08

Chen, B. J., Leser, G. P., Morita, E., & Lamb, R. A. (2007). Influenza Virus Hemagglutinin and Neuraminidase, but Not the Matrix Protein, Are Required for Assembly and Budding of Plasmid-Derived Virus-Like Particles. *Journal of Virology*, *81*(13), 7111–7123. doi:10.1128/JVI.00361-07

Chen, C.-J., Ermler, M. E., Tan, G. S., Krammer, F., Palese, P., & Hai, R. (2016). Influenza A viruses expressing intra- or inter-group chimeric hemagglutinins. *Journal of Virology*, *90*(January), JVI.03060-15. doi:10.1128/JVI.03060-15

Chen, M. W., Cheng, T. J., Huang, Y., Jan, J. T., Ma, S. H., Yu, A. L., et al. (2008). A consensus-hemagglutinin-based DNA vaccine that protects mice against divergent H5N1 influenza viruses. *Proc Natl Acad Sci U S A*, *105*(36), 13538–13543. doi:10.1073/pnas.0806901105

Chen, M. W., Liao, H. Y., Huang, Y., Jan, J. T., Huang, C. C., Ren, C.-T., et al. (2011). Broadly neutralizing DNA vaccine with specific mutation alters the antigenicity and sugar-binding activities of influenza hemagglutinin. *Proceedings of the National Academy of Sciences*, *108*(9), 3510–3515. doi:10.1073/pnas.1019744108

Chen, W., Calvo, P. A., Malide, D., Gibbs, J., Schubert, U., Bacik, I., et al. (2001). A novel influenza A virus mitochondrial protein that induces cell death. *Nature Medicine*, *7*(12), 1306–1312. doi:10.1038/nm1201-1306

Cheng, A., Wong, S. M., & Yuan, Y. A. (2009). Structural basis for dsRNA recognition by NS1 protein of influenza A virus. *Cell Research*, *19*(2), 187–195. doi:10.1038/cr.2008.288

Cheresiz, S. V., Kononova, A. A., Razumova, Y. V., Dubich, T. S., Chepurnov, A. A., Kushch, A. A., et al. (2014). A vesicular stomatitis pseudovirus expressing the surface glycoproteins of influenza A virus. *Archives of Virology*, *159*(10), 2651–2658. doi:10.1007/s00705-014-2127-y

Ciampor, F., Thompson, C. A., Grambas, S., & Hay, A. J. (1992). Regulation of pH by the M2 protein of influenza A viruses. *Virus Research*, *22*(3), 247–258. doi:10.1016/0168-1702(92)90056-F

Cohen, M., Zhang, X.-Q., Senaati, H. P., Chen, H.-W., Varki, N. M., Schooley, R. T., & Gagneux, P. (2013). Influenza A penetrates host mucus by cleaving sialic acids with neuraminidase. *Virology Journal*, *10*(1), 321. doi:10.1186/1743-422X-10-321

Colman, P. M. (1994). Influenza virus neuraminidase: Structure, antibodies, and inhibitors. *Protein Science*, *3*(10), 1687–1696. doi:10.1002/pro.5560031007

Colman, P. M., Varghese, J. N., & Laver, W. G. (1983). Structure of the catalytic and antigenic sites in influenza virus neuraminidase. *Nature*, *303*(5912), 41–44. doi:10.1038/303041a0

Corti, D., Suguitan, A. L., Pinna, D., Silacci, C., Fernandez-Rodriguez, B. M., Vanzetta, F., et al. (2010). Heterosubtypic neutralizing antibodies are produced by individuals immunized with a seasonal influenza vaccine. *Journal of Clinical Investigation*, *120*(5), 1663–1673. doi:10.1172/JCI41902DS1

Corti, D., Voss, J., Gamblin, S. J., Codoni, G., Macagno, A., Jarrossay, D., et al. (2011). A Neutralizing Antibody Selected from Plasma Cells That Binds to Group 1 and Group 2 Influenza A Hemagglutinins. *Science*, *333*(6044), 850–6. doi:10.1126/science.1205669

Couzens, L., Gao, J., Westgeest, K. B., Sandbulte, M. R., Lugovtsev, V. Y., Fouchier, R. A. M., & Eichelberger, M. C. (2014). An optimized enzyme-linked lectin assay to measure influenza A virus neuraminidase inhibition antibody titers in human sera. *Journal of Virological Methods*, *210*, 7–14. doi:10.1016/j.jviromet.2014.09.003

Cox, R. J. (2013). Correlates of protection to influenza virus, where do we go from here? *Human Vaccines and Immunotherapeutics*, *9*(2), 405–408. doi:10.4161/hv.2290

Cox, R. J., Mykkeltvedt, E., Robertson, J. S., & Haaheim, L. R. (2002). Non-lethal viral challenge of influenza haemagglutinin and nucleoprotein DNA vaccinated mice results in reduced viral replication. *Scandinavian Journal of Immunology*, *55*(1), 14–23. doi:10.1046/j.1365-3083.2002.01015.x

Davey, ard T., Dodd, L., Proschan, M. A., Neaton, J., Neuhaus Nordwall, J., Koopmeiners, J. S., et al. (2016). A Randomized, Controlled Trial of ZMapp for Ebola Virus Infection. *N Engl J Med*, *375*, 1448–56. doi:10.1056/NEJMoa1604330

Dawood, F. S., Iuliano, A. D., Reed, C., Meltzer, M. I., Shay, D. K., Cheng, P.-Y., et al. (2012). Estimated global mortality associated with the first 12 months of 2009 pandemic influenza A H1N1 virus circulation: a modelling study. *The Lancet Infectious Diseases*, *12*(9), 687–695. doi:10.1016/S1473-3099(12)70121-4

de Boer, G. F., Back, W., & Osterhaus, A. D. (1990). An ELISA for detection of antibodies against influenza A nucleoprotein in humans and various animal species. *Archives of virology*, *115*(1–2),

47–61. http://www.ncbi.nlm.nih.gov/pubmed/2174233. Accessed 24 August 2017

De Clercq, E. (2004). Antivirals and antiviral strategies. *Nature Reviews Microbiology*, *2*(9), 704–721. doi:10.1038/nrmicro975

De Clercq, E. (2006). Antiviral agents active against influenza A viruses. *Nature reviews. Drug discovery*, *5*(December), 1015–1025. doi:10.1038/nrd2175

de Jong, J. C., Beyer, W. E. P., Palache, A. M., Rimmelzwaan, G. F., & Osterhaus, A. D. (2000). Mismatch between the 1997/1998 influenza vaccine and the major epidemic A(H3N2) virus strain as the cause of an inadequate vaccine-induced antibody response to this strain in the elderly. *Journal of Medical Virology*, *61*(1), 94–99. doi:10.1002/(SICI)1096-9071(200005)61:1<94::AID-JMV15>3.0.CO;2-C

de Jong, J. C., Palache, A. M., Beyer, W. E. P., Rimmelzwaan, G. F., Boon, A., & Osterhaus, A. D. (2003). Haemagglutination-inhibiting antibody to influenza virus. *Dev Biol (Basel)*, 63–73.

de St.Groth, F., & Webster, R. G. (1966a). Disquisitions on Original Antigenic Sin: Ii. Proof in Lower Creatures. *Journal of Experimental Medicine*, *124*(3), 347–361. doi:10.1084/jem.124.3.347

de St.Groth, F., & Webster, R. G. (1966b). Disquisition on original antigenic sin. I. Evidence in man. *J.Exp.Med.*, *124*(3), 331–345. http://www.ncbi.nlm.nih.gov/pubmed/5922742. Accessed 26 September 2017

Demaison, C., Parsley, K., Brouns, G., Scherr, M., Battmer, K., Kinnon, C., et al. (2002). High-level transduction and gene expression in hematopoietic repopulating cells using a human immunodeficiency [correction of imunodeficiency] virus type 1-based lentiviral vector containing an internal spleen focus forming virus promoter. *Human gene therapy*, *13*(7), 803–813. doi:10.1089/10430340252898984

Desai, T. M., Marin, M., Chin, C. R., Savidis, G., Brass, A. L., & Melikyan, G. B. (2014). IFITM3 Restricts Influenza A Virus Entry by Blocking the Formation of Fusion Pores following Virus-Endosome Hemifusion. *PLoS Pathogens*, *10*(4), e1004048. doi:10.1371/journal.ppat.1004048

Di Pietro, A., Kajaste-Rudnitski, A., Oteiza, A., Nicora, L., Towers, G. J., Mechti, N., & Vicenzi, E. (2013). TRIM22 inhibits influenza A virus infection by targeting the viral nucleoprotein for degradation. *J Virol*, *87*(8), 4523–4533. doi:10.1128/JVI.02548-12

Dias, A., Bouvier, D., Crepin, T., McCarthy, A. A., Hart, D. J., Baudin, F., et al. (2009). The cap-snatching endonuclease of influenza virus polymerase resides in the PA subunit. *Nature*, *458*(7240), 914–918. doi:10.1038/nature07745

Diebold, S. S., Kaisho, T., Hemmi, H., Akira, S., & Reis e Sousa, C. (2004). Innate Antiviral Responses by Means of TLR7-Mediated Recognition of Single-Stranded RNA. *Science*, *303*(5663), 1529–

1531. doi:10.1126/science.1093616

DiLillo, D. J., Tan, G. S., Palese, P., & Ravetch, J. V. (2014). Broadly neutralizing hemagglutinin stalk-specific antibodies require FcγR interactions for protection against influenza virus in vivo. *Nature medicine*, *20*(2), 143–51. doi:10.1038/nm.3443

Ding, H., Tsai, C., Zhou, F., Buchy, P., Deubel, V., & Zhou, P. (2011). Heterosubtypic antibody response elicited with seasonal influenza vaccine correlates partial protection against highly pathogenic H5N1 virus. *PLoS ONE*, *6*(3), e17821. doi:10.1371/journal.pone.0017821

Doms, R. W., Lamb, R. A., Rose, J. K., & Helenius, A. (1993). Folding and assembly of viral membrane proteins. *Virology*. doi:10.1006/viro.1993.1164

Dos Santos, G., Neumeier, E., & Bekkat-Berkani, R. (2016). Influenza: Can we cope better with the unpredictable? *Human Vaccines and Immunotherapeutics*, *12*(3), 699–708. doi:10.1080/21645515.2015.1086047

Dreyfus, C., Laursen, N. S., Kwaks, T., Zuijdgeest, D., Khayat, R., Ekiert, D. C., et al. (2013). Highly Conserved Protective Epitopes on Influenza B Viruses, *337*(6100), 1343–1348. doi:10.1126/science.1222908.Highly

Du, L., Zhao, G., Zhang, X., Liu, Z., Yu, H., Zheng, B. J., et al. (2010). Development of a safe and convenient neutralization assay for rapid screening of influenza HA-specific neutralizing monoclonal antibodies. *Biochemical and Biophysical Research Communications*, *397*(3), 580–585. doi:10.1016/j.bbrc.2010.05.161

Du, L., Zhou, Y., & Jiang, S. (2010). Research and development of universal influenza vaccines. *Microbes and Infection*, *12*(4), 280–286. doi:10.1016/j.micinf.2010.01.001

Du, N., Zhou, J., Lin, X., Zhang, Y., Yang, X., Wang, Y., & Shu, Y. (2010). Differential activation of NK cells by influenza A pseudotype H5N1 and 1918 and 2009 pandemic H1N1 viruses. *J Virol*, *84*(15), 7822–7831. doi:10.1128/JVI.00069-10

DuBois, R. M., Aguilar-Yañez, J. M., Mendoza-Ochoa, G. I., Oropeza-Almazán, Y., Schultz-Cherry, S., Alvarez, M. M., et al. (2011). The receptor-binding domain of influenza virus hemagglutinin produced in Escherichia coli folds into its native, immunogenic structure. *Journal of virology*, *85*(2), 865–72. doi:10.1128/JVI.01412-10

Dukes, J. D., Whitley, P., Chalmers, A. D., Gaush, C., Hard, W., Smith, T., et al. (2011). The MDCK variety pack: choosing the right strain. *BMC Cell Biology*, *12*(1), 43. doi:10.1186/1471-2121-12-43

Ebrahimi, K. H., & West, G. M. (2014). Mass Spectrometry Approach and ELISA Reveal the Effect of Codon Optimization on N-Linked Glycosylation of HIV-1 gp120.

Edwards, M. J., & Dimmock, N. J. (2001). Hemagglutinin 1-specific immunoglobulin G and Fab molecules mediate postattachment neutralization of influenza A virus by inhibition of an early fusion event. *Journal of virology*, *75*(21), 10208–10218. doi:10.1128/JVI.75.21.10208-10218.2001

Eggink, D., Goff, P. H., & Palese, P. (2014). Guiding the Immune Response against Influenza Virus Hemagglutinin toward the Conserved Stalk Domain by Hyperglycosylation of the Globular Head Domain. *Journal of virology*, *88*(1), 699–704. doi:10.1128/JVI.02608-13

Eichelberger, M. C., Couzens, L., Gao, Y., Levine, M., Katz, J. M., Wagner, R., et al. (2016). Comparability of neuraminidase inhibition antibody titers measured by enzyme-linked lectin assay (ELLA) for the analysis of influenza vaccine immunogenicity. *Vaccine*, *34*(4), 458–465. doi:10.1016/j.vaccine.2015.12.022

Eichelberger, M. C., & Wan, H. (2014). Influenza Neuraminidase as a Vaccine Antigen. In *Current topics in microbiology and immunology* (Vol. 386, pp. 275–299). doi:10.1007/82_2014_398

Eisfeld, A. J., Neumann, G., & Kawaoka, Y. (2014). At the centre : influenza A virus ribonucleoproteins. *Nature Publishing Group*, (November). doi:10.1038/nrmicro3367

Ekiert, D. C., Bhabha, G., Elsliger, M., Friesen, R. H. E., Jongeneelen, M., Throsby, M., et al. (2009). Antibody recognition of a highly conserved influenza virus epitope : implications for universal prevention and therapy. *Science*, *324*(5924), 246–251. doi:10.1126/science.1171491.Antibody

Ekiert, D. C., Friesen, R. H. E., Bhabha, G., Kwaks, T., Yu, W., Ophorst, C., et al. (2012). A Highly Conserved Neutralizing Epitope on Group 2 Influenza A Viruses. *Science*, *333*(6044), 843–850. doi:10.1126/science.1204839.A

Ellebedy, A. H., & Ahmed, R. (2012). Re-engaging cross-reactive memory B cells: The influenza puzzle. *Frontiers in Immunology*, *3*(MAR), 53. doi:10.3389/fimmu.2012.00053

EMA. (2010). Report from scientific workshop on serology assays and correlates of protection for influenza vaccines. http://www.ema.europa.eu/docs/en_GB/document_library/Report/2010/12/WC500100205.pdf. Accessed 12 June 2017

Engelman, A., & Cherepanov, P. (2012). The structural biology of HIV-1: mechanistic and therapeutic insights. *Nature reviews. Microbiology*, *10*(4), 279–90. doi:10.1038/nrmicro2747

Ermler, M. E., Kirkpatrick, E., Sun, W., Hai, R., Amanat, F., Chromikova, V., & Krammer, F. (2017). Chimeric Hemagglutinin Constructs Induce Broad Protection against Influenza B Virus Challenge in the Mouse Model. *J. Virol.*, *91*(12), 1–14. doi:10.1128/JVI.00286-17

Estmer Nilsson, C., Abbas, S., Bennemo, M., Larsson, A., Hämäläinen, M. D., & Frostell-Karlsson, Å.

(2010). A novel assay for influenza virus quantification using surface plasmon resonance. *Vaccine*, *28*(3), 759–766. doi:10.1016/j.vaccine.2009.10.070

Farazmandfar, T., Shahreza, H. K., Haghshenas, M. R., Janbabai, G., Azadeh, H., & Samaei, N. M. (2012). Use of integrase-minus lentiviral vector for transient expression. *Cell Journal*, *14*(2), 76–81.

Farrell, K. B., Ting, Y.-T., & Eiden, M. V. (2002). Fusion-Defective Gibbon Ape Leukemia Virus Vectors Can Be Rescued by Homologous but Not Heterologous Soluble Envelope Proteins. *Journal of Virology*, *76*(9), 4267–4274. doi:10.1128/JVI.76.9.4267-4274.2002

Fechter, P., & Brownlee, G. G. (2005). Recognition of mRNA cap structures by viral and cellular proteins. *Journal of General Virology*, *86*(5), 1239–1249. doi:10.1099/vir.0.80755-0

Fereidouni, S., Kwasnitschka, L., Balkema Buschmann, A., Müller, T., Freuling, C., Schatz, J., et al. (2015). No virological evidence for an influenza A - like virus in European bats. *Zoonoses and Public Health*, *62*(3), 187–189. doi:10.1111/zph.12131

Ferrara, F. (2015). *USING PSEUDOTYPES TO STUDY HETEROSUBTYPIC ANTIBODY RESPONSES ELICITED BY SEASONAL INFLUENZA VACCINATION - PhD Thesis*.

Ferrara, F., Molesti, E., Böttcher-Friebertshäuser, E., Cattoli, G., Corti, D., Scott, S. D., & Temperton, N. J. (2012). The human Transmembrane Protease Serine 2 is necessary for the production of Group 2 influenza A virus pseudotypes. *Journal of molecular and genetic medicine : an international journal of biomedical research*, *7*, 309–14. http://www.pubmedcentral.nih.gov/articlerender.fcgi?artid=3614188&tool=pmcentrez&rendertype=abstract

Finkelshtein, D., Werman, A., Novick, D., Barak, S., & Rubinstein, M. (2013). LDL receptor and its family members serve as the cellular receptors for vesicular stomatitis virus. *Proceedings of the National Academy of Sciences of the United States of America*, *110*(18), 7306–11. doi:10.1073/pnas.1214441110

Fodor, E. (2013). The RNA polymerase of influenza a virus: mechanisms of viral transcription and replication. *Acta virologica*, *57*(2), 113–22. http://www.ncbi.nlm.nih.gov/pubmed/23600869. Accessed 25 September 2017

Fouchier, R. A. M., Munster, V. J., Wallensten, A., Bestebroer, T. M., Herfst, S., Smith, D. J., et al. (2005). Characterization of a Novel Influenza A Virus Hemagglutinin Subtype (H16) Obtained from Black-Headed Gulls Characterization of a Novel Influenza A Virus Hemagglutinin Subtype (H16) Obtained from Black-Headed Gulls. *J. Virol.*, *79*(5), 2814–2822. doi:10.1128/JVI.79.5.2814

Francis, T. J. (1960). On the Doctrine of Original Antigenic Sin. *Proceedings of the American*

Philosophical Society. American Philosophical Society. doi:10.2307/985534

Freidl, G. S., Binger, T., Müller, M. A., De Bruin, E., Van Beek, J., Corman, V. M., et al. (2015). Serological evidence of influenza a viruses in frugivorous bats from Africa. *PLoS ONE*, *10*(5), 1–7. doi:10.1371/journal.pone.0127035

Friesen, R. H. E., Koudstaal, W., Koldijk, M. H., Weverling, G. J., Brakenhoff, J. P. J., Lenting, P. J., et al. (2010). New class of monoclonal antibodies against severe influenza: Prophylactic and therapeutic efficacy in ferrets. *PLoS ONE*, *5*(2), 1–7. doi:10.1371/journal.pone.0009106

Fritz, R., Sabarth, N., Kiermayr, S., Hohenadl, C., Howard, M. K., Ilk, R., et al. (2012). A Vero Cell-Derived Whole-Virus H5N1 Vaccine Effectively Induces Neuraminidase-Inhibiting Antibodies. *Journal of Infectious Diseases*, *205*(1), 28–34. doi:10.1093/infdis/jir711

Gack, M. U., Albrecht, R. A., Urano, T., Inn, K.-S., Huang, I. C., Carnero, E., et al. (2009). Influenza A Virus NS1 Targets the Ubiquitin Ligase TRIM25 to Evade Recognition by the Host Viral RNA Sensor RIG-I. *Cell Host & Microbe*, *5*(5), 439–449. doi:10.1016/j.chom.2009.04.006

Gaiotto, T., & Hufton, S. E. (2016). Cross-neutralising nanobodies bind to a conserved pocket in the hemagglutinin stem region identified using yeast display and deep mutational scanning. *PLoS ONE*, *11*(10), 1–27. doi:10.1371/journal.pone.0164296

Gao, J., Couzens, L., & Eichelberger, M. C. (2016). Measuring Influenza Neuraminidase Inhibition Antibody Titers by Enzyme-linked Lectin Assay. *Journal of visualized experiments : JoVE*, (115). doi:10.3791/54573

García-Sastre, A. (2012). The neuraminidase of bat influenza viruses is not a neuraminidase. *Proc Natl Acad Sci U S A*, *109*(46), 18635–18636. doi:10.1073/pnas.1215857109

García-Sastre, A., Egorov, A., Matassov, D., Brandt, S., Levy, D. E., Durbin, J. E., et al. (1998). Influenza A virus lacking the NS1 gene replicates in interferon-deficient systems. *Virology*, *252*(2), 324–30. http://www.ncbi.nlm.nih.gov/pubmed/9878611. Accessed 25 September 2017

Garcia, J. M., Gao, A., He, P.-L., Choi, J., Tang, W., Bruzzone, R., et al. (2009). High-throughput screening using pseudotyped lentiviral particles: A strategy for the identification of HIV-1 inhibitors in a cell-based assay. *Antiviral Research*, *81*, 239–247. doi:10.1016/j.antiviral.2008.12.004

Garcia, J. M., Lagarde, N., Ma, E. S. K., de Jong, M. D., & Peiris, J. S. M. (2010). Optimization and evaluation of an influenza A (H5) pseudotyped lentiviral particle-based serological assay. *Journal of Clinical Virology*, *47*(1), 29–33. doi:10.1016/j.jcv.2009.10.009

Garcia, J. M., & Lai, J. C. C. (2011). Production of influenza pseudotyped lentiviral particles and their use in influenza research and diagnosis: an update. *Expert review of anti-infective therapy*, *9*(4),

443–455. doi:10.1586/eri.11.25

Garcia, J. M., Pepin, S., Lagarde, N., Ma, E. S. K., Vogel, F. R., Chan, K. H., et al. (2009). Heterosubtype neutralizing responses to influenza A (H5N1) viruses are mediated by antibodies to virus haemagglutinin. *PLoS ONE*, *4*(11), 1–6. doi:10.1371/journal.pone.0007918

Garten, R. J., Davis, C. T., Russell, C. A., Shu, B., Lindstrom, S., Balish, A., et al. (2009). Antigenic and genetic characteristics of swine-origin 2009 A(H1N1) influenza viruses circulating in humans. *Science (New York, N.Y.)*, *325*(5937), 197–201. doi:10.1126/science.1176225

Gibson, D. G., Young, L., Chuang, R.-Y., Venter, J. C., Hutchison, C. a, Smith, H. O., et al. (2009). Enzymatic assembly of DNA molecules up to several hundred kilobases. *Nature methods*, *6*(5), 343–5. doi:10.1038/nmeth.1318

Glezen, W. P. (2004). Cold-adapted , live attenuated influenza vaccine, 131–139.

Glezen, W. P., Schmier, J. K., Kuehn, C. M., Ryan, K. J., & Oxford, J. (2013). The burden of influenza B: A structured literature review. *American Journal of Public Health*, *103*(3), 43–51. doi:10.2105/AJPH.2012.301137

Gómez-Puertas, P., Albo, C., Pérez-Pastrana, E., Vivo, a, & Portela, a. (2000). Influenza virus matrix protein is the major driving force in virus budding. *Journal of virology*, *74*(24), 11538–11547. doi:10.1128/JVI.74.24.11538-11547.2000

Gorai, T., Goto, H., Noda, T., Watanabe, T., Kozuka-Hata, H., Oyama, M., et al. (2012). F1Fo-ATPase, F-type proton-translocating ATPase, at the plasma membrane is critical for efficient influenza virus budding. *Proceedings of the National Academy of Sciences of the United States of America*, *109*(12), 4615–20. doi:10.1073/pnas.1114728109

Gorres, J. P., Lager, K. M., Kong, W.-P., Royals, M., Todd, J. P., Vincent, A. L., et al. (2011). DNA vaccination elicits protective immune responses against pandemic and classic swine influenza viruses in pigs. *Clinical and Vaccine Immunology*, *18*(11), 1987–1995. doi:10.1128/CVI.05171-11

Graham, B. S. (n.d.). *Universal Influenza Vaccines*. http://www.who.int/immunization/research/meetings_workshops/23_Universal_flu.pdf. Accessed 14 August 2017

Graves, P. N., Schulman, J. L., Young, J. F., & Palese, P. (1983). Preparation of influenza virus subviral particles lacking the HA1 subunit of hemagglutinin: Unmasking of cross-reactive HA2 determinants. *Virology*, *126*(1), 106–116. doi:10.1016/0042-6822(83)90465-8

Greenberg, S. B., Criswell, B. S., Six, H. R., & Couch, R. B. (1978). Lymphocyte cytotoxicity to influenza virus-infected cells: response to vaccination and virus infection. *Infection and immunity*, *20*(3), 640–5. http://www.ncbi.nlm.nih.gov/pubmed/669816. Accessed 24 August 2017

Guilligay, D., Tarendeau, F., Resa-Infante, P., Coloma, R., Crepin, T., Sehr, P., et al. (2008). The structural basis for cap binding by influenza virus polymerase subunit PB2. *Nature Structural & Molecular Biology*, *15*(5), 500–506. doi:10.1038/nsmb.1421

Guillot, L., Le Goffic, R., Bloch, S., Escriou, N., Akira, S., Chignard, M., & Si-Tahar, M. (2005). Involvement of Toll-like Receptor 3 in the Immune Response of Lung Epithelial Cells to Double-stranded RNA and Influenza A Virus. *Journal of Biological Chemistry*, *280*(7), 5571–5580. doi:10.1074/jbc.M410592200

Gulati, S., Smith, D. F., Cummings, R. D., Couch, R. B., Griesemer, S. B., St, K., et al. (2013). Human H3N2 Influenza Viruses Isolated from 1968 To 2012 Show Varying Preference for Receptor Substructures with No Apparent Consequences for Disease or Spread, *8*(6). doi:10.1371/journal.pone.0066325

Hai, R., Krammer, F., Tan, G. S., Pica, N., Eggink, D., Maamary, J., et al. (2012). Influenza Viruses Expressing Chimeric Hemagglutinins: Globular Head and Stalk Domains Derived from Different Subtypes. *Journal of Virology*, *86*(10), 5774–5781. doi:10.1128/JVI.00137-12

Hale, B. G., Randall, R. E., Ortin, J., & Jackson, D. (2008). The multifunctional NS1 protein of influenza A viruses. *Journal of General Virology*, *89*(10), 2359–2376. doi:10.1099/vir.0.2008/004606-0

Hall, T. (1999). BioEdit: a user-friendly biological sequence alignment editor and analysis program for Windows 95/98/NT. *Nucleic Acids Symposium Series*. doi:citeulike-article-id:691774

Haller, O., Staeheli, P., & Kochs, G. (2009). Protective role of interferon-induced Mx GTPases against influenza viruses. *Revue scientifique et technique (International Office of Epizootics)*, *28*(1), 219–31. http://www.ncbi.nlm.nih.gov/pubmed/19618628. Accessed 26 September 2017

Hanika, A., Larisch, B., Steinmann, E., Schwegmann-Weßels, C., Herrler, G., & Zimmer, G. (2005). Use of influenza C virus glycoprotein HEF for generation of vesicular stomatitis virus pseudotypes. *Journal of General Virology*, *86*(5), 1455–1465. doi:10.1099/vir.0.80788-0

Harris, A., Cardone, G., Winkler, D. C., Heymann, J. B., Brecher, M., White, J. M., & Steven, A. C. (2006). Influenza virus pleiomorphy characterized by cryoelectron tomography. *Proceedings of the National Academy of Sciences*, *103*(50), 19123–19127. doi:10.1073/pnas.0607614103

Harris, A. K., Meyerson, J. R., Matsuoka, Y., Kuybeda, O., Moran, A., Bliss, D., et al. (2013). Structure and accessibility of HA trimers on intact 2009 H1N1 pandemic influenza virus to stem region-specific neutralizing antibodies. *Proceedings of the National Academy of Sciences of the United States of America*, *110*(12), 4592–7. doi:10.1073/pnas.1214913110

Hartley, J. W., Rowe, W. P., & Huebner, R. J. (1970). Host-range restrictions of murine leukemia viruses in mouse embryo cell cultures. *Journal of virology*, *5*(2), 221–225.

Hashem, A. M., Gravel, C., Farnsworth, A., Zou, W., Lemieux, M., Xu, K., et al. (2013). A Novel Synthetic Receptor-Based Immunoassay for Influenza Vaccine Quantification. *PLoS ONE*, *8*(2), e55428. doi:10.1371/journal.pone.0055428

Hashem, A. M., Van Domselaar, G., Li, C., Wang, J., She, Y. M., Cyr, T. D., et al. (2010). Universal antibodies against the highly conserved influenza fusion peptide cross-neutralize several subtypes of influenza A virus. *Biochemical and Biophysical Research Communications*, *403*(2), 247–251. doi:10.1016/j.bbrc.2010.11.030

Hashimoto, G., Wright, P. F., & Karzon, D. T. (1983a). Antibody-dependent cell-mediated cytotoxicity against influenza virus-infected cells. *The Journal of infectious diseases*, *148*(5), 785–94. http://www.ncbi.nlm.nih.gov/pubmed/6605395. Accessed 24 August 2017

Hashimoto, G., Wright, P. F., & Karzon, D. T. (1983b). Ability of human cord blood lymphocytes to mediate antibody-dependent cellular cytotoxicity against influenza virus-infected cells. *Infection and immunity*, *42*(1), 214–8. http://www.ncbi.nlm.nih.gov/pubmed/6604697. Accessed 24 August 2017

Hashimoto, Y., Moki, T., Takizawa, T., Shiratsuchi, A., & Nakanishi, Y. (2007). Evidence for phagocytosis of influenza virus-infected, apoptotic cells by neutrophils and macrophages in mice. *Journal of immunology (Baltimore, Md. : 1950)*, *178*(4), 2448–57. http://www.ncbi.nlm.nih.gov/pubmed/17277152. Accessed 26 September 2017

Hassantoufighi, A., Zhang, H., Sandbulte, M. R., Gao, J., Manischewitz, J., King, L. R., et al. (2010). A practical influenza neutralization assay to simultaneously quantify hemagglutinin and neuraminidase-inhibiting antibody responses. *Vaccine*, *28*(3), 790–797. doi:10.1016/j.vaccine.2009.10.066

Hatziioannou, T., Delahaye, E., Martin, F., Russell, S. J., & Cosset, F. L. (1999). Retroviral display of functional binding domains fused to the amino terminus of influenza hemagglutinin. *Human gene therapy*, *10*, 1533–1544. doi:10.1089/10430349950017860

Hatziioannou, T., Valsesia-Wittmann, S., Russell, S. J., & Cosset, F. L. (1998). Incorporation of fowl plague virus hemagglutinin into murine leukemia virus particles and analysis of the infectivity of the pseudotyped retroviruses. *Journal of virology*, *72*(6), 5313–7. http://www.pubmedcentral.nih.gov/articlerender.fcgi?artid=116395&tool=pmcentrez&rendertype=abstract

Hause, B. M., Collin, E. A., Liu, R., Huang, B., Sheng, Z., Lu, W., et al. (2014). Characterization of a novel influenza virus in cattle and swine: Proposal for a new genus in the Orthomyxoviridae family. *mBio*, *5*(2), 1–10. doi:10.1128/mBio.00031-14

Haye, K., Burmakina, S., Moran, T. M., García-Sastre, A., & Fernandez-Sesma, A. (2009). The NS1

protein of a human influenza virus inhibits type I interferon production and the induction of antiviral responses in primary human dendritic and respiratory epithelial cells. *Journal of virology*, *83*(13), 6849–62. doi:10.1128/JVI.02323-08

Haynes, J. R., Dokken, L., Wiley, J. A., Cawthon, A. G., Bigger, J., Harmsen, A. G., & Richardson, C. (2009). Influenza-pseudotyped Gag virus-like particle vaccines provide broad protection against highly pathogenic avian influenza challenge. *Vaccine*, *27*(4), 530–541. doi:10.1016/j.vaccine.2008.11.011

He, X.-S., Draghi, M., Mahmood, K., Holmes, T. H., Kemble, G. W., Dekker, C. L., et al. (2004). T cell–dependent production of IFN-γ by NK cells in response to influenza A virus. *Journal of Clinical Investigation*, *114*(12), 1812–1819. doi:10.1172/JCI22797

Hefti, H. P., Frese, M., Landis, H., Di Paolo, C., Aguzzi, A., Haller, O., & Pavlovic, J. (1999). Human MxA protein protects mice lacking a functional alpha/beta interferon system against La crosse virus and other lethal viral infections. *Journal of virology*, *73*(8), 6984–91. http://www.ncbi.nlm.nih.gov/pubmed/10400797. Accessed 26 September 2017

Heikkinen, T., Ikonen, N., & Ziegler, T. (2014). Impact of influenza B lineage-level mismatch between trivalent seasonal influenza vaccines and circulating viruses, 1999-2012. *Clinical Infectious Diseases*, *59*(11), 1519–1524. doi:10.1093/cid/ciu664

Heil, F., Hemmi, H., Hochrein, H., Ampenberger, F., Kirschning, C., Akira, S., et al. (2004). Species-Specific Recognition of Single-Stranded RNA via Toll-like Receptor 7 and 8. *Science*, *303*(5663), 1526–1529. doi:10.1126/science.1093620

Herlocher, L. M., Carr, J., Ives, J., Elias, S., Truscon, R., Roberts, N. A., & Monto, A. S. (2002). Influenza virus carrying an R292K mutation in the neuraminidase gene is not transmitted in ferrets. *Antiviral research*, *54*(2), 99–111. http://www.ncbi.nlm.nih.gov/pubmed/12062395. Accessed 23 August 2017

Herlocher, L. M., Truscon, R., Elias, S., Yen, H., Roberts, N. A., Ohmit, S. E., & Monto, A. S. (2004). Influenza Viruses Resistant to the Antiviral Drug Oseltamivir: Transmission Studies in Ferrets. *The Journal of Infectious Diseases*, *190*(9), 1627–1630. doi:10.1086/424572

Hirst, G. K. (1941). THE AGGLUTINATION OF RED CELLS BY ALLANTOIC FLUID OF CHICK EMBRYOS INFECTED WITH INFLUENZA VIRUS. *Science*, *94*(2427), 22–23. doi:10.1126/science.94.2427.22

Hoa, L. N. M., Mai, L. Q., Bryant, J. E., Thai, P. Q., Hang, N. L. K., Yen, N. T. T., et al. (2016). Association between HA stem-reactive antibodies and influenza A/H1N1 infection during the 2009 pandemic. *Journal of Virology*, *90*(May), JVI.00093-16. doi:10.1128/JVI.00093-16

Hobson, D., Curry, R. L., Beare, A. S., Ward-Gardner, A., & Refinery, E. (1972). The role of serum

haemagglutination-inhibiting antibody in protection against challenge infection with influenza A2 and B viruses. *The Journal of hygiene*, *70*(4), 767–77. doi:10.1017/S0022172400022610

Hoffmann, M., Krüger, N., Zmora, P., Wrensch, F., Herrler, G., & Pöhlmann, S. (2016). The hemagglutinin of bat-associated influenza viruses is activated by TMPRSS2 for pH-dependent entry into bat but not human cells. *PLoS ONE*, *11*(3), 1–18. doi:10.1371/journal.pone.0152134

Hoffmann, T. W., Munier, S., Larcher, T., Soubieux, D., Ledevin, M., Esnault, E., et al. (2012). Length variations in the NA stalk of an H7N1 influenza virus have opposite effects on viral excretion in chickens and ducks. *Journal of virology*, *86*(1), 584–8. doi:10.1128/JVI.05474-11

Hofmann, C., Sandig, V., Jennings, G., Rudolph, M., Schlag, P., & Strauss, M. (1995). Efficient gene transfer into human hepatocytes by baculovirus vectors. *Proc Natl Acad Sci U S A*, *92*(22), 10099–10103. doi:10.1073/pnas.92.22.10099

Holsinger, L. J., Nichani, D., Pinto, L. H., & Lamb, R. A. (1994). Influenza A virus M2 ion channel protein: a structure-function analysis. *Journal of virology*, *68*(3), 1551–63. http://www.pubmedcentral.nih.gov/articlerender.fcgi?artid=236612&tool=pmcentrez&rendertype=abstract

Honda, K., Ohba, Y., Yanai, H., Negishi, H., Mizutani, T., Takaoka, A., et al. (2005). Spatiotemporal regulation of MyD88–IRF-7 signalling for robust type-I interferon induction. *Nature*, *434*(7036), 1035–1040. doi:10.1038/nature03547

Hooper, K. A., & Bloom, J. D. (2013). A Mutant Influenza Virus That Uses an N1 Neuraminidase as the Receptor-Binding Protein. *Journal of Virology*, *87*(23), 12531–12540. doi:10.1128/JVI.01889-13

Hornung, V., Ellegast, J., Kim, S., Brzozka, K., Jung, A., Kato, H., et al. (2006). 5'-Triphosphate RNA Is the Ligand for RIG-I. *Science*, *314*(5801), 994–997. doi:10.1126/science.1132505

Hsueh-Ling, J. O., Kerström, S. Å., Shen, S., Bereczky, S., Karlberg, H., Klingström, J., et al. (2010). An Antibody against a Novel and Conserved Epitope in the Hemagglutinin 1 Subunit Neutralizes Numerous H5N1 Influenza Viruses. *Journal of Virology*, *84*(16), 8275–8286. doi:10.1128/JVI.02593-09

Huang, I. C., Bailey, C. C., Weyer, J. L., Radoshitzky, S. R., Becker, M. M., Chiang, J. J., et al. (2011). Distinct patterns of IFITM-mediated restriction of filoviruses, SARS coronavirus, and influenza A virus. *PLoS Pathogens*, *7*(1). doi:10.1371/journal.ppat.1001258

Huang, I. C., Li, W., Sui, J., Marasco, W. A., Choe, H., & Farzan, M. (2008). Influenza A virus neuraminidase limits viral superinfection. *J Virol*, *82*(10), 4834–4843. doi:10.1128/JVI.00079-08

Huang, K.-Y. Y. A., Li, C. K.-F. F., Clutterbuck, E., Chui, C. S. C., Wilkinson, T. M. a., Gilbert, A., et al. (2014). Virus-specific antibody secreting cell, memory B-cell, and sero-antibody responses in

the human influenza challenge model. *Journal of Infectious Diseases*, *209*(9), 1354–1361. doi:10.1093/infdis/jit650

Hultberg, A., Temperton, N. J., Rosseels, V., Koenders, M., Gonzalez-Pajuelo, M., Schepens, B., et al. (2011). Llama-derived single domain antibodies to build multivalent, superpotent and broadened neutralizing anti-viral molecules. *PLoS ONE*, *6*(4), e17665. doi:10.1371/journal.pone.0017665

Hutchinson, E. C., & Fodor, E. (2013). Transport of the influenza virus genome from nucleus to nucleus. *Viruses*, *5*(10), 2424–2446. doi:10.3390/v5102424

Ichinohe, T., Lee, H. K., Ogura, Y., Flavell, R. A., & Iwasaki, A. (2009). Inflammasome recognition of influenza virus is essential for adaptive immune responses. *The Journal of Experimental Medicine*, *206*(1), 79–87. doi:10.1084/jem.20081667

Imai, M., Kawasaki, K., & Odagiri, T. (2008). Cytoplasmic domain of influenza B virus BM2 protein plays critical roles in production of infectious virus. *Journal of virology*, *82*(2), 728–39. doi:10.1128/JVI.01752-07

Imai, M., Watanabe, S., Ninomiya, A., Obuchi, M., & Odagiri, T. (2004). Influenza B virus BM2 protein is a crucial component for incorporation of viral ribonucleoprotein complex into virions during virus assembly. *Journal of virology*, *78*(20), 11007–11015. doi:10.1128/JVI.78.20.11007-11015.2004

Impagliazzo, A., Milder, F., Kuipers, H., Wagner, M. V., Zhu, X., Hoffman, R. M. B., et al. (2015). A stable trimeric influenza hemagglutinin stem as a broadly protective immunogen. *Science*, *349*(6254), 1301–1306. doi:10.1126/science.aac7263

Inglis, S. C., Barrett, T., Brown, C. M., & Almond, J. W. (1979). The smallest genome RNA segment of influenza virus contains two genes that may overlap. *Proceedings of the National Academy of Sciences of the United States of America*, *76*(8), 3790–4. http://www.ncbi.nlm.nih.gov/pubmed/291039. Accessed 2 October 2017

Iwasaki, A., & Pillai, P. S. (2014). Innate immunity to influenza virus infection. *Nature Reviews Immunology*, *14*(5), 315–328. doi:10.1038/nri3665

Jacks, T., Power, M. D., Masiarz, F. R., Luciw, P. A., Barr, P. J., & Varmus, H. E. (1988). Characterization of ribosomal frameshifting in HIV-1 gag-pol expression. *Nature*, *331*(6153), 280–3. doi:10.1038/331280a0

Jagger, B. W., Wise, H. M., Kash, J. C., Walters, K.-A., Wills, N. M., Xiao, Y.-L., et al. (2012). An overlapping protein-coding region in influenza A virus segment 3 modulates the host response. *Science (New York, N.Y.)*, *337*(6091), 199–204. doi:10.1126/science.1222213

Jegaskanda, S., Vandenberg, K., Laurie, K. L., Loh, L., Kramski, M., Winnall, W. R., et al. (2014). Cross-Reactive Influenza-Specific Antibody-Dependent Cellular Cytotoxicity in Intravenous Immunoglobulin as a Potential Therapeutic Against Emerging Influenza Viruses. *Journal of Infectious Diseases*, *210*(11), 1811–1822. doi:10.1093/infdis/jiu334

Jin, H., Leser, G. P., Zhang, J., & Lamb, R. A. (1997). Influenza virus hemagglutinin and neuraminidase cytoplasmic tails control particle shape. *EMBO Journal*, *16*(6), 1236–1247. doi:10.1093/emboj/16.6.1236

Joyce, M. G., Wheatley, A. K., Thomas, P. V., Chuang, G. Y., Soto, C., Bailer, R. T., et al. (2016). Vaccine-Induced Antibodies that Neutralize Group 1 and Group 2 Influenza A Viruses. *Cell*, *166*(3), 609–623. doi:10.1016/j.cell.2016.06.043

Julkunen, I., Melén, K., Nyqvist, M., Pirhonen, J., Sareneva, T., & Matikainen, S. (2000). Inflammatory responses in influenza A virus infection. *Vaccine*, *19 Suppl 1*, S32-7. http://www.ncbi.nlm.nih.gov/pubmed/11163460. Accessed 26 September 2017

Julkunen, I., Pyhälä, R., & Hovi, T. (1985). Enzyme immunoassay, complement fixation and hemagglutination inhibition tests in the diagnosis of influenza A and B virus infections. Purified hemagglutinin in subtype-specific diagnosis. *Journal of virological methods*, *10*(1), 75–84. http://www.ncbi.nlm.nih.gov/pubmed/3882733. Accessed 27 June 2017

Jung, H., Lee, K. P., Park, S. J., Park, J. H., Jang, Y. S., Choi, S. Y., et al. (2008). TMPRSS4 promotes invasion, migration and metastasis of human tumor cells by facilitating an epithelial-mesenchymal transition. *Oncogene*, *27*(18), 2635–2647. doi:10.1038/sj.onc.1210914

Juozapaitis, M., Aguiar Moreira, E., Mena, I., Giese, S., Riegger, D., Pohlmann, A., et al. (2014). An infectious bat-derived chimeric influenza virus harbouring the entry machinery of an influenza A virus. *Nat Commun*, *5*, 4448. doi:10.1038/ncomms5448

Kamali, A., & Holodniy, M. (2013). Influenza treatment and prophylaxis with neuraminidase inhibitors: A review. *Infection and Drug Resistance*, *6*, 187–198. doi:10.2147/IDR.S36601

Kamlangdee, A., Kingstad-Bakke, B., & Osorio, J. E. (2016). Mosaic H5 Hemagglutinin Provides Broad Humoral and Cellular Immune Responses against Influenza Viruses. *Journal of Virology*, *90*(15), 6771–6783. doi:10.1128/JVI.00730-16

Kanekiyo, M., Wei, C.-J., Yassine, H. M., McTamney, P. M., Boyington, J. C., Whittle, J. R. R., et al. (2013). Self-assembling influenza nanoparticle vaccines elicit broadly neutralizing H1N1 antibodies. *Nature*, *499*(7456), 102–106. doi:10.1038/nature12202

Karageorgopoulos, D. E., Vouloumanou, E. K., Korbila, I. P., Kapaskelis, A., & Falagas, M. E. (2011). Age distribution of cases of 2009 (H1N1) pandemic influenza in comparison with seasonal

influenza. *PLoS ONE*, *6*(7). doi:10.1371/journal.pone.0021690

Kato, H., Sato, S., Yoneyama, M., Yamamoto, M., Uematsu, S., Matsui, K., et al. (2005). Cell Type-Specific Involvement of RIG-I in Antiviral Response. *Immunity*, *23*(1), 19–28. doi:10.1016/j.immuni.2005.04.010

Kendal, A. P., Bozeman, F. M., & Ennis, F. A. (1980). Further studies of the neuraminidase content of inactivated influenza vaccines and the neuraminidase antibody responses after vaccination of immunologically primed and unprimed populations. *Infection and immunity*, *29*(3), 966–71. http://www.ncbi.nlm.nih.gov/pubmed/7429641. Accessed 12 June 2017

Kendal, A. P., & Cate, T. R. (1983). Increased sensitivity and reduced specificity of hemagglutination inhibition tests with ether-treated influenza B/Singapore/222/79. *Journal of Clinical Microbiology*, *18*(4), 930–934. http://www.ncbi.nlm.nih.gov/pubmed/6630472. Accessed 27 June 2017

Khurana, S., King, L. R., Manischewitz, J., Coyle, E. M., & Golding, H. (2014). Novel antibody-independent receptor-binding SPR-based assay for rapid measurement of influenza vaccine potency. *Vaccine*, *32*(19), 2188–2197. doi:10.1016/j.vaccine.2014.02.049

Kilbourne, E. D. (1976). Comparative efficacy of neuraminidase-specific and conventional influenza virus vaccines in induction of antibody to neuraminidase in humans. *The Journal of infectious diseases*, *134*(4), 384–94. http://www.ncbi.nlm.nih.gov/pubmed/789791. Accessed 4 May 2017

Kirchenbaum, G. A., Carter, D. M., & Ross, T. M. (2015). Sequential Infection in Ferrets with Antigenically Distinct Seasonal H1N1 Influenza Boosts Hemagglutinin Stalk-Specific Antibodies. *Journal of Virology*, *90*(2), 1116–1128. doi:10.1128/JVI.02372-15

Klenk, H.-D., & Rott, R. (1988). The Molecular Biology of Influenza Virus Pathogenicity. *Advances in Virus Research*, *34*(C), 247–281. doi:10.1016/S0065-3527(08)60520-5

Klenk, H.-D., Rott, R., Orlich, M., & Blödorn, J. (1975). Activation of influenza A viruses by trypsin treatment. *Virology*, *68*(2), 426–439. doi:10.1016/0042-6822(75)90284-6

Komiya, N., Gu, Y., Kamiya, H., Yahata, Y., Matsui, T., Yasui, Y., & Okabe, N. (2009). Clinical Features of Cases of Influenza A (H1N1)v in Osaka Prefecture, Japan, May 2009. *Eurosurveillance*, *14*(1). http://www.eurosurveillance.org/images/dynamic/EE/V14N29/art19272.pdf. Accessed 22 August 2017

Kong, W.-P., Hood, C., Yang, Z.-Y., Wei, C.-J., Xu, L., García-Sastre, A., et al. (2006). Protective immunity to lethal challenge of the 1918 pandemic influenza virus by vaccination. *Proceedings of the National Academy of Sciences of the United States of America*, *103*(43), 15987–15991. doi:10.1073/pnas.0607564103

Konishi, M., Kawamoto, K., Izumikawa, M., Kuriyama, H., & Yamashita, T. (2008). Gene transfer into guinea pig cochlea using adeno-associated virus vectors. *The journal of gene medicine*, *10*(6), 610–618. doi:10.1002/jgm

Krammer, F. (2016). Novel universal influenza virus vaccine approaches. *Current Opinion in Virology*, *17*, 95–103. doi:10.1016/j.coviro.2016.02.002

Krammer, F., Hai, R., Yondola, M., Tan, G. S., Leyva-Grado, V. H., Ryder, A. B., et al. (2014). Assessment of influenza virus hemagglutinin stalk-based immunity in ferrets. *Journal of virology*, *88*(6), 3432–42. doi:10.1128/JVI.03004-13

Krammer, F., Margine, I., Hai, R., Flood, A., Hirsh, A., Tsvetnitsky, V., et al. (2014). H3 Stalk-Based Chimeric Hemagglutinin Influenza Virus Constructs Protect Mice from H7N9 Challenge. *Journal of Virology*, *88*(4), 2340–2343. doi:10.1128/JVI.03183-13

Krammer, F., & Palese, P. (2013). Influenza virus hemagglutinin stalk-based antibodies and vaccines. *Current Opinion in Virology*, *3*(5), 521–530. doi:10.1016/j.coviro.2013.07.007

Krammer, F., & Palese, P. (2014). Universal influenza virus vaccines: need for clinical trials. *Nature immunology*, *15*(1), 3–5. doi:10.1038/ni.2761

Krammer, F., & Palese, P. (2015). Advances in the development of influenza virus vaccines. *Nature reviews. Drug discovery*, *14*(3), 167–82. doi:10.1038/nrd4529

Krammer, F., Pica, N., Hai, R., Margine, I., & Palese, P. (2013). Chimeric hemagglutinin influenza virus vaccine constructs elicit broadly protective stalk-specific antibodies. *J Virol*, *87*(12), 6542–6550. doi:10.1128/jvi.00641-13

Krammer, F., Pica, N., Hai, R., Tan, G. S., & Palese, P. (2012). Hemagglutinin Stalk-Reactive Antibodies Are Boosted following Sequential Infection with Seasonal and Pandemic H1N1 Influenza Virus in Mice. *Journal of Virology*, *86*(19), 10302–10307. doi:10.1128/JVI.01336-12

Krug, R. M., & Etkind, P. R. (1973). Cytoplasmic and nuclear virus-specific proteins in influenza virus-infected MDCK cells. *Virology*, *56*(1), 334–48. http://www.ncbi.nlm.nih.gov/pubmed/4795673. Accessed 25 September 2017

Kuck, L. R., Sorensen, M., Matthews, E., Srivastava, I., Cox, M. M. J., & Rowlen, K. L. (2014). Titer on chip: New analytical tool for influenza vaccine potency determination. *PLoS ONE*, *9*(10), e109616. doi:10.1371/journal.pone.0109616

Kumar, A., Haque, J., Lacoste, J., Hiscott, J., & Williams, B. R. G. (1994). Double-stranded RNA-dependent protein kinase activates transcription factor NF-kappa B by phosphorylating I kappa B. *Proceedings of the National Academy of Sciences of the United States of America*, *91*(14), 6288–92. http://www.ncbi.nlm.nih.gov/pubmed/7912826. Accessed 26 September 2017

Kumari, K., Gulati, S., Smith, D. F., Gulati, U., Cummings, R. D., & Air, G. M. (2007). Receptor binding specificity of recent human H3N2 influenza viruses, *12*, 1–11. doi:10.1186/1743-422X-4-42

La Montagne, J. R., Noble, G. R., Quinnan, G. V, Curlin, G. T., Blackwelder, W. C., Smith, J. I., et al. (1983). Summary of clinical trials of inactivated influenza vaccine - 1978. *Reviews of infectious diseases*, *5*(4), 723–736. http://www.ncbi.nlm.nih.gov/pubmed/6353529. Accessed 24 April 2017

Labrosse, B., Tourdjman, M., Porcher, R. L., Legoff, J., de Lamballerie, X., Simon, F., et al. (2010). Detection of extensive cross-neutralization between pandemic and seasonal A/H1N1 influenza viruses using a pseudotype neutralization assay. *PLoS ONE*, *5*(6), 4–7. doi:10.1371/journal.pone.0011036

Lacek, K., Urbanowicz, R. A., Troise, F., De Lorenzo, C., Severino, V., Di Maro, A., et al. (2014). Dramatic potentiation of the antiviral activity of HIV antibodies by cholesterol conjugation. *Journal of Biological Chemistry*, *289*(50), 35015–35028. doi:10.1074/jbc.M114.591826

Lakadamyali, M., Rust, M. J., & Zhuang, X. (2004). Endocytosis of influenza viruses Melike. *Microbes Infect.*, *6*(10), 929–936. doi:10.1016/j.micinf.2004.05.002.Endocytosis

Lamb, R. A., & Choppin, P. W. (1979). Segment 8 of the influenza virus genome is unique in coding for two polypeptides. *Proceedings of the National Academy of Sciences of the United States of America*, *76*(10), 4908–12. http://www.ncbi.nlm.nih.gov/pubmed/291907. Accessed 2 October 2017

Lamb, R. A., & Lai, C. J. (1980). Sequence of interrupted and uninterrupted mRNAs and cloned DNA coding for the two overlapping nonstructural proteins of influenza virus. *Cell*, *21*(2), 475–85. http://www.ncbi.nlm.nih.gov/pubmed/7407920. Accessed 2 October 2017

Lamb, R. A., Zebedee, S. L., & Richardson, C. D. (1985). Influenza virus M 2 protein is an integral membrane protein expressed on the infected-cell surface. *Cell*, *40*(3), 627–633.

Lambré, C. R., & Kasturi, K. N. (1979). A microplate immunoenzyme assay for anti-influenza antibodies. *Journal of Immunological Methods*, *26*(1), 61–67. doi:10.1016/0022-1759(79)90041-3

Lambré, C. R., Terzidis, H., Greffard, A., & Webster, R. G. (1991). An enzyme-linked lectin assay for sialidase. *Clinica chimica acta; international journal of clinical chemistry*, *198*(3), 183–93. http://www.ncbi.nlm.nih.gov/pubmed/1716184. Accessed 4 May 2017

Lande, R., Gregorio, J., Facchinetti, V., Chatterjee, B., Wang, Y.-H., Homey, B., et al. (2007). Plasmacytoid dendritic cells sense self-DNA coupled with antimicrobial peptide. *Nature*, *449*(7162), 564–569. doi:10.1038/nature06116

Laurie, K. L., Engelhardt, O. G., Wood, J. M., Heath, A., Katz, J. M., Peiris, J. S. M., et al. (2015). International laboratory comparison of influenza microneutralization assays for A(H1N1)pdm09, A(H3N2), and A(H5N1) influenza viruses by CONSISE. *Clinical and vaccine immunology : CVI*, *22*(8), 957–64. doi:10.1128/CVI.00278-15

Laver, G., & Garman, E. (2002). Pandemic influenza: Its origin and control. *Microbes and Infection*, *4*(13), 1309–1316. doi:10.1016/S1286-4579(02)00013-8

Lazarowitz, S. G., & Choppin, P. W. (1975). Enhancement of the infectivity of influenza A and B viruses by proteolytic cleavage of the hemagglutinin polypeptide. *Virology*, *68*(2), 440–454. doi:10.1016/0042-6822(75)90285-8

Lazarowitz, S. G., Goldberg, A. R., & Choppin, P. W. (1973). Proteolytic cleavage by plasmin of the HA polypeptide of influenza virus: Host cell activation of serum plasminogen. *Virology*, *56*(1), 172–180. doi:10.1016/0042-6822(73)90296-1

Le Goffic, R., Balloy, V., Lagranderie, M., Alexopoulou, L., Escriou, N., Flavell, R. A., et al. (2006). Detrimental Contribution of the Toll-Like Receptor (TLR)3 to Influenza A Virus–Induced Acute Pneumonia. *PLoS Pathogens*, *2*(6), e53. doi:10.1371/journal.ppat.0020053

Le Goffic, R., Pothlichet, J., Vitour, D., Fujita, T., Meurs, E., Chignard, M., & Si-Tahar, M. (2007). Cutting Edge: Influenza A virus activates TLR3-dependent inflammatory and RIG-I-dependent antiviral responses in human lung epithelial cells. *Journal of immunology (Baltimore, Md. : 1950)*, *178*(6), 3368–72. http://www.ncbi.nlm.nih.gov/pubmed/17339430. Accessed 26 September 2017

Leber, J. H., Crimmins, G. T., Raghavan, S., Meyer-Morse, N. P., Cox, J. S., & Portnoy, D. A. (2008). Distinct TLR- and NLR-Mediated Transcriptional Responses to an Intracellular Pathogen. *PLoS Pathogens*, *4*(1), e6. doi:10.1371/journal.ppat.0040006

Ledgerwood, J. E., Hu, Z., Gordon, I. J., Yamshchikov, G., Enama, M. E., Plummer, S., et al. (2012). Influenza virus H5 DNA vaccination is immunogenic by intramuscular and intradermal routes in humans. *Clinical and Vaccine Immunology*, *19*(11), 1792–1797. doi:10.1128/CVI.05663-11

Ledgerwood, J. E., Wei, C.-J., Hu, Z., Gordon, I. J., Enama, M. E., Hendel, C. S., et al. (2011). DNA priming and influenza vaccine immunogenicity: Two phase 1 open label randomised clinical trials. *The Lancet Infectious Diseases*, *11*(12), 916–924. doi:10.1016/S1473-3099(11)70240-7

Ledgerwood, J. E., Zephir, K., Hu, Z., Wei, C.-J., Chang, L., Enama, M. E., et al. (2013). Prime-boost interval matters: A randomized phase 1 study to identify the minimum interval necessary to observe the h5 dna influenza vaccine priming effect. *Journal of Infectious Diseases*, *208*(3), 418–422. doi:10.1093/infdis/jit180

Lentz, M. R., & Air, G. M. (1986). Loss of enzyme activity in a site-directed mutant of influenza neuraminidase compared to expressed wild-type protein. *Virology*, *148*(1), 74–83. doi:10.1016/0042-6822(86)90404-6

Li, F., Ma, C., DeGrado, W. F., & Wang, J. (2016). Discovery of Highly Potent Inhibitors Targeting the Predominant Drug-Resistant S31N Mutant of the Influenza A Virus M2 Proton Channel. *Journal of medicinal chemistry*, *59*(3), 1207–16. doi:10.1021/acs.jmedchem.5b01910

Li, Q., Sun, X., Li, Z., Liu, Y., Vavricka, C. J., Qi, J., & Gao, G. F. (2012). Structural and functional characterization of neuraminidase-like molecule N10 derived from bat influenza A virus. *Proceedings of the National Academy of Sciences of the United States of America*, *109*(46), 18897–18902. doi:10.1073/pnas.1211037109

Li, S., Min, J.-Y., Krug, R. M., & Sen, G. C. (2006). Binding of the influenza A virus NS1 protein to PKR mediates the inhibition of its activation by either PACT or double-stranded RNA. *Virology*, *349*(1), 13–21. doi:10.1016/j.virol.2006.01.005

Li, W., Cowley, A. P., Uludag, M., Gur, T., McWilliam, H., Squizzato, S., et al. (2015). The EMBL-EBI bioinformatics web and programmatic tools framework. *Nucleic acids research*, *43*(W1), W580-4. doi:10.1093/nar/gkv279

Li, Y., Chen, S., Zhang, X., Fu, Q., Zhang, Z., Shi, S., et al. (2014). A 20-Amino-Acid Deletion in the Neuraminidase Stalk and a Five-Amino-Acid Deletion in the NS1 Protein Both Contribute to the Pathogenicity of H5N1 Avian Influenza Viruses in Mallard Ducks. *PLoS ONE*, *9*(4), e95539. doi:10.1371/journal.pone.0095539

Liang, M., Lye, D. C., Chen, M. I., Chow, A., Krishnan, P., Seow, E., & Leo, Y. S. (2009). New influenza A (H1N1) 2009 in Singapore: the first ten adult imported cases. *Singapore medical journal*, *50*(6), 581–3. http://www.ncbi.nlm.nih.gov/pubmed/19551309. Accessed 22 August 2017

Lin, A. H., & Cannon, P. M. (2002). Use of pseudotyped retroviral vectors to analyze the receptor-binding pocket of hemagglutinin from a pathogenic avian influenza A virus (H7 subtype). *Virus Research*, *83*(1–2), 43–56. doi:10.1016/S0168-1702(01)00407-5

Lin, X., Zhou, J., Zhang, Y., Wu, J., Zhang, F., Li, Z., et al. (2009). Oseltamivir boosts 2009 H1N1 virus infectivity in vitro. *Biochemical and Biophysical Research Communications*, *390*(4), 1305–1308. doi:10.1016/j.bbrc.2009.10.142

Lin, Y. P., Pu, Y., Gregory, V., Collins, P. J., Kloess, J., Wharton, S. A., et al. (2010). Neuraminidase Receptor Binding Variants of Human Influenza A(H3N2) Viruses Resulting from Substitution of Aspartic Acid 151 in the Catalytic Site: a Role in Virus Attachment? *Journal of Virology*, *84*(13), 6769–6781. doi:10.1128/JVI.00458-10

Lin, Y. P., Xiaoli, X., Wharton, S. A., Martin, S. R., Coombs, P. J., Vachieri, S. G., et al. (2012). Evolution of the receptor binding properties of the influenza A(H3N2) hemagglutinin, *109*(52). doi:10.1073/pnas.1301039110

Lingwood, D., McTamney, P. M., Yassine, H. M., Whittle, J. R. R., Guo, X., Boyington, J. C., et al. (2012). Structural and genetic basis for development of broadly neutralizing influenza antibodies. *Nature*, *489*(7417), 566–570. doi:10.1038/nature11371

Liu, L., Nachbagauer, R., Zhu, L., Huang, Y., Xie, X., Jin, S., et al. (2017). Induction of broadly cross-reactive stalk-specific antibody responses to influenza group 1 and group 2 hemagglutinins by natural H7N9 virus infection in humans. *Journal of Infectious Diseases*, *215*(4), 518–528. doi:10.1093/infdis/jiw608

Liu, W.-C., Lin, C.-Y., Tsou, Y.-T., Jan, J.-T., & Wu, S.-C. (2015). Cross-Reactive Neuraminidase-Inhibiting Antibodies Elicited by Immunization with Recombinant Neuraminidase Proteins of H5N1 and Pandemic H1N1 Influenza A Viruses. *Journal of Virology*, *89*(14), 7224–7234. doi:10.1128/JVI.00585-15

Long, J. S., Howard, W. A., Núñez, A., Moncorgé, O., Lycett, S. J., Banks, J., & Barclay, W. S. (2013). The effect of the PB2 mutation 627K on highly pathogenic H5N1 avian influenza virus is dependent on the virus lineage. *Journal of virology*, *87*(18), 9983–96. doi:10.1128/JVI.01399-13

Loureiro, S., Ren, J., Phapugrangkul, P., Colaco, C. a, Bailey, C. R., Shelton, H., et al. (2011). Adjuvant-free immunization with hemagglutinin-Fc fusion proteins as an approach to influenza vaccines. *Journal of virology*, *85*(6), 3010–3014. doi:10.1128/JVI.01241-10

Lu, Y., Wambach, M., Katze, M. G., & Krug, R. M. (1995). Binding of the influenza virus NS1 protein to double-stranded RNA inhibits the activation of the protein kinase that phosphorylates the eIF-2 translation initiation factor. *Virology*, *214*(1), 222–8. http://www.ncbi.nlm.nih.gov/pubmed/8525619. Accessed 25 September 2017

Lund, J. M., Alexopoulou, L., Sato, A., Karow, M., Adams, N. C., Gale, N. W., et al. (2004). Recognition of single-stranded RNA viruses by Toll-like receptor 7. *Proceedings of the National Academy of Sciences*, *101*(15), 5598–5603. doi:10.1073/pnas.0400937101

Ma, W., García-Sastre, A., & Schwemmle, M. (2015). Expected and Unexpected Features of the Newly Discovered Bat Influenza A-like Viruses. *PLoS Pathog*, *11*(6), e1004819. doi:10.1371/journal.ppat.1004819

Madden, T. L., Tatusov, R. L., & Zhang, J. (1996). Applications of network BLAST server. *Methods in enzymology*, *266*, 131–41. http://www.ncbi.nlm.nih.gov/pubmed/8743682. Accessed 17 August 2017

Mahallawi, W. H., Kasbekar, A. V., McCormick, M. S., Hoschler, K., Temperton, N. J., Leong, S. C., et al. (2013). Infection with 2009 H1N1 Influenza Virus Primes for Immunological Memory in Human Nose-Associated Lymphoid Tissue, Offering Cross-Reactive Immunity to H1N1 and Avian H5N1 Viruses. *Journal of Virology*, *87*(10), 5331–5339. doi:10.1128/JVI.03547-12

Mallajosyula, V. V. A., Citron, M., Ferrara, F., Lu, X., Callahan, C., Heidecker, G. J., et al. (2014). Influenza hemagglutinin stem-fragment immunogen elicits broadly neutralizing antibodies and confers heterologous protection. *Proc Natl Acad Sci U S A*, *111*(25), E2514-23. doi:10.1073/pnas.1402766111

Mänz, B., Brunotte, L., Reuther, P., & Schwemmle, M. (2012). Adaptive mutations in NEP compensate for defective H5N1 RNA replication in cultured human cells. *Nature Communications*, *3*, 802. doi:10.1038/ncomms1804

Marcelin, G., DuBois, R. M., Rubrum, A., Russell, C. J., McElhaney, J. E., & Webby, R. J. (2011). A Contributing Role for Anti-Neuraminidase Antibodies on Immunity to Pandemic H1N1 2009 Influenza A Virus. *PLoS ONE*, *6*(10), e26335. doi:10.1371/journal.pone.0026335

Marcelin, G., Sandbulte, M. R., & Webby, R. J. (2012). Contribution of antibody production against neuraminidase to the protection afforded by influenza vaccines. *Reviews in Medical Virology*, *22*(4), 267–279. doi:10.1002/rmv.1713

Margine, I., Hai, R., Albrecht, R. A., Obermoser, G., Harrod, A. C., Banchereau, J., et al. (2013). H3N2 Influenza Virus Infection Induces Broadly Reactive Hemagglutinin Stalk Antibodies in Humans and Mice. *Journal of Virology*, *87*(8), 4728–4737. doi:10.1128/JVI.03509-12

Martin, K., & Helenius, A. (1991). Nuclear transport of influenza virus ribonucleoproteins: The viral matrix protein (M1) promotes export and inhibits import. *Cell*, *67*, 117–130. doi:10.1016/0092-8674(91)90576-K

Maruyama, J., Miyamoto, H., Kajihara, M., Ogawa, H., Maeda, K., Sakoda, Y., et al. (2014). Characterization of the Envelope Glycoprotein of a Novel Filovirus, Lloviu Virus. *Journal of Virology*, *88*(1), 99–109. doi:10.1128/JVI.02265-13

Maruyama, J., Nao, N., Miyamoto, H., Maeda, K., Ogawa, H., Yoshida, R., et al. (2016). Characterization of the glycoproteins of bat-derived influenza viruses. *Virology*, *488*, 43–50. doi:10.1016/j.virol.2015.11.002

Mather, S. T., Wright, E., Scott, S. D., & Temperton, N. J. (2014). Lyophilisation of influenza, rabies and Marburg lentiviral pseudotype viruses for the development and distribution of a neutralisation -assay-based diagnostic kit. *Journal of Virological Methods*, *210*, 51–58. doi:10.1016/j.jviromet.2014.09.021

Matlin, K. S., Reggio, H., Helenius, A., & Simons, K. (1981). Infectious entry pathway of influenza virus in a canine kidney cell line. *Journal of Cell Biology*, *91*(3 I), 601–613. doi:10.1083/jcb.91.3.601

Matrosovich, M. N., Matrosovich, T. Y., Gray, T., Roberts, N. A., & Klenk, H.-D. (2004). Neuraminidase Is Important for the Initiation of Influenza Virus Infection in Human Airway Epithelium. *Society*, *78*(22), 12665–12667. doi:10.1128/JVI.78.22.12665

McCown, M. F., & Pekosz, A. (2006). Distinct Domains of the Influenza A Virus M2 Protein Cytoplasmic Tail Mediate Binding to the M1 Protein and Facilitate Infectious Virus Production. *Journal of Virology*, *80*(16), 8178–8189. doi:10.1128/JVI.00627-06

Mccullers, J. a, Saito, T., & Iverson, A. R. (2004). Multiple Genotypes of Influenza B Virus Circulated between 1979 and 2003 Multiple Genotypes of Influenza B Virus Circulated between 1979 and 2003, *78*(23), 12817–12828. doi:10.1128/JVI.78.23.12817

McKay, T., Patel, M., Pickles, R. J., Johnson, L. G., & Olsen, J. C. (2006). Influenza M2 envelope protein augments avian influenza hemagglutinin pseudotyping of lentiviral vectors. *Gene therapy*, *13*(8), 715–724. doi:10.1038/sj.gt.3302715

McNab, F., Mayer-Barber, K., Sher, A., Wack, A., & O'Garra, A. (2015). Type I interferons in infectious disease. *Nature Reviews Immunology*, *15*(2), 87–103. doi:10.1038/nri3787

McWilliam, H., Li, W., Uludag, M., Squizzato, S., Park, Y. M., Buso, N., et al. (2013). Analysis Tool Web Services from the EMBL-EBI. *Nucleic acids research*, *41*(Web Server issue), W597-600. doi:10.1093/nar/gkt376

Medeiros, R., Escriou, N., Naffakh, N., Manuguerra, J., & Werf, S. Van Der. (2001). Hemagglutinin Residues of Recent Human A (H3N2) Influenza Viruses That Contribute to the Inability to Agglutinate Chicken Erythrocytes, *85*, 74–85. doi:10.1006/viro.2001.1121

Medina, R. a, Manicassamy, B., Stertz, S., Seibert, C. W., Hai, R., Belshe, R. B., et al. (2010). Pandemic 2009 H1N1 vaccine protects against 1918 Spanish influenza virus. *Nature communications*, *1*(May), 28. doi:10.1038/ncomms1026

Medzhitov, R., & Janeway, C. (2000). Innate immune recognition: mechanisms and pathways. *Immunological reviews*, *173*, 89–97. http://www.ncbi.nlm.nih.gov/pubmed/10719670. Accessed 26 September 2017

Mibayashi, M., Martinez-Sobrido, L., Loo, Y.-M., Cardenas, W. B., Gale, M., & García-Sastre, A. (2007). Inhibition of Retinoic Acid-Inducible Gene I-Mediated Induction of Beta Interferon by the NS1 Protein of Influenza A Virus. *Journal of Virology*, *81*(2), 514–524. doi:10.1128/JVI.01265-06

Mildner, A., & Jung, S. (2014). Immunity Review Development and Function of Dendritic Cell Subsets.

Immunity, *40*, 642–656. doi:10.1016/j.immuni.2014.04.016

Min, J.-Y., & Krug, R. M. (2006). The primary function of RNA binding by the influenza A virus NS1 protein in infected cells: Inhibiting the 2'-5' oligo (A) synthetase/RNase L pathway. *Proceedings of the National Academy of Sciences*, *103*(18), 7100–7105. doi:10.1073/pnas.0602184103

Min, J.-Y., Li, S., Sen, G. C., & Krug, R. M. (2007). A site on the influenza A virus NS1 protein mediates both inhibition of PKR activation and temporal regulation of viral RNA synthesis. *Virology*, *363*(1), 236–243. doi:10.1016/j.virol.2007.01.038

Mitnaul, L. J., Matrosovich, M. N., Castrucci, M. R., Tuzikov, A. B., Bovin, N. V, Kobasa, D., & Kawaoka, Y. (2000). Balanced hemagglutinin and neuraminidase activities are critical for efficient replication of influenza A virus. *Journal of virology*, *74*(13), 6015–20. doi:10.1128/JVI.74.13.6015-6020.2000

Molesti, E., Ferrara, F., Lapini, G., Montomoli, E., & Temperton, N. J. (2014). Discordant correlation between serological assays observed when measuring heterosubtypic responses against avian influenza H5 and H7 viruses in unexposed individuals. *BioMed Research International*, *2014*, 231365. doi:10.1155/2014/231365

Molesti, E., Milani, A., Terregino, C., Cattoli, G., & Temperton, N. J. (2013). Comparative serological assays for the study of H5 and H7 avian influenza viruses. *Influenza research and treatment*, *2013*, 286158. doi:10.1155/2013/286158

Monto, A. S., & Maassab, H. F. (1981). Ether treatment of type B influenza virus antigen for the hemagglutination inhibition test. *Journal of Clinical Microbiology*, *13*(1), 54–57. http://www.ncbi.nlm.nih.gov/pubmed/7462419. Accessed 24 April 2017

Moody, M. A., Zhang, R., Walter, E. B., Woods, C. W., Ginsburg, G. S., McClain, M. T., et al. (2011). H3N2 influenza infection elicits more cross-reactive and less clonally expanded anti-hemagglutinin antibodies than influenza vaccination. *PLoS ONE*, *6*(10). doi:10.1371/journal.pone.0025797

Moreira, É. A., Locher, S., Kolesnikova, L., Bolte, H., Aydillo, T., García-Sastre, A., et al. (2016). Synthetically derived bat influenza A-like viruses reveal a cell type- but not species-specific tropism. *Proceedings of the National Academy of Sciences*, 201608821. doi:10.1073/pnas.1608821113

Morgulis, A., Coulouris, G., Raytselis, Y., Madden, T. L., Agarwala, R., & Schäffer, A. A. (2008). Database indexing for production MegaBLAST searches. *Bioinformatics*, *24*(16), 1757–1764. doi:10.1093/bioinformatics/btn322

Morley, P. S., Hanson, L. K., Bogdan, J. R., Townsend, H. G., Appleton, J. A., & Haines, D. M. (1995).

The relationship between single radial hemolysis, hemagglutination inhibition, and virus neutralization assays used to detect antibodies specific for equine influenza viruses. *Veterinary microbiology*, *45*(1), 81–92. http://www.ncbi.nlm.nih.gov/pubmed/7653031. Accessed 24 August 2017

Moscona, A. (2005). Neuraminidase inhibitors for influenza. *The New England journal of medicine*, *353*(13), 1363–1373. doi:10.1056/NEJMra050740

Mossad, S. B. (2007). Influenza update 2007 – 2008 : Vaccine advances , pandemic preparation. *Cleveland Clinic Journal of Medicine*, *74*(12), 889–894.

Mossad, S. B. (2008). 2008-2009 Influenza update: A better vaccine match. *Cleveland Clinic Journal of Medicine*, *75*(12), 865–870. doi:10.3949/ccjm.75a.08088

Mullarkey, C. E., Boyd, A., Van Laarhoven, A., Lefevre, E. A., Veronica Carr, B., Baratelli, M., et al. (2013). Improved adjuvanting of seasonal influenza vaccines: Preclinical studies of MVA-NP+M1 coadministration with inactivated influenza vaccine. *European Journal of Immunology*, *43*(7), 1940–1952. doi:10.1002/eji.201242922

Muramoto, Y., Noda, T., Kawakami, E., Akkina, R., & Kawaoka, Y. (2013). Identification of novel influenza A virus proteins translated from PA mRNA. *Journal of virology*, *87*(5), 2455–62. doi:10.1128/JVI.02656-12

Muyldermans, S. (2013). Nanobodies: Natural Single-Domain Antibodies. *Annual Review of Biochemistry*, *82*(1), 775–797. doi:10.1146/annurev-biochem-063011-092449

Nachbagauer, R., Choi, A., Izikson, R., Cox, M. M. J., Palese, P., & Krammer, F. (2016). Age dependence and isotype specificity of influenza virus hemagglutinin stalk-reactive antibodies in humans. *mBio*, *7*(1), 1–10. doi:10.1128/mBio.01996-15

Nachbagauer, R., Kinzler, D., Choi, A., Hirsh, A., Beaulieu, E., Lecrenier, N., et al. (2016). A chimeric haemagglutinin-based influenza split virion vaccine adjuvanted with AS03 induces protective stalk-reactive antibodies in mice. *npj Vaccines*, *1*(1), 16015. doi:10.1038/npjvaccines.2016.15

Nachbagauer, R., & Krammer, F. (2017). Universal influenza virus vaccines and therapeutic antibodies. *Clinical Microbiology and Infection*, *23*(4), 222–228. doi:10.1016/j.cmi.2017.02.009

Nachbagauer, R., Wohlbold, T. J., Hirsh, A., Hai, R., Sjursen, H., Palese, P., et al. (2014). Induction of broadly reactive anti-hemagglutinin stalk antibodies by an H5N1 vaccine in humans. *Journal of virology*, *88*(22), 13260–8. doi:10.1128/JVI.02133-14

Naffakh, N., Tomoiu, A., Rameix-Welti, M.-A., & van der Werf, S. (2008). Host Restriction of Avian Influenza Viruses at the Level of the Ribonucleoproteins. *Annual Review of Microbiology*, *62*(1), 403–424. doi:10.1146/annurev.micro.62.081307.162746

Naldini, L., Blömer, U., Gage, F. H., Trono, D., & Verma, I. M. (1996). Efficient transfer, integration, and sustained long-term expression of the transgene in adult rat brains injected with a lentiviral vector. *Proceedings of the National Academy of Sciences of the United States of America*, *93*(21), 11382–8. doi:10.1073/pnas.93.21.11382

Nayak, B., Kumar, S., DiNapoli, J. M., Paldurai, A., Perez, D. R., Collins, P. L., & Samal, S. K. (2010). Contributions of the avian influenza virus HA, NA, and M2 surface proteins to the induction of neutralizing antibodies and protective immunity. *Journal of virology*, *84*(5), 2408–20. doi:10.1128/JVI.02135-09

Nayak, D. P., Balogun, R. A., Yamada, H., Hong Zhou, Z., & Barman, S. (2009). Influenza virus morphogenesis and budding. *Virus Research*, *143*(2), 147–161. doi:10.1124/dmd.107.016501.CYP3A4-Mediated

Nefkens, I., Garcia, J. M., Ling, C. S., Lagarde, N., Nicholls, J., Tang, D.-J. J., et al. (2007). Hemagglutinin pseudotyped lentiviral particles: Characterization of a new method for avian H5N1 influenza sero-diagnosis. *Journal of Clinical Virology*, *39*(1), 27–33. doi:10.1016/j.jcv.2007.02.005

Neumann, G., Ozawa, M., & Kawaoka, Y. (2012). Reverse Genetics of Influenza Viruses. In *Methods in molecular biology (Clifton, N.J.)* (Vol. 865, pp. 193–206). doi:10.1007/978-1-61779-621-0_12

Ng, A. K.-L., Wang, J.-H., & Shaw, P.-C. (2009). Structure and sequence analysis of influenza A virus nucleoprotein. *Science in China Series C: Life Sciences*, *52*(5), 439–449. doi:10.1007/s11427-009-0064-x

Ni, F., Kondrashkina, E., & Wang, Q. (2013). Structural basis for the divergent evolution of influenza B virus hemagglutinin. *Virology*, *446*(1–2), 112–122. doi:10.1016/j.virol.2013.07.035

Nobusawa, E., Ishihara, H., Morishita, T., Sato, K., & Nakajima, K. (2000). Change in Receptor-Binding Specificity of Recent Human Influenza A Viruses (H3N2): A Single Amino Acid Change in Hemagglutinin Altered Its Recognition of Sialyloligosaccharides, *596*, 587–596. doi:10.1006/viro.2000.0679

O'Brien, T. R., Prokunina-Olsson, L., & Donnelly, R. P. (2014). IFN-λ4: the paradoxical new member of the interferon lambda family. *Journal of interferon & cytokine research : the official journal of the International Society for Interferon and Cytokine Research*, *34*(11), 829–38. doi:10.1089/jir.2013.0136

O'Donnell, C. D., Wright, A., Vogel, L. N., Wei, C.-J., Nabel, G. J., & Subbarao, K. (2012). Effect of Priming with H1N1 Influenza Viruses of Variable Antigenic Distances on Challenge with 2009 Pandemic H1N1 Virus. *Journal of Virology*, *86*(16), 8625–8633. doi:10.1128/JVI.00147-12

Obenauer, J. C., Denson, J., Mehta, P. K., Su, X., Mukatira, S., Finkelstein, D. B., et al. (2006). Large-scale sequence analysis of avian influenza isolates. *Science (New York, N.Y.)*, *311*(5767), 1576–80. doi:10.1126/science.1121586

Oh, S., Selleck, P., Temperton, N. J., Chan, P. K. S., Capecchi, B., Manavis, J., et al. (2009). Neutralizing monoclonal antibodies to different clades of Influenza A H5N1 viruses. *Journal of Virological Methods*, *157*(2), 161–167. doi:10.1016/j.jviromet.2008.12.016

Ohuchi, M., Asaoka, N., Sakai, T., & Ohuchi, R. (2006). Roles of neuraminidase in the initial stage of influenza virus infection. *Microbes and Infection*, *8*(5), 1287–1293. doi:10.1016/j.micinf.2005.12.008

Okuno, Y., Isegawa, Y., Sasao, F., & Ueda, S. (1993). A common neutralizing epitope conserved between the hemagglutinins of influenza A virus H1 and H2 strains. *Journal of virology*, *67*(5), 2552–8. http://www.ncbi.nlm.nih.gov/pubmed/7682624%5Cnhttp://www.pubmedcentral.nih.gov/articlerender.fcgi?artid=PMC237575

Okuno, Y., Matsumoto, K., Isegawa, Y., & Ueda, S. (1994). Protection against the mouse-adapted A/FM/1/47 strain of influenza A virus in mice by a monoclonal antibody with cross-neutralizing activity among H1 and H2 strains. *Journal of virology*, *68*(1), 517–20.

Ong, A. K., Chen, M. I., Lin, L., Tan, A. S., Nwe, N. W., Barkham, T., et al. (2009). Improving the Clinical Diagnosis of Influenza—a Comparative Analysis of New Influenza A (H1N1) Cases. *PLoS ONE*, *4*(12), e8453. doi:10.1371/journal.pone.0008453

Oxford, J. S., Yetts, R., & Schild, G. C. (1982). Quantitation and analysis of the specificity of post-immunization antibodies to influenza B viruses using single radial haemolysis. *J Hyg (Lond)*, *88*(2), 325–333. doi:10.1017/S0022172400070170

Palese, P., Tobita, K., Ueda, M., & Compans, R. W. (1974). Characterization of temperature sensitive influenza virus mutants defective in neuraminidase. *Virology*, *61*(2), 397–410. doi:10.1016/0042-6822(74)90276-1

Palladino, G., Mozdzanowska, K., Washko, G., & Gerhard, W. (1995). Virus-neutralizing antibodies of immunoglobulin G (IgG) but not of IgM or IgA isotypes can cure influenza virus pneumonia in SCID mice. *Journal of virology*, *69*(4), 2075–81. http://www.ncbi.nlm.nih.gov/pubmed/7884853. Accessed 26 September 2017

Pan, K. (2011). Understanding original antigenic sin in influenza with a dynamical system. *PLoS ONE*, *6*(8). doi:10.1371/journal.pone.0023910

Pandey, A. K., Yang, Y., Jiang, Z., Fortune, S. M., Coulombe, F., Behr, M. A., et al. (2009). NOD2, RIP2

and IRF5 Play a Critical Role in the Type I Interferon Response to Mycobacterium tuberculosis. *PLoS Pathogens*, *5*(7), e1000500. doi:10.1371/journal.ppat.1000500

Pappas, L., Foglierini, M., Piccoli, L., Kallewaard, N. L., Turrini, F., Silacci, C., et al. (2014). Rapid development of broadly influenza neutralizing antibodies through redundant mutations. *Nature*, *516*(7531), 418–422. doi:10.1038/nature13764

Park, S. I., Kim, M. J., Hwang, H. Y., Oh, C. E., Lee, J. H., & Park, J. S. (2010). Clinical characteristics of children with 2009 pandemic influenza A (H1N1) admitted in a single institution. *Korean Journal of Pediatrics*, *53*(10), 886. doi:10.3345/kjp.2010.53.10.886

Park, S., Il Kim, J., Lee, I., Bae, J.-Y., Yoo, K., Nam, M., et al. (2017). Adaptive mutations of neuraminidase stalk truncation and deglycosylation confer enhanced pathogenicity of influenza A viruses. *Scientific Reports*, *7*(1), 10928. doi:10.1038/s41598-017-11348-0

Pascual Serrano, D., Vera Pasamontes, C., & Girón Moreno, R. (2016). Modelos animales de dolor neuropático. *Dolor*, *31*(2), 70–76. doi:10.1017/CBO9781107415324.004

Patel, M., Giddings, A. M., Sechelski, J., & Olsen, J. C. (2013). High efficiency gene transfer to airways of mice using influenza hemagglutinin pseudotyped lentiviral vectors. *Journal of Gene Medicine*, *15*(1), 51–62. doi:10.1002/jgm.2695

Pavlovic, J., Arzet, H. A., Hefti, H. P., Frese, M., Rost, D., Ernst, B., et al. (1995). Enhanced virus resistance of transgenic mice expressing the human MxA protein. *Journal of virology*, *69*(7), 4506–10. http://www.ncbi.nlm.nih.gov/pubmed/7769712. Accessed 26 September 2017

Pavlovic, J., Haller, O., & Staeheli, P. (1992). Human and mouse Mx proteins inhibit different steps of the influenza virus multiplication cycle. *Journal of virology*, *66*(4), 2564–9. http://www.ncbi.nlm.nih.gov/pubmed/1548781. Accessed 26 September 2017

Pei, J., Kim, B.-H., & Grishin, N. V. (2008). PROMALS3D: a tool for multiple protein sequence and structure alignments. *Nucleic Acids Research*, *36*(7), 2295–2300. doi:10.1093/nar/gkn072

Pestka, S., Krause, C. D., & Walter, M. R. (2004). Interferons, interferon-like cytokines, and their receptors. *Immunological Reviews*, *202*(1), 8–32. doi:10.1111/j.0105-2896.2004.00204.x

Pica, N., Hai, R., Krammer, F., Wang, T. T., Maamary, J., Eggink, D., et al. (2012). Hemagglutinin stalk antibodies elicited by the 2009 pandemic influenza virus as a mechanism for the extinction of seasonal H1N1 viruses. *Proceedings of the National Academy of Sciences of the United States of America*, *109*(7), 2573–8. doi:10.1073/pnas.1200039109

Pichlmair, A., Schulz, O., Tan, C. P., Naslund, T. I., Liljestrom, P., Weber, F., & Reis e Sousa, C. (2006). RIG-I-Mediated Antiviral Responses to Single-Stranded RNA Bearing 5'-Phosphates. *Science*, *314*(5801), 997–1001. doi:10.1126/science.1132998

Pichyangkul, S., Krasaesub, S., Jongkaewwattana, A., Thitithanyanont, A., Wiboon-ut, S., Yongvanitchit, K., et al. (2014). Short report: Pre-existing cross-reactive antibodies to avian influenza H5N1 and 2009 pandemic H1N1 in US military personnel. *American Journal of Tropical Medicine and Hygiene*, *90*(1), 149–152. doi:10.4269/ajtmh.13-0151

Pierce, C. L., Williams, T. L., Moura, H., Pirkle, J. L., Cox, N. J., Stevens, J., et al. (2011). Quantification of immunoreactive viral influenza proteins by immunoaffinity capture and isotope-dilution liquid chromatography-tandem mass spectrometry. *Analytical Chemistry*, *83*(12), 4729–4737. doi:10.1021/ac2006526

Pinilla, L. T., Holder, B. P., Abed, Y., Boivin, G., & Beauchemin, C. A. A. (2012). The H275Y Neuraminidase Mutation of the Pandemic A/H1N1 Influenza Virus Lengthens the Eclipse Phase and Reduces Viral Output of Infected Cells, Potentially Compromising Fitness in Ferrets. *Journal of Virology*, *86*(19), 10651–10660. doi:10.1128/JVI.07244-11

Pinto, L. H., Holsinger, L. J., & Lamb, R. A. (1992). Influenza virus M2 protein has ion channel activity. *Cell*, *69*(3), 517–528. doi:10.1016/0092-8674(92)90452-I

Pinto, L. H., & Lamb, R. A. (2006). The M2 proton channels of influenza A and B viruses. *Journal of Biological Chemistry*, *281*(14), 8997–9000. doi:10.1074/jbc.R500020200

Plessa, E., Diakakis, P., Gardelis, J., Thirios, A., Koletsi, P., & Falagas, M. E. (2010). Clinical features, risk factors, and complications among pediatric patients with pandemic influenza A (H1N1). *Clinical pediatrics*, *49*(8), 777–81. doi:10.1177/0009922810368558

Plotch, S. J., Bouloy, M., Ulmanen, I., & Krug, R. M. (1981). A unique cap(m7GpppXm)-dependent influenza virion endonuclease cleaves capped RNAs to generate the primers that initiate viral RNA transcription. *Cell*, *23*(3), 847–58. http://www.ncbi.nlm.nih.gov/pubmed/6261960. Accessed 25 September 2017

Poole, E., Elton, D., Medcalf, L., & Digard, P. (2004). Functional domains of the influenza A virus PB2 protein: identification of NP- and PB1-binding sites. *Virology*, *321*(1), 120–133. doi:10.1016/j.virol.2003.12.022

Potier, M., Mameli, L., Bélisle, M., Dallaire, L., & Melançon, S. B. (1979). Fluorometric assay of neuraminidase with a sodium (4-methylumbelliferyl-alpha-D-N-acetylneuraminate) substrate. *Analytical biochemistry*, *94*(2), 287–96. http://www.ncbi.nlm.nih.gov/pubmed/464297. Accessed 5 May 2017

Potter, C. W., & Oxford, J. (1979). Determinants of immunity to influenza infection in man. *British medical bulletin*, *35*(1), 69–75. http://www.ncbi.nlm.nih.gov/pubmed/367490. Accessed 24 April 2017

Powell, T. J., Silk, J. D., Sharps, J., Fodor, E., & Townsend, A. R. M. (2012). Pseudotyped Influenza A Virus as a Vaccine for the induction of Heterotypic Immunity. *Journal of Virology*, *86*(24), 13397–13406. doi:10.1128/JVI.01820-12

Prevato, M., Cozzi, R., Pezzicoli, A., Taddei, A. R., Ferlenghi, I., Nandi, A., et al. (2015). An innovative pseudotypes-based Enzyme-Linked Lectin Assay for the measurement of functional anti-neuraminidase antibodies. *PLoS ONE*, *10*(8), e0135383. doi:10.1371/journal.pone.0135383

Prokunina-Olsson, L., Muchmore, B., Tang, W., Pfeiffer, R. M., Park, H., Dickensheets, H., et al. (2013). A variant upstream of IFNL3 (IL28B) creating a new interferon gene IFNL4 is associated with impaired clearance of hepatitis C virus. *Nature Genetics*, *45*(2), 164–171. doi:10.1038/ng.2521

Pyhälä, R., Kleemola, M., & Visakorpi, R. (1985). The HI test modified by ether treatment in the sero-epidemiological surveillance of influenza B. *J Hyg (Lond)*, *94*(3), 341–348. doi:10.1017/S002217240006157X

Qian, X. Y., Alonso-Caplen, F., & Krug, R. M. (1994). Two functional domains of the influenza virus NS1 protein are required for regulation of nuclear export of mRNA. *Journal of virology*, *68*(4), 2433–41. http://www.ncbi.nlm.nih.gov/pubmed/8139028. Accessed 25 September 2017

Qiu, C., Huang, Y., Wang, Q., Tian, D., Zhang, W., Hu, Y., et al. (2012). Boosting heterosubtypic neutralization antibodies in recipients of 2009 pandemic H1N1 influenza vaccine. *Clinical Infectious Diseases*, *54*(1), 17–24. doi:10.1093/cid/cir753

Qiu, C., Huang, Y., Zhang, A., Tian, D., Wan, Y., Zhang, X., et al. (2013). Safe pseudovirus based assay for neutralization antibodies against influenza A(H7N9) virus. *Emerging Infectious Diseases*, *19*(10), 1685–1687. doi:10.3201/eid1910.130728

Qiu, X., Wong, G., Audet, J., Bello, A., Fernando, L., Alimonti, J. B., et al. (2014). Reversion of advanced Ebola virus disease in nonhuman primates with ZMapp. doi:10.1038/nature13777

Quan, F.-S., Huang, C., Compans, R. W., & Kang, S.-M. (2007). Virus-like particle vaccine induces protective immunity against homologous and heterologous strains of influenza virus. *Journal of virology*, *81*(7), 3514–24. doi:10.1128/JVI.02052-06

Quinnan, G. V, Ennis, F. A., Tuazon, C. U., Wells, M. A., Butchko, G. M., Armstrong, R., et al. (1980). Cytotoxic lymphocytes and antibody-dependent complement-mediated cytotoxicity induced by administration of influenza vaccine. *Infection and immunity*, *30*(2), 362–9. http://www.ncbi.nlm.nih.gov/pubmed/7439982. Accessed 26 September 2017

Rajendran, M., Nachbagauer, R., Ermler, M. E., Bunduc, P., Amanat, F., Izikson, R., et al. (2017). Analysis of Anti-Influenza Virus Neuraminidase Antibodies in Children, Adults, and the Elderly

by ELISA and Enzyme Inhibition: Evidence for Original Antigenic Sin. *mBio*, *8*(2), e02281-16. doi:10.1128/mBio.02281-16

Rajsbaum, R., Albrecht, R. A., Wang, M. K., Maharaj, N. P., Versteeg, G. A., Nistal-Villán, E., et al. (2012). Species-Specific Inhibition of RIG-I Ubiquitination and IFN Induction by the Influenza A Virus NS1 Protein. *PLoS Pathogens*, *8*(11), e1003059. doi:10.1371/journal.ppat.1003059

Ramos, E. L., Mitcham, J. L., Koller, T. D., Bonavia, A., Usner, D. W., Balaratnam, G., et al. (2015). Efficacy and Safety of Treatment With an Anti-M2e Monoclonal Antibody in Experimental Human Influenza. *Journal of Infectious Diseases*, *211*(7), 1038–1044. doi:10.1093/infdis/jiu539

Rao, S. S., Kong, W.-P., Wei, C.-J., Van Hoeven, N., Patrick Gorres, J., Nason, M., et al. (2010). Comparative efficacy of hemagglutinin, nucleoprotein, and matrix 2 protein gene-based vaccination against h5n1 influenza in mouse and ferret. *PLoS ONE*, *5*(3), e9812. doi:10.1371/journal.pone.0009812.g001

Rao, S. S., Kong, W.-P., Wei, C.-J., Yang, Z.-Y., Nason, M., Styles, D., et al. (2008). Multivalent HA DNA vaccination protects against highly pathogenic H5N1 avian influenza infection in chickens and mice. *PLoS ONE*, *3*(6). doi:10.1371/journal.pone.0002432

Reed, & Muench, H. (1938). A SIMPLE METHOD OF ESTIMATING FIFTY PER CENT ENDPOINTS. *Am. J. Epidemiol.*, *27*(3).

Rehwinkel, J., Tan, C. P., Goubau, D., Schulz, O., Pichlmair, A., Bier, K., et al. (2010). RIG-I Detects Viral Genomic RNA during Negative-Strand RNA Virus Infection. *Cell*, *140*(3), 397–408. doi:10.1016/j.cell.2010.01.020

Renegar, K. B., Small, P. A., Boykins, L. G., & Wright, P. F. (2004). Role of IgA versus IgG in the control of influenza viral infection in the murine respiratory tract. *Journal of immunology (Baltimore, Md. : 1950)*, *173*(3), 1978–86. http://www.ncbi.nlm.nih.gov/pubmed/15265932. Accessed 26 September 2017

Resa-Infante, P., Jorba, N., Coloma, R., & Ortin, J. (2011). The influenza virus RNA synthesis machine: advances in its structure and function. *RNA biology*, *8*(2), 207–15. doi:10.4161/rna.8.2.14513

Robb, N. C., Vreede, F. T., Smith, M., & Fodor, E. (2009). NS2/NEP protein regulates transcription and replication of the influenza virus RNA genome. *Journal of General Virology*, *90*(6), 1398–1407. doi:10.1099/vir.0.009639-0

Robertson, J. S., Naeve, C. W., Webster, R. G., Bootman, J. S., Newman, R. W., & Schild, G. C. (1985). Alterations in the hemagglutinin associated with adaptation of influenza B virus to growth in eggs. *Virology*, *143*(1), 166–74. http://www.ncbi.nlm.nih.gov/pubmed/4060580. Accessed 30 September 2017

Rossman, J. S., Jing, X., Leser, G. P., & Lamb, R. A. (2010). Influenza virus M2 protein mediates ESCRT-independant membrane scission. *Cell*, *142*(6), 902–913. doi:10.1016/j.cell.2010.08.029.Influenza

Rossman, J. S., & Lamb, R. A. (2011). Influenza virus assembly and budding. *Virology*, *411*(2), 229–236. doi:10.1016/j.virol.2010.12.003.Influenza

Rota, P. A., Wallis, T. R., Harmon, M. W., Rota, J. S., Kendal, A. P., & Nerome, K. (1990). Cocirculation of two distinct evolutionary lineages of influenza type B virus since 1983. *Virology*, *175*(1), 59–68. doi:10.1016/0042-6822(90)90186-U

Rowe, T., Abernathy, R. A., Hu-Primmer, J., Thompson, W. W., Lu, X., Lim, W., et al. (1999). Detection of antibody to avian influenza a (H5N1) virus in human serum by using a combination of serologic assays. *Journal of Clinical Microbiology*, *37*(4), 937–943.

Russell, R. J., Haire, L. F., Stevens, D. J., Collins, P. J., Lin, Y. P., Blackburn, G. M., et al. (2006). The structure of H5N1 avian influenza neuraminidase suggests new opportunities for drug design. *Nature*, *443*(7107), 45–49. doi:10.1038/nature05114

Ryder, A. B., Nachbagauer, R., Buonocore, L., Palese, P., Krammer, F., & Rose, J. K. (2016). Vaccination with Vesicular Stomatitis Virus-Vectored Chimeric Hemagglutinins Protects Mice against Divergent Influenza Virus Challenge Strains. *Journal of Virology*, *90*(5), 2544–2550. doi:10.1128/JVI.02598-15

Sadler, A. J., & Williams, B. R. G. (2007). Structure and function of the protein kinase R. *Current topics in microbiology and immunology*, *316*, 253–92. http://www.ncbi.nlm.nih.gov/pubmed/17969452. Accessed 26 September 2017

Sadler, A. J., & Williams, B. R. G. (2008). Interferon-inducible antiviral effectors. *Nature Reviews Immunology*, *8*(7), 559–568. doi:10.1038/nri2314

Saito, T., Nakaya, Y., Suzuki, T., Ito, R., Saito, T., Saito, H., et al. (2004). Antigenic alteration of influenza B virus associated with loss of a glycosylation site due to host-cell adaptation. *Journal of Medical Virology*, *74*(2), 336–343. doi:10.1002/jmv.20178

Sakuma, T., Barry, M. A., & Ikeda, Y. (2012). Lentiviral vectors: basic to translational. *Biochem J*, *443*(3), 603–618. doi:10.1042/BJ20120146

Sandbulte, M. R., Gao, J., Straight, T. M., & Eichelberger, M. C. (2009). A miniaturized assay for influenza neuraminidase-inhibiting antibodies utilizing reverse genetics-derived antigens. *Influenza and other Respiratory Viruses*, *3*(5), 233–240. doi:10.1111/j.1750-2659.2009.00094.x

Sandbulte, M. R., Gauger, P. C., Kitikoon, P., Chen, H., Perez, D. R., Roth, J. A., & Vincent, A. L. (2016). Neuraminidase inhibiting antibody responses in pigs differ between influenza A virus N2

lineages and by vaccine type. *Vaccine*, *34*(33), 3773–3779. doi:10.1016/j.vaccine.2016.06.001

Sandrin, V., & Cosset, F.-L. (2006). Intracellular versus cell surface assembly of retroviral pseudotypes is determined by the cellular localization of the viral glycoprotein, its capacity to interact with Gag, and the expression of the Nef protein. *Journal of Biological Chemistry*, *281*(1), 528–542. doi:10.1074/jbc.M506070200

Sant, A. J., Chaves, F. A., Krafcik, F. R., Lazarski, C. A., Menges, P., Richards, K., & Weaver, J. M. (2007). Immunodominance in CD4 T-cell responses: implications for immune responses to influenza virus and for vaccine design. *Expert Review of Vaccines*, *6*(3), 357–368. doi:10.1586/14760584.6.3.357

Sasai, M., Linehan, M. M., & Iwasaki, A. (2010). Bifurcation of Toll-Like Receptor 9 Signaling by Adaptor Protein 3. *Science*, *329*(5998), 1530–1534. doi:10.1126/science.1187029

Sawoo, O., Dublineau, A., Batéjat, C., Zhou, P., Manuguerra, J., & Leclercq, I. (2014). Cleavage of hemagglutinin-bearing lentiviral pseudotypes and their use in the study of influenza virus persistence. *PLoS ONE*, *9*(8), e106192. doi:10.1371/journal.pone.0106192

Schild, G. C., Pereira, M. S., & Chakraverty, P. (1975). Single-radial-hemolysis: a new method for the assay of antibody to influenza haemagglutinin. Applications for diagnosis and seroepidemiologic surveillance of influenza. *Bulletin of the World Health Organization*, *52*(1), 43–50. http://www.ncbi.nlm.nih.gov/pubmed/1082381. Accessed 15 June 2017

Schmeisser, F., Friedman, R., Besho, J., Lugovtsev, V. Y., Soto, J., Wang, W., et al. (2013). Neutralizing and protective epitopes of the 2009 pandemic influenza {H1N1} hemagglutinin. *Influenza and other respiratory viruses*, *7*(3), 480–490. doi:10.1111/irv.12029

Schmeisser, F., Vasudevan, A., Soto, J., Kumar, A., Williams, O., & Weir, J. P. (2014). A monoclonal antibody-based immunoassay for measuring the potency of 2009 pandemic influenza H1N1 vaccines. *Influenza and other Respiratory Viruses*, *8*(5), 587–595. doi:10.1111/irv.12272

Schmidt, A., Schwerd, T., Hamm, W., Hellmuth, J. C., Cui, S., Wenzel, M., et al. (2009). 5'-triphosphate RNA requires base-paired structures to activate antiviral signaling via RIG-I. *Proceedings of the National Academy of Sciences of the United States of America*, *106*(29), 12067–72. doi:10.1073/pnas.0900971106

Schoenborn, J. R., & Wilson, C. B. (2007). Regulation of Interferon-γ During Innate and Adaptive Immune Responses. In *Advances in immunology* (Vol. 96, pp. 41–101). doi:10.1016/S0065-2776(07)96002-2

Schotsaert, M., De Filette, M., Fiers, W., & Saelens, X. (2009). Universal M2 ectodomain-based influenza A vaccines: preclinical and clinical developments. *Expert Review of Vaccines*, *8*(4),

499–508. doi:10.1586/erv.09.6

Schotsaert, M., Ysenbaert, T., Smet, A., Schepens, B., Vanderschaeghe, D., Stegalkina, S., et al. (2016). Long-Lasting Cross-Protection Against Influenza A by Neuraminidase and M2e-based immunization strategies. *Scientific Reports*, *6*(April), 24402. doi:10.1038/srep24402

Schulz, O., Diebold, S. S., Chen, M., Näslund, T. I., Nolte, M. A., Alexopoulou, L., et al. (2005). Toll-like receptor 3 promotes cross-priming to virus-infected cells. *Nature*, *433*(7028), 887–892. doi:10.1038/nature03326

Scott, S. D., Molesti, E., Temperton, N. J., Ferrara, F., Böttcher-Friebertshäuser, E., & Daly, J. (2012). The use of equine influenza pseudotypes for serological screening. *Journal of molecular and genetic medicine : an international journal of biomedical research*, *6*, 304–8. http://www.pubmedcentral.nih.gov/articlerender.fcgi?artid=3601075&tool=pmcentrez&rendertype=abstract

Serra-Cobo, J., & López-Roig, M. (2016). Bats and Emerging Infections: An Ecological and Virological Puzzle. *Advances in experimental medicine and biology*, 1–14. doi:10.1007/5584_2016_131

Shaw, M. W., Xu, X., Li, Y., Normand, S., Ueki, R. T., Kunimoto, G. Y., et al. (2001). Reappearance and Global Spread of Variants of Influenza B/Victoria/2/87 Lineage Viruses in the 2000-2001 and 2001-2002 Seasons. doi:10.1006/viro.2002.1719

Shelton, H., Roberts, K. L., Molesti, E., Temperton, N. J., & Barclay, W. S. (2013). Mutations in haemagglutinin that affect receptor binding and pH stability increase replication of a PR8 influenza virus with H5 HA in the upper respiratory tract of ferrets and may contribute to transmissibility. *Journal of General Virology*, *94*(PART 6), 1220–1229. doi:10.1099/vir.0.050526-0

Shrestha, S. S., Swerdlow, D. L., Borse, R. H., Prabhu, V. S., Finelli, L., Atkins, C. Y., et al. (2011). Estimating the burden of 2009 pandemic influenza a (H1N1) in the United States (April 2009-April 2010). *Clinical Infectious Diseases*, *52*(SUPPL. 1), 75–82. doi:10.1093/cid/ciq012

Shtykova, E. V., Baratova, L. A., Fedorova, N. V., Radyukhin, V. A., Ksenofontov, A. L., Volkov, V. V., et al. (2013). Structural analysis of influenza a virus matrix protein M1 and Its self-assemblies at low pH. *PLoS ONE*, *8*(12), 1–10. doi:10.1371/journal.pone.0082431

Shtyrya, Y. A., Mochalova, L. V, & Bovin, N. V. (2009). Influenza virus neuraminidase: structure and function. *Acta naturae*, *1*(2), 26–32. http://www.ncbi.nlm.nih.gov/pubmed/22649600%5Cnhttp://www.pubmedcentral.nih.gov/articlerender.fcgi?artid=PMC3347517

Shuck, K., Lamb, R. A., & Pinto, L. H. (2000). Analysis of the pore structure of the influenza A virus

M(2) ion channel by the substituted-cysteine accessibility method. *Journal of virology*, *74*(17), 7755–7761. doi:10.1128/JVI.74.17.7755-7761.2000

Sievers, F., Wilm, A., Dineen, D., Gibson, T. J., Karplus, K., Li, W., et al. (2011). Fast, scalable generation of high-quality protein multiple sequence alignments using Clustal Omega. *Molecular systems biology*, *7*(1), 539. doi:10.1038/msb.2011.75

Skehel, J. J., & Waterfield, M. D. (1975). Studies on the primary structure of the influenza virus hemagglutinin. *Proceedings of the National Academy of Sciences of the United States of America*, *72*(1), 93–97. doi:10.1073/pnas.72.1.93

Skehel, J. J., & Wiley, D. C. (2000). Receptor binding and membrane fusion in virus entry: The Influenza Hemagglutinin. *Annual Review of Biochemistry*, *69*, 531–569. doi:10.1146/annurev.biochem.69.1.531

Smiley, S. T., & Grusby, M. J. (1998). Interleukin 4. In *Encyclopedia of Immunology* (pp. 1451–1453). Elsevier. doi:10.1006/rwei.1999.0368

Smith, G. J. D., Vijaykrishna, D., Bahl, J., Lycett, S. J., Worobey, M., Pybus, O. G., et al. (2009). Origins and evolutionary genomics of the 2009 swine-origin H1N1 influenza A epidemic. *Nature*, *459*(7250), 1122–1125. doi:10.1038/nature08182

Smith, S. E., Gibson, M. S., Wash, R. S., Ferrara, F., Wright, E., Temperton, N. J., et al. (2013). Chicken interferon-inducible transmembrane protein 3 restricts influenza viruses and lyssaviruses in vitro. *Journal of virology*, *87*(23), 12957–66. doi:10.1128/JVI.01443-13

Soneoka, Y., Cannon, P. M., Ramsdale, E. E., Griffiths, J. C., Romano, G., Kingsman, S. M., & Kingsman, A. J. (1995). A transient three-plasmid expression system for the production of high titer retroviral vectors. *Nucleic Acids Research*, *23*(4), 628–633. doi:10.1093/nar/23.4.628

Sonntag, M., Mühldorfer, K., Speck, S., Wibbelt, G., & Kurth, A. (2009). New adenovirus in bats, Germany. *Emerging Infectious Diseases*, *15*(12), 2052–2055. doi:10.3201/eid1512.090646

States, D. J., & Gish, W. (1994). Combined use of sequence similarity and codon bias for coding region identification. *Journal of computational biology : a journal of computational molecular cell biology*, *1*(1), 39–50. doi:10.1089/cmb.1994.1.39

Steel, J., Lowen, A. C., & Wang, T. T. (2010). Influenza Virus Vaccine Based on the Conserved Hemagglutinin Stalk. *mBio*, *1*(1), 1–9. doi:10.1128/mBio.00018-10.Editor

Stephenson, I., Heath, A., Major, D., Newman, R. W., Hoschler, K., Junzi, W., et al. (2009). Reproducibility of serologic assays for influenza virus A (H5N1). *Emerging Infectious Diseases*, *15*(8), 1250–1259. doi:10.3201/eid1508.081754

Su, B., Wurtzer, S., Rameix-Welti, M.-A., Dwyer, D., van der Werf, S., Naffakh, N., et al. (2009).

Enhancement of the influenza a hemagglutinin (HA)-mediated cell-cell fusion and virus entry by the viral neuraminidase (NA). *PLoS ONE*, *4*(12), e8495. doi:10.1371/journal.pone.0008495

Su, C. Y., Wang, S. Y., Shie, J. J., Jeng, K. S., Temperton, N. J., Fang, J. M., et al. (2008). In vitro evaluation of neuraminidase inhibitors using the neuraminidase-dependent release assay of hemagglutinin-pseudotyped viruses. *Antiviral Research*, *79*(3), 199–205. doi:10.1016/j.antiviral.2008.03.002

Su, Y., Zhu, X., Wang, Y., Wu, M., & Tien, P. (2008). Evaluation of Glu11 and Gly8 of the H5N1 influenza hemagglutinin fusion peptide in membrane fusion using pseudotype virus and reverse genetics. *Archives of Virology*, *153*(2), 247–257. doi:10.1007/s00705-007-1088-9

Sui, J., Hwang, W. C., Perez, S., Wei, G., Aird, D., Chen, L., et al. (2009). Structural and functional bases for broad-spectrum neutralization of avian and human influenza A viruses. *Nature structural & molecular biology*, *16*(3), 265–273. doi:10.1038/nsmb.1566

Sui, J., Hwang, W. C., Perez, S., Wei, G., Aird, D., Chen, L., et al. (2009). Strutural and Functional bases for broad spectrum neutralization of Avian and human influenza A viruses. *Nat Struct Mol Biol*, *16*(3), 265–273. doi:10.1038/nsmb.1566.Structural

Sui, J., Sheehan, J., Hwang, W. C., Bankston, L. A., Burchett, S. K., Huang, C. Y., et al. (2011). Wide prevalence of heterosubtypic broadly neutralizing human anti-influenza a antibodies. *Clinical Infectious Diseases*, *52*(8), 1003–1009. doi:10.1093/cid/cir121

Sulli, C., Banik, S. S. R., Schilling, J., Moser, A., Xiang, X., Payne, R., et al. (2013). Detection of proton movement directly across viral membranes to identify novel influenza virus M2 inhibitors. *Journal of virology*, *87*(19), 10679–86. doi:10.1128/JVI.01190-13

Sun, X., Shi, Y., Lu, X., He, J., Gao, F., Yan, J., et al. (2013). Bat-Derived Influenza Hemagglutinin H17 Does Not Bind Canonical Avian or Human Receptors and Most Likely Uses a Unique Entry Mechanism. *Cell Reports*, *3*(3), 769–778. doi:10.1016/j.celrep.2013.01.025

Sundquist, W. I., & Kräusslich, H. G. (2012). HIV-1 assembly, budding, and maturation. *Cold Spring Harbor Perspectives in Medicine*, *2*(7), 1–24. doi:10.1101/cshperspect.a006924

Takeda, K., & Akira, S. (2004). Microbial recognition by Toll-like receptors. *Journal of Dermatological Science*, *34*(2), 73–82. doi:10.1016/j.jdermsci.2003.10.002

Talekar, A., Pessi, A., Glickman, F., Sengupta, U., Briese, T., Whitt, M. A., et al. (2012). Rapid Screening for Entry Inhibitors of Highly Pathogenic Viruses under Low-Level Biocontainment. *PLoS ONE*, *7*(3), e30538. doi:10.1371/journal.pone.0030538

Tamura, S., & Kurata, T. (2004). Defense mechanisms against influenza virus infection in the respiratory tract mucosa. *Japanese journal of infectious diseases*, *57*(6), 236–47.

http://www.ncbi.nlm.nih.gov/pubmed/15623947. Accessed 26 September 2017

Tang, D.-J. J., Lam, Y.-M. M., Siu, Y.-L. L., Lam, C.-H. H., Chu, S.-L. L., Peiris, J. S. M., et al. (2012). A Single Residue Substitution in the Receptor-Binding Domain of H5N1 Hemagglutinin Is Critical for Packaging into Pseudotyped Lentiviral Particles. *PLoS ONE*, *7*(11), e43596. doi:10.1371/journal.pone.0043596

Tang, Y., Zaitseva, F., Lamb, R. A., & Pinto, L. H. (2002). The gate of the influenza virus M2 proton channel is formed by a single tryptophan residue. *Journal of Biological Chemistry*, *277*(42), 39880–39886. doi:10.1074/jbc.M206582200

Tanimoto, T., Nakatsu, R., Fuke, I., Ishikawa, T., Ishibashi, M., Yamanishi, K., et al. (2005). Estimation of the neuraminidase content of influenza viruses and split-product vaccines by immunochromatography. *Vaccine*, *23*(37), 4598–4609. doi:10.1016/j.vaccine.2005.04.042

Tao, L., Chen, J., Meng, J., Chen, Y., Li, H., Liu, Y., et al. (2013). Enhanced protective efficacy of H5 subtype influenza vaccine with modification of the multibasic cleavage site of hemagglutinin in retroviral pseudotypes. *Virologica Sinica*, *28*(3), 136–145. doi:10.1007/s12250-013-3326-5

te Velthuis, A. J. W., & Fodor, E. (2016). Influenza virus RNA polymerase: insights into the mechanisms of viral RNA synthesis. *Nature Reviews Microbiology*, *14*(8), 479–493. doi:10.1038/nrmicro.2016.87

Tefsen, B., Lu, G., Zhu, Y., Haywood, J., Zhao, L., Deng, T., et al. (2014). The N-Terminal Domain of PA from Bat-Derived Influenza-Like Virus H17N10 Has Endonuclease Activity. *Journal of Virology*, *88*(4), 1935–1941. doi:10.1128/JVI.03270-13

Temperton, N. J., Hoschler, K., Major, D., Nicolson, C., Manvell, R., Hien, V. M., et al. (2007). A sensitive retroviral pseudotype assay for influenza H5N1-neutralizing antibodies. *Influenza and other respiratory viruses*, *1*(3), 105–112. doi:10.1111/j.1750-2659.2007.00016.x

Tete, S. M., Krammer, F., Lartey, S., Bredholt, G., Wood, J. M., Skrede, S., & Cox, R. J. (2016). Dissecting the hemagglutinin head and stalk-specific IgG antibody response in healthcare workers following pandemic H1N1 vaccination. *npj Vaccines*, *1*(May), 16001. doi:10.1038/npjvaccines.2016.1

Thompson, M. R., Kaminski, J. J., Kurt-Jones, E. A., Fitzgerald, K. A., Kaminski@umassmed, J., Edu, J. J. K., et al. (2011). Pattern Recognition Receptors and the Innate Immune Response to Viral Infection. *Viruses*, *3*, 920–940. doi:10.3390/v3060920

Thomson, C. A., Wang, Y., Jackson, L. M., Olson, M., Wang, W., Liavonchanka, A., et al. (2012). Pandemic H1N1 influenza infection and vaccination in humans induces cross-protective antibodies that target the hemagglutinin stem. *Frontiers in Immunology*, *3*(MAY), 1–19.

doi:10.3389/fimmu.2012.00087

Throsby, M., van den Brink, E., Jongeneelen, M., Poon, L. L. M., Alard, P., Cornelissen, L. A. H. M., et al. (2008). Heterosubtypic neutralizing monoclonal antibodies cross-protective against H5N1 and H1N1 recovered from human IgM+ memory B cells. *PLoS ONE*, *3*(12). doi:10.1371/journal.pone.0003942

Tisoncik, J. R., Guo, Y., Cordero, K. S., Yu, J., Wang, J., Cao, Y., & Rong, L. (2011). Identification of critical residues of influenza neuraminidase in viral particle release. *Virology journal*, *8*(1), 14. doi:10.1186/1743-422X-8-14

Tong, S., Li, Y., Rivailler, P., Conrardy, C., Castillo, D. A. A., Chen, L.-M., et al. (2012). A distinct lineage of influenza A virus from bats. *Proceedings of the National Academy of Sciences of the United States of America*, *109*(11), 4269–4274. doi:10.1073/pnas.1116200109

Tong, S., Zhu, X., Li, Y., Shi, M., Zhang, J., Bourgeois, M., et al. (2013). New World Bats Harbor Diverse Influenza A Viruses. *PLoS Pathogens*, *9*(10). doi:10.1371/journal.ppat.1003657

Tosh, P. K., Jacobson, R. M., & Poland, G. A. (2010). Influenza vaccines: from surveillance through production to protection. *Mayo Clinic Proceedings*, *85*(3), 257–273. doi:10.4065/mcp.2009.0615

Towers, G. J., Bock, M., Martin, S., Takeuchi, Y., Stoye, J. P., & Danos, O. (2000). A conserved mechanism of retrovirus restriction in mammals. *Proceedings of the National Academy of Sciences of the United States of America*, *97*(22), 12295–12299. doi:10.1073/pnas.200286297

Tran, E. E. H., Podolsky, K. A., Bartesaghi, A., Kuybeda, O., Grandinetti, G., Wohlbold, T. J., et al. (2016). Cryo-electron microscopy structures of chimeric hemagglutinin displayed on a universal influenza vaccine candidate. *mBio*, *7*(2), 1–9. doi:10.1128/mBio.00257-16

Treanor, J. J., Tierney, E. L., Zebedee, S. L., Lamb, R. A., & Murphy, B. R. (1990). Passively transferred monoclonal antibody to the M2 protein inhibits influenza A virus replication in mice. *Journal of virology*, *64*(3), 1375–7. http://www.ncbi.nlm.nih.gov/pubmed/2304147. Accessed 26 September 2017

Tripathi, S., White, M. R., & Hartshorn, K. L. (2015). The amazing innate immune response to influenza A virus infection. *Innate Immunity*, *21*(1), 73–98. doi:10.1177/1753425913508992

Trombetta, C., Perini, D., Mather, S. T., Temperton, N. J., & Montomoli, E. (2014). Overview of Serological Techniques for Influenza Vaccine Evaluation: Past, Present and Future. *Vaccines*, *2*(4), 707–734. doi:10.3390/vaccines2040707

Tsai, C., Caillet, C., Hu, H., Zhou, F., Ding, H., Zhang, G., et al. (2009). Measurement of neutralizing antibody responses against H5N1 clades in immunized mice and ferrets using pseudotypes

expressing influenza hemagglutinin and neuraminidase. *Vaccine*, *27*(48), 6777–6790. doi:10.1016/j.vaccine.2009.08.056

Turan, K., Mibayashi, M., Sugiyama, K., Saito, S., Numajiri, A., & Nagata, K. (2004). Nuclear MxA proteins form a complex with influenza virus NP and inhibit the transcription of the engineered influenza virus genome. *Nucleic Acids Research*, *32*(2), 643–652. doi:10.1093/nar/gkh192

Turner, R., Lathey, J. L., Van Voris, L. P., & Belshe, R. B. (1982). Serological diagnosis of influenza B virus infection: comparison of an enzyme-linked immunosorbent assay and the hemagglutination inhibition test. *J Clin Microbiol*, *15*(5), 824–829. http://www.ncbi.nlm.nih.gov/pubmed/7047553. Accessed 24 April 2017

Vaerman, J, P. (1981). Single radial immunodiffusion. *Methods in Enzymology*, *73*, 291–305.

Valkenburg, S. A., Mallajosyula, V. V. A., Li, O. T. W., Chin, A. W. H., Carnell, G. W., Temperton, N. J., et al. (2016). Stalking influenza by vaccination with pre-fusion headless HA mini-stem. *Nature Publishing Group*, *6*, 1–11. doi:10.1038/srep22666

Van Kerkhove, M. D., Broberg, E., Engelhardt, O. G., Wood, J. M., Nicoll, A., & CONSISE steering committee. (2013). The consortium for the standardization of influenza seroepidemiology (CONSISE): a global partnership to standardize influenza seroepidemiology and develop influenza investigation protocols to inform public health policy. *Influenza and Other Respiratory Viruses*, *7*(3), 231–234. doi:10.1111/irv.12068

Varghese, J. N., & Colman, P. M. (1991). Three-dimensional structure of the neuraminidase of influenza virus A/Tokyo/3/67 at 2·2 Å resolution. *Journal of Molecular Biology*, *221*(2), 473–486. doi:10.1016/0022-2836(91)80068-6

Vella, S., Rocchi, G., Resta, S., Marcelli, M., & Felici, A. De. (1980). Antibody reactive in antibody-dependent cell-mediated cytotoxicity following influenza virus vaccination. *Journal of Medical Virology*, *6*(3), 203–211. doi:10.1002/jmv.1890060303

Verma, S., Soto, J., Vasudevan, A., Schmeisser, F., Alvarado-Facundo, E., Wang, W., et al. (2017). Determination of influenza B identity and potency in quadrivalent inactivated influenza vaccines using lineage-specific monoclonal antibodies. *Plos One*, *12*(4), e0175733. doi:10.1371/journal.pone.0175733

Vlahos, R., Stambas, J., Bozinovski, S., Broughton, B. R. S., Drummond, G. R., & Selemidis, S. (2011). Inhibition of Nox2 Oxidase Activity Ameliorates Influenza A Virus-Induced Lung Inflammation. *PLoS Pathogens*, *7*(2), e1001271. doi:10.1371/journal.ppat.1001271

Wallerstrom, S., Lagerqvist, N., Temperton, N. J., Cassmer, M., Moreno, A., Karlsson, M., et al. (2014). Detection of antibodies against H5 and H7 strains in birds: evaluation of influenza

pseudovirus particle neutralization tests. *Infection Ecology and Epidemiology*, *4*, 1–8. doi:10.3402/iee.v4.23011

Wang, C., Lamb, R. A., & Pinto, L. H. (1995). Activation of the M2 ion channel of influenza virus: a role for the transmembrane domain histidine residue. *Biophysical Journal*, *69*(4), 1363–1371. doi:10.1016/S0006-3495(95)80003-2

Wang, H., Ma, C., Lu, Y., Ji, X., Pang, Y., Hua, F., et al. (2013). Generation of human neutralizing monoclonal antibodies against the 2009 pandemic H1N1 virus from peripheral blood memory B lymphocytes. *Cellular & molecular immunology*, *10*(May), 1–10. doi:10.1038/cmi.2013.25

Wang, J., Cheng, H., Ratia, K., Varhegyi, E., Hendrickson, W. G., Li, J., & Rong, L. (2014). A comparative high-throughput screening protocol to identify entry inhibitors of enveloped viruses. *Journal of biomolecular screening*, *19*(1), 100–7. doi:10.1177/1087057113494405

Wang, S.-Y., Su, C.-Y., Mengi Lin, Huang, S.-Y., Huang, W.-I., Wang, C.-C., et al. (2009). HA-pseudotyped retroviral vectors for influenza antagonist screening. *Journal of Biomolecular Screening*, *14*(3), 294–302. doi:10.1177/1087057108330786

Wang, T. T., Tan, G. S., Hai, R., Pica, N., Petersen, E., Moran, T. M., & Palese, P. (2010). Broadly protective monoclonal antibodies against H3 influenza viruses following sequential immunization with different hemagglutinins. *PLoS Pathogens*, *6*(2), e1000796. doi:10.1371/journal.ppat.1000796

Wang, W., Anderson, C. M., de Feo, C. J., Zhuang, M., Yang, H., Vassell, R., et al. (2011). Cross-neutralizing antibodies to pandemic 2009 H1N1 and recent seasonal H1N1 influenza a strains influenced by a mutation in hemagglutinin subunit 2. *PLoS Pathogens*, *7*(6), e1002081. doi:10.1371/journal.ppat.1002081

Wang, W., Butler, E. N., Veguilla, V., Vassell, R., Terrig Thomas, J., Moos, M., et al. (2008). Establishment of retroviral pseudotypes with influenza hemagglutinins from H1, H3, and H5 subtypes for sensitive and specific detection of neutralizing antibodies. *Journal of Virological Methods*, *153*(2), 111–119. doi:10.1016/j.jviromet.2008.07.015

Wang, W., Castelán-Vega, J. A., Jiménez-Alberto, A., Vassell, R., Ye, Z., & Weiss, C. D. (2010). A mutation in the receptor binding site enhances infectivity of 2009 H1N1 influenza hemagglutinin pseudotypes without changing antigenicity. *Virology*, *407*(2), 374–380. doi:10.1016/j.virol.2010.08.027

Wang, W., Peng, H., Tao, Q., Zhao, X., Tang, H., Tang, Z., et al. (2014). Serologic assay for avian-origin influenza A (H7N9) virus in adults of Shanghai, Guangzhou and Yunnan, China. *Journal of Clinical Virology*, *60*(3), 305–308. doi:10.1016/j.jcv.2014.04.006

Wang, W., Xie, H., Ye, Z., Vassell, R., & Weiss, C. D. (2010). Characterization of lentiviral pseudotypes with influenza H5N1 hemagglutinin and their performance in neutralization assays. *Journal of Virological Methods*, *165*(2), 305–310. doi:10.1016/j.jviromet.2010.02.009

Warren, L. (1959). The Thiobarbituric Acid Assay of Sialic Acids. *The Journal of biological chemistry*, *234*(8), 1971–1975.

Wei, C.-J., Boyington, J. C., Dai, K., Houser, K. V, Pearce, M. B., Kong, W.-P., et al. (2010). Cross-neutralization of 1918 and 2009 influenza viruses: role of glycans in viral evolution and vaccine design. *Science translational medicine*, *2*(24), 24ra21. doi:10.1126/scitranslmed.3000799

Wei, C.-J., Boyington, J. C., McTamney, P. M., Kong, W.-P., Pearce, M. B., Xu, L., et al. (2010). Induction of broadly neutralizing H1N1 influenza antibodies by vaccination. *Science (New York, N.Y.)*, *329*(5995), 1060–4. doi:10.1126/science.1192517

Wei, C.-J., Xu, L., Kong, W.-P., Shi, W., Canis, K., Stevens, J., et al. (2008). Comparative efficacy of neutralizing antibodies elicited by recombinant hemagglutinin proteins from avian H5N1 influenza virus. *Journal of virology*, *82*(13), 6200–6208. doi:10.1128/JVI.00187-08

Wei, C.-J., Yassine, H. M., McTamney, P. M., Gall, J. G. D., Whittle, J. R. R., Boyington, J. C., & Nabel, G. J. (2012). Elicitation of Broadly Neutralizing Influenza Antibodies in Animals with Previous Influenza Exposure. *Science Translational Medicine*, *4*(147), 147ra114-147ra114. doi:10.1126/scitranslmed.3004273

Weir, J. P., & Gruber, M. F. (2016). An overview of the regulation of influenza vaccines in the United States. *Influenza and other Respiratory Viruses*, *10*(5), 354–360. doi:10.1111/irv.12383

Wen, Y., Han, L., Palladino, G., Ferrari, A., Xie, Y., Carfi, A., et al. (2015). Conformationally selective biophysical assay for influenza vaccine potency determination. *Vaccine*, *33*(41), 5342–5349. doi:10.1016/j.vaccine.2015.08.077

West, A. P., Shadel, G. S., & Ghosh, S. (2011). Mitochondria in innate immune responses. *Nature Reviews Immunology*, *11*(6), 389–402. doi:10.1038/nri2975

Westgeest, K. B., Bestebroer, T. M., Spronken, M. I. J., Gao, J., Couzens, L., Osterhaus, A. D., et al. (2015). Optimization of an enzyme-linked lectin assay suitable for rapid antigenic characterization of the neuraminidase of human influenza A(H3N2) viruses. *Journal of Virological Methods*, *217*, 55–63. doi:10.1158/1078-0432.CCR-15-0428.Bioactivity

Wetherall, N. T., Trivedi, T., Zeller, J., Hodges-Savola, C., McKimm-Breschkin, J. L., Zambon, M. C., & Hayden, F, G. (2003). Evaluation of Neuraminidase Enzyme Assays Using Different Substrates To Measure Susceptibility of Influenza Virus Clinical Isolates to Neuraminidase Inhibitors: Report of the Neuraminidase Inhibitor Susceptibility Network. *Journal of Clinical Microbiology*,

41(2), 742–750. doi:10.1128/JCM.41.2.742

Whittaker, G. R., Bui, M., & Helenius, A. (1996). The role of nuclear import and export in influenza virus infection. *Trends in cell biology*, *6*(2), 67–71. http://www.ncbi.nlm.nih.gov/pubmed/15157497

Whittle, J. R. R., Wheatley, A. K., Wu, L., Lingwood, D., Kanekiyo, M., Ma, S. S., et al. (2014). Flow cytometry reveals that H5N1 vaccination elicits cross-reactive stem-directed antibodies from multiple Ig heavy-chain lineages. *J Virol*, *88*(8), 4047–4057. doi:10.1128/JVI.03422-13

WHO. (2003). WHO Factsheet FS211. http://www.who.int/mediacentre/factsheets/2003/fs211/en/

WHO. (2011). World Health Organization Global Influenza Surveillance Network (GISN). 2011. Manual for the laboratory diagnosis and virological surveillance of influenza.

WHO. (2014). Who Fact Sheet. *WHO Fact Sheets*. http://www.who.int/mediacentre/factsheets/fs312/en/#

WHO. (2016). Weekly epidemiological record:, *88*(7), 73–81. doi:10.1016/j.actatropica.2012.04.013.

Wiley, D. C., & Skehel, J. J. (1987). The Structure and Function of the Haemagglutinin Membrane Glycoprotein of Influenza Virus. *Annu. Rev. Biochem.*, *56*, 365–394. doi:10.1146/annurev.biochem.56.1.365

Wiley, D. C., Wilson, I. A., & Skehel, J. J. (1981). Structural identification of the antibody-binding sites of Hong Kong influenza haemagglutinin and their involvement in antigenic variation. *Nature*, *289*(5796), 373–378. doi:10.1038/289373a0

Williams, C. J., Schweiger, B., Diner, G., Gerlach, F., Haaman, F., Krause, G., et al. (2010). Seasonal influenza risk in hospital healthcare workers is more strongly associated with household than occupational exposures: results from a prospective cohort study in Berlin, Germany, 2006/07. *BMC infectious diseases*, *10*, 8. doi:10.1186/1471-2334-10-8

Williams, M. S. (1993). Single-radial-immunodiffusion as an in vitro potency assay for human inactivated viral vaccines. *Veterinary Microbiology*, *37*(3–4), 253–262. doi:10.1016/0378-1135(93)90027-5

Williams, M. S., Mayner, R. E., Daniel, N. J., Phelan, M. A., Rastogi, S. C., Bozeman, F. M., & Ennis, F. A. (1980). New developments in the measurement of the hemagglutinin content of influenza virus vaccines by single-radial-immunodiffusion. *Journal of Biological Standardization*, *8*(4), 289–96. doi:10.1016/S0092-1157(80)80006-0

Wise, H. M., Foeglein, A., Sun, J., Dalton, R. M., Patel, S., Howard, W. A., et al. (2009). A complicated message: Identification of a novel PB1-related protein translated from influenza A virus segment 2 mRNA. *Journal of virology*, *83*(16), 8021–31. doi:10.1128/JVI.00826-09

Wise, H. M., Hutchinson, E. C., Jagger, B. W., Stuart, A. D., Kang, Z. H., Robb, N. C., et al. (2012). Identification of a Novel Splice Variant Form of the Influenza A Virus M2 Ion Channel with an Antigenically Distinct Ectodomain. *PLoS Pathogens*, *8*(11), e1002998. doi:10.1371/journal.ppat.1002998

Wise, T. G., Dolin, R., Mazur, M. H., Top, F. H., Edelman, R., & Ennis, F. A. (1977). Serologic responses and systemic reactions in adults after vaccination with bivalent A/victoria/75-A/new jersey/76 and monovalent B/hong kong/72 influenza vaccines. *Journal of Infectious Diseases*, *136*(4), S507–S517. doi:10.1093/infdis/136.Supplement_3.S507

Wisskirchen, C., Ludersdorfer, T. H., Muller, D. A., Moritz, E., & Pavlovic, J. (2011). The Cellular RNA Helicase UAP56 Is Required for Prevention of Double-Stranded RNA Formation during Influenza A Virus Infection. *Journal of Virology*, *85*(17), 8646–8655. doi:10.1128/JVI.02559-10

Witte, K., Witte, E., Sabat, R., & Wolk, K. (2010). IL-28A, IL-28B, and IL-29: Promising cytokines with type I interferon-like properties. *Cytokine & Growth Factor Reviews*, *21*(4), 237–251. doi:10.1016/j.cytogfr.2010.04.002

Wohlbold, T. J., & Krammer, F. (2014). In the shadow of hemagglutinin: A growing interest in influenza viral neuraminidase and its role as a vaccine antigen. *Viruses*, *6*(6), 2465–2494. doi:10.3390/v6062465

Wolint, P., Betts, M. R., Koup, R. A., & Oxenius, A. (2004). Immediate cytotoxicity but not degranulation distinguishes effector and memory subsets of CD8+ T cells. *The Journal of experimental medicine*, *199*(7), 925–36. doi:10.1084/jem.20031799

Wood, J. M., Schild, G. C., Newman, R. W., & Seagroatt, V. (1977). An improved single-radial-immunodiffusion technique for the assay of influenza haemagglutinin antigen: Application for potency determinations of inactivated whole virus and subunit vaccines. *Journal of Biological Standardization*, *5*(3), 237–47. doi:10.1016/S0092-1157(77)80008-5

Wrammert, J., Koutsonanos, D., Li, G. M., Edupuganti, S., Sui, J., Morrissey, M., et al. (2011). Broadly cross-reactive antibodies dominate the human B cell response against 2009 pandemic H1N1 influenza virus infection. *The Journal of Experimental Medicine*, *208*(1), 181–193. doi:10.1084/jem.20101352

Wright, E., Hayman, D. T. S., Vaughan, A., Temperton, N. J., Wood, J. L. N., Cunningham, A. A., et al. (2010). Virus neutralising activity of African fruit bat (Eidolon helvum) sera against emerging lyssaviruses. *Virology*, *408*(2), 183–189. doi:10.1016/j.virol.2010.09.014

Wright, P. F., Cherry, J. D., Foy, H. M., Glezen, W. P., Hall, C. B., McIntosh, K., et al. (1983). Antigenicity and reactogenicity of influenza A/USSR/77 virus vaccine in children--a multicentered evaluation of dosage and safety. *Rev Infect Dis*, *5*(4), 758–764.

http://www.ncbi.nlm.nih.gov/pubmed/6353530. Accessed 24 April 2017

Wu, A., Peng, Y., Du, X., Shu, Y., & Jiang, T. (2010). Correlation of influenza virus excess mortality with antigenic variation: Application to rapid estimation of influenza mortality burden. *PLoS Computational Biology*, *6*(8). doi:10.1371/journal.pcbi.1000882

Wu, J., Zhang, F., Wang, M., Xu, C., Song, J., Zhou, J., et al. (2010). Characterization of neuraminidases from the highly pathogenic avian H5N1 and 2009 pandemic H1N1 influenza a viruses. *PLoS ONE*, *5*(12), e15825. doi:10.1371/journal.pone.0015825

Wu, Q., Fang, L., Wu, X., Li, B., Luo, R., Yu, Z., et al. (2009). A pseudotype baculovirus-mediated vaccine confers protective immunity against lethal challenge with H5N1 avian influenza virus in mice and chickens. *Molecular Immunology*, *46*(11–12), 2210–2217. doi:10.1016/j.molimm.2009.04.017

Xu, R., Ekiert, D. C., Krause, J. C., Hai, R., Crowe, J. E., & Wilson, I. A. (2010). Structural basis of pre-existing immunity to the 2009 H1N1 pandemic influenza virus, *328*(5976), 357–360. doi:10.1126/science.1186430.Structural

Yamayoshi, S., Watanabe, M., Goto, H., & Kawaoka, Y. (2015). Identification of a Novel Viral Protein Expressed from the PB2 Segment of Influenza A Virus. *Journal of virology*, *90*(1), 444–56. doi:10.1128/JVI.02175-15

Yan, N., & Chen, Z. J. (2012). Intrinsic antiviral immunity. *Nature immunology*, *13*(3), 214–22. doi:10.1038/ni.2229

Yang, D.-G., Chung, Y.-C., Lai, Y.-K., Lai, C.-W., Liu, H.-J., & Hu, Y.-C. (2007). Avian Influenza Virus Hemagglutinin Display on Baculovirus Envelope: Cytoplasmic Domain Affects Virus Properties and Vaccine Potential. *Molecular Therapy*, *15*(5), 989–996. doi:10.1038/mt.sj.6300131

Yang, J., Li, W., Long, Y., Song, S., Liu, J., Zhang, X., et al. (2014). Reliability of pseudotyped influenza viral particles in neutralizing antibody detection. *PLoS ONE*, *9*(12), e113629. doi:10.1371/journal.pone.0113629

Yassine, H. M., Boyington, J. C., McTamney, P. M., Wei, C.-J., Kanekiyo, M., Kong, W.-P., et al. (2015). Hemagglutinin-stem nanoparticles generate heterosubtypic influenza protection. *Nature Medicine*, *21*(9), 1065–1070. doi:10.1038/nm.3927

Yen, H., Herlocher, L. M., Hoffmann, E., Matrosovich, M. N., Monto, A. S., Webster, R. G., & Govorkova, E. A. (2005). Neuraminidase inhibitor-resistant influenza viruses may differ substantially in fitness and transmissibility. *Antimicrobial agents and chemotherapy*, *49*(10), 4075–84. doi:10.1128/AAC.49.10.4075-4084.2005

Yen, H., Ilyushina, N. A., Salomon, R., Webster, R. G., Govorkova, E. A., & Hoffmann, E. (2007).

Neuraminidase inhibitor-resistant recombinant A/Vietnam/1203/04 (H5N1) Influenza Viruses Retain Their Replication Efficiency and Pathogenicity In Vitro and In Vivo. *Journal of Virology*, *4*(22), 12418–12426. doi:10.1128/JVI.01067-07

Yin, C., Khan, J. A., Swapna, G. V. T., Ertekin, A., Krug, R. M., Tong, L., & Montelione, G. T. (2007). Conserved Surface Features Form the Double-stranded RNA Binding Site of Non-structural Protein 1 (NS1) from Influenza A and B Viruses. *Journal of Biological Chemistry*, *282*(28), 20584–20592. doi:10.1074/jbc.M611619200

Yoshimura, A., & Ohnishi, S. (1984). Uncoating of influenza virus in endosomes. *Journal of virology*, *51*(2), 497–504. http://www.pubmedcentral.nih.gov/articlerender.fcgi?artid=254465&tool=pmcentrez&rendertype=abstract

Yuan, P., Bartlam, M., Lou, Z., Chen, S., Zhou, J., He, X., et al. (2009). Crystal structure of an avian influenza polymerase PAN reveals an endonuclease active site. *Nature*, *458*(7240), 909–913. doi:10.1038/nature07720

Zhang, J., & Madden, T. L. (1997). PowerBLAST: a new network BLAST application for interactive or automated sequence analysis and annotation. *Genome research*, *7*(6), 649–56. http://www.ncbi.nlm.nih.gov/pubmed/9199938. Accessed 17 August 2017

Zhang, K., Wang, Z., Liu, X., Yin, C., Basit, Z., Xia, B., & Liu, W. (2012). Dissection of influenza A virus M1 protein: PH-dependent oligomerization of N-terminal domain and dimerization of C-terminal domain. *PLoS ONE*, *7*(5), 1–12. doi:10.1371/journal.pone.0037786

Zhang, S., Xiao, L., Zhou, H., Yu, Z., Chen, H., Guo, A., & Jin, M. (2008). Generation and characterization of an H5N1 avian influenza virus hemagglutinin glycoprotein pseudotyped lentivirus. *Journal of Virological Methods*, *154*(1–2), 99–103. doi:10.1016/j.jviromet.2008.08.016

Zhang, Y., Lin, X., Wang, G., Zhou, J., Lu, J., Zhao, H., et al. (2010). Neuraminidase and hemagglutinin matching patterns of a highly pathogenic avian and two pandemic H1N1 influenza A viruses. *PLoS ONE*, *5*(2). doi:10.1371/journal.pone.0009167

Zhang, Y., Lin, X., Zhang, F., Wu, J., Tan, W., Bi, S., et al. (2009). Hemagglutinin and neuraminidase matching patterns of two influenza A virus strains related to the 1918 and 2009 global pandemics. *Biochemical and Biophysical Research Communications*, *387*(2), 405–408. doi:10.1016/j.bbrc.2009.07.040

Zhang, Z., Schwartz, S., Wagner, L., & Miller, W. (2000). A Greedy Algorithm for Aligning DNA Sequences. *Journal of Computational Biology*, *7*(1–2), 203–214. doi:10.1089/10665270050081478

Zhao, R., Cui, S., Guo, L., Wu, C., Gonzalez, R., Paranhos-Baccalà, G., et al. (2011). Identification of a highly conserved H1 subtype-specific epitope with diagnostic potential in the hemagglutinin protein of influenza A virus. *PLoS ONE*, *6*(8), e23374. doi:10.1371/journal.pone.0023374

Zheng, L., Chi, M., Zhonghua, L., Wei, H., Li, Z., Ma, C., et al. (2011). Serologic cross-reactivity among humans and birds infected with highly pathogenic avian influenza A subtype H5N1 viruses in China. *Immunology Letters*, *135*(1–2), 59–63. doi:10.1016/j.imlet.2010.09.012

Zheng, M., Luo, J., & Chen, Z. (2014). Development of universal influenza vaccines based on influenza virus M and NP genes. *Infection*, *42*(2), 251–262. doi:10.1007/s15010-013-0546-4

Zhong, W., Liu, F., Wilson, J. R., Holiday, C., Li, Z.-N., Bai, Y., et al. (2016). Antibody-Dependent Cell-Mediated Cytotoxicity to Hemagglutinin of Influenza A Viruses After Influenza Vaccination in Humans. *Open Forum Infectious Diseases*, *3*(2), ofw102. doi:10.1093/ofid/ofw102

Zhou, B., Ma, J., Liu, Q., Bawa, B., Wang, W., Shabman, R. S., et al. (2014). Characterization of Uncultivable Bat Influenza Virus Using a Replicative Synthetic Virus. *PLoS Pathogens*, *10*(10), e1004420. doi:10.1371/journal.ppat.1004420

Zhou, F., Wang, G., Buchy, P., Cai, Z., Chen, H., Chen, Z., et al. (2012). A triclade DNA vaccine designed on the basis of a comprehensive serologic study elicits neutralizing antibody responses against all clades and subclades of highly pathogenic avian influenza H5N1 viruses. *J Virol*, *86*(12), 6970–6978. doi:10.1128/JVI.06930-11

Zhou, Y., Wu, C., Zhao, L., & Huang, N. (2014). Exploring the early stages of the pH-induced conformational change of influenza hemagglutinin. *Proteins: Structure, Function and Bioinformatics*, *82*(10), 2412–2428. doi:10.1002/prot.24606

Zhu, B., Cai, G., Hall, E. O., & Freeman, G. J. (2007). In-Fusion™ assembly: Seamless engineering of multidomain fusion proteins, modular vectors, and mutations. *BioTechniques*, *43*(3), 354–359. doi:10.2144/000112536

Zhu, X., Yang, H., Guo, Z., Yu, W., Carney, P. J., Li, Y., et al. (2012). Crystal structures of two subtype N10 neuraminidase-like proteins from bat influenza A viruses reveal a diverged putative active site. *Proceedings of the National Academy of Sciences of the United States of America*, *109*(46), 18903–18908. doi:10.1073/pnas.1212579109

Zhu, X., Yu, W., McBride, R., Li, Y., Chen, L.-M., Donis, R. O., et al. (2013). Hemagglutinin homologue from H17N10 bat influenza virus exhibits divergent receptor-binding and pH-dependent fusion activities. *Proceedings of the National Academy of Sciences of the United States of America*, *110*(4), 1458–63. doi:10.1073/pnas.1218509110

Zimmer, G., Locher, S., Rentsch, M. B., & Halbherr, S. J. (2014). Pseudotyping of vesicular stomatitis

virus with the envelope glycoproteins of highly pathogenic avian influenza viruses. *Journal of General Virology*, *95*(PART 8), 1634–1639. doi:10.1099/vir.0.065201-0

Zmora, P., Blazejewska, P., Moldenhauer, A.-S., Welsch, K., Nehlmeier, I., Wu, Q., et al. (2014). DESC1 and MSPL activate influenza A viruses and emerging coronaviruses for host cell entry. *Journal of virology*, *88*(20), 12087–97. doi:10.1128/JVI.01427-14

Zufferey, R., Dull, T., Mandel, R. J., Bukovsky, A., Quiroz, D., Naldini, L., & Trono, D. (1998). Self-inactivating lentivirus vector for safe and efficient in vivo gene delivery. *Journal of virology*, *72*(12), 9873–80. doi:99030895

Zufferey, R., Nagy, D., Mandel, R. J., Naldini, L., & Trono, D. (1997). Multiply attenuated lentiviral vector achieves efficient gene delivery in vivo. *Nat Biotechnol*, *15*(9), 871–875. doi:10.1038/nbt0997-871

Appendix

Appendix X1

Jenner Sera, obtained from the Jenner institute laboratories, University of Oxford. Serum ID#, age at enrolment (if available), date of sample collection as well as pMN neutralising antibody titres (IC_{50}) against A/duck/Memphis/546/1974, A/California/7/2009 and CS CHM are displayed.

			Average IC_{50}		
ID#	**Age at enrolment**	**Sample date**	**H11**	**CA/09**	**CHM**
1	47	29.07.08	5	2263	194
2	31	29.07.08	10	3263	287
3	28	31.07.08	0	2629	68
4	-	04.08.08	0	2172	136
5	34	12.08.08	35	2307	512
6	23	13.08.08	17	2931	174
7	24	14.08.08	0	2958	149
8	-	14.08.08	100	3924	1242
9	43	21.08.08	2	4050	674
10	21	29.08.08	6	4956	169
11	32	11.09.08	4	4146	1167
12	27	15.09.08	0	3275	421
13	49	16.10.08	0	2085	141
14	25	05.01.09	0	2389	126
15	24	05.01.09	10	3271	77
16	22	22.01.09	0	1716	78
17	-	28.01.09	0	9274	308
18	20	10.02.09	0	7388	801
19	41	19.02.09	45	3321	423
20	23	7.09.09	0	1116	137
21	45	16.03.10	1883	13444	3492
22	35	16.03.10	40	3223	613
23	18	16.03.10	0	1414	108
24	-	07.04.10	429	2033	1820
25	28	13.04.10	10	1757	132
26	47	13.04.10	423	2374	543
27	23	15.04.10	0	7171	1217
28	23	27.04.10	853	6139	2826
29	29	17.05.10	0	2116	554
30	51	17.05.10	33	1470	739
31	-	24.05.10	108	1492	756

32	-	24.05.10	133	3217	1440
33	54	15.06.10	851	2943	2887
34	-	17.08.10	503	3869	1368
35	66	07.09.10	49	2035	257
36	63	24.09.10	54	2866	530
37	50	05.10.10	284	5356	2122
38	91	26.10.10	126	4208	1540
39	66	26.10.10	435	3076	1194
40	54	17.11.10	207	3540	2942
41	54	17.11.10	93	4109	225
42	-	17.11.10	95	1616	211
43	58	17.11.10	288	3143	812
44	59	14.12.10	1257	7956	1921
45	63	14.12.10	553	2194	755
46	54	14.12.10	151	2555	1654
47	61	14.12.10	336	9401	5420
48	-	03.08.11	547	3472	1924
49	-	09.08.11	45	1728	775
50	59	16.08.11	78	1989	484
51	62	25.08.11	-	2684	612
52	59	25.08.11	37	1524	282
53	78	13.09.11	165	5547	1038
54	61	13.09.11	157	2267	1058
55	75	29.09.11	394	3152	863
56	65	29.09.11	268	4016	2767
57	-	27.10.11	791	1757	3250
58	-	01.11.11	3	1802	851
59	-	02.11.11	107	6219	901
60	85	15.12.11	68	7505	1103
61	63	04.01.12	211	4797	2264
62	60	31.01.12	-	4101	458
63	58	01.02.12	380	6718	1563
64	63	01.03.12	428	4623	1656
65	76	28.03.12	3	3349	786
66	82	28.03.12	935	7547	3043
67	56	28.03.12	2	1337	225
68	72	04.05.12	1429	-	4248
69	63	04.05.12	398	6729	2547
70	80	09.05.12	157	3184	1005
71	75	09.05.12	80	6473	711
72	83	22.05.12	3	2838	396
73	60	16.05.12	233	6134	804
74	40	20.06.12	25	2191	552
75	58	12.07.12	63	4008	1508
76	57	12.07.12	132	6236	1071

77	62	25.07.12	204	4430	6625
78	28	31.07.12	23	2806	591
79	26	02.08.12	-	2686	1033
80	62	02.08.12	539	--	1632
81	65	20.08.12	409	3708	1235
82	24	23.08.12	-	2490	779
83	29	28.08.12	12	4356	216
84	26	28.08.12	302	6078	1010
85	-	30.08.12	401	2528	650
86	23	12.09.12	-	11547	668
87	-	12.09.12	-	23954	901
88	79	12.09.12	272	3011	1120
89	67	13.09.12	38	6161	1294
90	42	19.09.12	213	5824	4322
91	-	20.09.12	89	3770	1350
92	47	20.09.12	196	3757	2466
93	53	21.11.12	306	-	722
94	32	03.10.12	-	1882	524
95	49	09.10.12	145	1758	653
96	21	09.10.12	79	684	489
97	20	31.10.12	9	10636	561
98	21	31.10.12	1	4586	811
99	21	31.10.12	-	3738	3277
100	21	09.01.13	128	3429	775
101	-	19.08.13	8	5586	138
102	22	26.09.13	183	6212	1977
103	22	26.09.13	3	2417	166
104	20	18.10.13	-	4022	760
105	22	12.12.13	117	5947	578
106	21	05.03.14	491	15535	5008
107	-	19.03.14	340	7964	1071
108	-	19.03.14	490	6071	435
109	20	10.04.14	98	7487	724
110	20	10.04.14	98	7487	724
111	39	28.04.14	425	5789	1206
112	22	13.05.14	61	8123	343
113	21	15.05.14	185	-	312
114	24	15.07.14	1	3803	53
115	22	25.09.14	43	6998	106
116	29	04.11.14	63	5386	484
117	23	08.01.15	39	8407	440
118	20	13.01.15	144	7016	1649
119	64	15.01.15	7	5090	313
120	27	23.02.15	239	9394	2773
121	25	26.01.15	-	6179	691

122	21	28.01.15	8	7687	630
123	24	04.02.15	9	6208	1524
124	24	04.02.15	5	8423	485
125	25	04.02.15	7	-	1021
126	22	05.02.15	47	8611	2017
127	22	10.02.15	532	-	8445
128	25	11.02.15	357	7630	2302
129	45	11.02.15	39	3560	396
130	78	12.02.15	3	2347	561
131	23	18.02.15	7	8166	235
132	46	04.03.15	72	9743	1297
133	21	05.03.15	2	4205	439
134	21	09.03.15	11	6524	475
135	21	09.03.15	178	6163	1336
136	58	21.03.15	66	4149	1471
137	36	26.03.15	93	2742	830
138	21	26.03.15	3	5628	80
139	52	26.03.15	493	4760	1111
140	60	26.03.15	174	2969	1262
141	61	26.03.15	35	3023	579
142	62	15.04.15	-	1726	1307
143	57	15.04.15	549	4207	2528
144	52	16.04.15	154	7658	3148
145	65	16.04.15	752	4691	2604
146	64	16.04.15	6	2735	713
147	38	23.04.15	97	4203	959
148	29	24.04.15	45	6531	638
149	21	3.05.15	-	6084	634
150	24	20.05.15	15	3384	1009
151	20	14.05.15	198	8530	1672
152	22	13.05.15	1	5890	5540
153	28	19.05.15	3	3991	461
154	21	13.05.15	7	5833	2160
155	26	13.05.15	167	5040	1405
156	24	20.05.15	7	17860	883
157	19	13.05.15	434	7965	2206
158	27	27.05.15	84	3382	595
159	66	11.05.15	387	3249	1338
160	54	11.05.15	280	4451	3634
161	68	18.05.15	-	1354	1627
162	-	18.05.15	143	3279	-
163	56	11.05.15	705	11462	1856
164	63	11.05.15	39	4910	1471
165	70	18.05.15	510	8439	3141
166	67	18.05.15	382	3581	2633

167	50	21.05.15	25	1128	229
168	72	11.05.15	746	17958	6739
169	55	13.05.15	-	867	226
170	52	18.05.15	147	1573	2863
171	63	18.05.15	292	7916	1636
172	67	21.05.15	236	4075	1333
173	-	21.05.15	-	3683	363
174	22	01.06.15	42	7759	1192
175	22	01.06.15	66	8711	754
176	22	04.06.15	46	4219	702
177	23	08.06.15	42	4488	612
178	54	28.09.16	165	1490	578
179	-	26.10.16	191	-	923

Appendix X2

Sports Science Sera, obtained from Dr Glen Davidson, University of Kent. Serum ID# is displayed alongside pMN neutralising antibody titres (IC50) against group 1 (A/Brisbane/59/2007 (H1) and A/Vietnam/1194/2004 (H5)) and group 2(A/Udorn/307/1972 (H3) and A/Shanghai/2/2013 (H7)) influenza PV.

Group 1 Influenza PV

A/Brisbane/59/2007 (H1) IC_{50}		
ID	**0V**	**12V**
0	761	752
1	1504	5122
2	2404	937
3	1845	2202
4	9188	6515
5	7013	16548
6	783	1156
7	9226	2823
8	6817	3761
9	7032	2035
11	5309	5035
12	3161	2825
13	757	438
14	690	578
15	13736	2646
16	1771	2196
18	2592	4539
19	3194	4794
21	2303	2011
22	6050	2223
23	5298	4303
24	2716	3429
26	2600	9783
27	3699	1959
28	1580	3660
29	6089	8584
30	3832	10660
31	4251	5016
32	1301	15391
34	2100	2537
35	10275	6095
36	4683	17408
37	4319	3011

A/Vietnam/1194/2004 (H5) IC_{50}		
ID	**0V**	**12V**
0	332	123
1	233	262
2	102	257
3	531	1126
4	427	518
5	6107	2421
6	1209	1039
7	2257	1835
8	1105	7007
9	1256	1211
11	459	355
12	655	665
13	355	383
14	382	404
15	1006	1082
16	725	122
18	754	366
19	259	172
21	203	375
22	419	1342
23	1107	1364
24	1047	2074
26	1285	1701
27	171	229
28	413	538
29	1063	688
30	846	545
31	467	639
32	175	161
34	19	41
35	1107	1086
36	62	85
37	1058	828

38	7181	1986	**38**	94	63
39	4255	3561	**39**	226	137
40	1661	4148	**40**	33	23
41	44354	27972	**41**	724	584
42	8286	3528	**42**	40	25
44	10186	7586	**44**	169	175
45	4013	6750	**45**	736	386
46	6091	5213	**46**	288	763
47	9125	3779	**47**	99	187
48	1450	1953	**48**	60	52
49	13533	14031	**49**	799	415
50	14443	3830	**50**	509	628
51	2221	9298	**51**	63	109
53	1415	4478	**53**	125	6
54	19333	32973	**54**	140	3
55	2137	3694	**55**	9	34
56	4016	3747	**56**	414	670
57	1650	1614	**57**	-	5
58	25325	89154	**58**	36	25
59	8931	25241	**59**	204	206
60	45409	10518	**60**	187	1782

Group 2 Influenza PV

A/Udorn/307/1972 (H3) IC_{50}			**A/Shanghai/2/2013 (H7) IC_{50}**		
ID	**0V**	**12V**	**ID**	**0V**	**12V**
0	1484	3747	**0**	602	914
1	1535	3249	**1**	590	921
2	3106	2482	**2**	899	483
3	4437	5858	**3**	963	1423
4	1508	1244	**4**	1760	774
5	5856	4769	**5**	412	781
6	1169	1837	**6**	917	1623
7	2401	2622	**7**	554	507
8	3084	2441	**8**	1129	341
9	8170	5560	**9**	3323	1797
11	1511	4293	**11**	212	153
12	1618	6789	**12**	1106	582
13	1764	3013	**13**	281	602
14	1548	7454	**14**	665	202
15	2300	1629	**15**	376	1100
16	2351	3341	**16**	21	87
18	3834	16920	**18**	243	365
19	4374	5416	**19**	121	254

21	2124	11279	**21**	211	149
22	6242	5500	**22**	226	272
23	4618	7714	**23**	416	987
24	7580	2574	**24**	402	674
26	4371	8359	**26**	782	1423
27	2379	2151	**27**	423	378
28	8138	15213	**28**	840	2236
29	3061	4473	**29**	75	165
30	4230	3679	**30**	442	781
31	6590	5422	**31**	256	514
32	4263	8172	**32**	183	416
33	-	-	**33**	-	-
34	542	1216	**34**	102	45
35	2688	1433	**35**	246	113
36	1403	2408	**36**	187	334
37	4879	3538	**38**	347	397
38	3520	2734	**39**	252	179
39	12763	1456	**40**	160	336
40	1247	1583	**41**	1612	2258
41	5959	9512	**42**	515	391
42	17384	5599	**44**	300	425
44	6163	4559	**45**	315	147
45	2532	3014	**46**	74	424
46	939	2417	**47**	205	690
47	1420	1210	**48**	609	521
48	1920	1591	**49**	283	201
49	3009	1770	**50**	132	84
50	1093	957	**51**	118	637
51	1139	1491	**53**	293	1070
53	1515	21139	**54**	180	260
54	2231	7856	**55**	470	96
55	4974	5001	**56**	363	412
56	4793	2836	**57**	230	505
57	2014	6418	**58**	1569	513
58	6099	5539	**59**	317	553
60	14047	2292	**60**	380	159

Appendix X3 – List of publications

Carnell, G. W., Grehan, K., Ferrara, F., Molesti, E., Temperton, N. J. (2017). An Optimized Method for the Production Using PEI, Titration and Neutralization ofo SARS-CoV Spike Luciferase Pseudotypes. *Bio-Protocol*, 7 (16). Doi: 10.21769/BioProtoc.2514

Valkenburg, S. A., Mallajosyula, V. V. A., Li, O. T. W., Chin, A. W. H., **Carnell, G. W.,** Temperton, N. J., Varadarajan, R., Poon, L. L. M. (2016). Stalking influenza by vaccination with pre-fusion headless HA mini-stem. *Nature Publishing Group, Scientific Reports*. 6: 1-11. Doi: 10.1038/srep22666.

Carnell, G. W., Ferrara, F., Grehan, K., Thompson, C. P., Temperton, N. J. (2015). Pseudotype-based neutralization assays for influenza: A systematic analysis. *Frontiers in Immunology*. 6(MAR): 1-17. Doi: 10.3389/fimmu.2015.00161.

Hernandez-Triana, L. M., Jeffries, C. L., Mansfield, K. L., **Carnell, G. W.,** Fooks, A. R., Johnson, N. (2014). Emergence of West Nile Virus Lineage 2 in Europe: A Review on the Introduction and Spread of a Mosquito-Borne Disease. *Frontiers in Public Health*. 2:271. Doi: 10.3389/fpubh.2014.00271